DESIGN OF NEW MONODENTATE LIGANDS FOR REGIOSELECTIVITY AND

ENANTIOSELECTIVITY TUNING IN LATE TRANSITION METAL CATALYSIS

Aaron A. Ruch

Dissertation Prepared for the Degree of

DOCTOR OF PHILOSOPHY

UNIVERSITY OF NORTH TEXAS

May 2016

APPROVED:

LeGrande M. Slaughter, Major Professor
Weston Borden, Committee Member
Francis D'Souza, Committee Member
Tom Cundari, Committee Member
Jean-Luc Montchamp, Committee Member
Michael Richmond, Committee Member and
      Chair of the Department of Chemistry

Ruch, Aaron A. *Design of New Monodentate Ligands for Regioselectivity and Enantioselectivity Tuning in Late Transition Metal Catalysis.* Doctor of Philosophy (Chemistry-Organic Chemistry), May 2016, 247 pp., 51 tables, 50 figures, references, 28 titles.

The ability of gold(I) to activate many types of unsaturated bonds toward nucleophilic attack was not widely recognized until the early 2000s. One major challenge in gold catalysis is the control over regioselectivity when there are two or more possible products as a result of complicated mechanistic pathways. It is well know that the choice of ligand can have dramatic effects on which pathway is being followed but very rarely are the reasons for this selectivity understood. The synthesis of new acyclic diaminocarbenes was developed and a study of the ligand effects on the regioselectivity of a gold-catalyzed domino enyne cyclization hydroarylation reaction and a Nazarov cyclization was undertaken. New chiral acyclic diaminocarbenes were also developed and tested along side new C3-symmetric phosphite ligands in an asymmetric intramolecular hydroamination of allenes. Structure activity correlations were developed for the potential use in further rational ligand design. The synthesis of 6a,7-dihydro-5-amino-dibenzo[c,g]chromene derivatives via a gold-catalyzed domino reaction of alkynylbenzaldehydes in the presence of secondary amines was developed. These were sent to be screened for biological activity.

ACKNOWLEDGEMENTS

TABLE OF CONTENTS

LIST OF TABLES

LIST OF FIGURES

LIST OF ABBREVIATIONS

ADC ....Acyclic diaminocarbene

NHC .... N-heterocyclic carbene

iPr .... Isopropyl

Cy .... Cyclohexyl

PMP.. 4-methoxyphenyl

TMP 2,4,6-trimethoxyphenyl

Mes..2,4,6-trimethylphenyl

ADF.. Amsterdam Density Functional

DFT .... Density Functional Theory

ETS-NOCV ....extended transition state-natural orbitals for chemical valence

OTf...Triflate

HOMO ....Highest Occupied Molecular Orbital

LUMO...Lowest Unoccupied Molecular Orbital

%V_{bur}..Percent Buried Volume

Cbz ....Carboxybenzyl

TEP .... Tolman Electronic Parameter

IR .... Infrared Spectroscopy

NMR .... Nuclear Magnetic Spectroscopy

EXSY .... Exchange Spectroscopy

NOESY .... Nuclear Overhauser Effect Spectroscopy

DIPEA...Diisopropylethylamine

PG ....Protecting Group

Ts .... p-toluenesulfonyl

Ms ....methanesulfonyl

Fmoc ....Fluorenylmethyloxycarbonyl

Piv .... Pivaloyl

Ac ....Acetyl

MOM...Methoxymethyl acetal

%ee... percent enantiomeric excess

BINOL ....1,1′-Binaphthyl-2,2′-diol

BINAM .... 1,1′-Binaphthyl-2,2′-diamine

Xantphos .... 4,5-Bis(diphenylphosphino)-9,9-dimethylxanthene

Bn .... Benzyl

THT.. Tetrahydrothiophene

HOESY .... Heteronuclear Overhauser Effect Spectroscopy

acac ....Acetylacetone

TADDOL .... (4R,5R)-2,2-Dimethyl-$\alpha,\alpha,\alpha',\alpha'$-tetraphenyldioxolane-4,5-dimethanol

Ad ....Adamantyl

dppe.. 1,2-Bis(diphenylphosphino)ethane

θ ....Tolman Cone Angle

G .... Solid Angle G-parameter

CAAC ....Cyclic Alkyl Amino Carbene

TLC...Thin Layer Chromatography

HOMOGENEOUS GOLD CATALYSIS

1.1 Introduction

   Although gold has historically been regarded as too inert to be useful in transition metal

catalysis, there has been a surge in the last 16 years in the use of gold to catalyze a wide range of

organic transformations. Metallic gold is very inert and has been a part of human history for

centuries, being used as the basis of currency, in jewelry, and more recently in electronics. The

two most common oxidation states of gold, gold(I) and gold(III), are, however, both catalytically

active. One of the first gold-catalyzed reactions involved hydrochlorination of alkynes with a

heterogeneous gold(III) catalyst **(Scheme 1.1).**[1] An early example of homogeneous gold

catalysis, and the first asymmetric gold catalyzed reaction, appeared in 1986, when an

asymmetric aldol reaction was reported by Hayashi and co-workers (**Scheme 1.2**).[2]
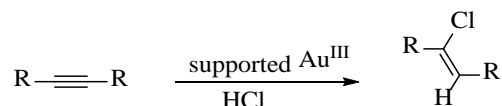
Scheme 1.1: Gold Catalyzed Hydrochlorination of Alkynes
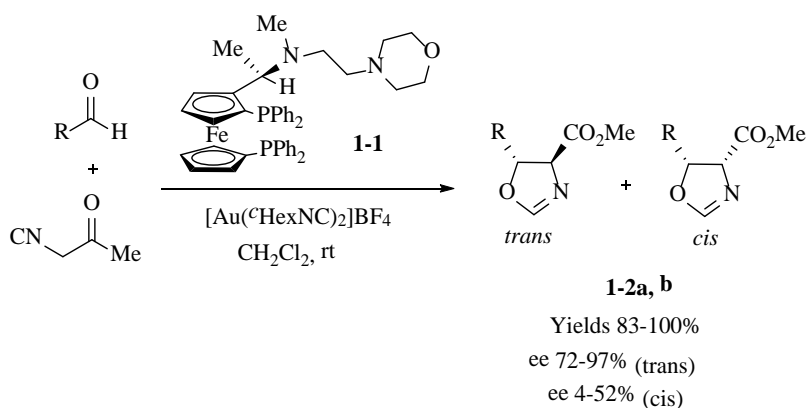
Scheme 1.2: First Asymmetric Gold Catalyzed Reaction

Even with these early promising results occurring almost 3 decades ago, it was not until the late 1990s and early 2000s that the study of gold catalysis really took off, when Teles's group showed that ketones, enol ethers, and ketals could be synthesized by the gold(I) catalyzed addition of alcohols and water to alkynes as well as Hashmi's phenol synthesis (**Scheme 1.3**).[3] Probably the most distinguishing characteristic of gold in catalysis is its carbophilicity. As a soft Lewis acid, gold is arguably the best metal for activating π−bonds including alkynes, allenes, and alkenes. However, it should be noted that in the case of alkenes, some controversies have arisen suggesting that the alkenes are actually activated by trace amounts of strong Brønsted acid generated by the non-coordinating anions used to replace chloride upon activation of gold(I)-chloride precatalysts.[4] Gold has the added benefit of being an environmentally friendly alternative to other π-acids such as Hg. The number of gold catalyzed reactions that have appeared over the past few years has been growing at an accelerating rate.
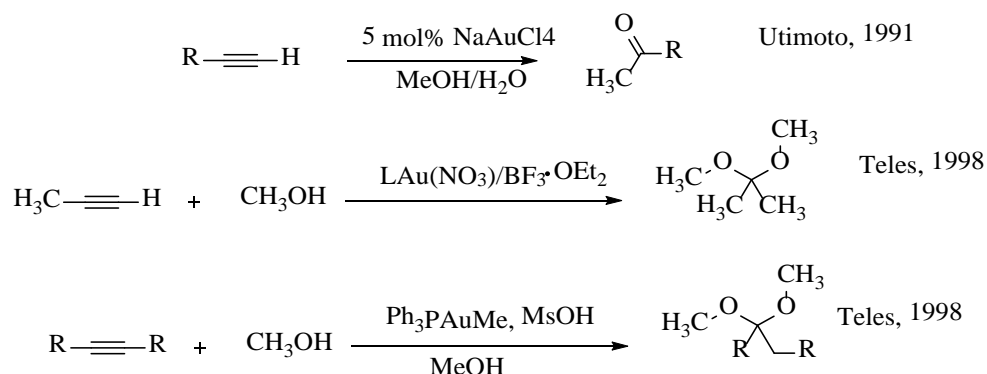
Scheme 1.3 Foundation of Au^I Catalysis

The groups of Toste, Echavarren, Michelet, and Hashmi, just to name a few, have demonstrated the wide applicability of gold catalysis. Some of the various reactions catalyzed by gold are outlined in **Scheme 1.4**.
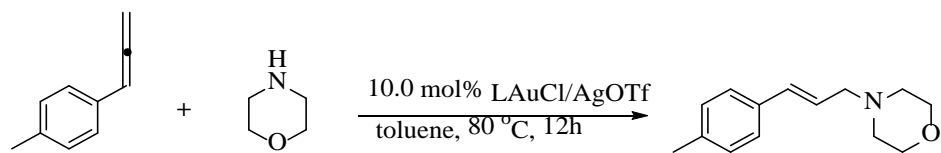
(a) Intermolecular hydroamination of allenes [5]
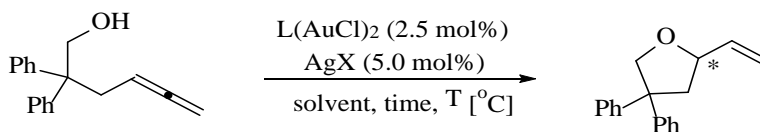
(b) Enantioselective intramolecular hydroalkoxylation of allenes. [6]
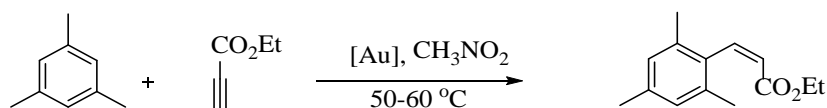
(c) Intermolecular hydroarylation of electron deficient alkyne[7]
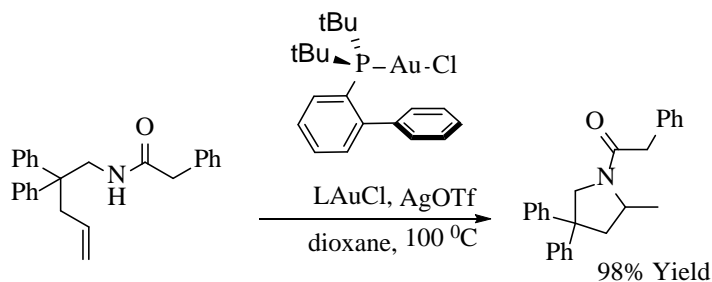
(d) Hydroamination of olefins[8]

Scheme 1.4: Examples of Gold Catalyzed Reactions

Even with all the gold-catalyzed reactions that have been studied, there is still significant work that needs to be done in discovering new reactions as well as understanding their mechanisms and how to control their chemo-, regio-, and stereoselectivities.

1.2 Advantages of Gold Catalysis

Due in part to relativistic effects, the reactivity of gold is very unique.[9] Gold generally shows superior activity to other metals when catalyzing the same reaction **(Scheme 1.5)**.[10] Au^I is a carbophilic soft Lewis acid that is isolobal with H^+.[11] This allows gold to go beyond typical Lewis

acid catalysis and also catalyze reactions that are more typically catalyzed by Brønsted acids. As mentioned before, gold has the added benefit of being an environmentally friendly alternative to other π-acids such as Hg. Arguably the most desirable attribute of Au^I from a synthetic standpoint is its low oxophilicity which often removes the requirement of removing oxygen or rigorously drying solvents that normally apply with other metals.
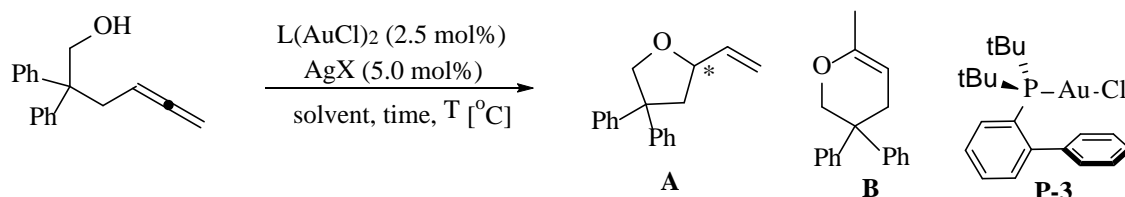
Scheme 1.5: Comparison of Au vs Pt in Intramolecular Allene Hydroalkoxylation[9]

Table 1.1: Hydroalkoxylation of Allenes

Catalyst (5 mol %)	% yield	A:B
PtCl(ethylene)2/(p-CF3-Ph)P	49	0:100
P-3/AgOTs	96	99:1

Some gold-catalyzed reactions can even be conducted in open flask, and sometimes the catalyst can even be recovered after column chromatography. In terms of characterizing the pre-catalyst, Au is very favorable in that both common oxidation states of gold are diamagnetic which allows for the use of NMR for both characterization and monitoring of reactions. There is also only one isotope of gold, ^{79}Au, which allows for easy interpretation of mass spectroscopy data. ^{79}Au is also NMR active but due to low sensitivity and a quadrupole moment, only a few ^{79}Au NMR spectra have been reported, and these were mostly in the solid state.[11] Attractive catalyst features, including the ability to run reactions typically at room temperature, low catalyst loadings, high turnover number, short reaction times, tolerance of a wide variety of solvents and functional

groups, ease of handling, and relatively low toxicity, have provided great advantages for Au^I catalysts in homogenous catalysis. Beyond all the chemical benefits of gold, assuming a comparable gold catalyst can be prepared, gold has an added benefit to potentially replace other more rare and expensive metals currently being used in catalysis. The influence of all of these benefits is suggested by **Figure 1.1**, which shows the number of publications based on a SciFinder search involving gold catalysis over the past 20 years increasing exponentially.[12]
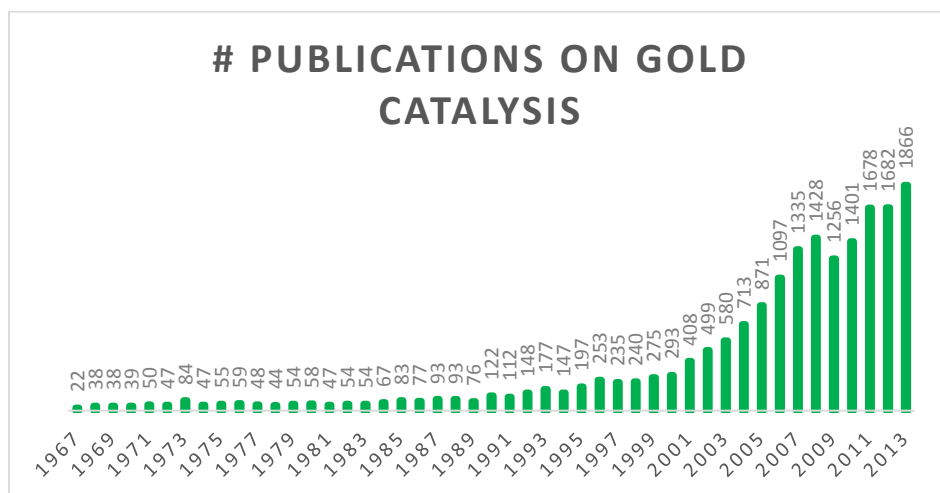
Figure 1.1: The Number of Publications Related to Gold Catalysis Per Year (1967-2013)

Despite the growing interest in discovering what new types of reactions gold can catalyze, relatively few of the publications cited in the figure above actually relate to understanding the mechanisms of reactions, and even fewer investigate how ligands can effect these intricate mechanistic pathways. The following section will give a brief introduction to the typical catalytic cycles involved in homogenous gold catalysis. The effects of ligands will be discussed more fully in Chapter 2.

1.3 Typical Gold Catalytic Cycles

A generic catalytic cycle for cationic gold(I)-catalyzed addition of nucleophiles to π-bonds is outlined in **Scheme 1.6**.[13] It is very well understood that the attack of the nucleophile to the cationic

gold complex in Stage 1 occurs via an anti-addition mechanism. The organogold intermediate then undergoes protodeauration in Stage 2 to regenerate the active "LAu$^+$" catalyst, which then reenters the catalytic cycle.
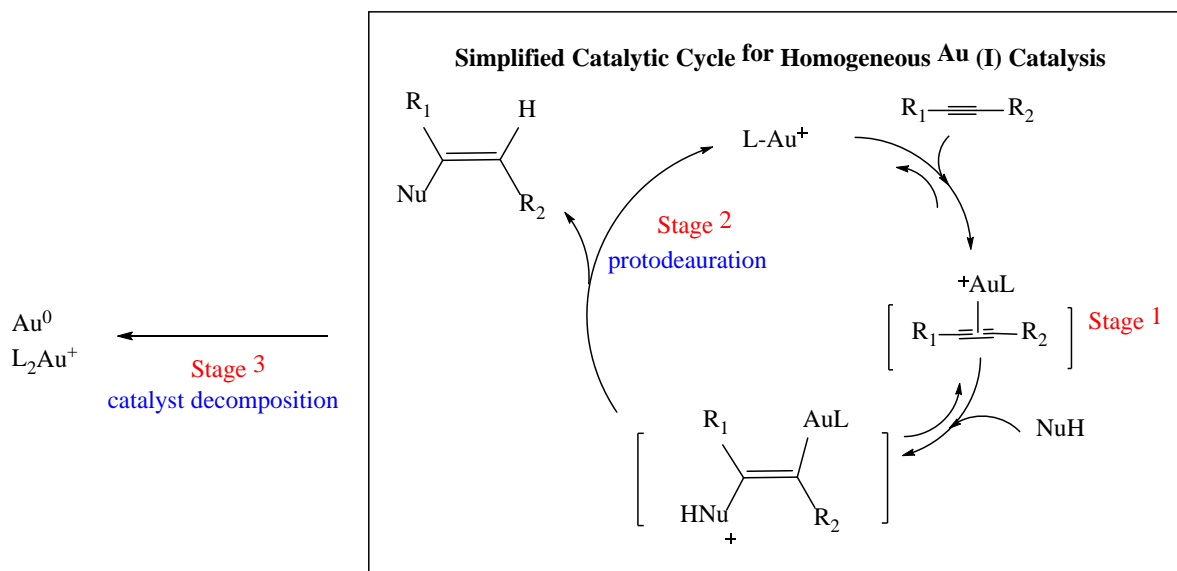
Scheme 1.6 Simplified Au^I Catalytic Cycle[13]

It was often assumed that the protodeauration step was very fast, and therefore the electrophilic activation of the π-bond should be the major factor in getting efficient turnover in gold catalysis.[14] However, this idea has been shown to be incorrect innumerous reactions, making it difficult to predict which ligands will be useful for certain gold-catalyzed organic transformations.[15] Hammond and co-workers recently published a study on ligand effects on various stages of this generic catalytic cycle for gold.[13] Some of the most common gold(I) complexes currently being used in gold catalysis are shown in **Figure 1.2.**
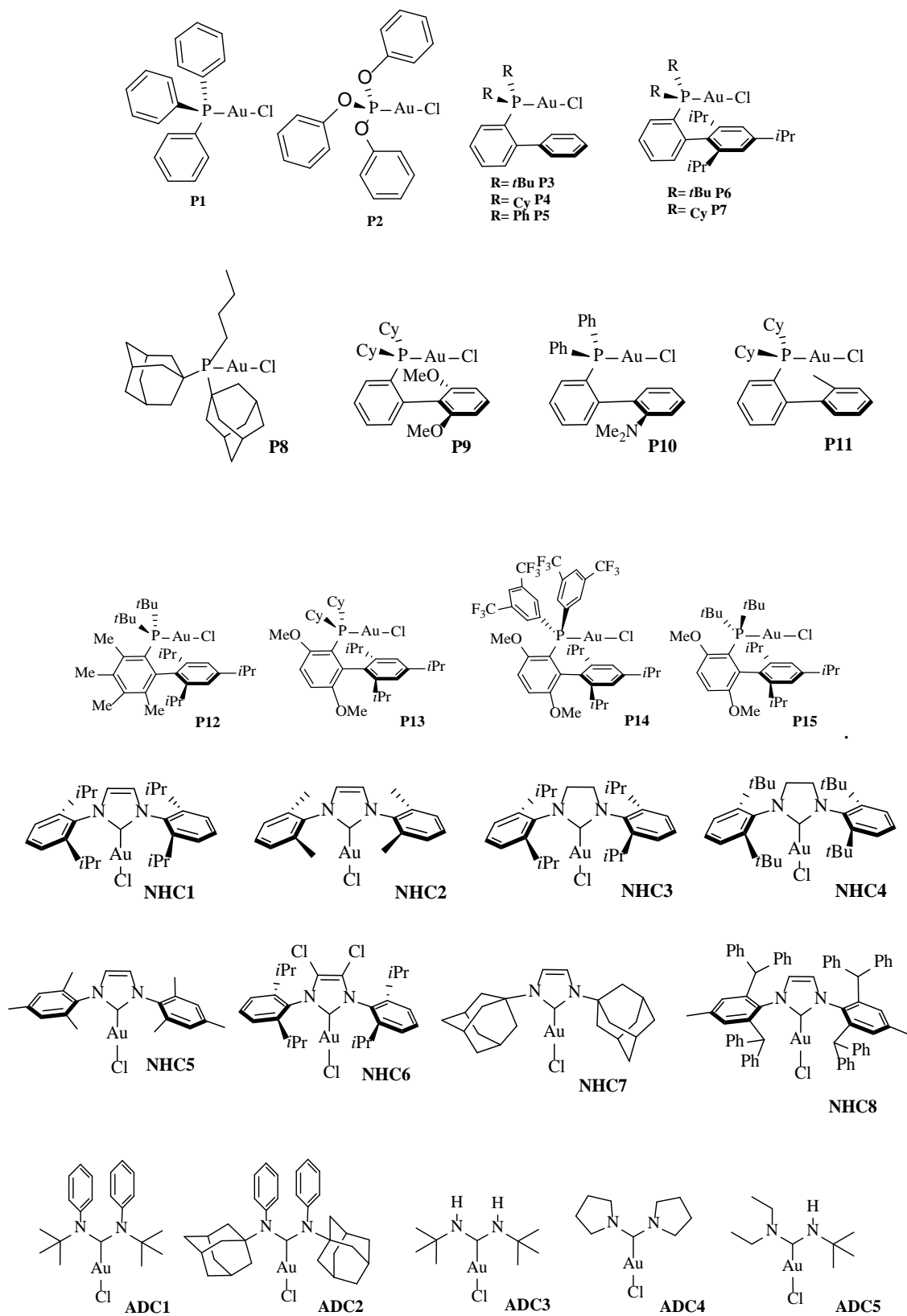
Figure 1.2: Complexes Commonly Used in Gold Catalysis

It was determined that electron-deficient ligands can facilitate activation of the π–bond by the cationic gold complex whereas electron-rich ligands can facilitate protodeauration. It was also determined that decay of the active catalyst to Au^0 could be inhibited by non-covalent secondary interactions with pendant aryl rings. These noncovalent interactions have actually become more important in various aspects of gold catalysis beyond just stabilizing the catalytically active intermediate.[16] This study is a rare example of an effort to understand ligand effects in gold catalysis. The present study gives some predictive understanding of which steps in a standard gold-catalytic cycle are affected by certain properties of the ligand, but most gold catalytic mechanism are very complex and may involve multiple additional steps.[17] Therefore, more experimental studies need to be done to gain a better understanding of the mechanisms. To expand on the simplified mechanism scheme detailed above, there are of several different reaction pathways that the organogold intermediate involved in many gold catalyzed reactions can follow. Beyond the typical protodeauration step, the intermediate can undergo various α or β proto-deauration/functionalization steps to provide a range of products.[18] The wide range of reactions that can be catalyzed by this metal that was formerly thought to be inert are briefly discussed in the following sections. It is organized based on the type of nucleophile being added to the gold-activated π-system.

1.4 Gold-Catalyzed Nucleophilic Additions: Oxygen Nucleophiles

Due to relativistic effects and other factors, cationic gold(I) is a π-acid with low oxophilicity.[8] This makes gold an optimal choice in forming new C-O bonds, which behind C-H and C-C bonds are the most widespread bonds in organic chemistry. Both Au^I and Au^{III} are known to activate π-systems toward nucleophilic attack by various types of oxygen nucleophiles. With Au^{III} being more oxophillic in nature, its chemistry is less well developed when compared with Au^I. The

8

various reactions described in the following sections have been used to synthesize a wide variety

of synthetically useful compounds such as cyclic ethers, ketals, ketones, lactones, and phenols,

just to name a few. Some asymmetric versions of these reaction will be discussed more fully in

Chapter 3.

1.4.1 Gold Catalyzed Addition of O-Nucleophiles to Alkynes

   The alkynophilicity of Au(I) makes it arguably the best choice of π-acids to activate alkynes

toward nucleophilic attack, allowing the formation of numerous complex structures. The low

oxophilicity of Au(I) also makes it an ideal candidate for the addition of oxygen based

nucleophiles. Although Au(III) is more oxophilic relative to Au(I) it has also played an important

role in the synthesis of new C-O bonds. As mentioned in the previous section, some of the earliest

reports of gold catalyzed reactions were of the hydration of alkynes **(Scheme 1.3)**.[3] An example

in which the use of Au^{I} as compared to Au^{III} resulted in the formation of two different products is

shown in **Scheme 1.8**.[19] The use of AuCl$_3$ results in the formation of a dihydrofuran derivative,

whereas the use of (Ph$_3$P)AuCl with a silver salt to abstract the chloride results in the formation of

butenolides in the presence of oxygen. Interestingly, if one subjects the product obtained using

Au^{III} catalysis to the Au^{I} conditions, it results in formation of the same product obtained using an

Au^{I} catalyst with the original substrate.
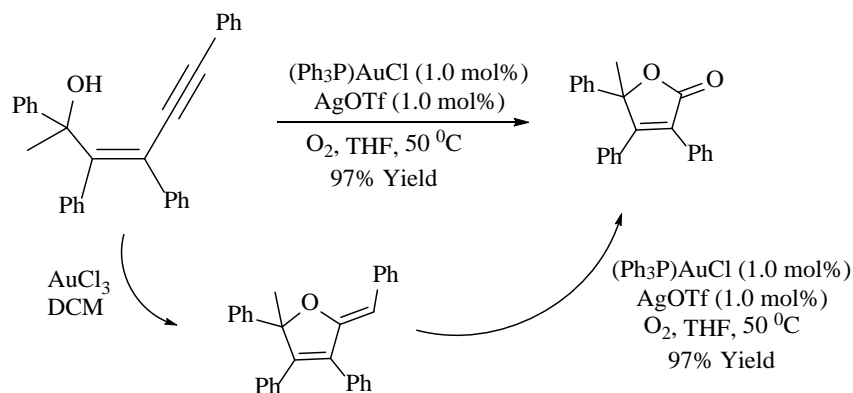
Scheme 1.8: Au^{I} vs. Au^{III} Product Selectivity

Besides alcohols and water, ethers can also be effective nucleophiles in gold catalysis. The synthesis of indenyl ethers is represented in **Scheme 1.9**.[20] The mechanism behind this reaction will prove to be important in Chapter 6. The initial activation of the π-bond by gold, followed by an intramolecular cyclization and bond rearrangement, results in the formation of indenyl ether derivatives.
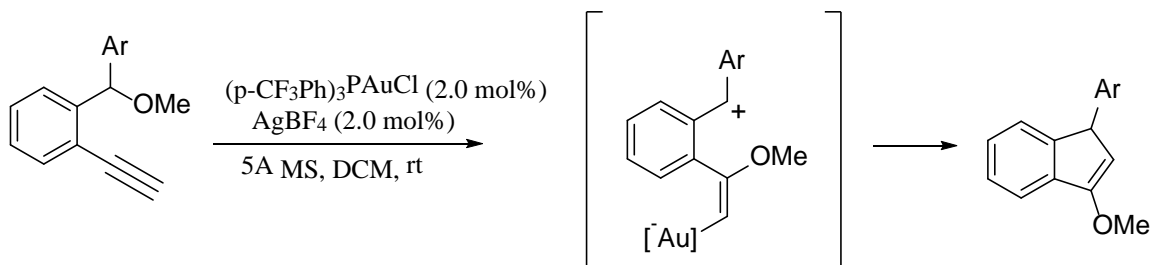
Scheme 1.9 Au-catalyzed indenyl ether synthesis

There are numerous occasions in which the choice of catalyst **(Scheme 1.8)** or choice of ancillary ligand has a dramatic effect on the reaction mechanism. These results can affect regioselectivity **(Table 1.2),**[21] reaction rate **(Table 1.3)**[22] or even enantioselectivity **(Table 1.4)**.[23] The simple fact that an ancillary ligand can result in such drastic changes in gold catalysis points toward the need for a better understanding of ligand effects in gold catalysis.[24]
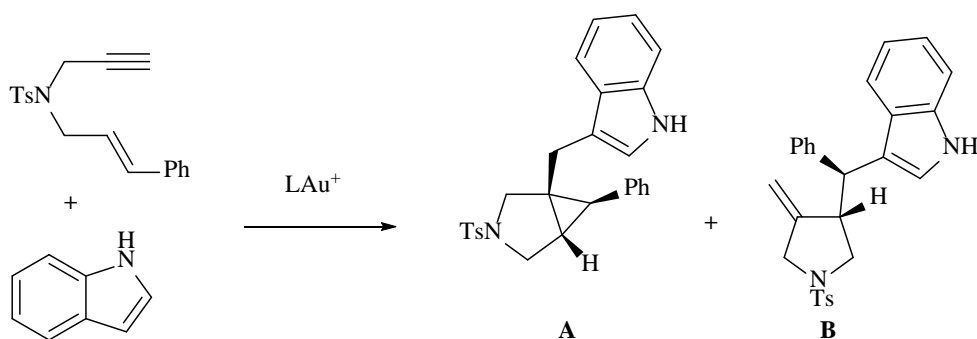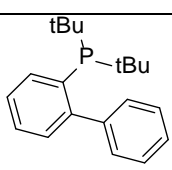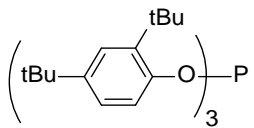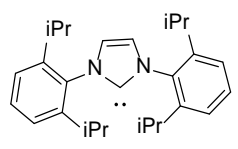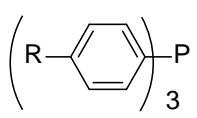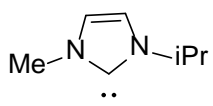
Table 1.2 Domino Enyne Cyclization/Hydroarylation Results

entry	L	% Yield	A:B
1		74	20:80
2		71	16:84
3		57	75:25
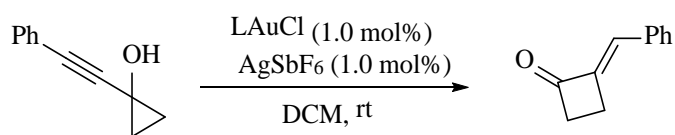
Table 1.3 Rate Enhanced Au Catalyzed Reaction Results

entry	L	R	% yield	time
1		H	95	115min
2		MeO	90	160min
3		Cl	97	85min
4		CF$_3$	99	25min
5			63	24hr
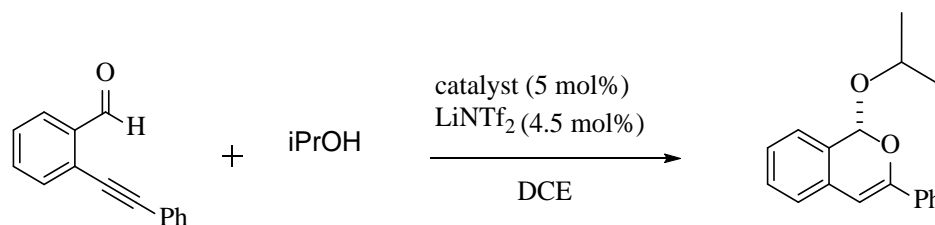
Table 1.4 Asymmetric Au^I Catalyzed Reaction Results

entry	L	R	% yield	%ee
1		H	12	8
2		Ph	28	61
3		3,5(bis-CF$_3$)Ph	68	84

1.4.2 Gold Catalyzed addition of O-nucleophiles to Allenes

Another type of widely studied π-system used in gold catalysis is allenes.[25] These are the substrates of choice for enantioselective gold catalysis. Of reported enantioselective reactions, the intramolecular hydroalkoxylation of allenes is probably one of the most well studied.[26] Toste's group was able to achieve very high enantioselectivities in the synthesis of tetrahydrofuran derivatives. From the **Table 1.5 entries 1-3**, the standard chiral bis-phosphine ligands were not very enantioselective. However, when a chiral counterion was used (**entry 4** in the reaction) there was a dramatic increase in selectivity.
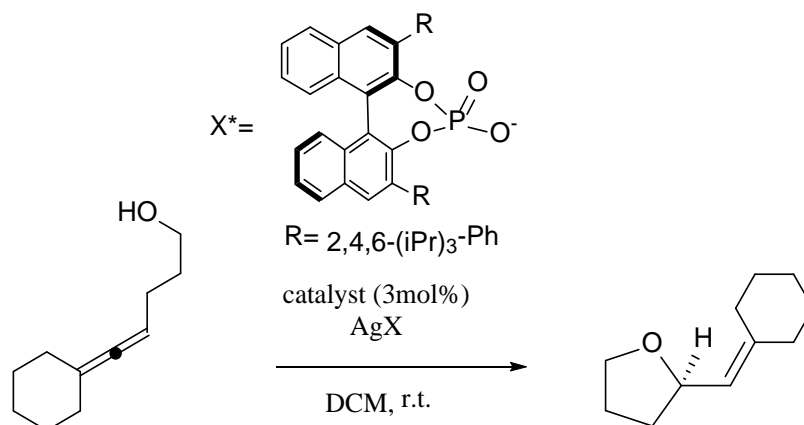
Table 1.5 Asymmetric Intramolecular Hydroalkoxylation Results

entry	L	X	% yield	%ee
1	(R)-3,5-xylyl-BINAP	BF4	68	0
2	(R)-3,5-xylyl-BINAP	OPNB	89	8
3	(R)-DTBM-Segphos	BF4	79	2
4	dppm	X*	76	65

There has been a recent surge of studies on counterion effects in gold catalysis.[27] It is one area, similar to ligand choice, where there is a lack of predictive knowledge, and currently a catalyst screening process involves running numerous reactions and testing various counterions.

1.4.3 Gold Catalyzed Addition of O-nucleophiles to Alkenes

Intermolecular addition of phenols and carboxylic acids to olefins was first developed in 2005 (**Scheme 1.10**).[28] It has been argued that some of the reactions are actually catalyzed by trace amounts of Brønsted acid formed under the catalytic reaction conditions.[29] Due to the lesser reactivity of alkenes and problems associated with competing acid-catalyzed pathways, gold chemistry of alkenes is less well developed when compared to that of alkynes and allenes.
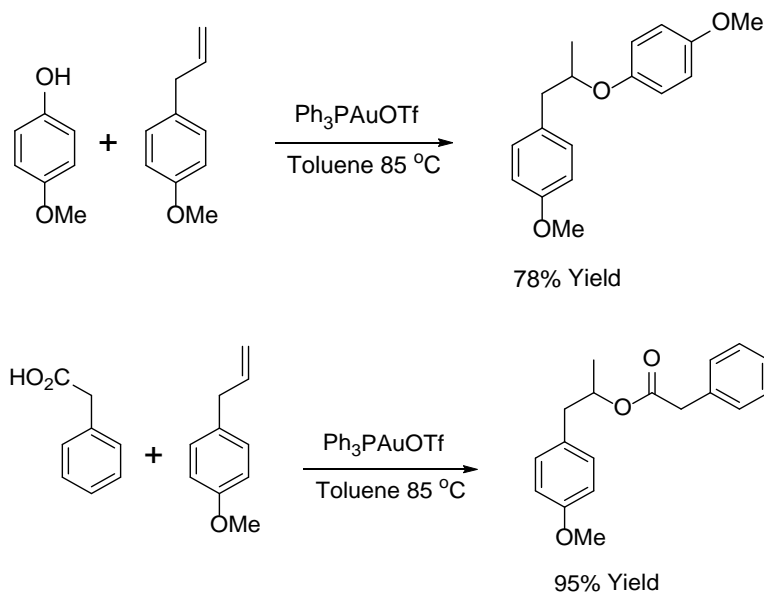
Scheme 1.10 Gold-Catalyzed Hydroalkoxylation of Olefins

1.5 Gold-Catalyzed Nucleophilic Additions: Carbon Nucleophiles

The gold(I) catalyzed addition of carbon nucleophiles to activated π-systems is an extremely powerful tool for creating new C-C bonds. This reaction can be thought of as a very mild Friedel-Crafts-type reaction in which gold acts as the Lewis acid. As with other types of nucleophilic additions, gold more readily activates alkynes and allenes than alkenes. Typical examples of each substrate type will be briefly discussed in the ensuing sections.

1.5.1 Gold Catalyzed Addition of C-nucleophiles to Alkynes

The typical C-nucleophile used in gold catalysis is an electron rich aryl ring. The alkynophilicity of gold makes it ideal for forming new C-C bonds between an activated alkyne and an aryl ring. A few examples of such reactions are outlined in **Scheme 1.11**.[30] The first is an intramolecular hydroarylation of a pendant alkyne resulting in a tricyclic structure.[30a] The second reaction depicts the use of an electron-rich heteroaryl indole derivative for the synthesis of a 7-member lactam.[30b] Both indole derivatives and lactam derivatives are biologically important.[31]
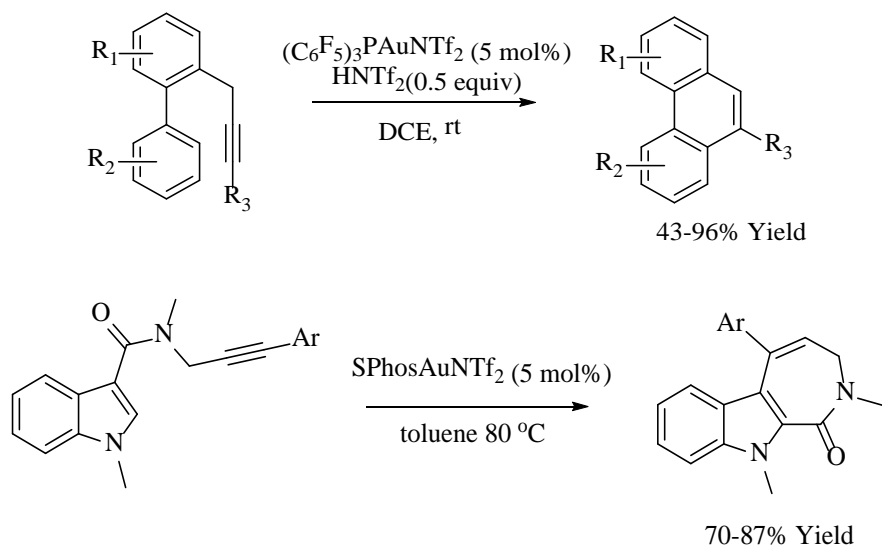
Scheme 1.11 Hydroarylation of Alkynes

1.5.2 Gold Catalyzed Addition of C-nucleophiles to Allenes

The second most common substrate studied in hydroarylation reactions are allenes. Although they are a little less reactive than alkynes, they have the potential of forming chiral products, which makes them valuable for researchers pursuing asymmetric gold catalysis. One example of a hydroarylation reaction involving an allene is depicted in **Scheme 1.12**[32] and results in the formal synthesis of the biologically active compound (-)-Rhazinilam.[33]
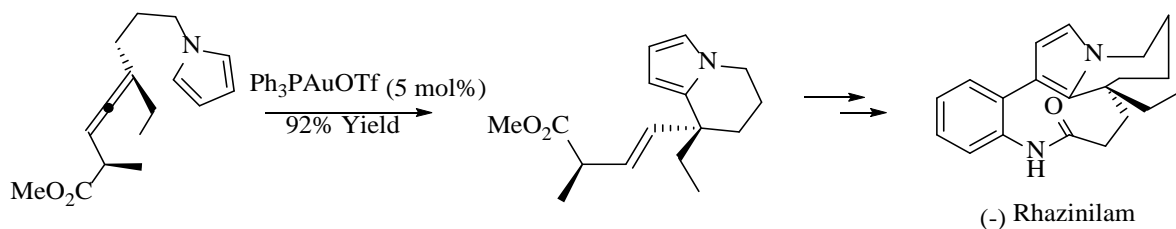
Scheme 1.12 Hydroarylation of Allenes: Formal Synthesis of Rhazinilam

1.5.3 Gold Catalyzed Addition of C-nucleophiles to Alkenes

Compared with other nucleophiles, additions to alkenes are fairly limited, and in some

circumstances the possibility of catalysis by trace Brønsted acids should be considered. The example depicted in **Scheme 1.13** is actually a domino process that begins with an intermolecular hydroarylation of the diene.[34]
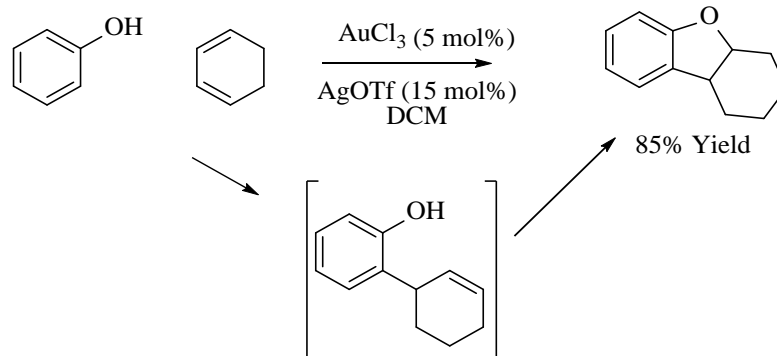
Scheme 1.13 Domino Hydroarylation of Diene

1.6 Gold-Catalyzed Nucleophilic Additions: Nitrogen Nucleophiles

Because amines have a higher binding affinity toward gold than C-C π-bonds,[35] protected amines are typically used as nitrogen nucleophiles in gold catalysis. This can lower the efficiency of the overall reaction by adding two extra steps if the amine is the desired product, but the mild conditions under which gold can catalyze the hydroamination reactions makes up for the extra synthetic effort.

1.6.1 Gold Catalyzed Addition of N-nucleophiles to Alkynes

The intramolecular hydroamination of alkynes is one of the mildest and most versatile ways of synthesizing substituted indoles.[36] The reaction of the alkynyl aniline derivative is depicted in **Scheme 1.14**. By simply starting with various substituted aniline derivatives, a researcher could synthesize an entire library of indole derivatives very quickly and under mild conditions by this method. The mild conditions might allow the incorporation of sensitive functional groups that are not compatible with other methods. Numerous groups have studied this reaction with various types

of ligands. Several comprehensive reviews of this area are available.[37]
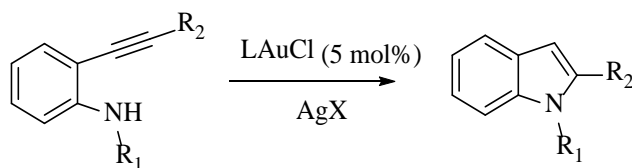
Scheme 1.14 Indole Synthesis via Intramolecular Hydroamination of Alkyne

1.6.2 Gold-Catalyzed Addition of N-Nucleophiles to Allenes

The ability to generate chiral centers when using allenes as substrates is one reason that the hydroamination reaction of allenes is one of the most well studied reactions in asymmetric gold catalysis.[38] With various nitrogen-containing heterocycles being biologically important, it is easy to understand the level of interest achieving high selectivities in this reaction. A few examples in which high levels of asymmetric induction were achieved are depicted in **Scheme 1.15.**[39] The first example shows the promise of using a chiral counterion rather than a chiral ligand to achieve high levels of asymmetric induction in the synthesis of enantioenriched pyrollidines.[39a] The second example, reported by Widenhoefer and coworkers, represent a somewhat rare example of an enantioselective intermolecular hydroamination reaction.[39b]

H$_2$NCbz + Ph〜•〜 → Ph〜〜*

[Biphep(AuCl)$_2$] (2.5 mol%)
AgBF$_4$ (5 mol%)
dioxane, rt, 24h

NHCbz
89% Yield, 72%ee

MeO, MeO — PAr$_2$, PAr$_2$

4-MeO-3,5-(^{t}-Bu)$_2$ MeO-BIPHEP
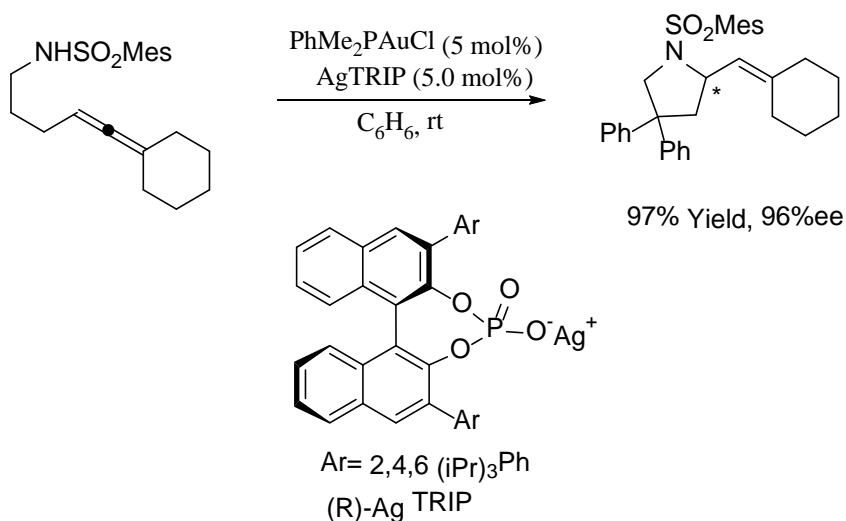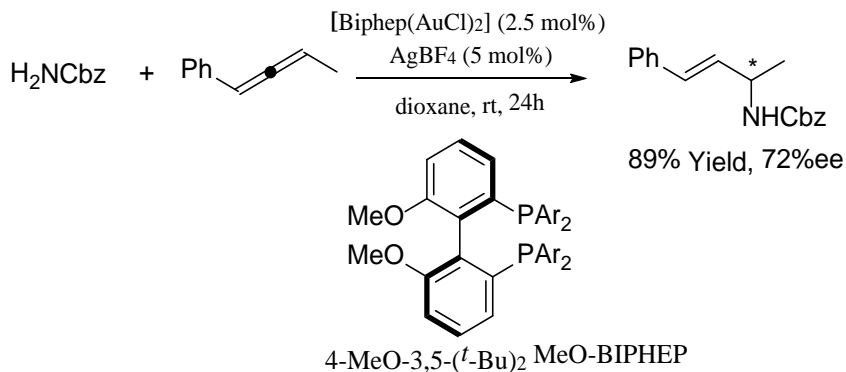
Scheme 1.15 Asymmetric Gold-Catalyzed Hydroamination of Allenes

1.6.3 Gold Catalyzed Addition of N-nucleophiles to Alkenes

Alkenes offer the same benefits as allenes in that they can be used to generate chiral centers under the appropriate conditions. One example of an asymmetric gold-catalyzed hydroamination of olefins is depicted in **Scheme 1.16**[40] This is one case in which one would have a hard time arguing that the reaction is Brønsted acid catalyzed, since significant enantioselecivities were achieved. For a more detailed introduction to the various types of reactions catalyzed by gold, there are several comprehensive reviews available.[37]

(a).

RN〜NH + 〜〜Me$_n$ →

[Biphep(AuCl)$_2$] (2.5 mol%)
AgOTf (5 mol%)
m-xylene, 100 °C

O Me
RN〜N〜*〜Me$_n$

R = alkyl, aryl   n = 5,7,9

MeO, MeO — PAr$_2$, PAr$_2$

4-MeO-3,5-(^{t}-Bu)$_2$ MeO-BIPHEP

6 examples
76-89% yield
71-78% ee
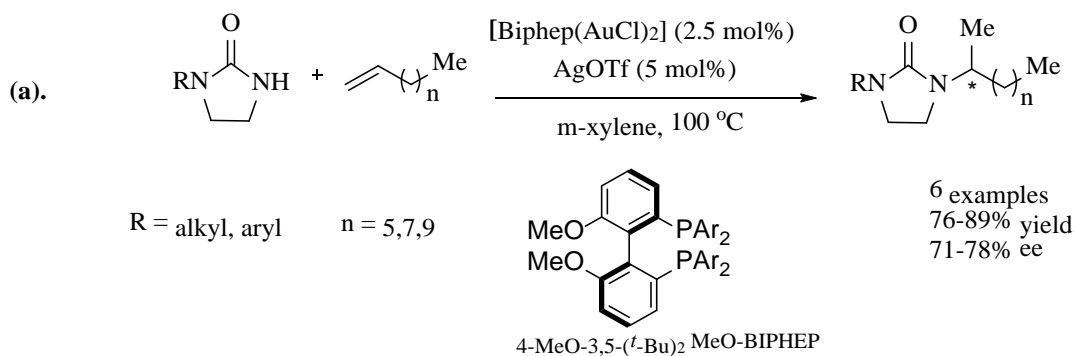
Scheme 1.16 Asymmetric Gold Catalyzed Hydroamination of Alkenes

1.7 Carbene Ligands in Gold Catalysis

Without question, phoshines have dominated ligand design in catalysis with all types of transition metals. Carbenes such as N-heterocyclic carbenes (NHCs)[41a] and more recently acyclic

diaminocarbenes (ADCs),[41b] have made some dramatic impacts in transition metal catalysis, including in gold catalysis. There are numerous examples in which a simple switch from a phosphorus-ligated catalyst to a carbene-ligated catalyst led to catalytic outcomes that are completely different (**Scheme 1.17**)[42]
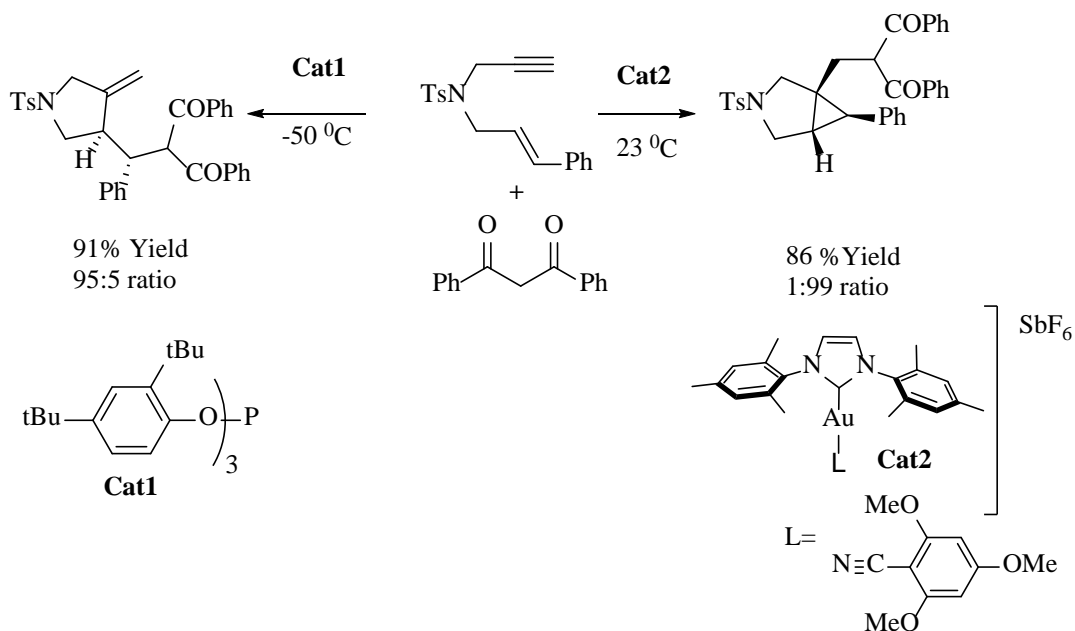
Scheme 1.17 Ligand-Controlled Regioselective Hydroarylation/Enyne Cyclization Reaction

The more electron-rich NHC ligand favors the fused bicyclic product, whereas the electron-deficient phosphite favors the olefin product. NHCs have become ubiquitous in gold catalysis because of their ability to promote unique reaction pathways, in addition to the facts that they are generally less sensitive and easier to handle than phosphine-ligated gold complexes. The acyclic counterparts of NHCs, ADCs, have shown promising and possibly advantageous features in recent years in reports from the groups of Hashmi, Hong, Toste, and Slaughter. ADCs have shown some unique and sometimes unexpected results when used as ancillary ligands in gold catalysis. One of the most notable examples is a variation of the reaction shown in **Scheme 1.21** reported by Sukwon Hong's group.[43] It was calculated that the ligand of **Cat1** should have better σ-donating capability

than NHC (**Cat2**) by calculating the energy of the HOMO orbital of the free carbenes (-4.57 eV vs -5.61), which led to an initial hypothesis that this ligand would result in higher selectivity for the bicyclic product. However, the observed product selectivity was completely opposite (**Scheme 1.18**).
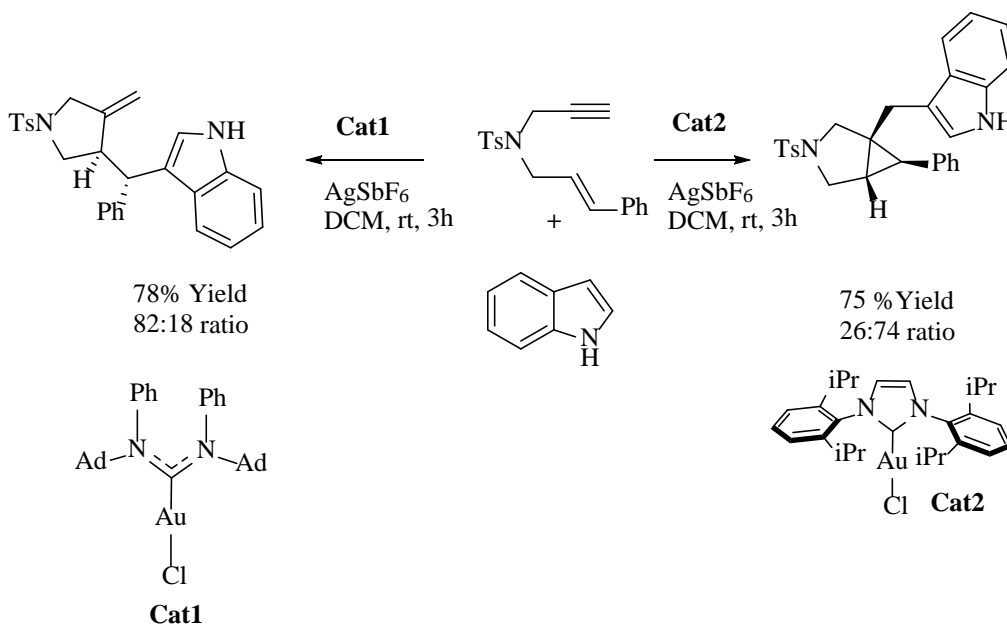
Scheme 1.18 Unusual Selectivity in an Enyne Reaction Catalyzed by an ADC Gold Complex.[43]

The authors initially looked towards steric explanations, since electronic factors did not seem to account for the observed results. Although the original method for describing the steric hindrance of a ligand is the Tolman cone angle, buried volume (**Figure 1.3**) has recently emerged as a substitute for carbenes to account for the fact they aren't cone shaped. However, the buried volumes of each were calculated and only differed by ~0.1%. This suggest that steric influences on selectivity are minimal. Hong and coworkers pointed out the distorted dihedral angle (41^0) of the ADC complex, which might potentially make the ligand more π-accepting, possibly causing it to favor the observed exocyclic olefin product. Although no evidence for this conclusion was provided, it helped to explain the observed results.
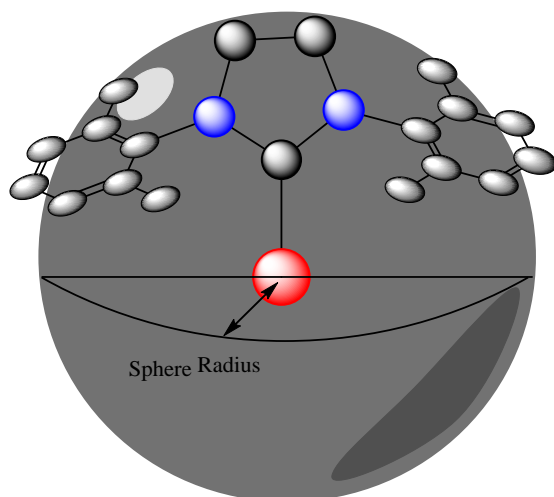
Percent buried volume
$\%V_{bur} =$ percent of the total volume
of a sphere occupied by a ligand.

Figure 1.3 $\%V_{bur}$ Diagram

1.8 Conclusion

Gold catalysis has undergone enormous growth just over the past 16 years, making it difficult

to predict in which direction the field will go in the future. There are still some key problems that

need to be addressed in gold catalysis, such a designing ligands that allow high levels of

asymmetric induction for diverse types of reactions instead of being specific for a certain reaction.

Gold-catalyzed asymmetric intermolecular reactions of allenes and alkenes are still very rare and

problematic. Probably one of the most important things left to accomplish in gold catalysis is an

asymmetric Au^{III}-catalyzed reaction. With a rationally designed ligand that stabilizes the gold(III)

active catalyst and prevents it from decomposing, this goal should be achievable. Further

understanding of subtle ligand effects in gold catalysis is another area that deserves much more

attention than it has received in the past. Probably the last big area of research left in the field is

an understanding of counterion effects or the "silver effect" in gold catalysis.[27] The requirement

of screening a large range of counterions with no predictive information as to why one works over

21

the others creates burdens on researchers and slows down progress in the field. The following chapters will address the problems of understanding subtle ligand effects in gold catalysis by investigation some structure-activity and structure-selectivity relationships in gold catalysis with various chiral and achiral ligands.

1.9 References

1.   Hutchings, G. J. *J. Catal.* **1985**, *96*, 292. Nkosi, B.; Coville, N. J.; Hutchings, G. J. *J. Chem. Soc. Chem. Commun.* **1988**, 71. (b) Nkosi, B.; Coville, N. J.; Hutchings, G. J. *Appl. Catal.* **1988**, *43*, 33. (c) Nkosi, B.; Coville, N. J.; Hutchings,G. J.; Adams, M. D.; Friedl, J.; Wagner, F. E. *J. Catal.* **1991**, *128*,366. (d) Nkosi, B.; Adams, M. D.; Coville, N. J.; Hutchings, G. J. *J. Catal.* **1991**, *128*, 378. (e) Hutchings, G. J. *Gold Bull.* **1996**, *29*, 123; *Catal. Today* **2002**, *72*, 11. (f) Hutchings, G. J. *Spec. Chem. Mag.* **2003**, 12.

2.   Ito, Y.; Sawamura, M.; Hayashi, T., *J. Am. Chem. Soc.,* **1986,** *108*, 6405-6406.

3.   (a) Teles, J. H.; Schulz, M. BASF AG, WO-A1 9721648, 1997 (*Chem. Abstr.* **1997**, *127*, 121499). (b) Teles, J. H.; Brode, S.; Chabanas, M. *Angew. Chem.* **1998**, *110*, 1475; *Angew. Chem., Int. Ed.* **1998**, *37*, 1415.

4.   LaLonde, R. L.; Sherry, B. D.; Kang, E. J.; Toste, F. D. *J. Am. Chem. Soc.* **2007**, *129*, 2452.

5.   (a) Aikawa, K.; Kojima, M.; Mikami, K., *Adv. Synth. Catal.,* **2010,** *352*, 3131-3135; (b) Aikawa, K.; Kojima, M.; Mikami, K., *Adv. Synth. Catal.,* **2011,** *353*, 2882-2883; (c) Zhang, Z.; Widenhoefer, R. A., *Angew. Chem., Int. Ed.,* **2007,** *46*, 283-285. (d) Hamilton, G. L.; Kang, E. J.; Mba, M.; Toste, F. D., *Science,* **2007,** *317*, 496-499; (e) Aponick, A.; Biannic, B., *Org. Lett.,* **2011,** *13*, 1330-1333..

6.   Reetz, M. T.; Sommer, K. *Eur. J. Org. Chem.* **2003**, 3485.

7.   (a) Bender, C. F.; Widenhoefer, R. A. *Chem. Commun.* **2008**, 2741 (b) Giner, X.; Najera, C.; Kovacs, G.; Lledos, A.; Ujaque, G. *Adv. Synth. Catal.* **2011**, *353*, 3451 (c) Kitahara, H.; Sakurai, H. *Chem. Lett.* **2010**, *39*, 46 (d) Giner, X.; Najera, C. *Org. Lett.* **2008**, *10*, 2919. (e) Bender, C. F.; Widenhoefer, R. A. *Org. Lett.* **2006**, *8*, 5303.

8.   (a) Gorin, D. J.; Toste, F. D. *Nature* **2007**, *446*, 395. (b) Pyykko, P. *Angew. Chem. Int. Ed.* **2004**, *43*, 4412. (c)Pyykko, P. *Inorg. Chim. Acta* **2005**, *358*, 4113.

9.   (a) Widenhoefer, *J. Am. Chem Soc.* **2006**, *128*, 9066 (b) Widenhoefer, *J. Am. Chem. Soc.* **2004**, *126*, 9536

10.   R. Hoffmann *Angew. Chem. Int. Ed. Engl.*, **1982**, *21*, 711–724

11.   (a) Narath, A. *Phys. ReV.* **1967**, *163*, 232. (b) Narath, A. *Phys. ReV.* **1968**, *175*, 696. (c) Goodfellow, R. J. In *Multinuclear NMR*; Mason, J., Ed.; Plenum: New York, 1987; p 563 (specific on p 567). (d) Kawakami, M.; Enokiya, H.; Okamoto, T. *J. Phys. F: Met. Phys.* **1985**, *15*, 1613. (e) Zangger, K.; Armitage, I. M. *Metal-Based Drugs* **1999**, *6*, 239.

12.   Subject Search Gold Catalysis in title

13.   Wang, W.; Hammond, G.B.; Xu, B. *J. Am. Chem. Soc.*, **2012**, *134*, 5697–5705

14.   (a). Wang, J.Z.; Benitez, D.; Goddard, W.A.; Toste, D.F.; *J. Am. Chem. Soc.*, **2010**, *132*, 13064–13071. (b). Markham, J. P.; Staben, S. T.; Toste, F. D. *J. Am. Chem. Soc.* **2005**, *127*, 9708-9709.

15.   Gorin, D.J.; Sherry, B.D.; Toste, D.F.; *Chem. Rev.,* **2008**, *108,* 3351-3378.

16.   (a). Tarselli, M.A.; Chianese, A.R.; Gagne, M.R.; *Angew. Chem. Int. Ed.*, **2007**, *46*, 6670-6673. (b). *Angew. Chem. Int. Ed.* **2010**, *49*, 1949-1953.

17.   Obradors, C.; Echavarren, A.M.; *Chem. Comm.*, **2014**, *50*, 16-28

18.   Miles, D.H.; Veguillas, M.; Toste, D.F.; *Chem. Sci.*, **2013**, *4*, 3427-3431

19.   Genin, E.; Toullec, P. Y.; Antoniotti, S.; Brancour, C.; Genêt, J.-P.; Michelet, V. *J. Am. Chem. Soc.* **2006**, *128*, 3112.

20.   Dubé, P.; Toste, F. D. *J. Am. Chem. Soc.* **2006**, *128*, 12062.

21.   Amijs, C.H.; Carrillo, V.; Raducan, M.; Galan, P.; Ferrer, C.; Echavarren, A.M. *J. Org. Chem.*, **2008**, *73*, 7721–7730

22.   Markham, J. P.; Staben, S. T.; Toste, F. D. *J. Am. Chem. Soc.* **2005**, *127*, 9708.

23.   Handa, S.; Slaughter, L.M.; *Angew. Chem. Int. Ed.* **2012**, *51*, 2912-2915

24.   Gorin, D,; Sherry, B.; Toste, D.F.; *Chem. Rev.*, **2008**, *108*, 3351-3378

25.   Widenhoefer, R.A. *Chem. Eur. J.*, **2008**, 14: 5382–5391.

26.   Hamilton, G. L.; Kang, E. J.; Mba, M.; Toste, F. D., *Science,***2007,** *317*, 496-499

27.   Minqiang, J.; Bandini, M.; *ACS Catalysis*, **2015**, *5*, 1638-1652

28.   Yang, C.-G.; He, C. *J. Am. Chem. Soc.* **2005**, *127*, 6966.

29.   Hashmi, S.A.K.; *Catalysis Today*, **2007**, *122*, 211-214

30. (a). Shu, C.; Li, L.; Chen, C. B.; Shen, H. C.; Ye, L. W. *Chem. Asian J*. **2014**, *9*, 1525−1529. (b). Hashmi, A. S. K.; Yang, W.; Rominger, F. *Adv. Synth. Catal*. **2012**, *354*, 1273−1279.

31. Sharma, V.; Kumar, P.; Pathak, D.; *J. Heterocyclic Chem.* , **2010**, *47*, 491-502

32. Liu, Z.; Wasmuth, A. S.; Nelson, S. G. *J. Am. Chem. Soc.* **2006**, *128*, 10352.

33. Alazard, j.P.; Boye, O.; Thal, C.; *Bioorg. Med. Chem. Lett.*, **1991**, *1*, 725.

34. Nguyen, R.-V.; Yao, X.; Li, C.-J. *Org. Lett.* **2006**, *8*, 2397.

35. Zhdanko, A., Ströbele, M. and Maier, M. E., *Chem. Eur. J.* **2012**, 18, 14732-14744

36. (a) G. Abbiati, F. Marinelli, E. Rossi and A. Arcadi, *Isr. J. Chem*., **2013**, *53*, 856–868. (b) A. Zhdanko and M. E. Maier, *Angew. Chem., Int. Ed*., **2014**, *53*, 7760–7764. (c) O. S. Morozov, A. V. Lunchev, A. A. Bush, A. A. Tukov, A. F. Asachenko, V. N. Khrustalev, S. S. Zalesskiy, V. P. Ananikov and M. S. Nechaev, *Chem. Eur. J*., **2014**, *20*, 6162–6170. (d) X. Zeng, R. Kinjo, B. Donnadieu and G. Bertrand, *Angew. Chem., Int. Ed*., **2010**, *49*, 942–945.

37. (a) M. Rudolph and A. S. K. Hashmi, *Chem. Soc. Rev*., **2012**, *41*,2448–2462; (b) Z. Li, C. Brouwer and C. He, *Chem. Rev*., **2008**, *108*,3239–3265; (c) E. Jimenez-Nun˜ez and A. M. Echavarren, *Chem. Rev*., **2008**, *108*, 3326–3350. (d). Dorel, R.; Echavarren, A.M.; *Chem. Rev.* **2015**, *115*, 9028-9072

38. For pertinent reviews on asymmetric gold catalysis, see: (a) Pradal, A.; Toullec, P. Y.; Michelet, V. *Synthesis* **2011**, 1501. (b) Shapiro, N. D.; Toste, F. D. *Synlett* **2010**, 675. (c)

Bongers, N.;Krause, N. *Angew. Chem., Int. Ed*. **2008**, *47*, 2178. (d) Widenhoefer, R.A.

Chem. Eur. J. **2008**, *14*, 5382.

39.　　(a). Hamilton, G. L.; Kang, E. J.; Mba, M.; Toste, F. D., *Science,***2007,** *317*, 496-

499; (b). Butler, K.L.; Tragni, M.; Widenhoefer, R.A., *Angew. Chem. Int. Ed.*, **2012**, *51*,

5175-5178.

40.　　Zhang, Z.; Lee, S. D.; Widenhoefer, R. A., *J. Am. Chem. Soc.,***2009,** *131*,

5372-5373.

41.　　(a) Hopkinson, M.N.; Richter, C.; Schedler, M.; Glorius, F. *Nature,* **2014**, *510,*, 485-496

(b). Slaughter, L.M., *ACS Catalysis*, **2012**, 2, 1802-1816.

42.　　(a) Amijs, C. H. M.; López-Carrillo, V.; Raducan, M.; Pérez- Galán, P.; Ferrer, C.;

Echavarren, A. M. *J. Org. Chem.* **2008**, *73*, 7721− 7730. (b) Toullec, P. Y.; Genin, E.;

Leseurre, L.; Genêt, J.-P.; Michelet, V. *Angew. Chem., Int. Ed.* **2006**, *45*, 7427−7430. (c)

Komeyama, K.; Miyagi, M.; Takaki, K. *Heteroat. Chem.* **2008**, *19*, 644−648. (d) de

Frémont, P.; Clavier, H.; Rosa, V.; Avilés, T.; Braunstein, P. *Organometallics* **2011**, *30*,

2241−2251.

43.　　H. Seo, B. P. Roberts, K. A. Abboud, K. M. Merz Jr., S. Hong, *Org. Lett.* **2010**, *12*,

4860–4863.

CHAPTER II

DEVELOPMENT AND REACTIVITY OF STERICALLY HINDERED ACYCLIC

DIAMINOCARBENE GOLD COMPLEXES

2.1 Introduction

Ligands have the ability to tune various properties of transition metals, including their

catalytic activities and selectivities. One key issue left to solve in homogeneous gold catalysis is

the ability to lower catalyst loadings to levels comparable to those attained with palladium or

rhodium catalysts, which in some cases can be as low as ppm catalyst loadings.[1] The prevailing

standard catalyst loading for a gold catalyzed reaction is around five mole percent, which is

acceptable by academic standards but not feasible on an industrial scale. With the ability of

ligands to tune the catalytic reactivity of transition metals, it has recently become more important

not only to find a ligand that works for a particular reaction but to fully understand why that

particular ligand works better than the other ligands that have been tested. This leads us into

rational ligand design. There has been a significant gap in knowledge between the number

publications of the various reactions gold can catalyze[2] and efforts to understand the role of the

ligands. This lack of understanding of the role of the ligand is also one of the reasons for the

slow development of asymmetric gold catalysis. With the number of intricate mechanism

involved in gold catalysis, the lack of understanding of what roles the ligands play in gold

catalysis results in scientist in the field having to run numerous reaction somewhat depending on

luck to achieve desired reactivity or selectivity. Recently, there has been a surge of studies being

undertaken to elucidate the role of the ligands in gold catalysis.[3] Most of these studies focus on

the electronic properties of ligands. This is likely due to the availability of experimental methods

for evaluating electronic factors such as σ-donating ability and π-backbonding capabilities of

various types of ligands.[4] The classic method for measuring σ-donating ability is by the use of the Tolman Electronic Parameter (TEP) **(Figure 2.1)**.[5] The TEP takes advantage of the ease and availability of infrared (IR) spectroscopy. By measuring the A_1 carbonyl stretching frequencies of various ligated nickel tricarbonyl complexes the σ-donating ability of the ligand can be determined. The stronger σ-donor the ligand is the more the metal will π-backbond to the carbonyl ligands resulting in a lower stretching frequency observed by IR. As shown in **Figure 2.1,** there have been a few modifications to the original TEP analysis to circumvent having to use toxic nickel tetracarbonyl.[6]
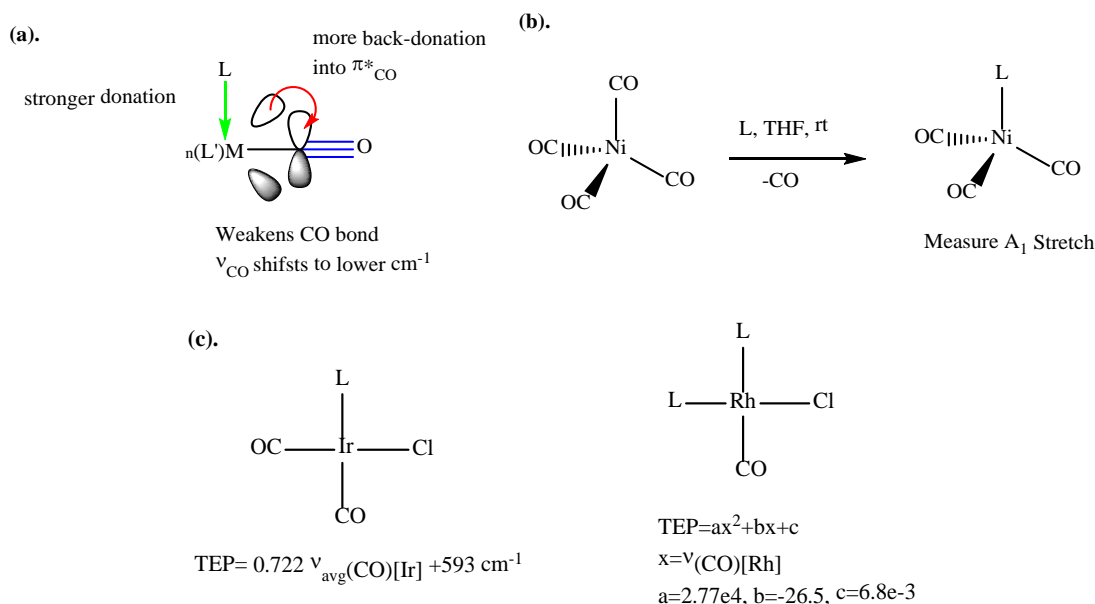
(a). Orbital picture of π-backbonding from filled d-orbitals to empty π* orbital on CO. (b). Original complex used for measuring TEP. (c). More recent version of to measure modified TEP and equations to relate them back to original TEP.

Figure 2.1 Various Methods for Measuring σ-Donating Ability of Ligands

In Tolman's original work, it was stated that the choice of the transition metal carbonyl complex was arbitrary. However, the situation is actually more complicated, as shown by TEP correlations using the iridium Vaska's type complex in **Figure 2.1.c.** The correlation requires a quadratic function to relate the measured stretching frequency back to the original TEP.[7] There are other cases where there is practically no correlation with $LNi(CO)_3$, such as $[LFe(CO)_4]$.[8] There is even some debate as to whether one can correctly compare different types of ligands, e.g. N-heterocyclic carbenes (NHCs) versus phosphines, even using the same method for measuring the TEP values.[9] Due to the issues with TEP, other methods have been developed for measuring σ-donating capabilities of various types of ligands, including the Lever electronic parameter[10], $^{1}J_{Se-P}$ coupling constants in ^{77}Se NMR[11], and computational methods.[12] Some of the computational methods currently being used include charge displacement analysis[12], simply calculating the energy of the HOMO[12], and ETS-NOCV (extended transition state-natural orbitals for chemical valence), with the latter being a method for bond energy analysis. A major benefit of using the ETS-NOCV method is that one can actually dissect the interaction between the metal and the ligand into both σ- and π-bonding components.[13] Experimentally, there are only a few methods for measuring π-acidity of a ligand.[14] One of these methods, developed by Guy Bertrand's group, is to use phosphorus-31 (^{31}P) NMR to measure the chemical shifts of various phosphinidine adducts.[15] Another method is to use ^{77}Se NMR, which has the great benefit that the chemical shift indicates the π-accepting capability of the ligand while the coupling constant indicates the σ-donating capability of the ligand.[16] Based on the seminal work of Fischer and Maasböl,[17] who related the rotation of the heteroatom-carbenic bond to the extent of back-donation, a recent paper on gold acyclic diaminocarbene (ADC) complexes used

exchange spectroscopy (EXSY) NMR to measure the rotational barriers of the ADC ligands and correlated those to π-acidity, which was also analyzed by charge displacement analysis.[18]

Some of the first quantitative evidence for steric effects in reactions between metal carbonyls and other organometallic compounds was published by Basolo and co-workers in 1966.[19] This requires a method to quantitatively describe the steric environment of a metal coordination sphere. This goes back to the seminal work of Tolman defining the ligand cone angle (**Figure 2.2**).[5] The cone angle was originally used to describe the steric encumbrance of a wide range of phosphorus donor ligands, and it providing useful correlations with catalytic activity despite the fact that it was originally measured using simple hand-made molecular models. However, this method has some inherent limitations, which are most apparent with other classes of ligands, such as carbenes, which are not cone shaped like phosphorus ligands.
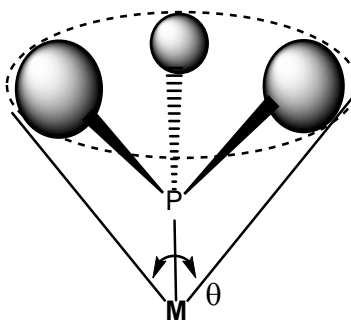
Figure 2.2: Illustration of Tolman Cone Angle

Clavier and Nolan created an alternative steric descriptor that works well for NHC ligands, known as Percent Buried Volume (%V_{bur}).[20] The calculation of this descriptor can be easily done using a web based program called SambVca.[20b] Solid Angle [21] is another steric descriptor that is compatible with all types of ligands but has not yet been widely adopted. Both descriptors are illustrated in **Figure 2.3**. There are numerous other descriptors being developed in attempts

to better describe the steric environment around a metal.[22] One inherent problem with the two methods shown in the figure below is they are usually based upon solid state crystal structure data which, might not accurately reflect what is occurring in solution.
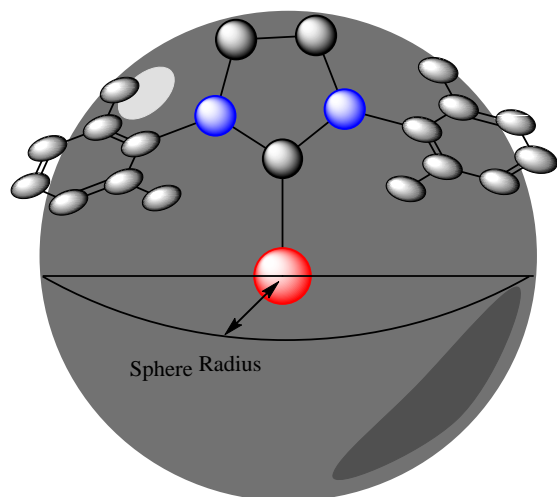
Percent buried volume
$\%V_{bur}$ = percent of the total volume
of a sphere occupied by a ligand.
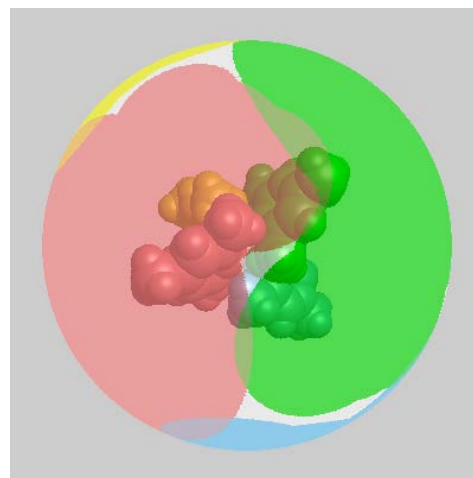
Solid Angle: $G_M(L) = (A/4pr^2) * 100$.
= % of metal coordination
sphere shielded by L

Figure 2.3: Description for $\%V_{bur}$ and Solid Angle G

With the numerous reactions that have are known to be dramatically influenced by choice of ligand in gold catalysis the use of some of the methods described previously in this chapter should be used to properly understand the role of ligand. In particular the remainder of the chapter will discuss the use of some of these methods of quantifying electronic and steric parameters in the context of catalysis by bulky acyclic diaminocarbene gold complexes. The goal of this study was to relate catalytic activities and regioselectivities to these quantifiable parameters for a set of test reactions catalyzed by the bulky gold ADC complexes It was anticipated that this could lead to a better understanding of the factors influencing the catalytic reactions tested and provide a foundation for a more effective rational ligand design.

31

2.2 Results and Discussion

Given the significant attention already devoted to variation of the electronic properties of ligands in gold catalysis,[2-4] it was decided to prepare a series of ligands that could potentially probe steric effects in gold catalysis. As outlined in **Scheme 2.1**, a set of four primary and secondary amines were allowed to react with 2-mesitylphenylisocyanide and 2,6-dimesitylphenylisocyanide gold chloride complexes to synthesize a small library of acyclic diaminocarbene (ADCs) gold complexes **2a-2h** shown in **Table 2.1** in good to moderate yields. Similar biphenyl isocyanides were originally prepared by Nagashima whereas Figueroa used the terphenyl isocyanide to stabilized various low coordinate zero valent metal complexes.[23]

When using unsymmetrical amines, inspection of the ^{1}H NMR (**Figure 2.4**) showed that there were mixtures of conformers.[24] The ratio of the products depended on sterics, with the 2,6-dimesitylphenyl ADCs strongly favoring the amphi conformer. By using a 1D-NOSEY experiment it was shown that the equilibrium was dynamic. Upon saturation of the minor isomer methyl substituent on the nitrogen in **2b** results in a transfer of polarization to the major isomer, indicating that the two are interchanging faster than the NMR time scale (**Figure 2.5**).[25]

(i) Amine (2 equiv), dry CH$_2$Cl$_2$, rt, 2 h, (ii) Acetonitrile, 40 °C 1 h.
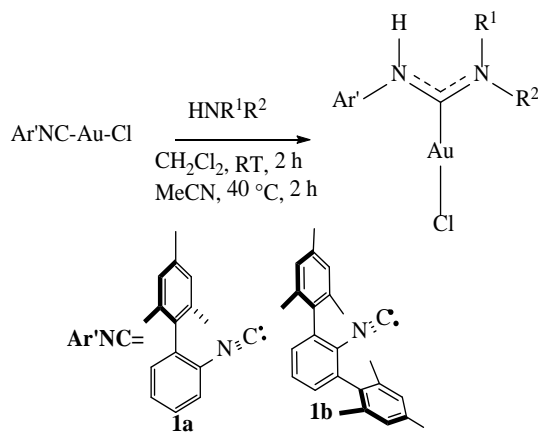
Scheme 2.1 Generic Reaction for ADC Gold Complex Formation

2a 83 % **2b** 86% **2c** 83% **2d** 83%

2e 82% **2f** 85% **2g** 88% **2h** 84%
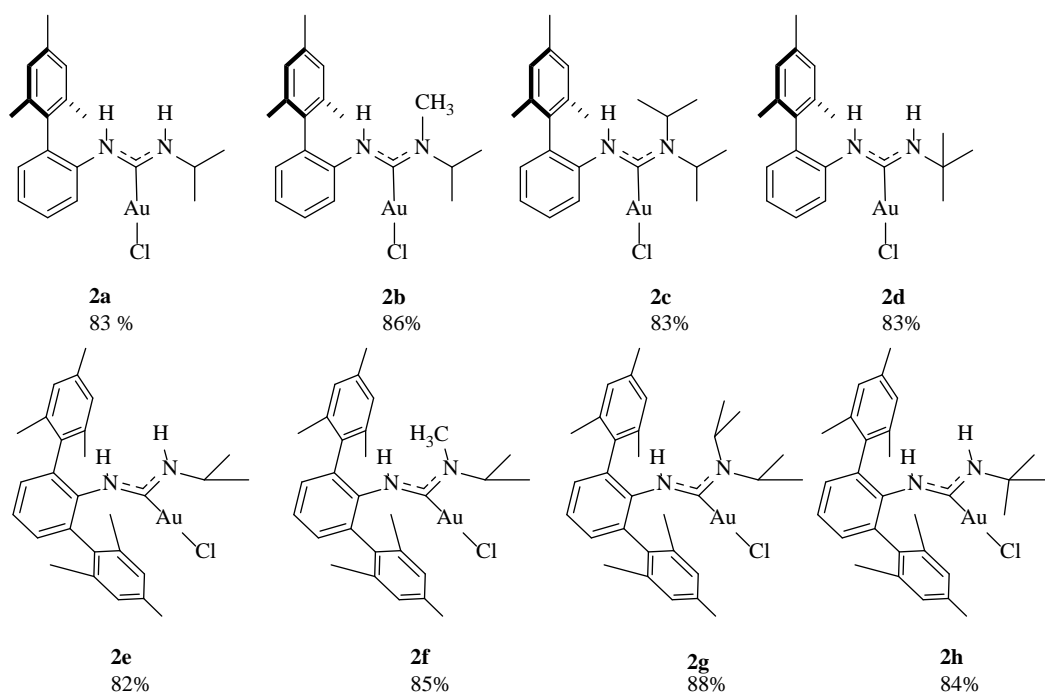
Table 2.1: Results of ADC Gold Complex Syntheses

ADC Au Complex	Major Isomer	Minor Isomer(s)
2a	64	36
2b	95	5
2c	N/A	N/A
2d	57	43
2e	95	5
2f	94	6
2g	N/A	N/A
2h	94	6

Table 2.2: Ratio of Isomers based on ^{1}H NMR
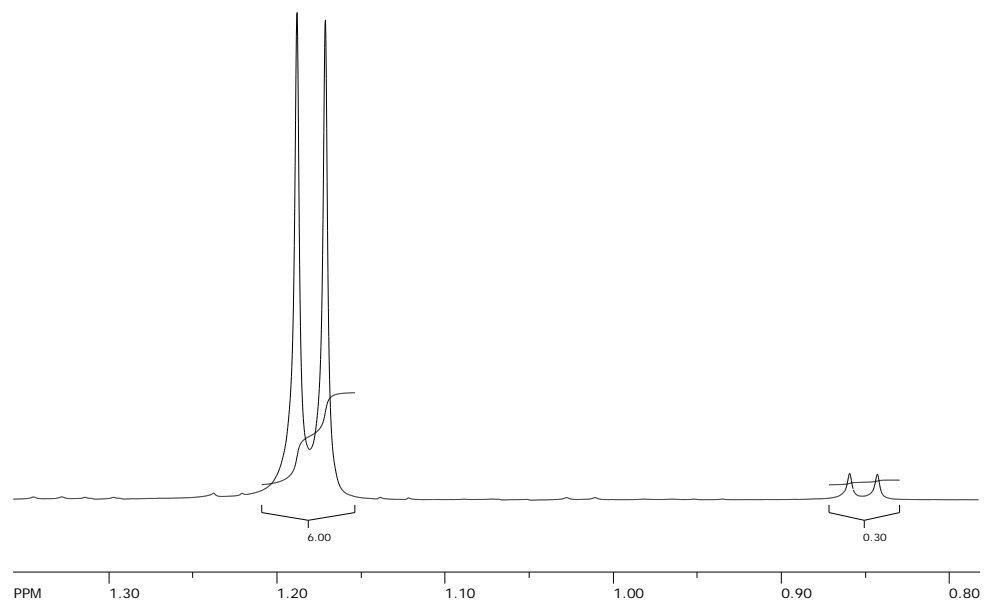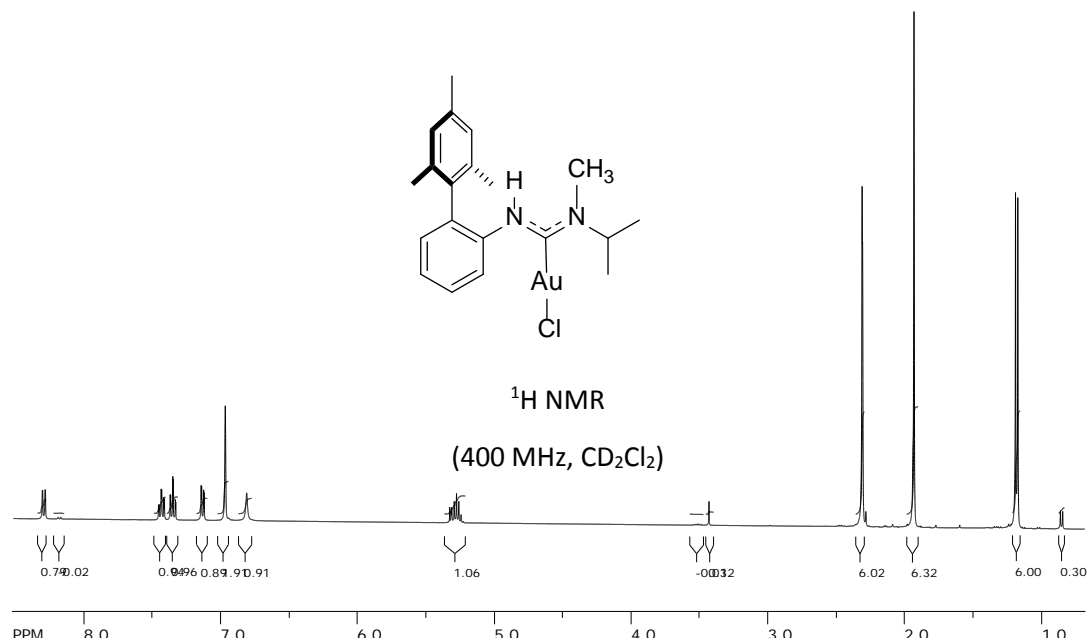
Figure 2.4 ^{1}H NMR of **2b**
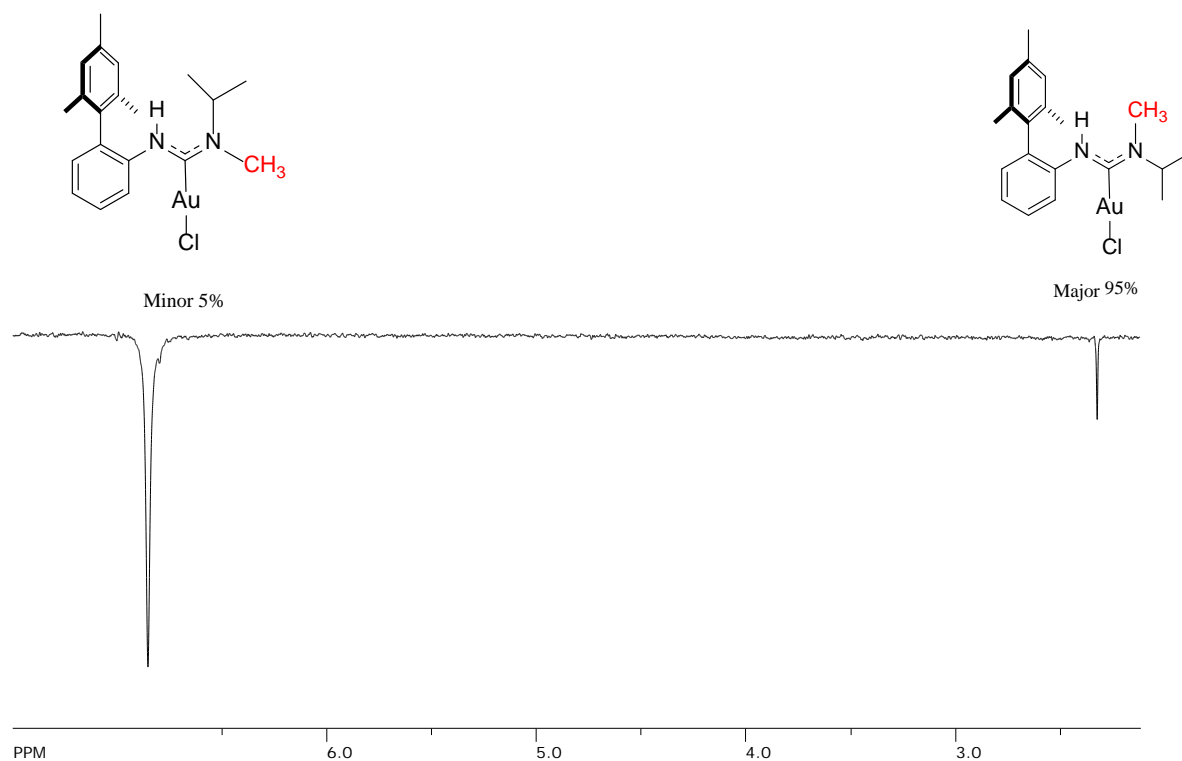
Figure 2.5 1D-NOSEY NMR of **2b** showing exchange of two methyl substituents

X-ray quality crystals were obtained by slow diffusion of pentane into a saturated dichloromethane solution of all of the ADC complexes except **2d** (**Figure 2.6**).The structure of **2d** was obtained via DFT calculations, because X-ray quality crystals were not obtainable. As shown in **Figure 2.6**, the ADC ligand favored amphi conformation with the sterically encumbered groups next to the gold atom.

2a

35
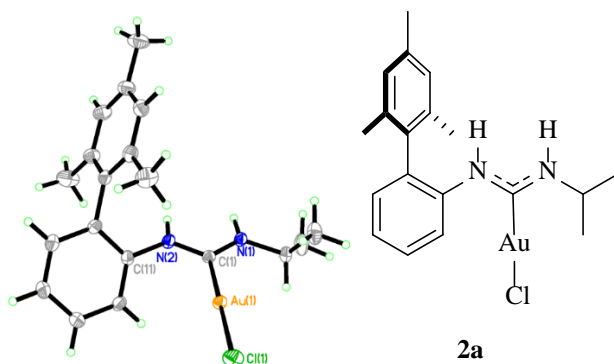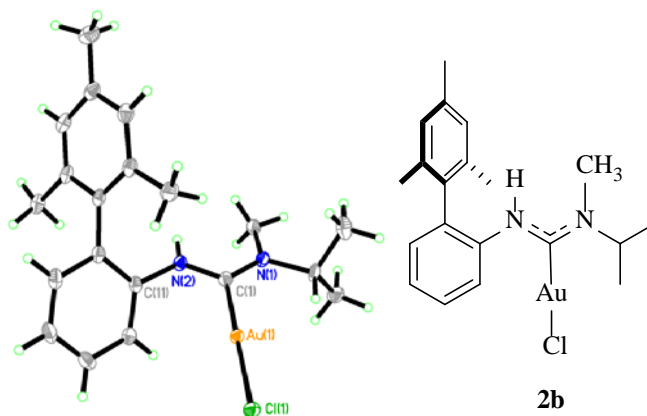
Figure 2.6b: X-ray structure of **2b** with 50% probability ellipsoids
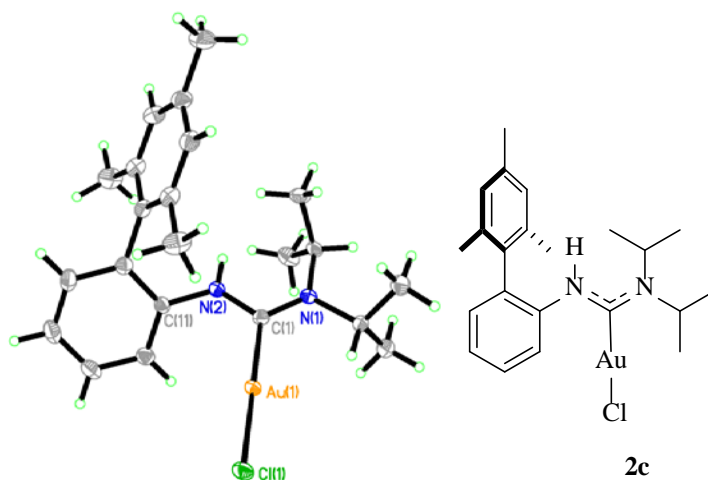
Figure 2.6c: X-ray structure of **2c** with 50% probability ellipsoids
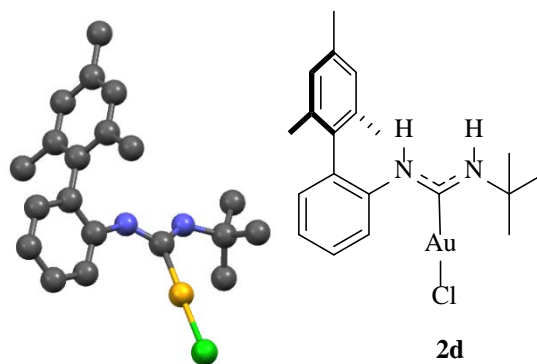
Figure 2.6d: Computed Structure of **2d**. B3LYP/CEP-31g*

2e
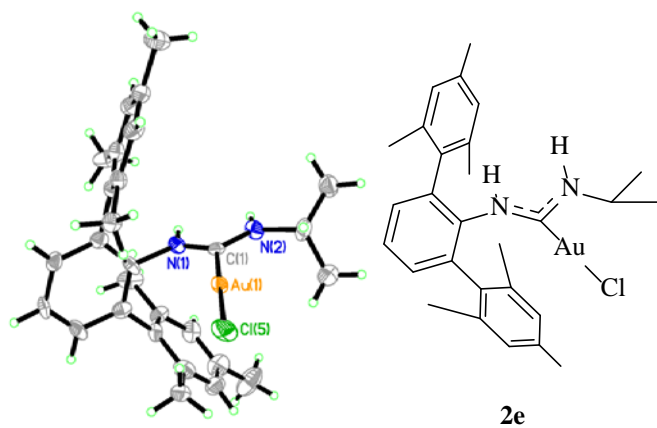
Figure 2.6e: X-ray structure of **2e** with 50% probability ellipsoids

2f
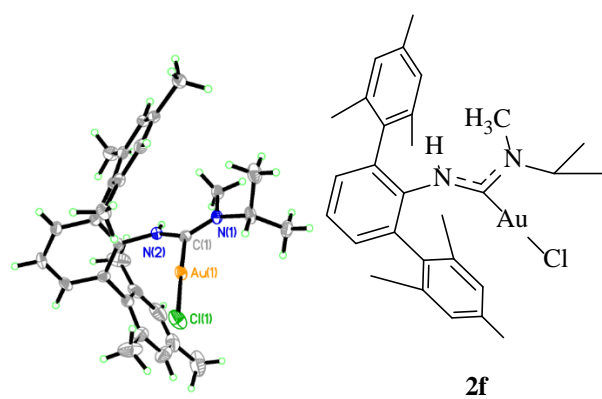
Figure 2.6f: X-ray structure of **2f** with 50% probability ellipsoids

2g

2h
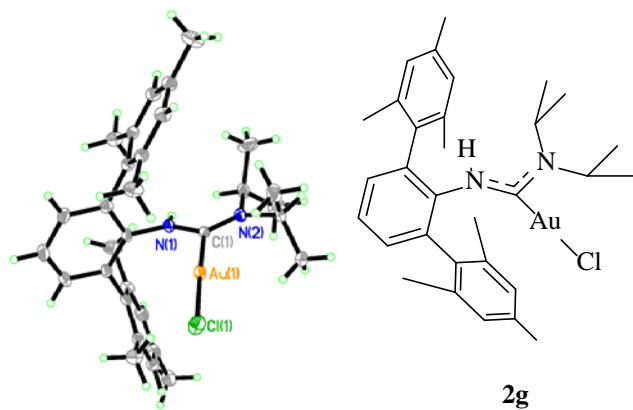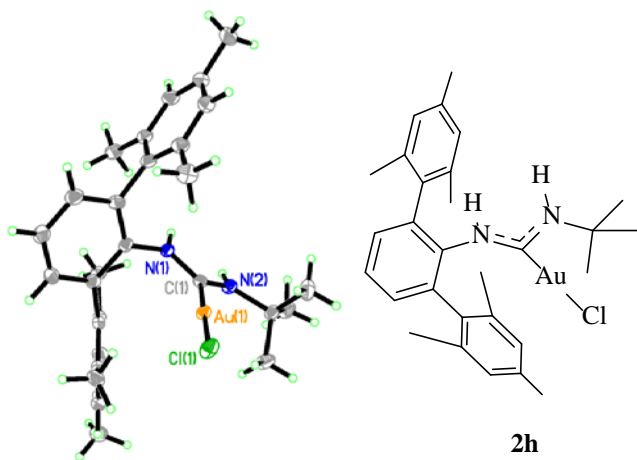
Figure 2.6h: X-ray structure of **2h** with 50% probability ellipsoids

ADC Au Complex	C-Au (Å)	Au-Cl (Å)	N-C-N (°)	C_1-N_1 (Å)	C_1-N_2 (Å)
2a	1.991	2.291	115.7	1.325	1.341
2b	2.006	2.292	117.7	1.334	1.347
2c	2.005	2.291	116.8	1.328	1.349
2d	2.040	2.330	112.2	1.355	1.366
2e	1.979	2.298	114.9	1.326	1.329
2f	1.990	2.287	117.0	1.331	1.341
2g	2.001	2.293	119.2	1.344	1.335
2h	1.984	2.288	115.3	1.329	1.343

Table 2.3 Structural Data for compounds **2a-2h**

Metal-bound NHCs typically have N-C-N bond angles of about 104-107°;[26] however these

ADCs have N-C-N bond angles between 112 and 119° (**Table 2.3**). The wider N-C-N bond

angle has been proposed to have some interesting consequences on selectivity of catalytic

reactions.[26] It was hypothesized that they would result in a more sterically encumbered

coordination sphere. Buried volume calculations and solid angle calculations of complexes **2a-2h**

were done to test this hypothesis. The results are outlined in **Table 2.4**. The advantage of using

the isocyanide route to synthesizing ADCs[27] can be seen in these results. The steric bulk of the

ligand can be easily modified simply by switching the amine. This allows for systematic ligand

variation to obtain the desired catalytic activity and/or selectivity. One notable result is that **2g**

has a calculated buried volume of 52.4%, which is higher than that of the very bulky NHC IPr

which has a corresponding buried volume of 44.5% and is shown in **Figure 2.7**.[28]

ADC Au Complex	% V_{bur}	G
2a	34.3	31.97
2b	37.2	33.41
2c	35.7	32.0
2d	36.5	31.74
2e	46.4	45.22
2f	46.35	45.83
2g	52.4	48.28
2h	48.5	45.93

Table 2.4 % V_{bur} Results
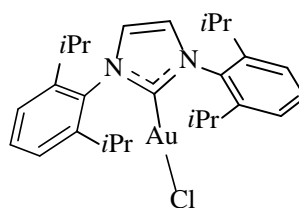
IPrAuCl
% V_{Bur} = 44.5%

Figure 2.7 % V_{bur} Resuts for IPrAuCl

As mentioned previously, it is problematic to measure the donating ability of a ligand on one metal and assumes it has the same properties on a very different metal.[7-9] This is especially true with gold. A recent study has found that although phosphines and NHCs have comparable donor properties when bound with nickel, they actually turn out to be very different on gold. This study actually predicted that phosphines donate more electron density to gold than NHCs, even though the conventional view is that NHCs are stronger donors.[29] One might be tempted to simply create a gold analogue of the Tolman electronic parameter by utilizing gold carbonyl complexes. However, there are only a handful of gold carbonyl compounds[30] known, likely because transition metal carbonyl compounds are only stable when the carbon is bound to a metal that can engage in strong π-backbonding. Another problem with trying to use Au-CO complexes as an IR probe is that typically these are non-classical carbonyl complexes, in that the IR stretching frequency of CO shifts to higher wavenumbers relative to the free ligand.[30] The first classical Au-CO complex has only recently been synthesized.[30e] An alternative IR probe ligand that has been previously used by the Slaughter group is methylisocyanide,[31] which is isoelectronic with CO and binds strongly with gold. One major advantage of this method is that the chloride from the (ADC)AuCl complex can be simply replaced with methyl isocyanide after abstraction with a silver salt (**Scheme 2.2**). This removes the need to synthesize another set of metal complexes and provides the advantage that the electronic propoerties are being measured on the same metal used in the catalytic study. By measuring the difference in the stretching frequency of the methyl isocyanide relative to free methyl isocyanide (2160 cm^{-1}), a descriptor for the σ-donating capabilities of the ADC ligands was obtained.
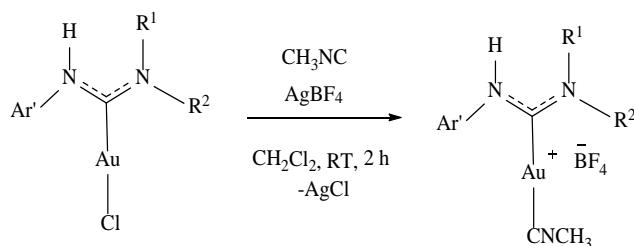
Scheme 2.2 Generic Reaction Scheme for Gold Methyl Isocyanide Complex Formation

ADC Au Complex	% Yield	Δv (cm^{-1})
3a	36	114
3b	32	116
3c	40	118
3d	36	116
3e	42	113
3f	27	114
3g	31	113
3h	24	111

*free methyl MeNC 2160 cm^{-1}

Table 2.5 Results of Methyl Isocyanide Probe Study of Cationic Gold Complex

In a simple bonding depiction, A low Δv indicates a strongly sigma donating ligand, whereas a large Δv indicates a weakly σ-donating ligand. This was originally proposed on the assumption that the amount of π-backbonding to the methyl isocyanide ligand would be negligible, and therefore the only influence on the IR stretching frequency would be the amount of donation from the lone pair on carbon. However, an ETS-NOCV analysis of the bonding in these gold methylisocyanide adducts (**Figure 2.8)** proved this assumption to be incorrect. The π-component

of the bonding interaction between the metal and methylisocyanide actually account for over

30% of the overall orbital interaction. Just as the choice of transition metal when using CO as an

IR probe is not arbitrary, the same problem may exist when using methylisocyanide.

$\sigma_1 = 53.8\%$ $\pi_\perp = 15.4\%$ $\pi_\parallel = 15.4\%$
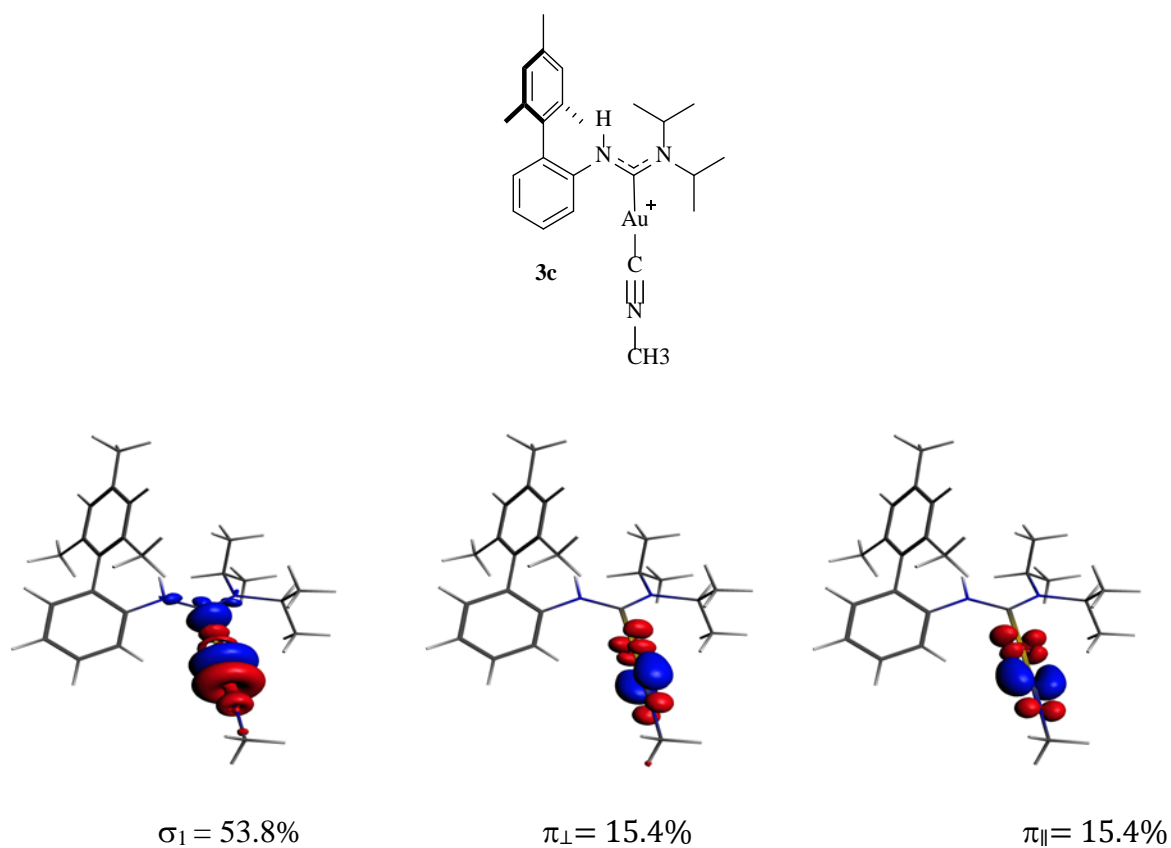
(a). Flow of electrons is from red to blue. (b) $\Delta E_{orbital}$= -70.25 kcal.mol (c). Percentages

calculated by $E_{deformation\ density}/ \Delta E_{orbital}$ x 100

Figure 2.8: ETS-NOCV Deformation Densities of **3c**

There has been a long debate about the actual structure of proposed gold carbenoid

intermediates in many gold catalyzed organic transformations.[32] It is clear that the ancillary

ligand can have a dramatic impact on the outcome of numerous reactions that are catalyzed by

gold, possibly by influencing the nature of such intermediates.[33] With descriptors in hand for

both the steric properties and electronic properties of the ligands, we chose to examine two gold-catalyzed organic transformations in which there would likely be strong effects on catalytic selectivity resulting from the ligand structure. The first reaction examined was the 1,6-enyne cyclization-hydroarylation domino reaction **(Scheme 2.3)**.[34] This reaction has been studied by many groups, and the product ratio has been shown very recently by Bielawski's group, using NHC gold complexes, to be strongly dependent on the σ-donating capabilities of the NHCs.[35] As shown in **Table 2.6**, ADC gold complexes **2b** and **2c** provide significant selectivity preferentially favoring the bicyclic product **10**. Whereas the other complexes gave almost no selectivity.
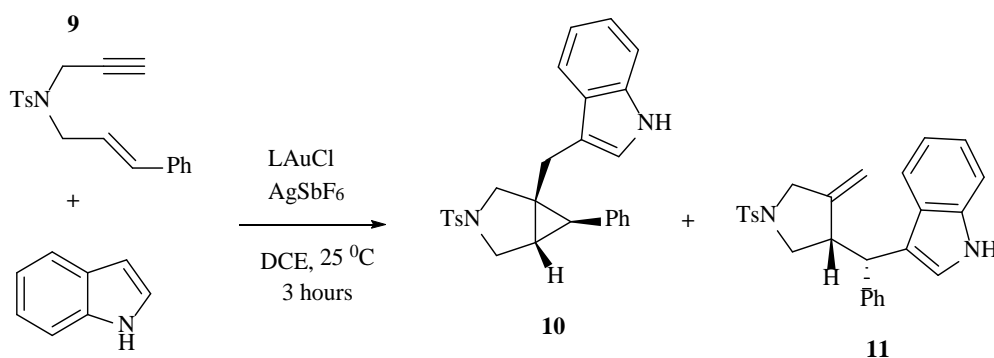
(a). 1equiv **9**, 1.15 equiv indole 5 mol% [Au], 5 mol% AgOTf, 0.15 M DCE (dry), N_2

Scheme 2.3: Tandem Gold Catalyzed Enyne-Cyclization/ Hydroarylation Reaction

ADC Au Complex	% Yield*	10:11 Ratio
2a	46	64:36
2b	75	75:25
2c	88	75:25
2d	64	65:35
2e	63	62:38

2f	86	52:48
2g	89	52:48
2h	76	56:44

* Isolated Yields

Table 2.6 Tandem Enyne Cyclization-Hydroarylation Results

The use of the Δν parameter from the methylisocyanide adducts proves not to be as useful as expected after considering the bonding analysis described above and the catalytic results. The strongest donating ADC according to the Δν parameter does not give the best selectivity. Hong's group studied this reaction with very bulky gold ADC complexes proposed that the observed reversal of product selectivity was potentially due to these ADCs being more π-accepting due to their distorted-N-C-N dihedral angles (**Figure 2.9**). [36] Guy Bertrand's group also found acyclic diaminocarbenes to be more π-accepting when compared to NHCs using carbene-phosphinidine adducts.[15]

%V_{bur} 45.7
Dev. From Planarity 41^0
10:11 ratio = 18:82

distorted dihedral results in less overlap

Therefore Allowing More π-backbonding from Au
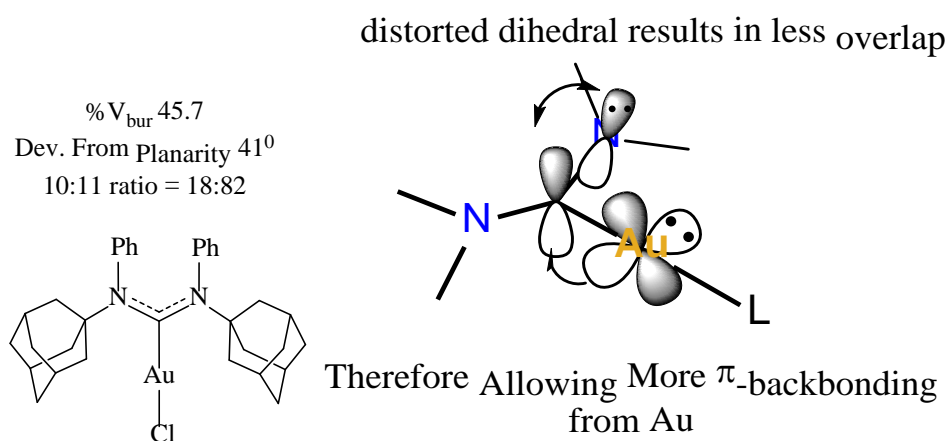
Figure 2.9: Hong's Bulky ADC and Illustration of Au π-backdonation

The argument for the distorted dihedral appears potentially valid if one considers how

distorting the planarity of the carbene disrupts the overlap of the π-orbitals on the nitrogen atom,

which should make the empty π-orbital on carbon more susceptible to back-donation from gold.

Something comparable can also be seen for Alder's tetraisopropyl carbene in that one of the

nitrogen atoms is pyramidalized, which prevents the lone pair from interacting with the vacant

orbital on carbon.[37] This causes Alder's carbene to be more π-acidic. An ETS-NOCV analysis

was performed on a simplified system to see if distorting the dihedral does make a carbene more

π-acidic and it seems to suggest that Hong's prediction was correct. **(Figure 2.10)**

Dihedral Angle 0°
$\pi_\perp$ = 14.7%
$\Delta E_{orbital}$ = -72.31 kcal.mol

Dihedral Angle 45°
$\pi_\perp$ = 17.2%
$\Delta E_{orbital}$ = -74.84 kcal.mol

(a). Flow of electrons is from red to blue. (b) Percentages = $E_{deformation\ density}$/ $\Delta E_{orbital}$ x 100
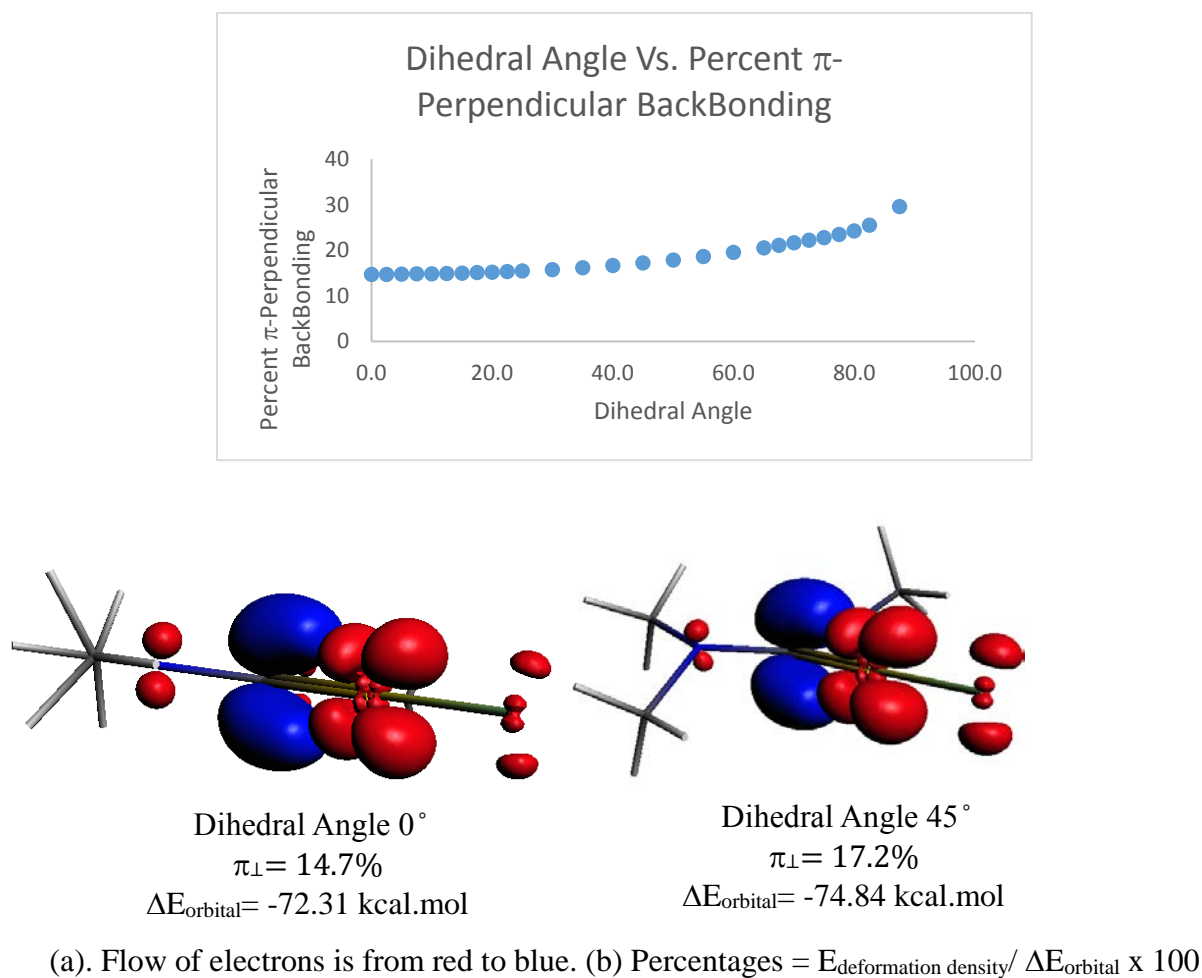
Figure 2.10: Extent of π-Backbonding vs Dihedral Angle of Carbene

If one compares the deviation from planarity (180-dihedral angle) of this series **(Table 2.7)** of ADCs to the product selectivity, there is a weak correlation (**Figure 2.11**), supporting the hypothesis that ADCs with a distorted dihedral angle are potentially more π-accepting and tend to disfavor the bicyclic product. The ADCs with less undistorted dihedral angles (**2b/2c**) behave like standard strongly σ-donating carbene ligands, favoring the bicyclic product **10**.

Table 2.7 Mesityl ADC Deviation From Planarity

ADC Au Complex	Deviation from Planarity* (degrees)
2a	6
2b	3.7
2c	3.3
2d	0.6
2e	2.8
2f	15.9
2g	13.5
2h	13.2

Deviation From Planarity= 180-Average Dihedral Angle
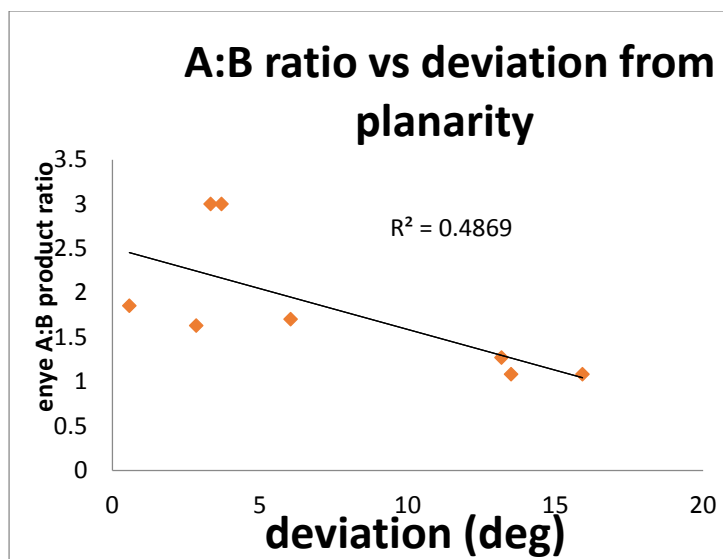
Figure 2.11 Enyne Cyclization Product Selectivity vs. Deviation from Planarity

The second reaction studied was a gold-catalyzed Nazarov cyclization.[38] A classic Nazarov cyclization is a Lewis or Bronsted acid catalyzed 4π electrocyclic ring closure of a divinyl ketone to a 2-cyclopentenone. The resulting products are common structural motifs in biologically active compounds.[39] One key problem left to solve is control over the termination step to localize the double bond in the final product. This is typically done through substrate engineering.[39] The substrate used in this study is one such substrate that was engineered by Frontiers group in which the intermediate after cyclization is polarized resulting in localization of the double bond on one side of the five membered ring. Although our group has previously achieved some selectivity in the palladium catalyzed Nazarov cyclization with a limited set of substrates,[40] examination of one substrate with bulky Au-ADC catalysts **2a-2h** revealed another example of gold outperforming palladium **(Scheme 2.4)**. It is important to note that this reaction appears to have no selectivity when catalyzed by simple Lewis acids, such as $Cu(OTf)_2$,.[41] As a comparison, a gold catalysts containing a standard NHC ligand (IMes) was also examined. The reaction

selectivities, i.e. the ratios of the endo:exo product for the Nazarov reaction, are presented in

Table 2.8.
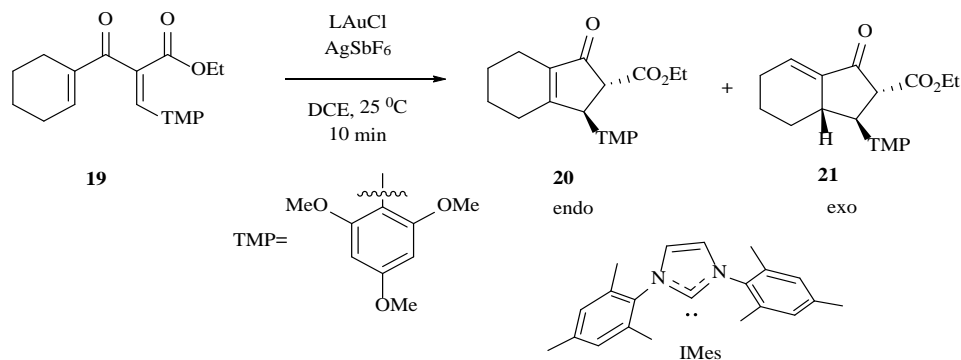
(a). 1 equiv **19**, 5 mol% [Au], 5 mol% AgOTf, 0.15M DCE (dry), N_2

Scheme 2.4: Gold Catalyzed Nazarov Cyclization

Table 2.8 Au Catalyzed Nazarov Endo:Exo Product Selectivities

ADC Au Complex	% Yield*	**20:21** ratio
2a	78	3.47:1
2b	74	2.58:1
2c	76	3.39:1
2d	64	3.23:1
2e	66	1.83:1
2f	76	1.21:1
2g	78	1.56:1
2h	60	1.85:1
IMes	60	4:1
AgCl	0	N/A

*Isolated Yields

There seems to be very poor correlation between σ-donating capacity of the ADC as measured by Δv parameter and the endo:exo selectivity (**Figure 2.12**). However, there does seem to be a meaningful correlation between the steric encumbrance of the ADCs, as measured by buried volume or solid angle, and the endo:exo selectivity (**Figure 2.13**). It appears that less sterically hindered ligands tend to favor the endo product. There are other reports of gold-catalyzed reactions in which the regioselectivity appears to be affected by sterics.[42] However, these other reports only provide speculations about what part of the mechanism is actually affected by sterics, thus leading to the observed regioselectivities. Most Lewis acids activate the carbonyl for cyclization but the low oxophilicity and high carbophilicity[2d] of gold suggest that activation of one of the alkenes is a possible alternative mechanism. Although this is probably unlikely due to some speculation of whether or not trace acids are catalyzing many of the "gold" catalyzed alkene transformations.[43] The relative stereochemistry observed in the product is yet another reason to disfavor a gold activated alkene pathway. The cis relationship observed in the exo product between the H_A and the TMP substituent is what one would expect if the reaction followed the Woodward-Hoffman rules.[44] A gold activated alkene process could potentially result in a mixture of cis and trans.
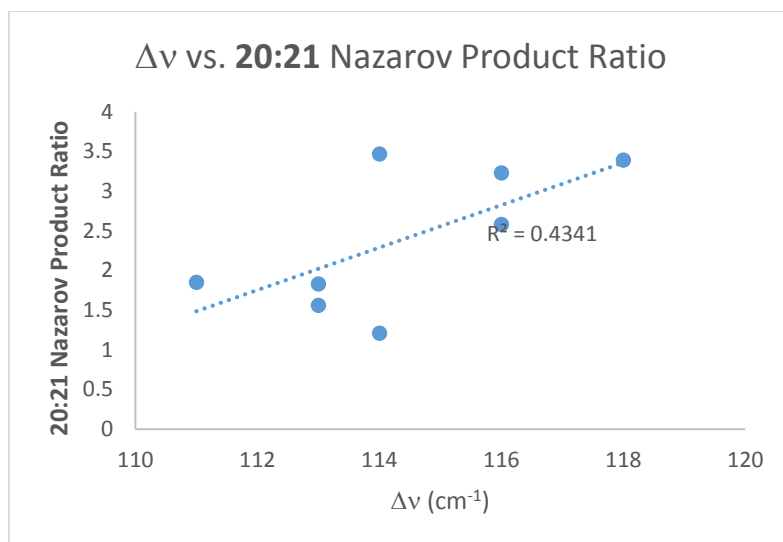
Figure 2.12: Correlation of Δν with endo:exo Selectivities in the Nazarov Cyclization.
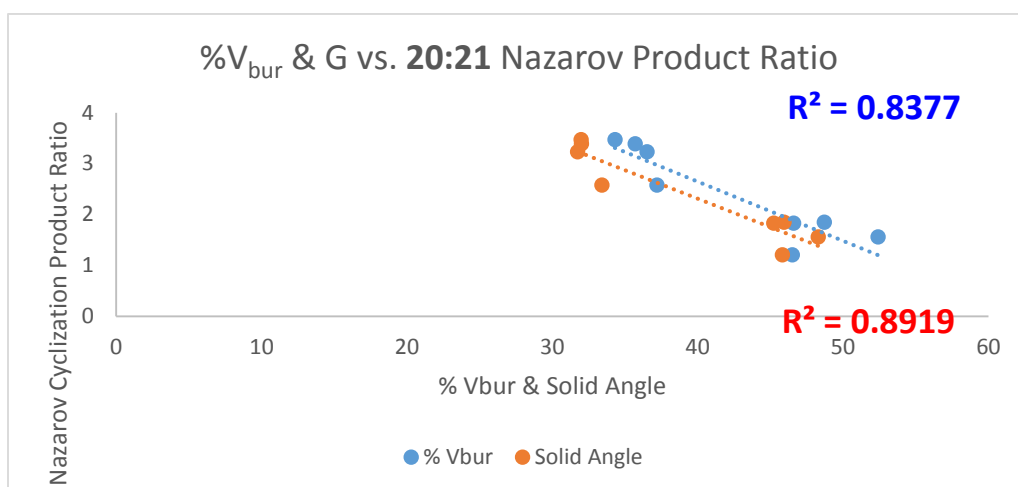
Figure 2.13: Correlation of %V_{bur} or G with endo:exo Selectivities in the Nazarov Cyclization.

A plausible mechanism for a gold catalyzed Nazarov cyclization is outlined **Figure 2.14.** Coordination of the alkene to gold **1** is likely in equilibrium with the oxygen bound substrate **1'** which allows for a prototypical Lewis acid activation of the substrate. The resulting carbocationic intermediate is also likely an equilibrium between an O-bound gold enolate **2** and a C-bound gold enolate **2'**. The C-bound enolate **2'** is proposed to be more favorable due to gold's

carbophilicity and low oxophilicity. A relevant example is the LAu(acac) complex shown in **Figure 2.15** in which the C-bound complex is formed with no observable amounts of the O-bound.[45] An argument could be made that the carbocation is more stabilized in the O-bound complex **2** however these substrates were engineered by Frontier and coworkers to polarize this intermediate to the carbocation being located as pictured.[38] In the C-bound gold enolate **2'** the ligand is in a position to sterically hinder the deprotonation of H_a which would result in the formation of **3** which after protodeauration would form the endo product **20**. The fact the C-bound enolate puts the ligand in proximity of H_a explains why larger ligands (**2f** $\%V_{bur}$ 47%) start to disfavor deprotnation of H_a (**20:21** 1.56:1). If the ligand is less sterically encumbering (**2b** $\%V_{bur}$ 35%) then the ligand could potentially be acting as a directing group for the base to selectively deprotonate H_a. With an N-H moiety on the ADC ligand it could potentially hydrogen bond with the counterion x^- or even with another molecule of the substrate that could be doing the deprotonation. It has been shown that the location of the counterion has had effects on catalysitc activity and selectivity in gold catalysis.[46] It was also shown in that paper that for NHCs the counterion is generally located near the ligand which supports where the counterion might be located with ADCs.
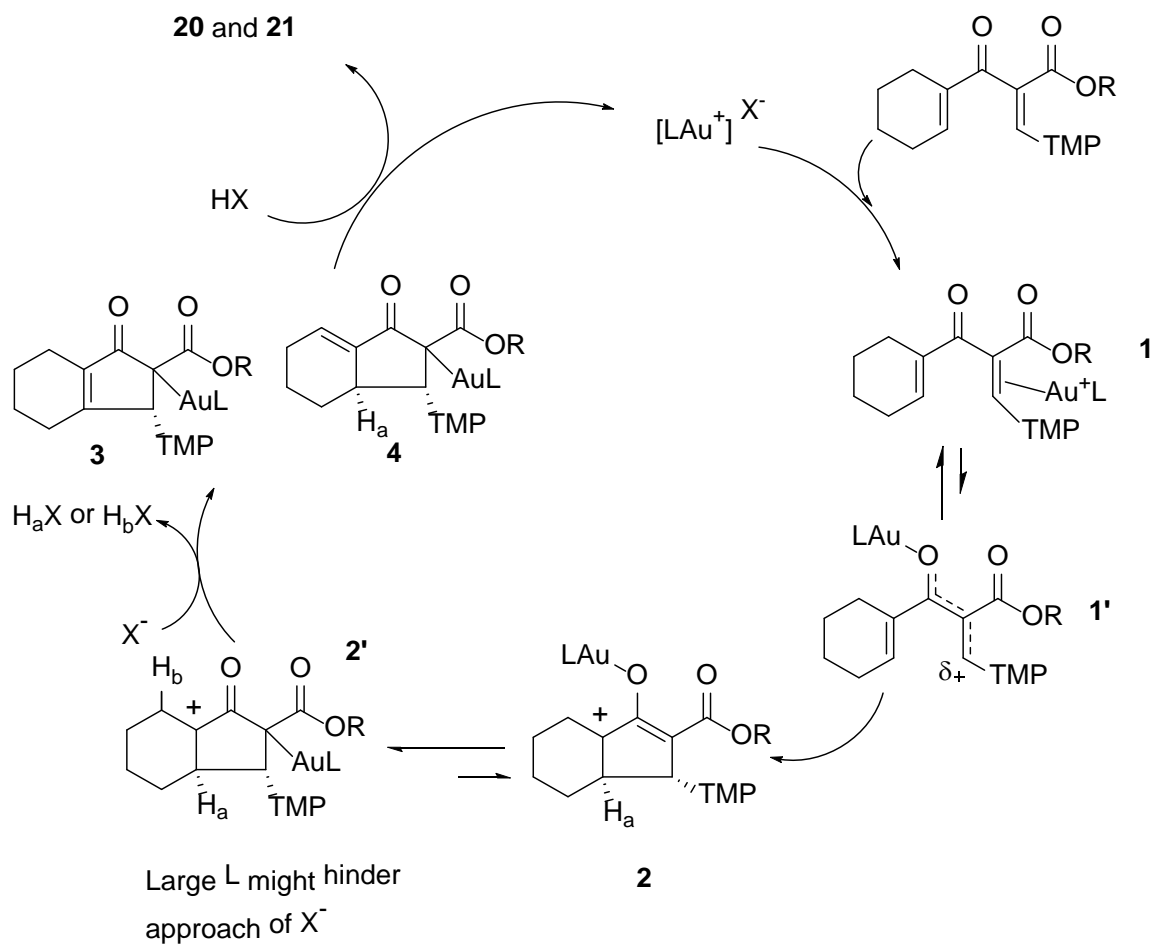
Figure 2.14 Proposed Gold Catalyzed Nazarov Cyclization Mechanism
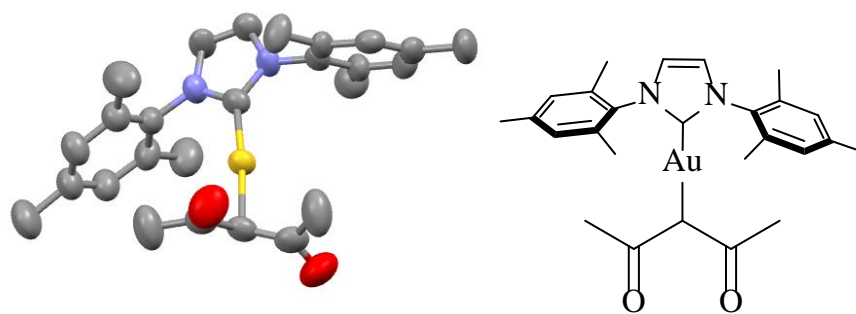
Figure 2.15 (NHC)Au(acac) X-ray Structure[45]

2.3 Conclusions

Gold ADC complexes were shown as a viable substitute for the more well-known NHC complexes in two gold catalyzed transformations. Larger N-C-N bond angles offers a highly sterically encumbered environment around the metal, notably in catalyst **2g**, which has one of the highest buried volumes reported for any carbene ligand 52.4%. It was also shown that using the metal-templated isocyanide-based synthetic route provided the ability to easily tune the steric properties, and to some extent the electronic properties of the ancillary ligands. This was shown to have important implications for two gold catalyzed organic transformations. The results were in agreement with previous studies of gold catalyzed 1,6-enyne cyclization/hydroarylation reactions in that the product ratio appeared to be controlled primarily by ligand electronic properties.[35] Although typically regarded as strongly σ-donating ligands, there are indications that the π-accepting capabilities of ADCs may need to be considered if the C-N-C-N dihedral angles of the carbenes are distorted. The first systematic study of ligand effects in a Nazarov cyclization was undertaken and ADC gold complexes are introduced as a new class of catalyst for this reaction. The data suggest that the termination step of the Nazarov cyclization is significantly influenced by ligand steric properties, and the resulting selectivities can be rationalized by a newly proposed mechanism. The ligand could potentially be acting as a directing group promoting the endo product. However, large groups might actually block the endo position so that the elimination giving the exo product starts to become competitive. This could potentially eliminate the need for substrate engineering to localize the double bond. This study provides a pathway to understanding the underlying mechanisms leading to product selectivity in the Nazarov cyclization and could provide a starting point for additional rational ligand design leading to even better selectivities.

2.4 Experimental Section

General Information:

All air-sensitive synthesis steps were performed under Argon atmosphere using Vacuum line or under Nitrogen atmosphere using glovebox unless otherwise noted. All solvent for reactions were dried before use. (Tetrahydrofuran, toluene and 1, 4-Dioxane were dried over and stored on sodium with benzophenone under vacuum. Dichloromethane were washed with concentrated Sulfuric acid, deionized water, saturated Sodium bicarbonate and deionized water, then pre-dried over anhydrous Calcium chloride, followed by refluxed and distilled from phosphorus pentoxide under nitrogen, stored over phosphorus pentoxide under vacuum.). Palladium Tetrakis was bought from Chem-Impex Interantional and used as such. All other reagents were used directly from the vendors. The reported chemical shifts in NMR spectra were referenced to residual solvent peaks.[47] (CDCl$_3$, ^{1}HNMR: 7.26 ppm, ^{13}CNMR: 77.18 ppm; CD$_2$Cl$_2$, ^{1}HNMR: 5.32 ppm, ^{13}CNMR: 53.84 ppm) CD$_2$Cl$_2$ was dried over and stored on activated 4 Å molecular sieves under vacuum. (THT)AuCl[48], 2,6-dimesitylphenyl isocyanide[49], methyl isocyanide[50], Nazarov substrate **19** were synthesized according to literature procedures. [53] IR spectra were performed from Nujol mulls on a Nicolet Protégé 460 FT-IR spectrometer. ^{1}H and ^{13}C NMR were taken on Varian GEMINI 2000 (300 MHZ) and Varian Unity INOVA (400 and 600 MHz) spectrometers. Elemental analyses were performed by Midwest Microlab, Indiana.
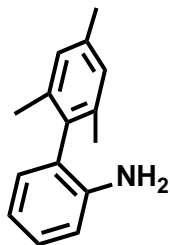
Synthesis of 2-mesitylaniline: [51]

^{1}H NMR data matches literature values [52].
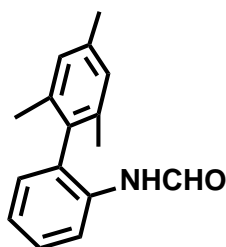
Synthesis of N-(2',4',6'-trimethyl-[1,1'-biphenyl]-2-yl)formamide: [51]

To a stirred solution of 2',4',6'-trimethyl-[1,1'-biphenyl]-2-amine (4.74mmol) in 100 mL of benzene hooked up to a Dean stark apparatus was added formic acid(71.03mmol) and the reaction mixture was refluxed for 8 hours with periodically removal of water from the Dean Stark apparatus. Upon completion the reaction is added to water and extracted into EtOAc, then washed with NaHCO$_3$. Organic layer is dried over Na$_2$SO$_4$ followed by removal of EtOAc under reduced pressure. The resulting product is purified by flash chromatography on silica (5:1 Hexane:EtOAc). White solid, yield 1.02 g (90%) ^{1}H NMR mixture of rotamers (600 MHz, CDCl$_3$): δ= 8.74 (d, J= 11.5 Hz, 1H), 8.48 (d, J=7.8 Hz, 1H), 8.20 (s, 1H), 8.19 (s, 1H), 7.39 (q, J= 7.8 Hz, 2H), 7.33 (d, J=7.8 Hz, 1H), 7.24 (t, J=7.8 Hz, 1H, 7.19 (t, J=7.8 Hz, 1H), 7.13 (d, J=7.8 Hz, 1H), 7.07 (d, J=7.8 Hz, 1H), 7.00 (s, 2H) 6.97 (s, 2H), 6.94 (bs, 1H, NH), 6.81 (bs, 1H, NH), 2.35 (s, 3H), 2.33 (s, 3H), 1.96 (s, 6H), 1.93 (s, 6H). ^{13}C NMR (150 MHz, CDCl$_3$): δ=

161.4, 158.9, 138.3, 138.2, 137.1, 136.6, 134.7, 133.0, 132.6, 131.0, 130.9, 129.8, 129.7, 129.0, 128.9, 128.6, 128.4, 125.2, 124.7, 120.7, 116.4, 21.2, 21.1, 20.2. IR (Nujol): 3268 cm^{-1}, 1693 cm^{-1} 1661 cm^{-1}. Anal. Calcd. For $C_{16}H_{17}NO$: C, 80.30; H, 7.16; N, 5.85%. Found: C, 80.38; H, 7.21; N, 5.90%.
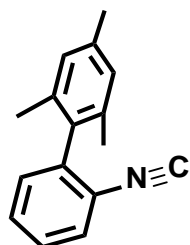
Synthesis of 2-mesitylphenylisocyanide: [51]

To a stirred solution of N-(2',4',6'-trimethyl-[1,1'-biphenyl]-2-yl)Formamide (4.19mmol) and triethylamine (20.94mmol) in CH_2Cl_2 (50mL) at 0 ^{0}C under nitrogen is added freshly distilled $POCl_3$ (8.37mmol) the reaction mixture is then stirred and monitored by TLC until complete. Upon completion the reaction mixture is washed with water (100mL X 3) followed by saturated $NaHCO_3$ solution, then brine, then dried over Na_2SO_4. The CH_2Cl_2 is removed under reduced pressure and the product is purified by flash chromatography on silica (4:1 Hexane:CH_2Cl_2). White solid, yield 852mg (92 %). ^{1}H NMR (400MHz, CD_2Cl_2): δ = 7.51-7.46 (m, 2H), 7.41 (dt, J=7.6 Hz, 1.6Hz, 1H), 7.23 (dd, J=7.6Hz, 1.6Hz, 1H) 6.99 (s, 2H), 2.34 (s, 3H) 1.97(s, 6H). ^{13}C NMR (101 MHz, CD_2Cl_2): δ = 165.9, 139.1, 138.2, 136.1, 134.2, 131.2, 129.9, 128.6, 128.4, 127.3, 126.4, 21.2, 20.2. IR (nujol): 2118 cm^{-1} Anal. Calcd. For $C_{16}H_{15}N$: C, 86.84; H, 6.83; N, 6.20%. Found: C, 87.02; H, 6.83; N, 6.20%.
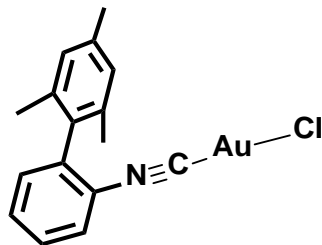
Synthesis of 2-mesitylphenylisocyanide Gold Chloride:

2-mesitylphenylisocyanide (0.90mmol) and tetrahydrothiophene gold chloride (0.86mmol) were dissolved in dry CH_2Cl_2 and allowed to stir for 12 hours at room temperature under nitrogen. The solvent was removed under reduced pressure and the resulting product was washed with Et_2O and purified by recrystalization in CH_2Cl_2/pentane. White crystalline solid, yield 354mg (91%).

^{1}H NMR (400 MHz, CD_2Cl_2): δ = 7.68-7.64 (m, 2H), 7.53-7.49 (m, 1H), 7.35-7.33 (m, 1H), 7.01 (d, J=0.80Hz, 2H), 2.35 (s, 3H) 1.96 (s, 6H). ^{13}C NMR (151MHZ, CD_2Cl_2): δ = 142.3, 140.5, 139.0, 135.8, 132.6, 132.2, 131.8, 129.0, 128.9, 127.7, 124.3, 21.2, 20.2. IR (Nujol) 2234.8 cm^{-1}. Anal. Calcd. For $C_{16}H_{15}NAuCl$: C, 42.36; H, 3.33; N, 3.09%. Found: C, 42.65; H, 3.46; N, 3.09%.

General Procedure for Synthesis of N-2-mesitylphenyl-N',N'-diaminocarbene gold chloride:

Various primary and secondary alkyl amines (2 equiv) were dissolved in 4mL of dry CH_2Cl_2 and added to a solution of 2-mesitylphenylisocyanide Gold Chloride (0.22mmol) in dry CH_2Cl_2 (10mL/mmol of 1) via syringe pump at a rate of 2mL/hour. After addition was complete, the reaction mixture was allowed to stir an additional hour at room temperature, after which the solvent was evaporated under reduced pressure. Dry acetonitrile (10mL/mmol of 1) was then added along with one more equivalent of amine, and the reaction mixture was heated at 40 °C for one hour. The solvent was then evaporated under reduced pressure, and the crude product was washed with pentane (3 x 10mL). The resulting product was purified by recrystallization from

CH₂Cl₂/pentane to give the pure product. Compounds were characterized by ^{1}H NMR, ^{13}C NMR, and elemental analysis.
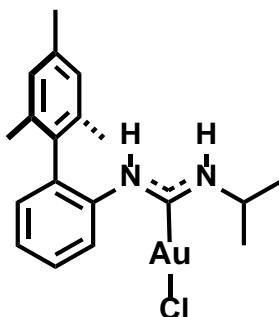
N-2-Mesitylphenyl-N'-isopropyldiaminocarbene gold chloride (2a)

White solid, yield 94mg (83%). Mixture of two isomers: major 64%, minor 36% by ^{1}H NMR. ^{1}H NMR (400 MHz, CD₂Cl₂): δ = 8.39 (d, J=8 Hz, 1H, major), 8.19 (bs, 1H, minor), 7.47-7.42 (m, 3H, major & minor), 7.39-7.35 (m, 4H, major & minor), 7.29 (bs, 2H, major & minor), 7.17-7.14 (m, 2H, (major & minor), 7.00 (s, 2H, minor), 6.97 (s, 2H, major), 6.60 (bs, 2H, major), 4.45-4.40 (m, 1H, major), 3.15 (septet, J=7Hz, 1H, minor), 2.32 (s, 3H, major), 2.30 (s, 3H, minor) 1.95 (s, 6H, minor), 1.92 (s, 6H, major), 1.22 (d, J=4Hz, 3H, major), 0.90 (d, J=4Hz, 3H, minor). ^{13}C NMR (101 MHz, CD₂Cl₂): δ = 186.3, 138.8, 138.3, 137.5, 136.7, 133.7, 133.2, 130.3, 129.1, 129.0, 128.5, 127.2, 125.7, 122.3, 53.4, 45.2, 23.2, 21.5, 21.2, 21.1, 20.6, 20.5. Anal. Calcd. for C₁₉H₂₄N₂AuCl: C, 44.50; H, 4.72; N, 5.46 %. Found: C, 44.39; H, 4.67; N, 5.36 %.
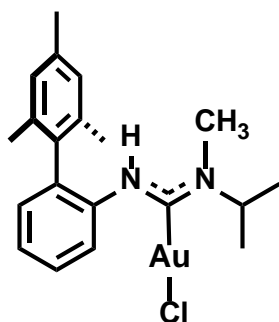
N-2-mesitylphenyl-N',N'-isopropylmethyldiaminocarbene gold chloride (2b)

White solid, yield 100mg (86%). Mixture of two isomers: major 93%, minor 7% by ^{1}H NMR. ^{1}H NMR (400 MHz, CD$_2$Cl$_2$): δ = 8.36-8.34 (m, 1H, major), 7.49-7.45 (m, 2H, major & minor), 7.40-7.36 (m, 2H, major & minor), 7.18 (dd, J=4Hz, 2H, major & minor), 7.00 (s, 4H, major & minor), 6.85 (bs, 2H, major & minor), 5.30 (m, 1H, major), 3.46 (s, 3H, minor), 2.33 (s, 6H, major), 2.31 (s, 3H, minor), 1.97 (s, 6H, minor), 1.96 (s, 6H, major), 1.22 (d, J=8Hz, 6H, major), 0.90 (d, J=8Hz, 6H, minor). ^{13}C NMR (101 MHZ, CD$_2$Cl$_2$): δ = 189.0, 138.6, 138.1, 136.7, 136.6, 134.0, 133.4, 130.3, 130.1, 129.0, 128.3, 128.2, 127.0, 123.6, 123.5, 61.7, 48.7, 40.6, 27.6, 21.2, 21.1, 20.6, 20.5, 20.3, 19.1. Anal. Calcd. for C$_{20}$H$_{26}$N$_2$AuCl: C, 45.57; H, 4.98; N, 5.32 %. Found: C, 45.43; H, 4.88; N, 5.23 %.
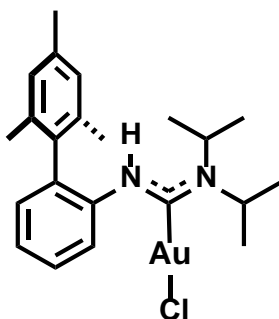
N-2-mesitylphenyl-N',N'-diisopropyldiaminocarbene gold chloride (2c)

White solid, 102mg (83%). ^{1}H NMR (400 MHZ, CD$_2$Cl$_2$): δ= 8.29 (d, J=8Hz, 1H), 7.46 (m, 1H), 7.37 (m,1H), 7.11 (m, 2H), 6.97 (s, 2H), 5.38 (bs, 1H), 3.66 (septet, J=7.2Hz, 2H), 2.27 (s, 3H), 1.95 (s, 6H), 1.24 (d, J=8Hz, 6H), 0.84 (d, J=8Hz, 6H). ^{13}C NMR (101MHZ, CD$_2$Cl$_2$): δ= 189.2, 138.8, 138.7, 136.8, 134.0, 133.8, 130.1, 129.1, 128.2, 127.0, 123.8, 46.6, 21.1, 20.6, 20.0. Anal. Calcd. for C$_{22}$H$_{30}$N$_2$AuCl: C, 47.62; H, 5.45; N, 5.05 %. Found: C, 47.44; H, 5.52; N, 4.85 %.

N-2-mesitylphenyl-N'-t-butyldiaminocarbene gold chloride (2d):

White solid, 89mg (77%).multiple isomers: 68% major 15% minor A 17% minor B. ^{1}H NMR (400 MHZ, CD$_2$Cl$_2$): δ = 8.47 (d, J= 8Hz, 1H, major), 8.39 (d, J=8Hz, 1H, minorA), 8.214 (bs, 1H, minor), 7.48-7.29 (m, major and minor) 7.18-7.10 (m, major and minor), 7.08 (s, 1H, major), 7.07 (s, 1H,major), 6.96 (s, 2H, minor), 6.62 (bs,1H, *NH,* major), 6.47 (d, J=8Hz, 1H, minor B), 2.36 (s, 3H, minor), 2.33(s, 3H, major), 2.29 (s, 3H, major), 1.95, 1.92, 1.87, 1.77 , 1.53 (bs, 9H), 1.00 (s, 9H). ^{13}C NMR (100 MHz, CD2Cl2): δ = 187.6, 138.9, 138.3, 137.7, 136.9, 136.0, 133.5, 130.2, 129.2, 129.0, 128.5, 127.2, 122.1, 54.9, 31.2, 29.0, 21.2, 21.1, 20.6, 20.5, 20.3. Anal. Calcd. for C$_{20}$H$_{26}$N$_2$AuCl: C, 45.59; H, 4.97; N, 5.32 %. Found: C, 45.92; H, 4.92; N, 4.93 %.
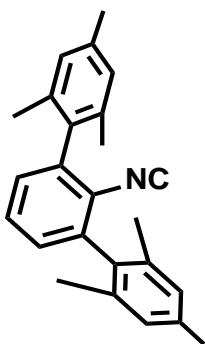
^{1}H NMR data matches literature values.[49]
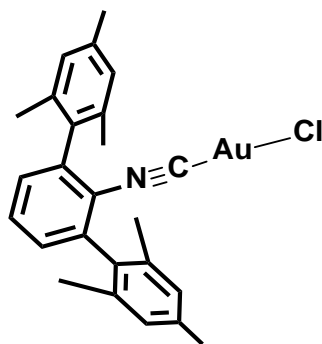
**Synthesis of 2,6-dimesitylphenylisocyanide gold chloride:**

2,6-dimesitylphenylisocyanide (0.589mmol) and tetrahydrothiophene gold chloride (0.560mmol) were dissolved in dry CH_2Cl_2 and allowed to stir for 12 hours at room temperature under nitrogen. The resulting product was washed with Et_2O and purified by recrystallization in CH_2Cl_2/pentane. White crystalline solid, yield 294mg (92%). ^{1}H NMR (400 MHz, CD_2Cl_2): δ= 7.70 (t, J=8Hz, 1H), 7.34 (d, J=8Hz, 2H), 7.02 (d, 0.8Hz, 4H), 2.35 (s, 6H), 2.01 (s, 12H). ^{13}C NMR (151MHz, CD_2Cl_2): δ= 143.8, 140.9, 139.0, 135.7, 133.0, 132.1, 130.3, 129.0, 124.0, 21.3, 20.2. IR (nujol): 2205 cm^{-1}. Anal. Calcd For $C_{25}H_{25}NAuCl$: C, 52.50; H, 4.41; N, 2.45%. Found: C, 49.69; H, 4.39; N, 2.05%.

General Procedure for synthesis of N,N'-2,6-dimesitylphenyl-N',N'-diaminocarbene gold chloride: The primary or secondary alkyl amine (2 equiv) was dissolved in 4mL of dry CH_2Cl_2 and added to a solution of 2,6-dimesitylphenylisocyanide gold chloride (0.175mmol) in dry CH_2Cl_2 (10mL/mmol of 2) via syringe pump at a rate of 2mL/hour. After addition was complete, the reaction mixture was allowed to stir an additional two hours at room temperature, after which the solvent was evaporated under reduced pressure. Dry acetonitrile (10mL/mmol of 2) was then added along with one more equivalent of amine, and the reaction mixture was heated at 40 °C for three hours. The solvent was then evaporated under reduced pressure and the crude product was washed with pentane (3 x10mL). The resulting product was purified by recrystallization in

CH₂Cl₂/pentane to give the pure product. The compounds were characterized by ^{1}H NMR, ^{13}C NMR, and elemental analysis.
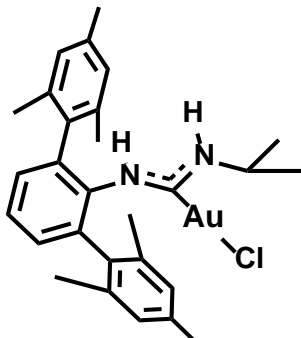
N,N'-2,6-dimesitylphenyl-N'-isopropyldiaminocarbene gold chloride (2e)

White solid, yield 90 mg (82%). Mixture of two isomers: major 95%, minor 5% by ^{1}H NMR. ^{1}H NMR (400 MHz, CD₂Cl₂): δ= 7.56 (t, J=7.6Hz, 1H, major & minor), 7.30 (d, J=7.6Hz, 2H, major & minor), 6.99(s, 4H, major)), 6.94 (s, 4H, minor), 6.74 (bs, 1H, N*H*, major), 5.72 (d, J=8Hz, 1H, N*H*, major), 4.10(m, 1H, major), 2.32 (s, 3H, major), 2.29(s, 3H, minor), 2.17 (s, 6H minor), 2.05 (s, 6H, major) 0.96 (d, J=6.4Hz, 6H, major), 0.83 (d, J=6.4Hz, 6H, minor). ^{13}C NMR (101MHz, CD₂Cl₂): δ= 187.8, 139.1, 138.3, 135.3, 134.3, 132.1, 131.6, 130.8, 129.6, 129.5, 128.9, 53.1, 22.7, 21.7, 21.2, 21.0. Anal. Calcd. For C₂₈H₃₄N₂AuCl: C, 53.30; H, 5.43; N, 4.44%. Found: C,53.88; H, 5.49; N, 4.31%.
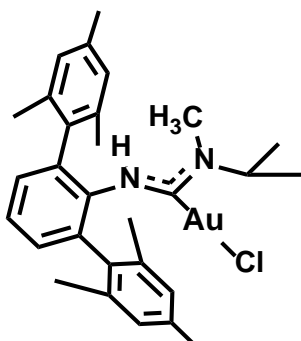

N,N'-2,6-dimesitylphenyl-N',N'-isopropylmethyldiaminocarbene gold chloride (2f)

White solid, yield 96mg (85%). Mixture of two isomers: major 94%, minor 6% by ^{1}H NMR. ^{1}H NMR (400 MHz, CD$_2$Cl$_2$): δ = 7.53(t, J=7.6Hz, 1H, major & minor), 7.28 (d, J=7.6Hz, 2H, major & minor), 6.92 (s, 4H, major & minor) 6.34 (s, 1H, N*H*, major & minor), 4.83 (septet, J=6.8Hz, 1H, major), 3.08 (s, 3H, minor), 2.30 (s, 3H, major), 2.28 (s, 6H, major), 2.20 (bs, 12H, major & minor), 0.88 (d, J=6.8Hz, 6H, major), 0.84 (d, J=6.8Hz, 6H, minor). ^{13}C NMR (101MHz, CD$_2$Cl$_2$): δ = 191.7, 140.6, 137.5, 136.5, 135.2, 130.7, 128.7, 68.1, 60.6, 26.9, 25.9, 21.8, 21.0, 19.8. Anal. Calcd. For C$_{29}$H$_{36}$N$_2$AuCl: C, 54.00; H, 5.63; N, 4.34%. Found: C, 53.89; H, 5.68; N, 4.43%.
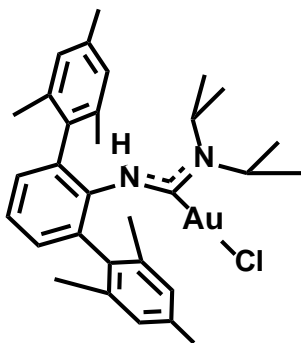
N,N'-2,6-dimesitylphenyl-N',N'-diisopropyldiaminocarbene gold chloride (2g)

White solid, yield 103mg (88%). ^{1}H NMR (400MHz, CD$_2$Cl$_2$): δ = 7.55 (t, J=7.6Hz, 1H), 7.28 (d, J=7.6Hz, 2H), 6.96 (bs, 2H), 6.86 (bs, 2H), 6.54 (bs, 1H, N*H*), 4.88 (bs, 1H, N*H*), 3.47 (m, 1H), 2.48(s, 6H), 2.26 (s, 6H), 1.93 (s, 6H), 0.96 (d, J=6.8Hz, 6H), 0.85 (d, J=7.2 Hz, 6H). ^{13}C NMR (101 MHz, CD$_2$Cl$_2$): δ = 191.9. 140.9. 137.6. 137.4. 137.1. 135.4. 134.8. 130.6. 129.3. 129.0. 128.9. 128.1. 46.0. 23.1. 21.1. 21.0. 20.4. Anal. Calcd. For C$_{31}$H$_{40}$N$_2$AuCl: C, 55.32; H, 5.99; N, 4.16%. Found: C, 55.25; H, 5.82; N, 4.31%.
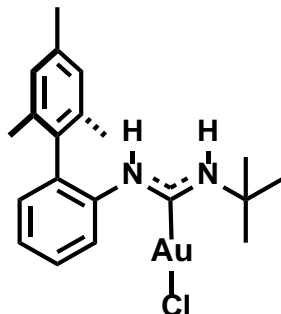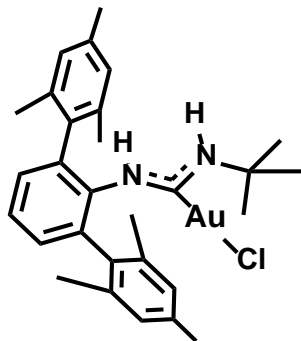
N,N'-2,6-dimesitylphenyl-N'-t-butyldiaminocarbene gold chloride (2h)

White solid, yield 95mg(84%). Mixture of two isomers: major 94%, minor 6% by ^{1}H NMR. ^{1}H NMR (400 MHz, CD$_2$Cl$_2$): δ = 7.57 (t, J=7.6Hz, 1H, major & minor), 7.32 (d, J=7.6Hz, 2H major), 7.28 (d, J=7.6Hz, 2H, minor), 7.00 (s, 4H, major), 6.94 (s, 4H, minor), 6.82 (bs, 1H, N*H*, major), 5.99 (bs, 1H, N*H*, major), 2.33 (s, 6H, major), 2.29 (s, 6H, minor), 2.06 (s, 12H, major & minor), 1.25 (s, 9H, major), 0.96 (s, 9H, minor). ^{13}C NMR (101MHz, CD$_2$Cl$_2$): δ = 188.4, 140.3, 139.8, 138.2, 137.7, 135.3, 135.2, 134.3, 131.6, 130.7, 129.7, 129.3, 129.1, 54.4, 30.8, 29.3, 21.2, 21.1. Anal. Calcd. For C$_{29}$H$_{36}$N$_2$AuCl: C, 54.00; H, 5.63; N, 4.34%. Found: C, 53.84; H, 5.67; N, 4.21%.
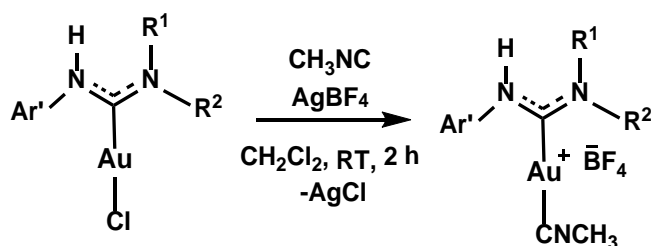
General Procedure for synthesis of methylisocyanide adducts:

To a stirred solution of ADC gold chloride (1 equiv) and methyl isocyanide (1.2 equiv) in dichloromethane (0.1M) under argon atomosphere was added AgBF$_4$ (1.1 equiv.) in one portion. The resulting reaction mixture was stirred overnight and solvent was removed under reduced

pressure. The crude product was sent into the glovebox and dissolved in dry CH_2Cl_2. Filtration of

the crude reaction mixture through a plug of Celite was followed by removal of solvent under

reduced pressure. This process was repeated 4 times to ensure complete removal of AgCl. The

product was then purified by recrystallization from CH_2Cl_2 and pentane.
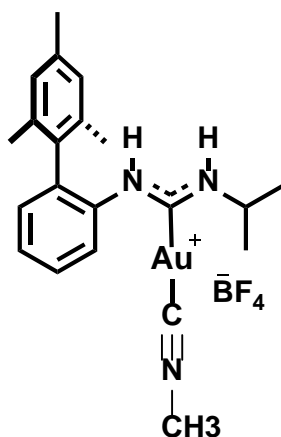
N-2-Mesitylphenyl-N'-isopropyldiaminocarbene gold methylisocyanide tetrafluoroborate

(3a)

White solid, yield 42mg (36%). Mixture of isomers: ^{1}H NMR (400 MHz, CD_2Cl_2): δ= 9.03 (bs),

8.69(bs), 8.41(d, J=8.8H), 7.65 (d, J=7.6Hz),7.48-6.90 (m), 4.02 (sept, J=5.6Hz, 1H, C_H, major),

3.40 (s, 3H, major), 2.31 (s, 3H, major), 1.92 (s, 6H, major) 1.23 (d, J=6.4Hz)^{13}C NMR

(101MHz, CD_2Cl_2): δ=195.7, 139.1, 137.9, 136.8, 136.4, 136.3, 134.1, 131.4, 130.8, 129.3,

129.1, 128.9, 128.8, 128.6, 128.3, 127.8, 126.0, 122.6, 45.5, 32.0, 29.9, 23.5, 21.3, 21.2, 21.1,

21.0, 20.9, 20.8, 20.6. IR(Nujol) 2274 cm^{-1} Anal. Calcd. For $C_{21}H_{27}N_3AuBF_4$: C, 41.67; H, 4.50;

N, 6.94%. Found: C, 41.58; H, 4.57; N, 6.86%.
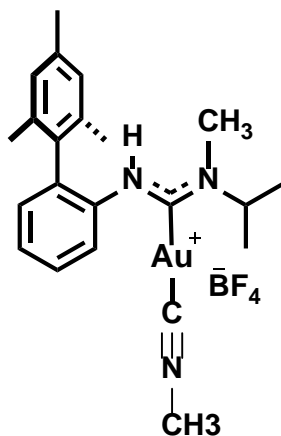
N-2-mesitylphenyl-N',N''-isopropylmethyldiaminocarbene gold methylisocyanide tertrafluoroborate (3b)

White solid, yield 38mg (32%). Mixture of isomers: ^{1}H NMR (400 MHz, CD$_2$Cl$_2$): δ=8.34 (d, J=8Hz, 1H, minor), 7.94 (d, J=7.6Hz, 1H,major), 7.9-7.81 (m, major & minor), 7.51-7.36 (m, major & minor) 7.22-7.14 (m, major & minor), 7.12 (bs, 1H) 6.99(s), 6.97 (s), 6.94 (bs), 6.86(bs), 5.32 (sept, J=6.8Hz, minor), 4.85 (sept, J=6.8 Hz, 1H, major), 4.45 (sept, J=6.8Hz, 1H, minor), 3.49 (s, 3H, major), 3.39 (s, 3H. minor), 2.45 (s, 3H, major), 2.35 (s, 3H, minor), 2.32 (s, 3H, major), 2.27 (s, 3H, minor), 1.96 (s, 6H, minor), 1.94 (s, 6H, major), 1.91 (s, 6H, minor), 1.25 (d, J=6.4Hz, 6H, major), 1.20 (d, J=6.4Hz, 6H, minor), 1.01 (d, J=6.8Hz, 6H, minor). ^{13}C NMR (101MHz, CD$_2$Cl$_2$): δ=200.3, 194.1, 138.8, 138.7, 138.2, 137.8, 136.6, 136.5, 136.2, 136.1, 135.6, 135.4, 133.3, 133.0, 131.1, 131.0, 130.3, 129.2, 129.1, 129.0, 128.4, 128.1, 128.0, 127.7, 127.0, 125.2, 124.2, 123.8, 123.7, 122.2, 62.4, 61.8, 60.4, 30.1, 28.4, 27.8, 21.2, 21.1, 20.8, 20.7, 20.6, 20.4, 20.3, 18.9. IR (Nujol) 2302, 2276, 2198 cm^{-1} Anal. Calcd. For C$_{22}$H$_{29}$N$_3$AuBF$_4$: C, 42.67; H, 4.72; N, 6.79%. Found: C, 42.71; H, 4.71; N, 6.77%.
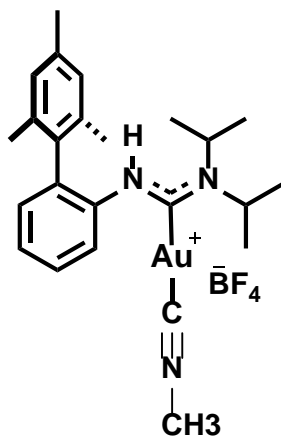
N-2-mesitylphenyl-N'N'-diisopropyldiaminocarbene gold methylisocyanide

tertrafluoroborate (3c)

White solid, yield 70mg (40%). Mixture of isomers: ^{1}H NMR (400 MHz, CD_2Cl_2) δ= 7.96 (d, J=7.6Hz, major), 7.92 (m, 1H minor), 7.52 (dt, J=7.6Hz, J=1.6Hz, 1H, major), 7.46 (dt, J=7.6Hz, J=1.6Hz, 1H, major), 7.40 (m, minor), 7.34 (bs, 1H, major), 7.25 (bs, 1H, minor) 7.20 (dd, J=7.6Hz, J=1.6Hz, 1H, major) 7.16 (m, minor), 7.00 (s, 2H, major), 6.99 (s, 2H minor), 6.94 (s, minor), 4.87 (bs, 1H, major), 4.6 (m, 1H, minor), 3.72 (septet, J=7.2Hz, 1H, major), 3.60 (septet, J=7.6Hz, 1H, minor), 3.50 (s, 3H, Major), 2.29 (s, 3H, major), 2.28 (s, 3H, minor), 1.97 (s, 6H, minor), 1.94 (s, 6H, major), 1.90 (s, 6H, minor), 1.31 (d, J=6.4Hz, 6H, minor), 1.02 (d, J=6.8Hz, 6H, minor), 0.89 (d, J=7.6Hz, 6H major), 0.85 (d, J=7.6Hz, 6H, minor). ^{13}C NMR (101MHz, CD_2Cl_2): δ=199.8, 194.0, 139.1, 139.0, 138.5, 138.2, 136.7, 136.4, 136.3, 134.7, 134.6, 133.6, 133.4, 130.9, 130.7, 129.3, 128.9, 128.3, 128.0, 127.4, 124.1, 123.5, 47.5, 46.9, 30.1, 21.1, 20.6, 20.5, 20.0, 19.8,. IR (Nujol) 2278 cm^{-1} Anal. Calcd. For $C_{24}H_{33}N_3AuBF_4$: C, 44.53; H, 5.14; N, 6.49%. Found: C, 44.31; H, 5.11; N, 6.42%.
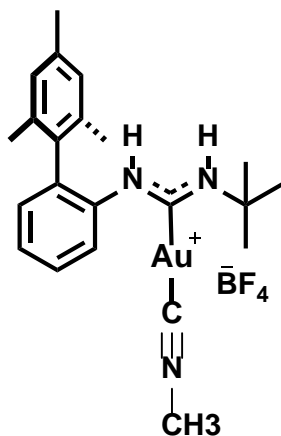
N-2-mesitylphenyl-N'-isopropyldiaminocarbene gold methylisocyanide tertrafluoroborate

(3d)

White solid, yield 42mg (36%). Mixture of isomers: ^{1}H NMR (400 MHz, CD$_2$Cl$_2$): δ= 8.43 (bs, 1H, major), 8.10 (d, J=7.6Hz, 1H, minor), 8.00 (bs, 1H, major), 7.69-6.85 (m, major and minor), 3.43 (s, 3H major), 2.993 (s, 3H, minor), 2.33 (s, 3H, major), 2.30 (s, 3H, minor), 2.26 (s, 3H, minor), 2.01 (s, 6H, minor), 1.94 (s, 6H, major), 1.90 (s, 6H, minor), 1.49 (s, 9H, major), 1.03 (s, 9H, minor). ^{13}C NMR (101MHz, CD$_2$Cl$_2$): δ= 197.2, 193.6, 139.6, 139.2, 137.9, 137.6, 137.0, 136.6, 136.4, 136.3, 136.2, 134.3, 133.9, 133.1, 131.3, 130.7, 130.3, 129.3, 128.8, 128.7, 128.3, 128.0, 127.9, 127.7, 126.6, 124.2, 122.1, 120.7, 55.5, 54.2, 31.5, 30.1, 29.8, 28.8, 21.3, 21.1, 20.8, 20.5. IR (Nujol) 2274 cm^{-1}Anal. Calcd. For C$_{22}$H$_{29}$N$_3$AuBF$_4$: C, 42.67; H, 4.72; N, 6.79%. Found: C, 41.89; H, 4.79; N, 7.01%.
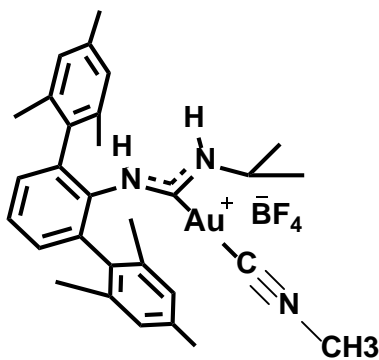
N-2-mesitylphenyl-N'-isopropyldiaminocarbene gold methylisocyanide tertrafluoroborate (3e)

White solid, yield 48 (42%). Mixture of isomers: ^{1}H NMR (400 MHz, CD$_2$Cl$_2$): δ= 7.84 (bs, 1H, major), 7.63-7.45 (m, major and minor), 7.33-7.29 (m, minor), 7.24 (d, J=7.6Hz, 2H, major), 7.06-6.76 (m, major and minor), 6.70 (bs, 1H, major), 5.96 (d, J=8.4Hz, minor), 3.87 (septet, J=7.6Hz, 1H, minor), 3.64 (septet, J=7.6Hz, major), 3.45 (s, 3H, minor), 3.43 (s, 3H, minor), 3.40 (s, 3H, major), 3.13 (m, minor), 2.32 (s, 3H, minor), 2.30 (s, 3H, major), 2.13 (s, 6H, major), 2.05 (s, 6H, minor), 0.99 (d, J=6.4Hz, 6H, minor), 0.90 (d, J=6.8Hz, 6H, major), 0.84 (d, J=6.4Hz, 6H, minor). ^{13}C NMR (101MHz, CD$_2$Cl$_2$): δ= 197.1, 147.4, 147.1, 146.9, 140.0, 139.1, 138.5, 138.3, 137.6, 136.2, 135.6, 135.4, 134.9, 134.3, 134.1, 131.9, 131.1, 130.9, 130.4, 129.5, 129.3, 128.8, 128.3, 53.0, 44.4, 30.0, 29.9, 23.0, 22.8, 21.7, 21.6, 21.3, 21.1, 21.0. IR (Nujol) 2273 cm^{-1} Anal. Calcd. For C$_{30}$H$_{37}$N$_3$AuBF$_4$: C, 49.81; H, 5.16; N, 5.81%. Found: C, 50.24; H, 5.28; N, 5.54%.
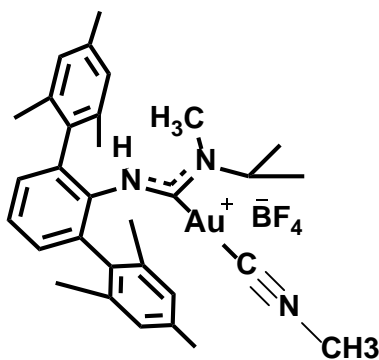
N-2-mesitylphenyl-N'-isopropyldiaminocarbene gold methylisocyanide tetrafluoroborate (3f)

White solid, yield 31mg (27%). Mixture of isomers: ^{1}H NMR (400 MHz, CD$_2$Cl$_2$): δ= 7.59-7.51 (m, major and minor), 7.37-7.26 (m, major and minor), 7.01 (s, 2H, minor), 6.96 (s, 2H, minor), 6.95 (s, 2H, minor), 6.92 (s, 2H, major), 6.85 (bs, minor), 6.55 (bs, minor), 6.35 (bs, major), 4.82 (septet, J=6.8Hz, 1H, major), 4.77 (septet, J=6.8Hz, 1H, minor), 4.41 (septet, J=6.8Hz, 1H, minor), 3.47 (s, 3h, major), 3.08 (s, 3H, minor), 3.04 (s, 3H, minor), 2.70 (s, 3H, minor), 2.37 (s,

3H, minor), 2.35 (s, 3H, minor), 2.31 (s, 3H, minor), 2.30 (s, 3H, minor), 2.28 (s, 3H, major),

2.20 (bs, 6H, minor), 2.14 (s, 6H, major), 2.12 (s, 6H, minor), 1.98 (s, 6H, minor), 1.90 (bs, 6H,

minor), 1.05 (d, J=6.8Hz, 6H, minor), 0.95 (d, J=6.8Hz, 6H, minor), 0.88 (d, J=6.8Hz, 6H,

major). ^{13}C NMR (101MHz, CD$_2$Cl$_2$): δ=196.0, 191.7, 140.7, 139.8, 139.0, 138.1, 137.9, 137.5,

136.5, 135.9, 135.8, 135.6, 135.2, 134.3, 131.1, 130.9, 130.7, 129.2, 129.1, 129.0, 128.7, 128.3,

68.1, 61.6, 60.6, 30.1, 27.5, 26.9, 26.0, 21.8, 21.4, 21.1, 20.5, 20.2, 20.0, 19.8, 19.3. IR (Nujol)

2274 cm^{-1}. Anal. Calcd. For C$_{31}$H$_{39}$N$_3$AuBF$_4$: C, 50.49; H, 5.33; N, 5.70%. Found: C, 50.61; H,

5.32; N, 5.62%.
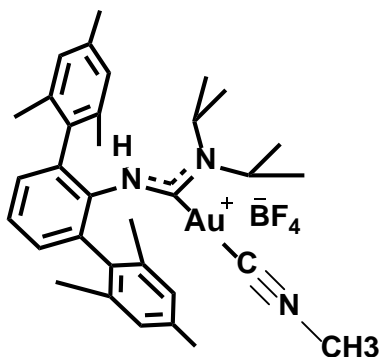
N-2-mesitylphenyl-N'-isopropyldiaminocarbene gold methylisocyanide tertrafluoroborate (3g)

White solid, yield 33mg (31%). Mixture of isomers: ^{1}H NMR (400 MHz, CD$_2$Cl$_2$): δ= 7.75 (m,

1H, minor), 7.57 (t, J=7.6Hz, 1H, major), 7.52 (t, J=8Hz, 1H, minor), 7.36 (m, 2H, minor), 7.32

(d, J=7.6Hz, 2H, major), 7.26 (d, J=7.6Hz, 2H, minor), 7.00 (s, 4H, minor), 6.95 (s, 4H, major),

6.85 (bs, 1H, major), 6.80 (s, minor), 6.75 (bs, 1H, minor), 6.66 (bs, minor), 6.54 (s, minor), 4.84

(bs, 2H, minor), 4.36 (bs, 2H, major), 3.93 (bs, 2H, minor), 3.55-.47 (m, minor), 3.46 (s, 3H,

major), 2.46 (s, 6H, minor), 2.35 (s, 6H, minor), 2.27 (s, 6H, major), 2.25 (s, 6H, minor), 2.14 (s,

12H, major), 2.01 (s, 12H, minor), 1.97 (s, 12H, minor), 1.92 (s, 12H, minor), 1.89 (s, 12H,

minor), 1.36 (d, J=7.2Hz, 12H, minor), 1.21 (d, J=6.4Hz, 12H, minor), 1.09 (d, J=6.4Hz, 12H,

minor), 1.02 (d, J=6.4 Hz, 12H, minor), 0.95 (d, J=6.4 Hz, 12H, minor), 0.85 (d, J=7.2 Hz, 12H,

major), 0.81 (d, J=7.2 Hz, 12H, minor). ^{13}C NMR (101MHz, CD$_2$Cl$_2$): δ=203.1, 195.7, 191.3, 140.3, 139.6, 138.3, 137.5, 137.4, 137.1, 136.9, 135.8, 135.1, 135.0, 134.8, 134.3, 133.9, 132.5, 132.3, 130.4, 130.2, 130.0, 128.8, 128.5, 128.4, 128.2, 127.9, 127.7, 66.8, 60.9, 46.7, 46.0, 45.5, 35.7, 29.4, 22.5, 21.4, 21.1, 20.9, 20.7, 20.4, 20.2, 19.9, 19.7, 19.6, 19.5. IR (Nujol) 2273 cm^{-1}

Anal. Calcd. For C$_{33}$H$_{43}$N$_3$AuBF$_4$: C, 51.78; H, 5.66 N, 5.49%. Found: C, 51.84; H, 5.70; N, 5.44%.
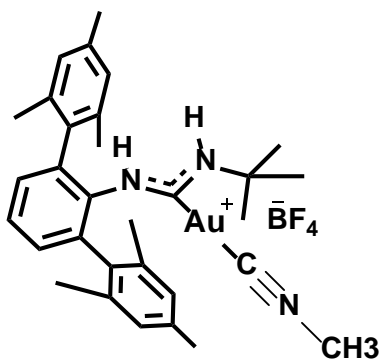
N-2-mesitylphenyl-N'-isopropyldiaminocarbene gold methylisocyanide tertrafluoroborate (3h)

White solid, yield 42mg (24%). Mixture of isomers: ^{1}H NMR (400 MHz, CD$_2$Cl$_2$): δ= 8.42 (bs,1H, major), 8.33 (bs, 1H, major), 7.70-7.55 (m, major and minor), 7.47 (t, J=7.6Hz, 1H, major), 7.34-7.28 (m, major and minor), 7.22 (d, J=7.6 Hz, 2H, major), 7.07 -7.05 (m, minor), 6.99 (s, 4H, minor), 6.97 (s, 4H, minor), 6.94 (s, 4H, major), 6.88 (s, 4H minor), 6.19 (bs, 1H minor), 5.99 (bs, 1H, minor), 3.42 (s, 3H, major and minor), 2.32 (s, 6H, minor), 2.29 (s, 6H, major), 2.15 (bs, 12H, major), 20.14 (s, 12H, minor), 2.06 (s, 12H, minor), 2.01 (s, 12H, minor), 1.26 (s, 9H, minor), 1.24 (s, 9H, minor), 1.22 (s, 9H, minor), 1.13 (s, 9H, major) ^{13}C NMR (101MHz, CD$_2$Cl$_2$): δ= 198.4, 146.5, 146.3, 146.0, 139.7, 138.2, 138.1, 137.2, 137.1, 136.2, 136.1, 135.4, 135.2, 134.8, 133.8, 131.6, 131.4, 130.8, 130.2, 129.6, 129.1, 128.6, 128.0, 127.8, 53.4, 31.1, 31.0, 30.7, 29.9, 29.8, 29.7, 29.0, 21.7, 20.9 . IR (Nujol) 2271 cm^{-1} Anal. Calcd. For C$_{31}$H$_{39}$N$_3$AuBF$_4$: C, 50.49; H, 5.33; N, 5.70%. Found: C, 50.08; H, 5.27; N, 5.54%.
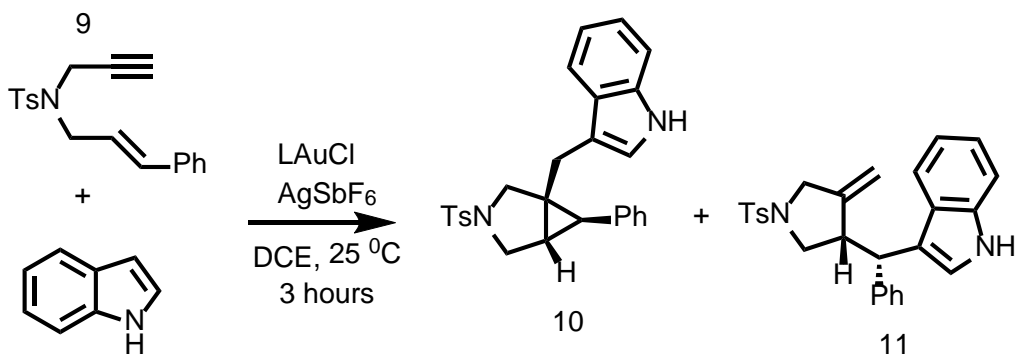
1,6-Enyne Cyclization/Hydroarylation Catalytic Study

A 2mL vial was charged with a stir bar, *N*-cinnamyl-4-methyl-*N*-(prop-2-yn-1-yl)benzenesulfonamide

(1,6-enyne) (0.050 g, 0.15 mmol) and indole (0.020 g, 0.17 mmol) in 1 mL of dry DCE in a nitrogen

filled drybox. To this homogeneous mixture was added a gold catalyst [(L)Au]$^+$[SbF6]$^-$, freshly prepared

by stirring 5 mol % of (L)AuCl (vs. enyne) and 5 % of AgSbF$_6$ (vs. enyne) in DCE

(1 mL) for 15 min, followed by filtration through plug of Celite. The resulting reaction mixture was

stirred at 25 °C for 3 hours. The mixture was dried under reduced pressure and purified using silica

column chromatography. The ratio of products **10** and **11** was obtained comparing the ^{1}H NMR integral

values of the two signals at δ = 6.59 ppm (d, J=1.9Hz, 1H, **10**), 4.75 (d, J=1.5Hz, 1H, **11**).
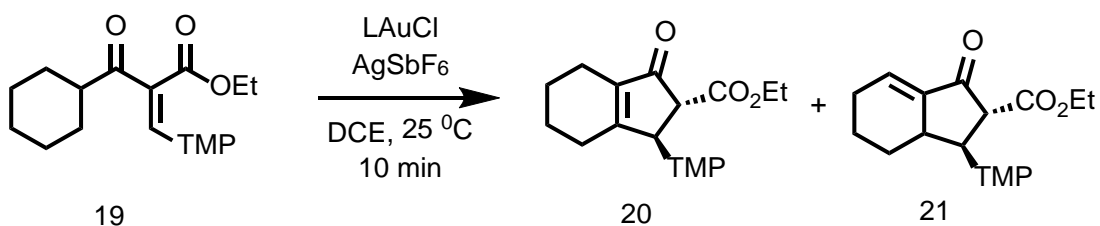
Nazarov Catalytic Study:

In a nitrogen glovebox, LAuCl (5 mol %) was combined with AgSbF$_6$ (4.5mol %) and freshly distilled

DCE (1mL) in a 2 mL reaction vial charged with a stir bar. The vial was sealed by a screw cap with a

PTFE/silicon septum and stirred at room temperature for 15 minutes. The AgCl was removed by filtration

through plug of Celite. A solution of **19** (0.134mmol) in freshly distilled DCE (1mL) was injected into the

reaction vial through the septum, and stirring was continued. Reaction progress was monitored by TLC until starting material had been consumed. After aqueous $NaHCO_3$ workup, products were purified by flash chromatography on silica with Et_2O:hexanes (3:2) mixtures as eluents. ^{1}H NMR data matched reported literature values. [4] The A:B ratios were determine from NMR analyses of the crude products.

X-ray Structural Data for 2a-2h

Crystal data and structure refinement for **2a**

Empirical formula	C19 H24 Au Cl N2	
Formula weight	512.82	
Temperature	115(2) K	
Wavelength	0.71073 Å	
Crystal system	Triclinic	
Space group	P -1	
Unit cell dimensions	a = 8.00640(10) Å	α= 95.8960(10)°.
	b = 10.6256(2) Å	β= 103.0150(10)°.
	c = 12.2089(2) Å	γ = 105.1440(10)°.
Volume	962.30(3) Å^3	
Z	2	
Density (calculated)	1.770 Mg/m^3	
Absorption coefficient	7.784 mm^{-1}	
F(000)	496	
Crystal size	0.30 x 0.12 x 0.04 mm^3	
Theta range for data collection	2.73 to 29.10°.	

Index ranges	-10<=h<=10, -14<=k<=14, -16<=l<=16
Reflections collected	21739
Independent reflections	5112 [R(int) = 0.0306]
Completeness to theta = 29.10°	99.2 %
Absorption correction	Semi-empirical from equivalents
Max. and min. transmission	0.7460 and 0.2036
Refinement method	Full-matrix least-squares on F^2
Data / restraints / parameters	5112 / 0 / 213
Goodness-of-fit on F^2	1.028
Final R indices [I>2sigma(I)]	R1 = 0.0170, wR2 = 0.0387
R indices (all data)	R1 = 0.0193, wR2 = 0.0394
Largest diff. peak and hole	0.910 and -0.558 e.Å^{-3}

Crystal data and structure refinement for **2b**

Empirical formula	C20 H26 Au Cl N2
Formula weight	526.84
Temperature	115(2) K
Wavelength	0.71073 Å
Crystal system	Monoclinic
Space group	P 2$_1$/c
Unit cell dimensions	a = 12.0932(2) Å $\quad\quad$ α= 90°.
	b = 10.37470(10) Å $\quad\quad$ β= 107.8330(10)°.
	c = 16.2882(2) Å $\quad\quad$ γ = 90°.
Volume	1945.38(4) Å^3

74

Z	4
Density (calculated)	1.799 Mg/m^3
Absorption coefficient	7.703 mm^{-1}
F(000)	1024
Crystal size	0.25 x 0.20 x 0.11 mm^3
Theta range for data collection	1.77 to 30.43°.
Index ranges	-17<=h<=17, -14<=k<=14, -23<=l<=23
Reflections collected	37331
Independent reflections	5887 [R(int) = 0.0315]
Completeness to theta = 30.43°	99.7 %
Absorption correction	Semi-empirical from equivalents
Max. and min. transmission	0.4845 and 0.2490
Refinement method	Full-matrix least-squares on F^2
Data / restraints / parameters	5887 / 0 / 223
Goodness-of-fit on F^2	1.054
Final R indices [I>2sigma(I)]	R1 = 0.0152, wR2 = 0.0320
R indices (all data)	R1 = 0.0197, wR2 = 0.0332
Largest diff. peak and hole	0.632 and -0.444 e.Å^{-3}

Crystal data and structure refinement for **2c**

Empirical formula	C23 H32 Au Cl3 N2
Formula weight	639.82
Temperature	115(2) K
Wavelength	0.71073 Å

Crystal system	Triclinic
Space group	P -1
Unit cell dimensions	a = 7.6872(3) Å $\alpha = 86.062(2)°$.
	b = 10.9274(4) Å $\beta = 78.745(2)°$.
	c = 15.3336(5) Å $\gamma = 79.790(2)°$.
Volume	1242.49(8) $Å^3$
Z	2
Density (calculated)	1.710 Mg/m^3
Absorption coefficient	6.255 mm^{-1}
F(000)	628
Crystal size	0.43 x 0.34 x 0.19 mm^3
Theta range for data collection	1.89 to 30.52°.
Index ranges	-10<=h<=10, -15<=k<=15, 0<=l<=21
Reflections collected	112255
Independent reflections	7525 [R(int) = 0.0340]
Completeness to theta = 30.52°	99.2 %
Absorption correction	Semi-empirical from equivalents
Max. and min. transmission	0.3828 and 0.1740
Refinement method	Full-matrix least-squares on F^2
Data / restraints / parameters	7525 / 0 / 269
Goodness-of-fit on F^2	1.054
Final R indices [I>2sigma(I)]	R1 = 0.0154, wR2 = 0.0404
R indices (all data)	R1 = 0.0166, wR2 = 0.0408

Largest diff. peak and hole 1.058 and -0.665 e.Å⁻

Input for **Figure 2.2d**: Computed Structure of **2d**. B3LYP/CEP-31g*

```
Au          2.1031    -0.56259   -0.14713
Cl          3.8315    -1.00806   -1.65862
C1          0.57564   -0.21707    1.15379
N1          0.37078   -0.89884    2.30323
H1         -0.451     -0.64342    2.85948
N2         -0.38016    0.71559    0.89306
H2         -1.19313    0.76499    1.51476
C2          1.19539   -1.99947    2.91905
C3          1.21656   -3.24436    1.99665
H3          0.19118   -3.59568    1.79007
H4          1.77469   -4.06061    2.4861
H5          1.70728   -3.01895    1.03779
C4          0.47758   -2.34946    4.24787
H6          0.44456   -1.47931    4.92769
H7          1.01867   -3.1579     4.7639
H8         -0.55497   -2.69866    4.06718
C5          2.63034   -1.49907    3.22125
H9          3.1653    -1.24157    2.29489
H10         3.19812   -2.29118    3.7382
H11         2.60443   -0.60552    3.86775
C6         -0.41485    1.62405   -0.23264
C7          0.77761    1.88963   -0.97009
C8          0.69935    2.81084   -2.04794
H12         1.60386    3.03145   -2.61862
C9         -0.51308    3.45977   -2.37043
H13        -0.54905    4.16771   -3.203
C10        -1.67399    3.2074    -1.60425
H14        -2.61084    3.71986   -1.83557
C11        -1.63946    2.29206   -0.52295
C12        -2.87348    2.07056    0.31277
C13        -3.89616    1.1787    -0.12983
C14        -5.04443    0.98884    0.68555
H15        -5.82273    0.30041    0.34384
C15        -5.2088     1.66518    1.91963
C16        -4.19021    2.56589    2.33041
H16        -4.30571    3.11748    3.26852
C17        -3.02921    2.7799     1.54577
C18        -3.78724    0.44085   -1.46241
H17        -3.7566     1.14403   -2.31238
H18        -4.6485    -0.22998   -1.6065
H19        -2.86986   -0.16849   -1.52012
C19        -6.44971    1.44637    2.7841
H20        -7.15802    0.75635    2.29795
H21        -6.97785    2.39757    2.97413
H22        -6.1824     1.01943    3.76758
C20        -1.98608    3.79753    2.01413
```

```
H23                        -2.30902    4.2816    2.94938
H24                        -1.82368    4.58539   1.25907
H25                        -0.99627    3.3416    2.20219
H26                         1.70931    1.40575  -0.71672
```

Crystal data and structure refinement for **2e**

Empirical formula	C28 H34 Au Cl N2
Formula weight	630.99
Temperature	115(2) K
Wavelength	0.71073 Å
Crystal system	Orthorhombic
Space group	F d d 2
Unit cell dimensions	a = 28.4766(4) Å $\quad \alpha = 90°.$
	b = 32.9002(3) Å $\quad \beta = 90°.$
	c = 11.79620(10) Å $\quad \gamma = 90°.$
Volume	11051.7(2) Å^3
Z	16
Density (calculated)	1.517 Mg/m^3
Absorption coefficient	5.438 mm^{-1}
F(000)	4992
Crystal size	0.22 x 0.11 x 0.10 mm^3
Theta range for data collection	1.89 to 28.19°.
Index ranges	-37<=h<=37, -43<=k<=43, -15<=l<=15
Reflections collected	29711

Independent reflections	6781 [R(int) = 0.0450]
Completeness to theta = 28.19°	100.0 %
Absorption correction	Semi-empirical from equivalents
Max. and min. transmission	0.6124 and 0.3809
Refinement method	Full-matrix least-squares on F^2
Data / restraints / parameters	6781 / 2 / 305
Goodness-of-fit on F^2	0.995
Final R indices [I>2sigma(I)]	R1 = 0.0257, wR2 = 0.0436
R indices (all data)	R1 = 0.0350, wR2 = 0.0457
Absolute structure parameter	-0.012(5)
Largest diff. peak and hole	0.976 and -0.440 e.$Å^{-3}$

Crystal data and structure refinement for **2f**

Empirical formula	C29.50 H37 Au Cl2 N2	
Formula weight	687.48	
Temperature	115(2) K	
Wavelength	0.71073 Å	
Crystal system	Triclinic	
Space group	P -1	
Unit cell dimensions	a = 9.11420(10) Å	α= 90.5550(10)°.
	b = 16.8134(2) Å	β= 99.2930(10)°.
	c = 18.4933(2) Å	γ = 91.2300(10)°.
Volume	2795.84(5) $Å^3$	
Z	4	

Density (calculated)	1.633 Mg/m^3
Absorption coefficient	5.473 mm^{-1}
F(000)	1364
Crystal size	0.20 x 0.16 x 0.14 mm^3
Theta range for data collection	1.64 to 28.25°.
Index ranges	-11<=h<=12, -22<=k<=22, -24<=l<=24
Reflections collected	56400
Independent reflections	13746 [R(int) = 0.0370]
Completeness to theta = 28.25°	99.4 %
Absorption correction	Semi-empirical from equivalents
Max. and min. transmission	0.5146 and 0.4074
Refinement method	Full-matrix least-squares on F^2
Data / restraints / parameters	13746 / 0 / 648
Goodness-of-fit on F^2	1.023
Final R indices [I>2sigma(I)]	R1 = 0.0253, wR2 = 0.0583
R indices (all data)	R1 = 0.0358, wR2 = 0.0621
Largest diff. peak and hole	1.202 and -1.199 e.Å^{-3}

Crystal data and structure refinement for **2g**

Empirical formula	C31 H40 Au Cl N2
Formula weight	673.07
Temperature	115(2) K
Wavelength	0.71073 Å
Crystal system	Monoclinic

Space group	P 21/n
Unit cell dimensions	a = 10.3393(2) Å α= 90°.
	b = 17.1048(3) Å β= 94.3060(10)°.
	c = 16.4509(2) Å γ = 90°.
Volume	2901.16(8) Å^3
Z	4
Density (calculated)	1.541 Mg/m^3
Absorption coefficient	5.184 mm^{-1}
F(000)	1344
Crystal size	0.25 x 0.25 x 0.20 mm^3
Theta range for data collection	1.72 to 30.43°.
Index ranges	-14<=h<=13, -23<=k<=24, -21<=l<=23
Reflections collected	50256
Independent reflections	8760 [R(int) = 0.0320]
Completeness to theta = 30.43°	99.5 %
Absorption correction	Semi-empirical from equivalents
Max. and min. transmission	0.4237 and 0.3573
Refinement method	Full-matrix least-squares on F^2
Data / restraints / parameters	8760 / 0 / 330
Goodness-of-fit on F^2	1.011
Final R indices [I>2sigma(I)]	R1 = 0.0182, wR2 = 0.0441
R indices (all data)	R1 = 0.0247, wR2 = 0.0467
Largest diff. peak and hole	0.650 and -0.540 e.Å^{-3}

Refinement method   Full-matrix least-squares on F^2

Goodness-of-fit on F^2 1.036

Crystal data and structure refinement for **2h**

Empirical formula   C29 H36 Au Cl N2

Formula weight   645.01

Temperature   115(2) K

Wavelength   0.71073 Å

Crystal system   Monoclinic

Space group   P 21/n

Unit cell dimensions   a = 12.4751(2) Å $\alpha = 90°$.

                           b = 17.3494(3) Å $\beta = 105.0750(10)°$.

                           c = 12.7598(2) Å $\gamma = 90°$.

Volume   2666.63(8) Å^3

Z   4

Density (calculated)   1.607 Mg/m^3

Absorption coefficient   5.636 mm^{-1}

F(000)   1280

Crystal size   0.25 x 0.20 x 0.12 mm^3

Theta range for data collection   2.03 to 30.43°.

Index ranges   -17<=h<=17, -23<=k<=24, -14<=l<=18

Reflections collected   34309

Independent reflections   8057 [R(int) = 0.0326]

Completeness to theta = 30.43°	99.7 %
Absorption correction	Semi-empirical from equivalents
Max. and min. transmission	0.5512 and 0.3331
Refinement method	Full-matrix least-squares on F^2
Data / restraints / parameters	8057 / 0 / 315
Goodness-of-fit on F^2	1.025
Final R indices [I>2sigma(I)]	R1 = 0.0201, wR2 = 0.0421
R indices (all data)	R1 = 0.0280, wR2 = 0.0442
Largest diff. peak and hole	1.084 and -0.377 e.Å^{-3}

2.5 References

1.   Hamasaka, G.; Sakurai, F., *Chem. Comm.,* **2015,** *51*, 3886-3888

2.   (a). He, C.; Brouwer, C.; Li, Z. *Chem. Rev.,* **2008**, *108,* 3239. (b). Hashmi, A. S. K. *Chem. Rev.*, **2007**, *107*, 3180. (c). Winter, C.; Krause, N., *Chem. Rev.*, **2011**, *111*, 1994-2009. (d) Dorel, R.; Echavarren, A.M.; *Chem. Rev.* **2015**, *115*, 9028-9072

3.   Gorin, D,; Sherry, B.; Toste, D.F.; *Chem. Rev.*, **2008**, *108*, 3351-3378.

4.   (a). Gusev, D., *Organometallics*, **2009**, 28,763-770. (b). Leeuwen, P.; Dierkes, P., *Chem. Rev.*, **2000**, 2741-2769. (c). Nolan, S.; Huang, J.; et al., *Organometallics*, **1999**, 18, 2370-2375. (d). Yang, J.; Huynh, H.V.; et al., **2009**, 28, 5395-5404.

5.   Tolman, C.A., *Chem. Rev.*, **1977**, 77, 313-348

6.   (a). Hermman, W.A.; Denk, K.; Sirsch, P., *J. Organomet. Chem.*, **2002**, 649, 219-224.

(b).   Kelly, R. A. I.; Clavier, H.; Giudice, S.; Scott, N. M.; Stevens, E. D.; Bordner, J.;

Smamardjiev, I.; Hoff, C. D.; Cavallo, L.; Nolan, S. P. *Organometallics* **2008**, 27, 202−210.

7.   Roodt, A.; Otto, S.; Steyl, G., *Coord. Chem. Rev*., **2003**, 245, 121.

8.   Kuehl, O. *Coord. Chem. Rev*. **2005**, 249, 693.

9.   Gusev, D. G., *Organometallics*, **2009**, 28, 763.

10.   (a). A. B. P. Lever, *Inorg. Chem*. **1990**, 29, 1271 –1285. (b). A. B. P. Lever, *Inorg. Chem*. **1991**, 30, 1980 –1985.

11.   (a). A. Liske, K. Verlinden, H. Buhl, K. Schaper, C. Ganter, *Organometallics,* **2013**, *32*, 5269– 5272. (b). Verlinden, K.; Buhl, H.; Frank, W.; Ganter, C. *Euro. J. Inorg. Chem.*, **2015**,   2416-2425

12.   (a). Belpassi, L.; Infante, I.; Tarantelli, F.; Visscher, L. *J. Am. Chem. Soc*. **2008**, 130, 1048. (b) Salvi, N.; Belpassi, L.; Tarantelli, F. *Chem. Eur. J*. **2010**, 16, 7231. (c) Cappelletti, D.; Ronca, E.; Belpassi, L.; Tarantelli, F.; Pirani, F. *Acc. Chem. Res*. **2012**, 45, 1571. (d) Bistoni, G.; Belpassi, L.; Tarantelli, F. *Angew. Chem., Int. Ed*. **2013**, 52, 11599. (e) Ronca, E.; Pastore, M.; Belpassi, L.; De Angelis, F.; Angeli, C.; Cimiraglia, R.; Tarantelli, F. *J. Chem. Phys*. **2014**, 140, No. 054110.

13.   (a). K. Morokuma*, J. Chem. Phys*. **1971**, 55, `1236. (b). C. Fonseca Guerra, J. G. Snijders, G. Te Velde, E. J. Baerends, *Theor. Chem. Acc*. **1998**, 99, 391; (c). G. Te Velde, F. M.   Bickelhaupt, E. J. Baerends, C. Fonseca Guerra, S. J. A. Van Gisbergen, J. G. Snijders, T. Ziegler, *J. Comput. Chem*. **2001**, 22, 931; (d) ADF2012, SCM, Theoretical Chemistry, Vrije Universiteit, Amsterdam, The Netherlands, http://www.scm.com.

14. (a). Bernhammer, J.C.; Frison, G.; Huynh, H.V. *Chem. Eur. J.* **2013**, 19, 12892-18905.

    (b). A. Liske, K. Verlinden, H. Buhl, K. Schaper, C. Ganter, *Organometallics,* **2013**, *32*, 5269– 5272.

15. Back, O.; Ellinger, MO.; Marting, C.D.; Martin, D.; Bertrand, G. *Angew. Chem. Int. Ed.*, **2013**, 52, 2939-2943

16. Verlinden, K.; Buhl, H.; Frank, W.; Ganter, C. *Euro. J. Inorg. Chem.*, **2015**, 2416-2425

17. (a) E. O. Fischer, A. Maasbçl, *Chem. Ber.* **1967**, 100, 2445 – 2456. (b). G. Seidel, R. Mynott, A. Furstner, *Angew. Chem. Int. Ed.* 2009, 48, 2510 –2513

18. Bernhammer, J.C.; Frison, G.; Huynh, H.V. *Chem. Eur. J.* **2013**, 19, 12892-18905

19. Baddley, W.H.; Basolo, F.; *J. Am. Chem. Soc.*, **1966**, 88 (13) 2944-2950

20. (a). Clavier, H.; Nolan, S.P.; *Chem. Comm.* **2010**, 46, 841 (b). http://www.molnac.unisa.it/OMtools/sambvca.php.

21. Guzei, I.A.; Wendt, W.; *Dalton Trans.,* **2006**, 3991-3999

22. Bilbrey, J.A.; Kazez, A.H.; Locklin, J.; Allen, W.D. *J. Comp. Chem.* **2013**, 34, 1189-1197. (b). T. L. Brown, K. J. Lee, *Coord. Chem. Rev*. **1993**, 128, 89.

23. (a). Wanniarachchi, Y. A.; Slaughter, L. M. *Chem. Commun*. **2007**, 3294−3296., (b). Wanniarachchi, Y. A.; Kogiso, Y.; Slaughter, L. M. *Organometallics,* **2008**, 27, 21−24.

24. (a). Kauffman, G. B. *Naturwissenschaften* **1976**, 63, 324−327. (b). Altenhoff, G.; Goddard, R.; Lehmann, C. W.; Glorius, F. *Angew. Chem., Int. Ed*. **2003**, 42, 3690−3693.

25. Hu, D.X.; Grice, P.; Ley, S.V. *J. Org. Chem.*, **2012**, 77, 5198-5202

26.   Slaughter, L.M., *ACS Catalysis*, **2012**, 2, 1802-1816.

27.   Tschugajeff (Chugaev), L.; Skanawy-Grigorjewa, M. *J. Russ. Chem. Soc*. **1915**, 47, 776.

28.   Clavier, H.; Nolan, S.P.; *Chem. Comm.* **2010**, 46, 841

29.   Cianacaleoni, G.; Scafuri, N.; Belpassi, L.; et al. *Inorg. Chem.*, **2014**, 53, 9907-9916

30.   (a) Dias, H. V. R.; Jin, W., *Inorg. Chem.***1996**, 35, 3687. (b). Kuster, R.; Seppelt, K.Z. *Anorg. Allg. Chem*. **2000**, 626, 236. (c). Dash, C.; Kroll, P.; Yousufuddin, M.; Dias, H. V. R. *Chem.Commun*., **2011**, 47, 4478. (d) Dias, H. V. R.; Dash, C.; Yousufuddin, M.; Celik, M. A.; Frenking, G. *Inorg. Chem.* **2011**, 50, 4253.

31.   Wanniarachchi, Y. A.; Kogiso, Y.; Slaughter, L. M. *Organometallics*, **2008**, 27, 21−24.

32.   Seidel, G.; Furstner, A., *Angew. Chem., Int. Ed*., **2014**, 53, 4807

33.   Hashmi, A. S. K. *Angew. Chem., Int. Ed*., **2010**, 49, 5232. (29) Arumugam, K.; Varghese, B.; Brantley, J. N.; Konda, S. S. M.; Lynch, V. M.; Bielawski, C. W. *Eur. J. Org. Chem*., **2014**, 2014 , 493.

34.   Nunez, E.J.; Echavarren, A.M. *Chem Rev*. **2008**, 108, 3326-3350. (b). Bartolome´, C.; Ramiro, Z.; Pe´rez-Gala´n, P.; Bour, C.; Raducan, M.; Echavarren, A. M.; Espinet, P. *Inorg. Chem.* **2008**, 47, 11391−11397.

35.   Arumugam, K., Varghese, B., Brantley, J. N., Konda, S. S. M., Lynch, V. M. and Bielawski, C. W. *Eur. J. Org. Chem*., **2014**: 493–497.

36.   H. Seo, B. P. Roberts, K. A. Abboud, K. M. Merz Jr., S. Hong, *Org. Lett.* **2010**, *12*, 4860–4863.

37.   Frey, G.D.; Lavallo, V.; Donnadieu, B.; Schoeller, W.W.; Bertrand, G. *Science*, **2007**, 316, 439-441

38.   For recent reviews of the Nazarov cyclization, see: (a) Grant, T. N.; Rieder, C. J.; West, F. G. *Chem. Commun*. **2009**, 5676. (b) W. W. Nakanishi, W. W.; West, F. G. *Curr. Opin. Drug Discovery Dev*. **2009**, 12, 732. (c) Vaidya, T.; Eisenberg, R.; Frontier, A. J. *ChemCatChem* **2011**, 3, 1531. (d) Shimada, N.; Stewart, C.; Tius, M. A. *Tetrahedron* **2011**, 67, 5851. (e) Spencer, W. T., III; Vaidya, T.; Frontier, A. *J. Eur. J. Org. Chem*. **2013**, 18, 3621. (f). Vaidya, T.; Cheng, R.; Carlsen, P. N.; Frontier, A. J.; Eisenberg, R. *Org. Lett*. **2014**,16, 800.

39.   (a). He. W.; Sun, X.; Frontier, A.J. *J. Am. Chem. Soc*. **2003**, 125, 14278-14279. (b). Johnson, R. et al. *Tetrahedron Lett*. **1986**, 5947-5950.

40.   Sri S. Subramanium, Sachin Handa, Anthea J. Miranda, and LeGrande M. Slaughter *ACS Catalysis* **2011** *1* (10), 1371-1374.

41.   He. W.; Sun, X.; Frontier, A.J. *J. Am. Chem. Soc*. **2003**, 125, 14278-14279

42.   Weidong Rao, Dewi Susanti, Benjamin James Ayers, and Philip Wai Hong Chan *J. Am. Chem. Soc.* **2015** *137* (19), 6350-6355

43.   Hashmi, S.A.K.; *Catalysis Today*, **2007**, *122*, 211-214

44.   R.B. Woodward and R. Hoffman, *The Conservation of Orbital Symmetry*, Academic Press, New York, 1920

45.   Fedorov, A.; Moret, M.-E.; Chen, P. *J. Am. Chem. Soc*. **2008**, *130*, 8880–8881

46.   Minqiang, J.; Bandini, M.; *ACS Catalysis*, **2015**, *5*, 1638-1652

47.   Fulmer, G.R.; Miller, A.J.M.; Stoltz, B.M.; Bercaw, J.E.; Goldberg, K.I.; *Organometallics*, **2010**, *29*,   2176-2179

48.   Inorg. Synth., Volume 26, Pg 86

49.   (a). Figueroa, J., Rheingold, A., et. al, *Inorg. Chem.*, **2008**, 47, 9010-9020. (b). Figueroa, J., Rheingold, A., et. al, *Inorg. Chem.*, **2009**, 48, 8362-8375.

50.   Schuster, R.E.; *Org. Synth.* **1966**, *46*, 75-77

51.   Nagashima, H., Tanabiki, M. et. al, *Organometallics*, **2004**, 23, 3976-3981

52.   Huang, C.Q.; *Bioorganic & Medicinal Chem, Lett.*, **2003**, *13*, 3375-3379

53.   Canterbury, D.P.; Herrick, I.R.; Um, J.; Houk, K.N.; Frontier, A.J.; *Tetrahedron* **2009**, *65*, 3165-3179

CHAPTER III

ENANTIOSELECTIVE GOLD CATALYSIS

3.1 Introduction

Homogeneous gold catalysis has recently emerged as a very powerful tool in the synthetic

chemist's toolbox for the synthesis of complex organic molecules. The emergence of gold

catalysis began with the use of gold (III) halide salts[1a-f] as catalysts, but more recently ligated

gold (I) complexes have become more prevalent. As mentioned in previous chapters, the 12-

electron [AuL]$^+$ fragment is a carbophilic soft Lewis acid that is excellent at activating π-bonds

toward nucleophilic attack. This would seem to make gold an ideal candidate for solving the

problem of enantioselective catalysis based on the π-activation of C-C multiple bonds. However,

the development of enantioselective gold catalysis lags far behind that of other transition metals

such as palladium or rhodium. This can be understood as due to the fact that gold(I) tends to

form linear, two-coordinate complexes, which places the substrate about 180° away from the

chiral ligand where the desired asymmetric induction originates. This problem is exacerbated by

the fact that the attacking the gold-activated π-bond does so in an outer sphere mechanism trans

to the gold center. This might lead one to choose a square planar gold (III) complex to achieve

high levels of asymmetric induction, but Au^{III} is more of a "hard" Lewis acid and is extremely

prone to reduction under catalytic conditions. There are no reports to date of enantioselective

gold (III) catalysis. Although an early report of enantioselective gold (I) catalysis appeared in a

study by Ito and Hayashi in 1986, **(Scheme 3.1)**[1g] it was not until 2005 that Echavarren

published the first example of enantioselective gold(I) catalysis involving π-activation **(Scheme

3.2)**.[2]
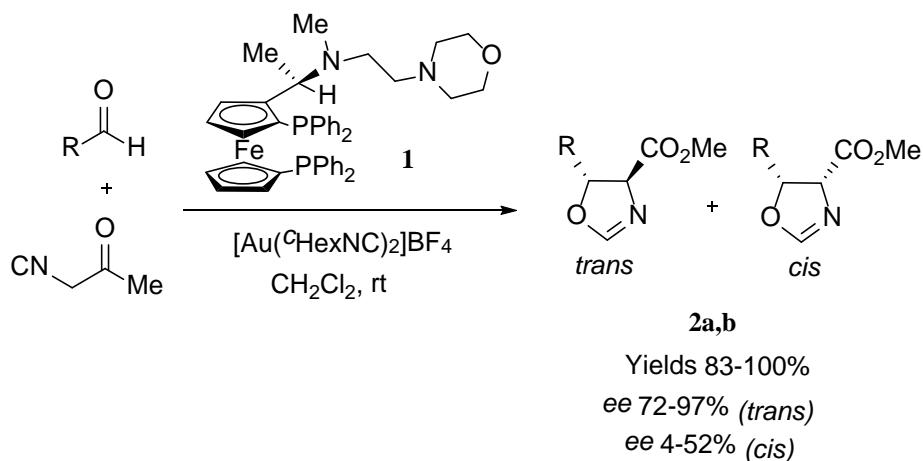
Scheme 3.1 Ito and Hayashi's Enantioselective Gold Catalyzed Aldol Reaction
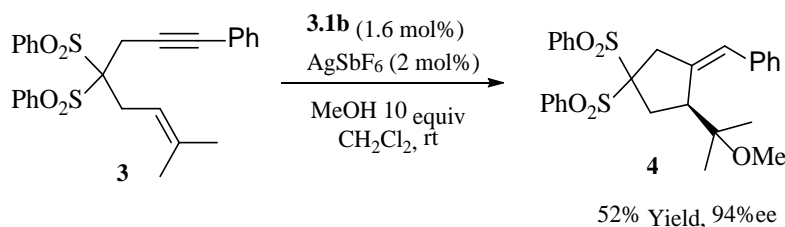
Scheme 3.2 Echavarren's Enantioselective Gold-Catalyzed Enyne Cyclization

Three major strategies have been employed to overcome these inherent problems with

enantioselective gold (I) catalysis. [3] The first strategy involves the use of a chiral counterion to

achieve asymmetric induction rather than a chiral ligand. As long as a sufficiently tight ion pair

is formed in solution, high levels of asymmetric induction can be achieved (**Scheme 3.3**). This

has allowed the synthesis of furan (**6**) and pyrrolidine (**8**) derivative with high

enantioselectivities. This idea was recently used by the Lipshutz group in which homogeneous

gold catalysis was carried out in micelles that forced a tight ion pair to form.[4]
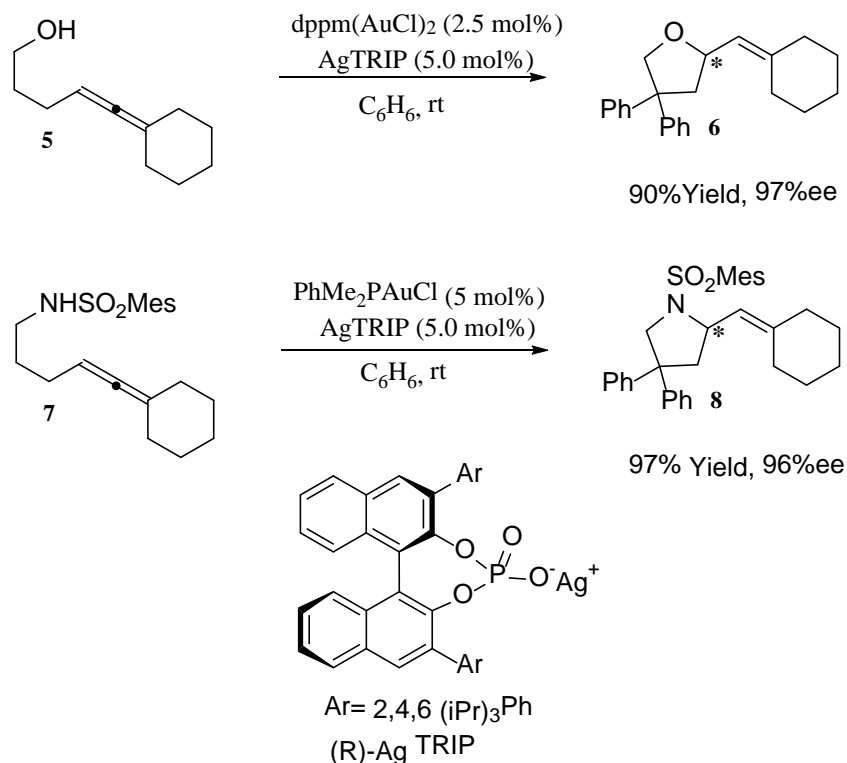
Scheme 3.3 Intramolecular Hydroamination and Hydroalkoxylation Using Chiral Counterions

The second strategy is the use of chiral bisphosphine complexes. Typically, these ligands use large aromatic groups on the phosphine to build a "wall" around the metal and create a well-defined chiral pocket. These bisphoshine complexes are dinuclear complexes **(Figure 3.1),** which potentially has advantages but also increase the overall cost of the catalyst. Although gold(I) has a propensity to form two coordinate complexes, the involvement of aurophilic interactions[5] between the two gold centers might play a role in achieving high levels of asymmetric induction or higher turnovers by stabilizing catalytic intermediates. However, there have also been reports that the level of selectivity is dependent on the amount of silver salt used to activate the dinucelar catalyst **(Scheme 3.4)**, which has led to the third strategy being employed.[6]
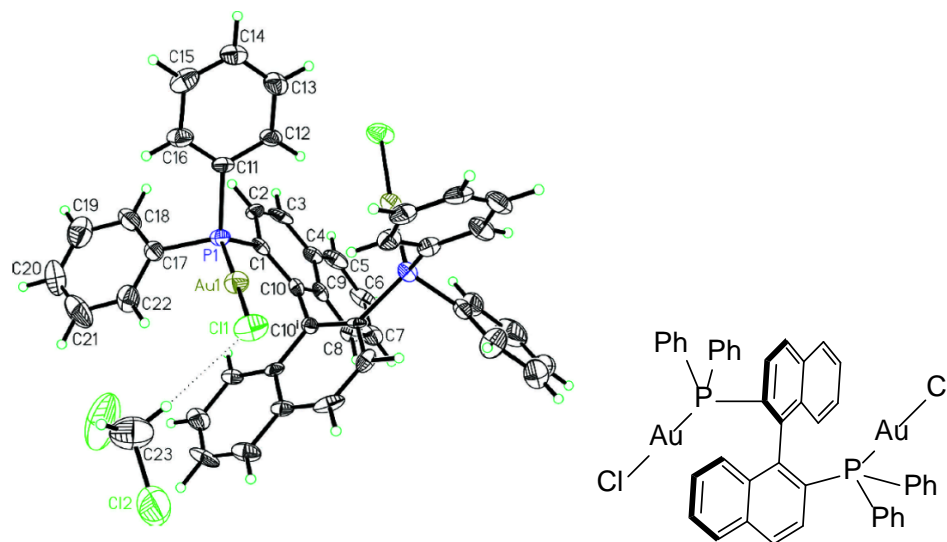
Figure 3.1 Crystal Structure **3.1a**[7]

A. X=6% 82% Yield, 1%ee
B. X=3% 81% Yield, 51%ee
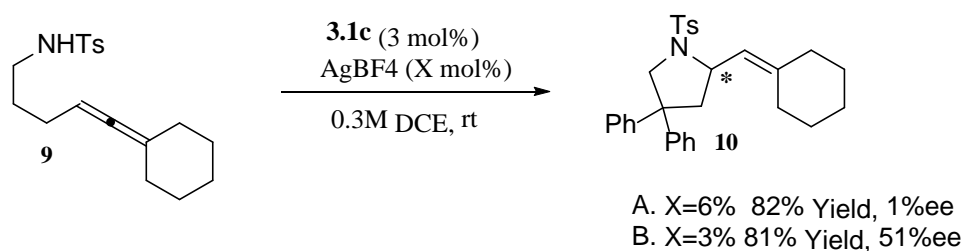
Scheme 3.4 Dependency of Enantioselectivity On The Number of Activated Metal Centers

The use of monodentate chiral ligands in enantioselective gold catalysis has recently shown significant promise and has some important potential benefits over the bisphosphine dinuclear complexes.[8] The most obvious advantage is the lower cost of the catalyst due to using less gold. The ability to use other ligand scaffolds besides phosphines, such as electron rich carbenes or electron deficient phosphite/phosphoramidite ligands, allows the possibility of catalyzing more types of reactions. The following sections will cover the typical ligand scaffolds currently being used in enantioselective gold catalysis as well as providing a brief introduction to the various reactions in which high levels of asymmetric induction have been achieved.

3.2 Common Chiral Ligands Currently Used

As mentioned in the introduction of this chapter, the most prevalent ligand type currently being used in enantioselective gold catalysis is bisphosphine ligands **(Figure 3.2)**. Typically, these ligands are based on axially chiral scaffolds represented by widely used ligand such as BINAP, SEGPHOS, and BIPHEP.[9] These tend to rely on the use of large aromatic substituents on the phosphorus atoms to obtain good selectivities. The amount of synthetic labor necessary to modify these scaffolds makes it extremely difficult for a researcher to investigate structure activity relationships with these types of ligands or to systematically tune electronic properties to allow them to catalyze a wide variety of reactions. These ligands might rely on secondary interactions such as π-π stacking and π-Au stacking to form rigid chiral pockets.[9i] The binuclear structures of gold complexes formed from these ligands has led to questions about the involvement of aurophilic interactions in catalytic intermediates, but the intrinsic role of the two gold atoms is still a matter of debate. Most mechanisms involving these binuclear complexes are depicted as only involving one of the metal centers, which has led to development of the other types of ligands commonly used.
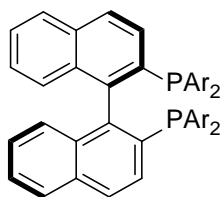
3.1a BINAP $(Ar = Ph)$
3.1b *tol*-BINAP $(Ar = p\text{-tolyl})$
3.1c 3,5-xylyl-BINAP
$(Ar = 3,5\text{-}C_6H_3Me_2)$
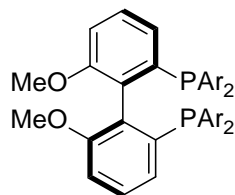
3.2a 4-MeO-3,5-(^{t}-Bu)$_2$ MeO-BIPHEP
$[Ar = 3,5\text{-}(^t\text{-Bu})_2\text{-}4\text{-MeOC}_6H_2]$
3.2b DM-MeOBIPHEP $(Ar = 3,5\text{-Me}_2C_6H_3)$
3.2c MeOBIPHEP $(Ar = Ph)$
3.2d MeO-DTB-BIPHEP
$[Ar = 3,5\text{-}(^t\text{-Bu})_2C_4H_3]$
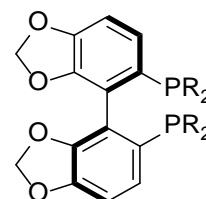
3.3a Cy-SEGPHOS $(R = Cy)$
3.3b DTBM-SEGPHOS
$[R = 3,5\text{-}(^t\text{-Bu})_2\text{-}4\text{-MeOC}_6H_2]$
3.3c = SEGPHOS $(R = Ph)$

n = 1, **3.4a** C$_1$-TUNEPHOS
n = 2, **3.4b** C$_2$-TUNEPHOS
n = 3, **3.4c** C$_3$-TUNEPHOS

3.5 Me-Duphos

3.6 DIPAMP

3.7 H$_8$-BINAP (Ar = Ph)
3.8 xyl-H$_8$-BINAP
(Ar = 3,5-Me$_2$C$_6$H$_3$)

3.9 BIPHEP (Ar = Ph)
3.10 (3,5-xyl)BIPHEP
[Ar = 3,5-Me$_2$C$_6$H$_3$]
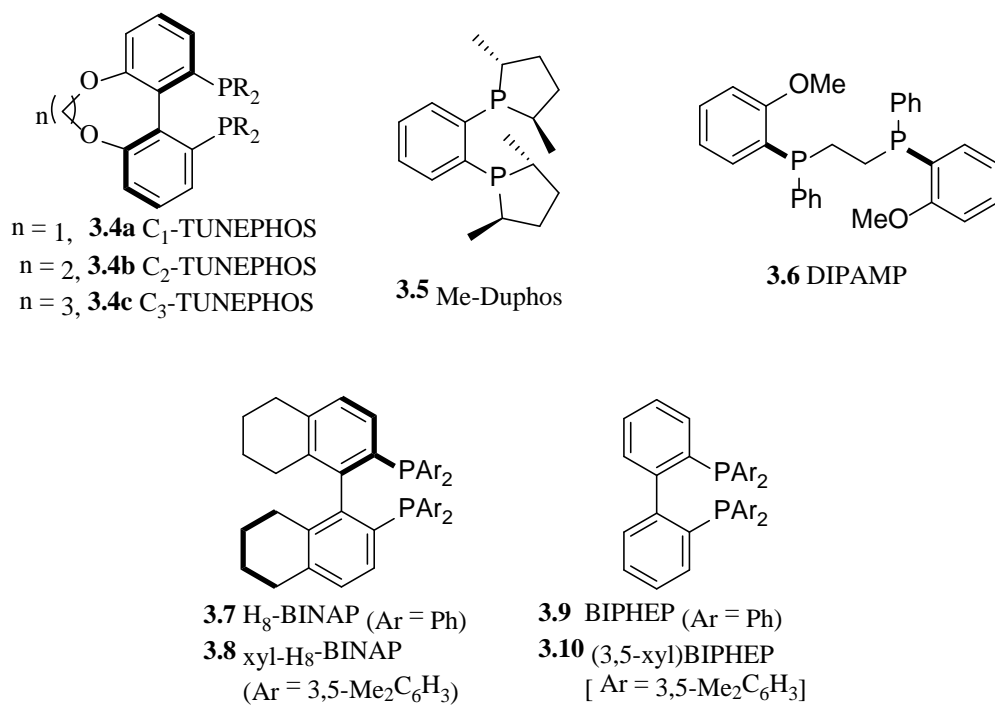
Figure 3.2 Typical Bisphosphines Currently Being Used in Enantioselective Gold Catalysis

The emergence of monodentate ligands in enantioselective gold catalysis has only recently become an active area of research.[8, 10] This has allowed for a wider variety of electron-rich carbene scaffolds and electron-deficient phosphites and phosphoramidites to be used **(Figure 3.3)**. This has significantly broadened the scope of enantioselective gold catalysis and resulted in some interesting debates on how the ligand is promoting high levels of asymmetric induction. The following sections will give a brief introduction into a few of the numerous enantioselective reactions that have been catalyzed using gold complexes of chiral ligands.
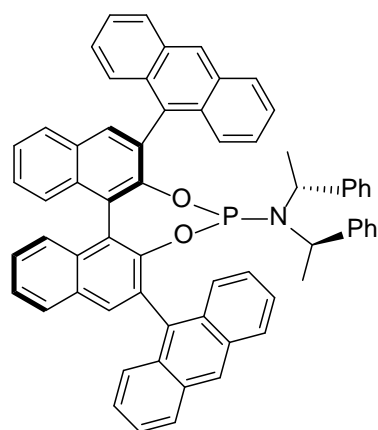
(R,R,R)-**3.11**
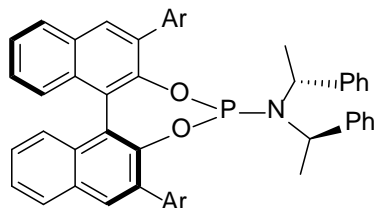
(S,R,R)-**3.12a** (Ar = Ph)
(S,R,R)-**3.12b** [Ar = 2,4,6-(^{i}Pr)$_3$C$_6$H$_2$]
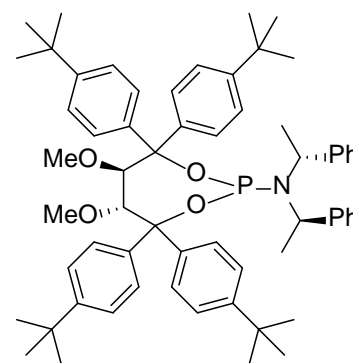
(R,R,R)-**3.13**
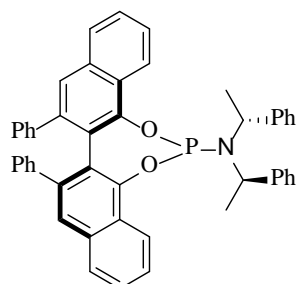
(S,R,R)-**3.14**
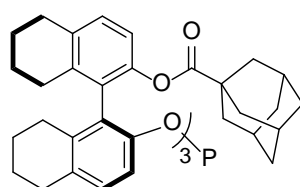
(S)-**3.15**
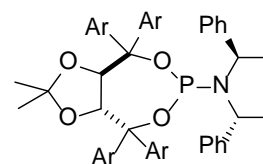
(R,R,R)-**3.16a** (Ar = Ph)
(R,R,R)-**3.16b** [Ar = 4-(OMe)-C$_6$H$_4$]
(R,R,R)-**3.16c** [Ar = 4-(Cl)-C$_6$H$_5$]
(R,R,R)-**3.16d** [Ar = 4-(F)-C$_6$H$_5$]
(R,R,R)-**3.16e** [Ar = 3,5-(CF$_3$)$_2$C$_6$H$_3$]
(R,R,R)-**3.16f** [Ar = 3,5-(^{t}-Bu)$_2$-(OMe)-C$_6$H$_2$]
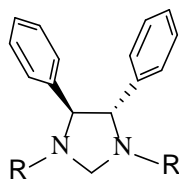
(S,S)-**3.17a** [2-(MeO)C$_6$H$_4$]
(S,S)-**3.17b** [2,4,6-(Me)$_3$Bn]
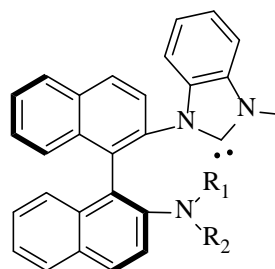
(S)-**3.18a** (R^2 = R^3 = nBu)
(S)-**3.18b** (R^2 = Me, R^3 = Me)
(S)-**3.18c** (R^2 = Bn, R^3 = H)
(S)-**3.18d** (R^2 = R^3 = Bn)

Figure 3.3 Selected Monodentate Ligands in Enantioselective Gold Catalysis

3.3 Enantioselective Gold Catalyzed Intramolecular Reactions

Intramolecular reactions involving gold activating a π-bond toward nucleophilic attack have been far more successful than their intermolecular counterparts. This has allowed the formation of complex bicyclic and heterocyclic compounds that would be very difficult to synthesize otherwise.

3.3.1 Enantioselective π-activation of Allenes

Allenes have proven to be the most succesful substrate for enantioselective gold catalysis. **Scheme 3.5** outlines some of the various skeletal rearrangements that have been catalyzed involving allenes. The first example is an allenene cyclization in which the allene on **11** is activated toward nucleophilic attack by the pendant olefin, resulting in the bicyclic compound **12**.[11] This particular report is interesting because it is one the first examples of moving away from the axially chiral binaphthyl scaffold used in most chiral ligands in gold catalysis. The use of TADDOL-based phosphoramidites allowed for a systematic variation of the ligand structure to achieve higher levels of asymmetric induction. These ligands help solve the issues involved in the tedious synthetic work necessary to derivatize the binaphthyl scaffold. It was found that having an acyclic backbone on the TADDOL phosphoramidite proved to be most efficient.[12] Toste and co-workers studied reactions of **13**, which is very similar substrate, but the resulting carbenoid intermediate reacts further with an alcohol nucleophile, resulting in an enantioselective domino process.[13]

(a).

LAuCl (5.5 mol%)
AgBF$_4$ (5 mol%)
CH$_2$Cl$_2$, rt

11 → **12**

1. **L = 3.16a-3.16f**,
   71-95% yield, 63-86% ee

2. **L = 3.13**
   79-88% yield, 79-965 ee

(b).

TsN + R-OH

[(**3.19**)AuCl] (6 mol%)
AgBF$_4$ (5 mol%)
CH$_3$NO$_2$, rt, 12h

13 → **14**

14 examples
39-95% yield, 72-96% ee

3.19

(c).

3.2b(AuCl)$_2$ (2.5 mol%)
NaBARF (5 mol5)
DCE, -30 °C, 24h

15 → **18**

61-99% yield
84-99% ee

16 → **17**
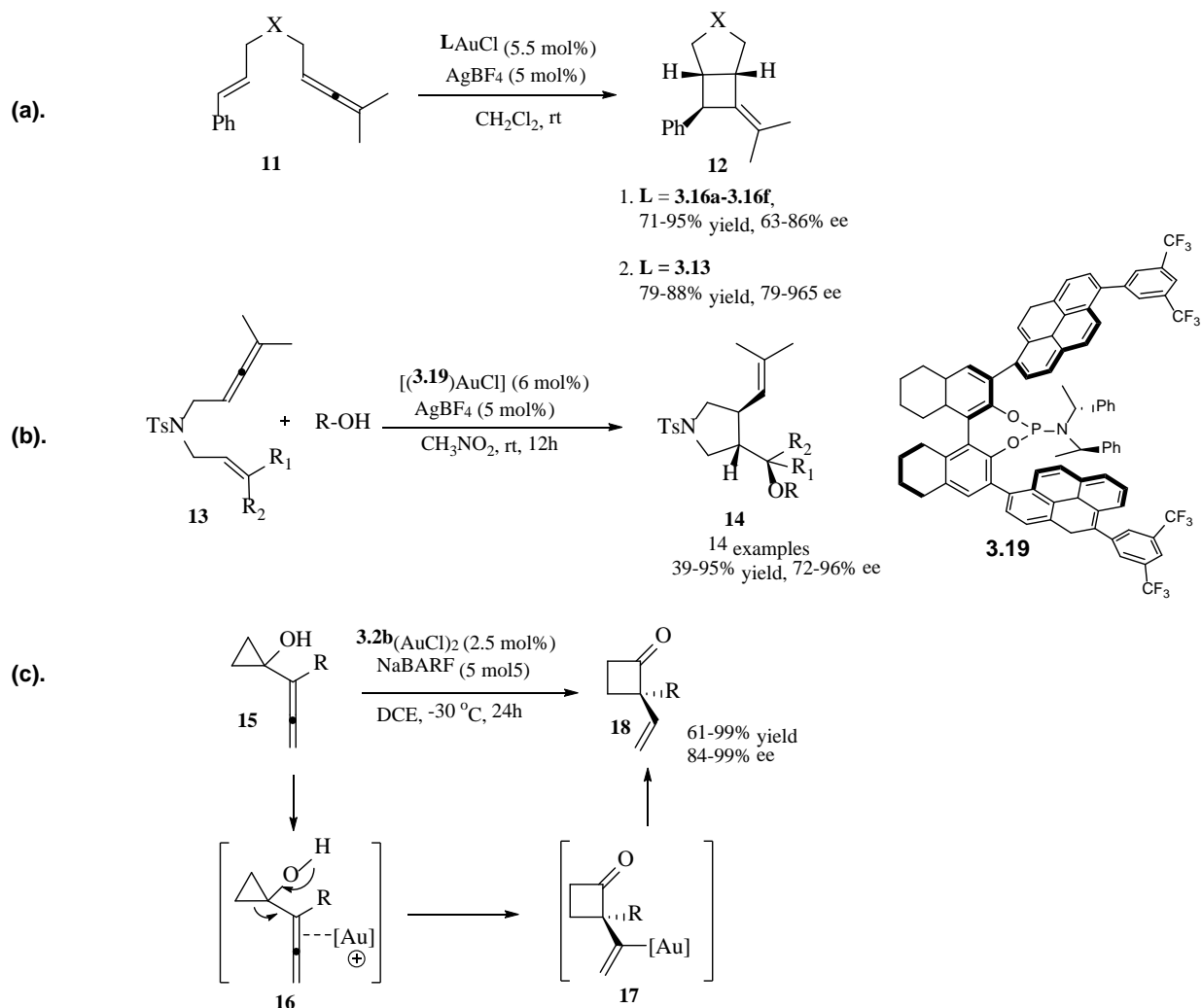
Scheme 3.5 Enantioselective Skeletal Rearrangements Involving Allenes

The ring expansion reaction of **15** was also studied by the Toste group.[14] This is but one of many examples from the Toste group of using of bisphosphine ligands to achieve high levels of enantioselectivity.[15] **Scheme 3.6** outlines a few examples of intramolecular reactions involving internal nucleophiles cyclizing with gold-activated allenes. The hydroarylation of **19** was studied by Widenhoefer and co-workers.[16] It was found that the enantioselectivity was very dependent not only on choice of ligand but also on solvent and counterion.

(a).

3.2a (2.5 mol%)
AgBF₄ (5 mol%)
toluene, -10 °C, 17h

19

20

88% Yield, 92%ee

(b).

NHCbz

[(S)-**3.2a**]Au₂Cl₂ (2.5 mol%)
AgClO₄ (5 mol%)
m-xylene, -40 °C, 24h

21

22

100% Conversion, 81%ee

(c).

OH

3.2a (2.5 mol%)
AgOTs (5 mol%)
toluene, -20 °C, 18h

23

24

76% Yield, 93%ee
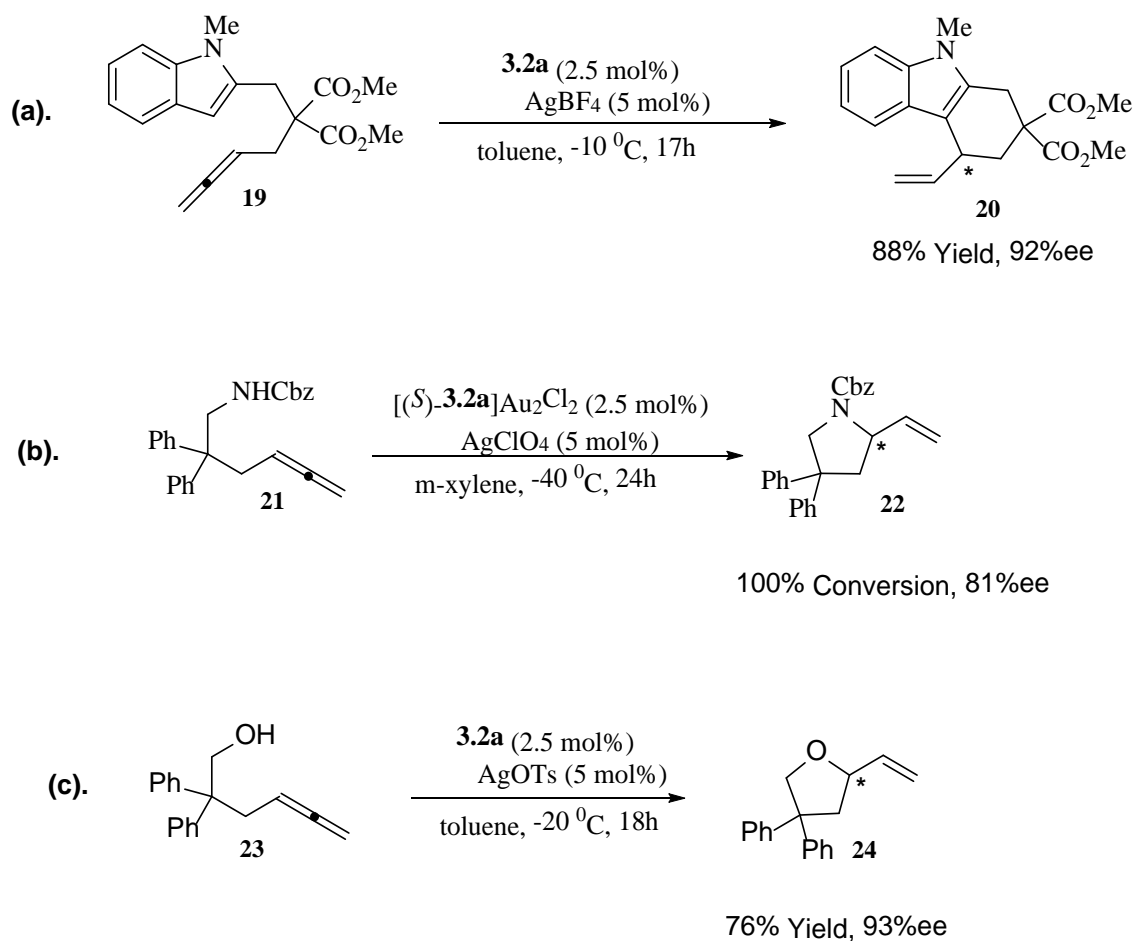
Scheme 3.6 Gold-Catalyzed Intramolecular Cyclization of Allenes

The intramolecular hydroamination of allenes has become one of the benchmark reactions used to test newly developed chiral gold catalysts. This reaction has been studied by numerous groups and has been shown to give a range of selectivities for many types of ligands.[17] In one particular example, the allenyl carbamate **21** was successfully converted to the substituted pyrrollidine using a BIPHEP based catalyst by the Widenhoefer group.[17a] In a similar fashion, the intramolecular hydroalkoxylation of allenols has also been studied by numerous groups, although with somewhat less success than the hydroamination reactions.[18]

3.3.2 Enantioselective π-activation of Alkynes and Alkenes

As mentioned above, enantioselective reactions involving alkynes and especially alkenes are much less developed than those of allenes. The most common enantioselective reactions involving activation of alkynes are enyne cyclizations **(Scheme 3.7)**. It is also well known that these types are reaction are very sensitive to choice of ligand and can give multiple reaction products, which can sometimes be selectively formed by careful choice of ligand.[19]
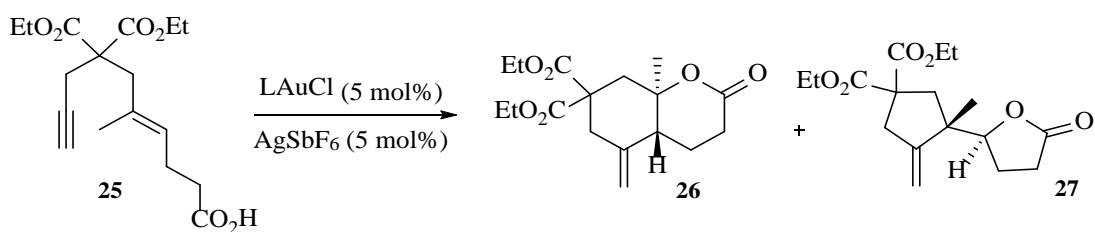
Scheme 3.7 Gold Catalyzed Enantioselective Domino Reaction

Table 3.1: Solvent and Ligand Effect on Gold-Catalyzed Enantioselective Domino Reaction[19]

Entry	Ligand (L)	Solvent	% Yield **26 (27)**	% ee
1	**3.3b**	CH_2Cl_2	81 (8)	2
2	**3.2a**	CH_2Cl_2	71 (7)	46
3	**3.2a**	benzene	76 (8)	83
4	**3.2a**	toluene	77 (9)	85
5	**3.2a**	*m*-xylene	76 (12)	87
6	**3.2d**	*m*-xylene	86 (11)	92

The above reaction proceeds via a competing 6-*exo-dig*/5-*exo-dig* cyclization of **25** upon activation of the alkyne. The resulting gold-carbenoid intermediate is then trapped upon cyclization of the pendant carboxylic acid, resulting in a mixture of **26** and **27**. This is actually a very mild example of how the product ratio can vary in these types of reaction by varying the ancillary ligand or even solvent conditions.[20] However the enantioselectivity is very sensitive to the choice of ligand, with **3.2a** outperforming **3.2b**. Another common reaction type that involves activation of alkynes is cyclopropanation reactions **(Scheme 3.8)**.[21] This particular reaction has an intramolecular variant as well as some intermolecular variants.

Scheme with reagents:

R_1, OR_3 ... **L**AuCl (2.5 mol%), AgSbF$_6$ (5 mol%), CH$_3$NO$_2$ → R_1, OR_3

14

n = 1,2
R_3 = Ac, Piv

L = $_{(R)}$ **3.1c**
or $_{(R)}$ **3.2a**

16

n = 1, 44-91 yields, 15-85% ee
n = 2, 80-98 yields, 75-92% ee
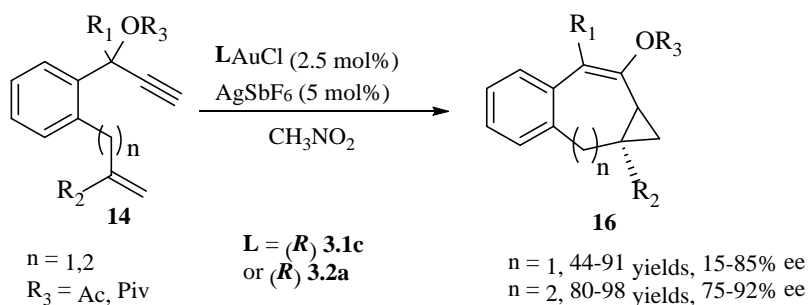
Scheme 3.8 Gold Catalyzed Intramolecular Cyclopropanation

This is another example in which bidentate phosphine ligands have been extensively studied in these particular types of reactions.[22] As mentioned earlier, the use of alkene substrates has been very limited, and it has been debated whether trace Brønsted acid in solution is actually catalyzing the addition to olefins in some cases. With the enantioselective versions, at least some of the reaction has to be catalyzed by the chiral gold complex to produce any asymmetric induction, unless a chiral counterion is being used to achieve asymmetric induction. **Scheme 3.9** outlines some of the few examples involving gold activation of alkenes.[23] Typically, these require activated alkenes such as dienes or allylic alcohols.
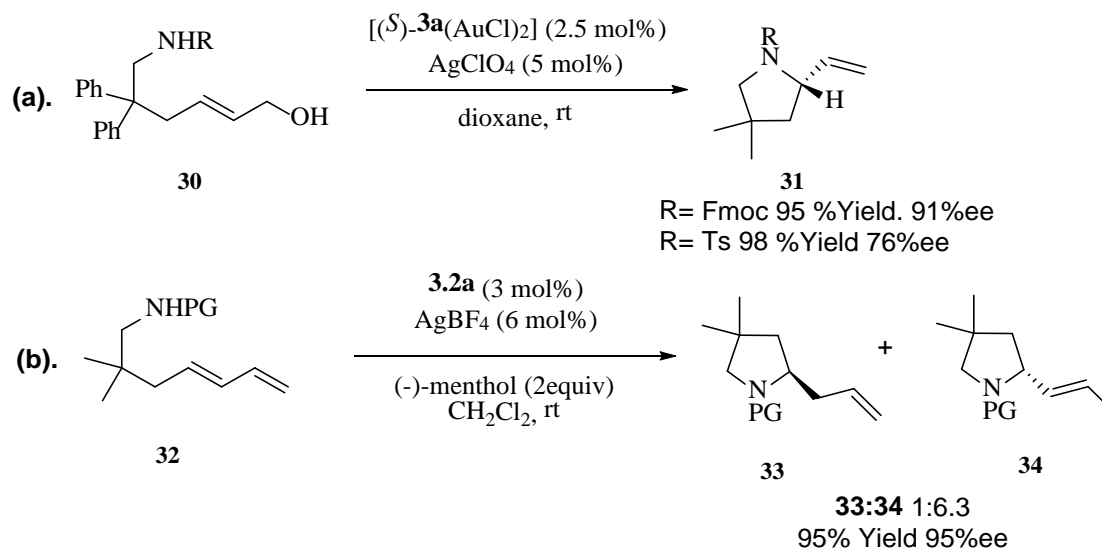
Scheme 3.9 Enantioselective Intramolecular Reactions with Activated Alkenes

The first reaction involves the intramolecular dehydrative hydroamination of allylic alcohols was studied by Widenhoefer's group.[24] It was noticed that the choice of protecting group had a substantial impact on the amount of selectivity achieved, with carbamate protecting groups outperforming sulfonamides. The regio- and enantioselective hydroamination of dienes **32** was studied by Toste group.[25] This is one of the pioneering examples of cooperative Brønsted acid- and gold catalysis where the use of (-)-menthol allowed for a higher level of regioselectivity and did not affect the enantioselectivity. More work is needed on enantioselective gold-catalyzed additions to alkenes to make these reactions comparable in scope to reactions of other π-systems.

3.4 Enantioselective Gold-Catalyzed Intermolecular Reactions

As mentioned in the previous section, the intermolecular addition of nucleophiles to activated C-C multiple bonds remains a challenge in enantioselective gold catalysis. **Scheme 3.9** outlines some of the few reactions that have been reported. The likely reason for intermolecular variations of the above reactions lagging in development behind intramolecular versions is the

inherent mechanism of gold (I) catalysis. The anti-attack of a nucleophile on the activated π-system makes it too difficult to achieve high levels of asymmetric induction.

(a).

[(S)**3.2a**(AuCl)$_2$] (2.5 mol%)
AgOTf (5 mol%)
m-xylene, 100 °C

35 **36**

R = alkyl, aryl   n = 5,7,9

37

6 examples
76-89% yield
71-78% ee

(b).

[(**3.12b**)AuCl] (5 mol%)
AgSbF$_6$ (5 mol%)
CH$_2$Cl$_2$, 25 °C

38 **39**

40

65% yield
88-91% ee

(c).

H$_2$NCbz + Ph

3.2a (2.5 mol%)
AgBF$_4$ (5 mol%)
dioxane, rt, 24h

Ph

NHCbz
89% Yield, 72%ee

41 **42**

43
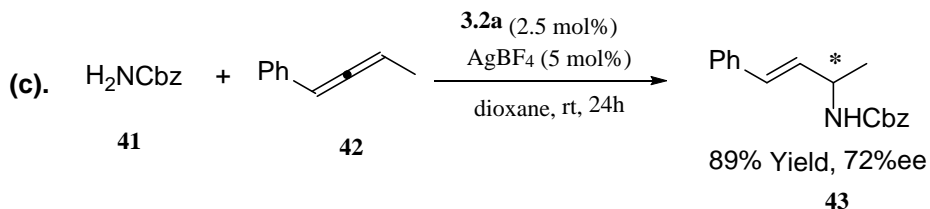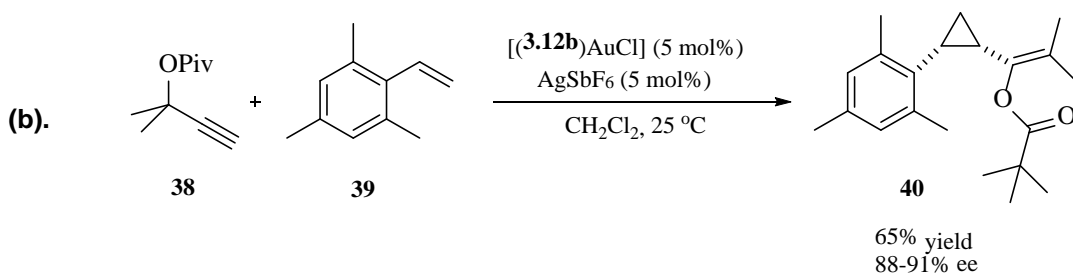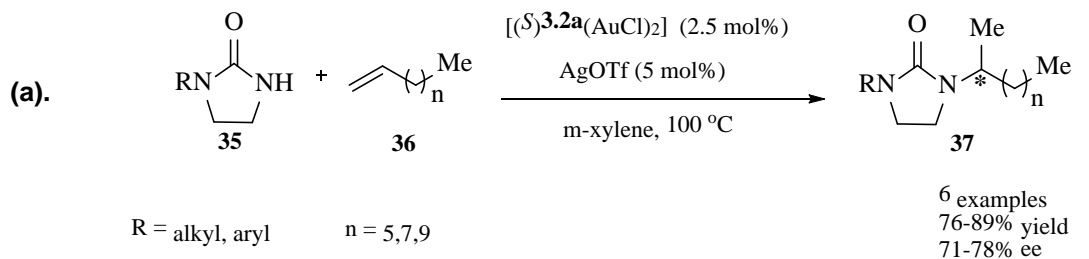
Scheme 3.9 Enantioselective sGold-Catalyzed Intermolecular Additions to Activated π-Systems

Widenhoefer and coworkers discovered the intermolecular hydroamination of olefins **36**[26] with ureas as well as the intermolecular hydroamination of allenes **42**.[27] Toste's group was able to achieve high levels of enantioselectivity in the intermolecular cyclopropanation of various styrene derivatives such as **39**.[28] The following section will discuss a relatively new class of chiral ligands that have started to show some promise in asymmetric gold catalysis.

3.5 Acyclic Diaminocarbenes in Enantioselective Gold Catalysis

The dominance of phosphorus-based ligands as ancillary ligands in enantioselective gold catalysis has been shown in the previous sections of this chapter. Although the first acyclic diaminocarbene complex[29] was synthesized long before the more prevalent NHCs, it was not until 2005 that Slaughter's[30] and Fürstner's[31] groups introduced acyclic carbenes as ancillary ligands in palladium catalysis. Since then, there has been a growing amount of research done with these ligands in several areas of transition metal catalysis. **Figure 3.4** shows some of the more recently reported chiral ADCs used in gold catalysis. The fact that ADCs have wider N-$C_{carbene}$-N bond angles and have more conformational freedom than NHCs will potentially allow for the chiral auxiliaries to be closer to the active site on the substrate. ADCs have also been shown to have some very different steric and electronic properties than NHCs.[30b]

(S)-**3.20a** (R = Ph)
(S)-**3.20b** [R = 4-(CF$_3$)C$_6$H$_4$]
(S)-**3.20c** [R = H]

(S)-**3.21a** (R = H, R' = Me)
(S)-**3.22b** (R = H, R' = iPr)
(S)-**3.23c** (R = Ph, R' = Me)
(S)-**3.24d** (R = Ph, R' = Et)

(S,S)-**3.25**

(R,R)-**3.26**

(R)-**3.27** (R)-**3.28** (S)-**3.29** (R,S,S)-**3.30**
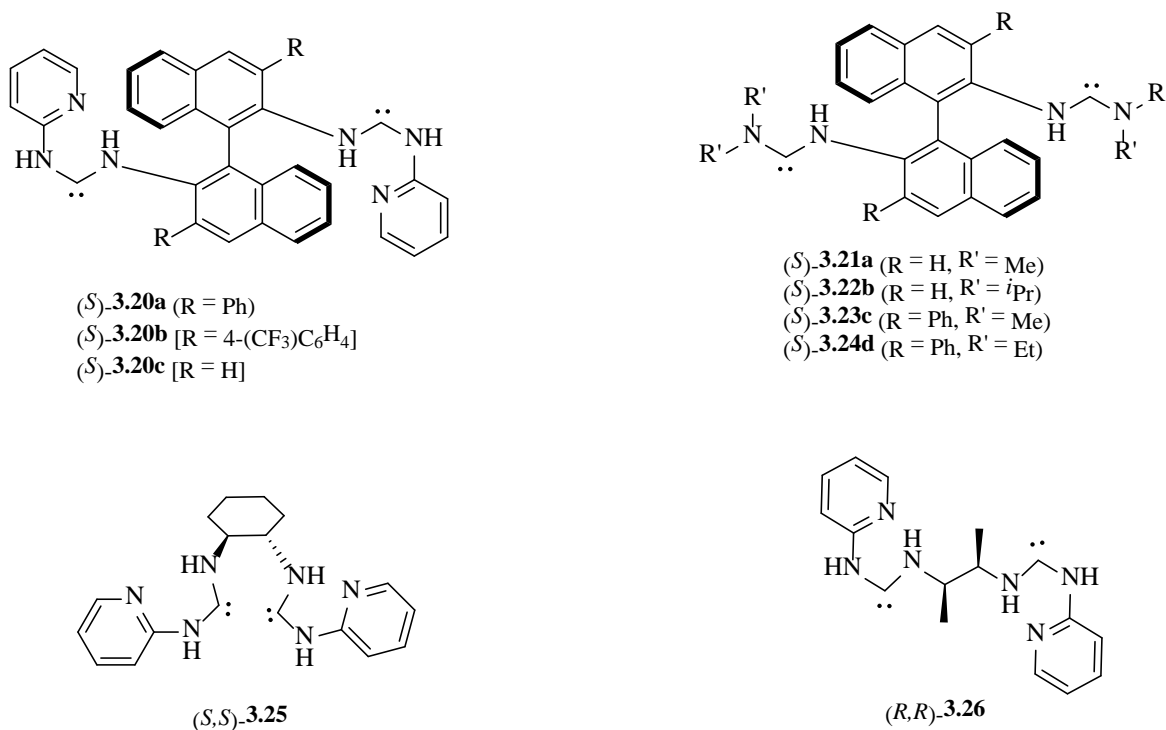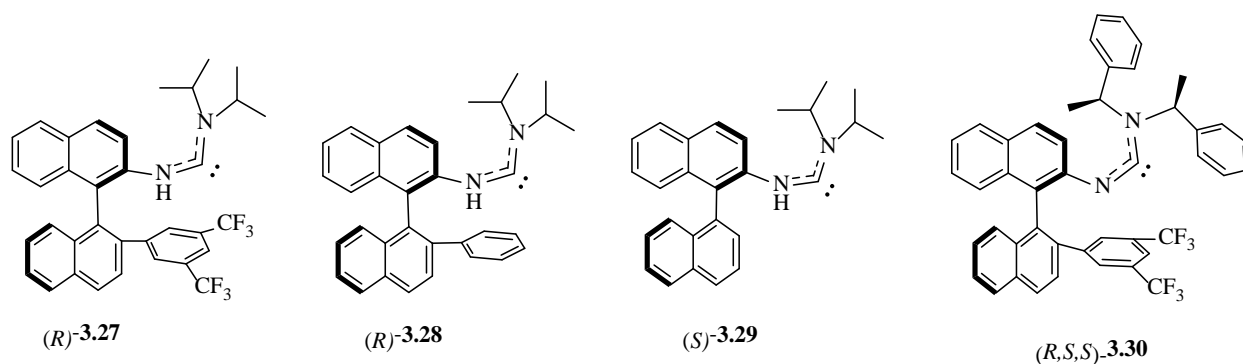
Figure 3.4 Examples of Chiral ADC ligands Used in Gold Catalysis

Espinet was the first to report the use of chiral ADC gold complexes in catalysis, with complex **3.2a** used in the cyclopropanation of styrene with propargyl pivaolate as well as in intramolecular hydroalkoxylations of allenes **(Scheme 3.10)**.[32] The results were discouraging, with only very low to moderate selectivities obtained.
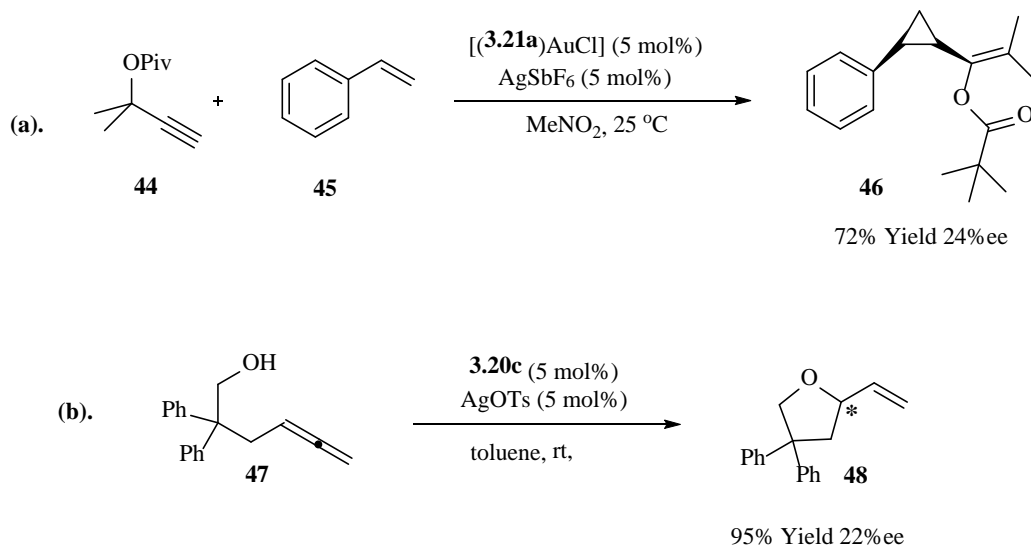
Scheme 3.10 Espinet's reported cyclopropanation and intramolecular hydroalkoxylation reactions catalyzed by Au-ADC complexes

Toste modified this ligand scaffold **(Scheme 3.11)** and was the first to obtain high levels of asymmetric induction using a carbene gold catalyst.[33] By adding the appropriate substituents at

the 3 and 3' positions of the binaphthyl backbone, his group was able to synthesize chromenyl

pivalates from phenols with high asymmetric induction.
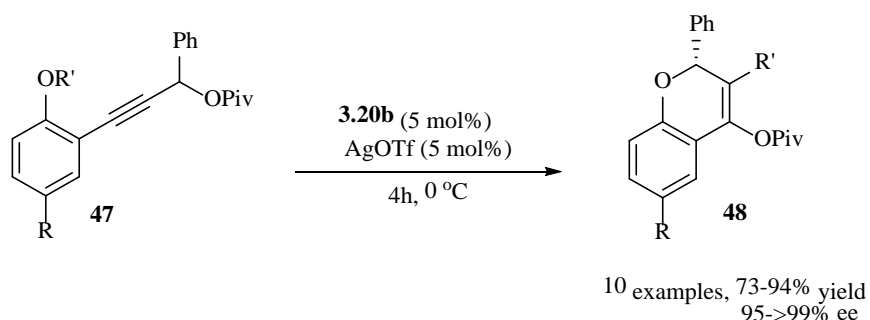
Scheme 3.11 Toste's Dynamic Kinetic Asymmetric Transformation of Propargyl Esters.

Shortly after Toste's publication, Slaughter and coworkers were able to achieve high levels

of asymmetric induction using a monodentate ADC gold complex with variation at the 2'-

position **(Scheme 3.12)**.[34] It was hypothesized that secondary interactions between the aryl

substituent at the 2'-position and the gold were responsible for higher catalytic activities and

higher levels of enantioselectivity.
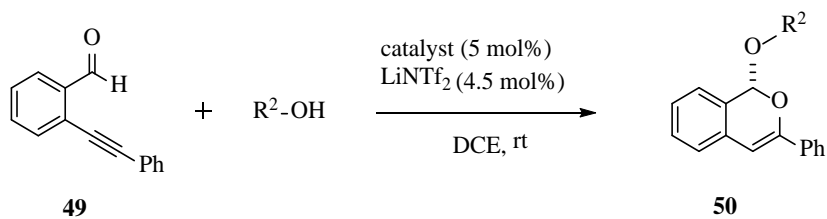
Scheme 3.12 Au-Catalyzed Enantioselective Alkynylbenzaldehyde Cyclizations

Table 3.2: Effect of Ligand on Gold Catalyzed Isochromene Synthesis

Entry	Catalyst	R^2	% Yield **50**	% ee
1	**3.29**	^{i}Pr	12	8

2	**3.28**	^{i}Pr	28	61
3	**3.27**	^{i}Pr	68	84
4	**3.29**	Cy	31	27
5	**3.28**	Cy	5	43
6	**3.27**	Cy	65	98

This is not the first report that invokes some sort of non-covalent interaction to explain how certain catalysts achieve higher levels of asymmetric induction (**Figure 3.5**). Gagné and co-workers invoked π–π stacking between aryl substituents in **A** to explain the formation of a more rigid chiral pocket.[35] Fürstner and coworkers suggested an interaction between the aryl ring of their TADDOL based phosphoramidte **B** and the metal center.[10]
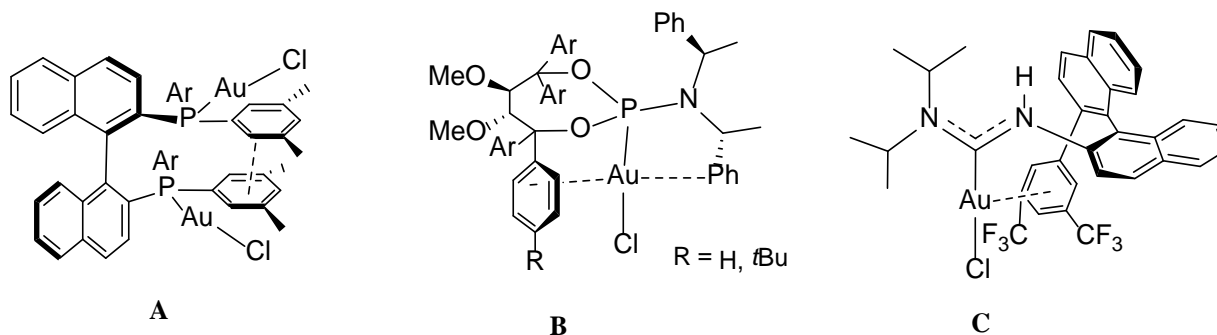
Figure 3.5 Ligand Secondary Interactions in Gold Catalysis

3.6 Conclusion

Gold's ability to create complex organic molecules under extremely mild conditions has led to the desire to achieve these synthetic transformations enantioselectively. Although there has been a lag of asymmetric gold catalysis behind reaction discovery, there have been some very interesting recent reports of enantioselective gold catalysis. This chapter is but a brief

introduction to enantioselective gold catalysis, and the interested reader is pointed to some excellent reviews written on the subject. [3] With improved understanding of the mechanisms behind the reactions catalyzed by gold, strategies to obtain high levels of asymmetric induction and overcome the inherent problems of gold catalysis will likely be discovered. The idea of secondary interactions appearing to be important in achieving better catalytic activities and selectivities might be important for the future for chiral ligand design in gold catalysis. Therefore, improved understanding of these interactions is necessary, as is a means of determining whether these interactions are present in solution as well as in the solid state. Another key issue left to solve in asymmetric gold catalysis is the design of ligands to achieve enantioselective gold (III) catalysis. Given the high activity in area of research by many groups, it seems likely that these issues will be addressed in time.

3.7 References

1.   Hutchings, G. J. *J. Catal.* **1985**, *96*, 292. Nkosi, B.; Coville, N. J.; Hutchings, G. J. *J. Chem. Soc. Chem. Commun.* **1988**, 71. (b) Nkosi, B.; Coville, N. J.; Hutchings, G. J. *Appl. Catal.* **1988**, *43*, 33. (c) Nkosi, B.; Coville, N. J.; Hutchings,G. J.; Adams, M. D.; Friedl, J.; Wagner, F. E. *J. Catal.* **1991**, *128*,366. (d) Nkosi, B.; Adams, M. D.; Coville, N. J.;   Hutchings, G. J. *J. Catal.* **1991**, *128*, 378. (e) Hutchings, G. J. *Gold Bull.* **1996**, *29*, 123; *Catal. Today* **2002**, *72*, 11. (f) Hutchings, G. J. *Spec. Chem. Mag.***2003**, 12. (g).Ito, Y.; Sawamura, M.; Hayashi, T., *J. Am. Chem. Soc.,***1986,** *108*, 6405-6406.

2.   Munoz, M. P.; Adrio, J.; Carretero, J. C.; Echavarren, A. M. *Organometallics,* **2005**, *24*, 1293–1300.

3.   For pertinent reviews on asymmetric gold catalysis, see: (a) Pradal, A.; Toullec, P. Y.; Michelet, V. *Synthesis* **2011**, 1501. (b) Shapiro, N. D.; Toste, F. D. *Synlett* **2010**, 675. (c)

Bongers, N.;Krause, N. *Angew. Chem., Int. Ed.* **2008**, *47*, 2178. (d) Widenhoefer, R.A. *Chem. Eur. J.* **2008**, *14*, 5382.

4.   Handa, S., Lippincott, D. J., Aue, D. H. and Lipshutz, B. H. *Angew. Chem. Int. Ed.* **2014**, *53*, 10658–10662

5.   Schmidbaur, H.; Schier, A. *Chem. Soc. Rev.* **2012**, *41*, 370.

6.   (a). Aikawa, K., Kojima, M. and Mikami, K., *Adv. Synth. Catal.*, **2010** *352*, 3131–3135. (b). Lalonde, R. L.; Sherry, B. D.; Kang, E. J.; Toste, F. D., *J. Am. Chem. Soc.* **2007**, *129*, 2452–2453.

7.   Bats, J.W.; Hamzic, M.; Hashmi, A.S.K,; *Acta. Cryst.* **2007,** E63, m2344

8.   Cera, G.; Bandini, M.; *Isr. J. Chem.* **2013**, *53*, 848-855

9.   (a) Johansson, M. J.; Gorin, D. J.; Staben, S. T.; Toste, F. D. *J. Am. Chem. Soc.* **2005**, *127*, 18002. (b) Munoz, M. P.; Adrio, J.;Carretero, J. C.; Echavarren, A. M. *Organometallics* **2005**, *24*, 1293.(c) Tarselli, M. A.; Chianese, A. R.; Lee, S. J.; Gagne, M. R. *Angew. Chem., Int. Ed.* **2007**, *46*, 6670. (d) Liu, C.; Widenhoefer, R. A. *Org. Lett.* **2007**, *9*, 1935. (e) Zhang, Z.; Widenhoefer, R. A. *Angew. Chem.,Int. Ed.* **2007**, *46*, 283. (f) LaLonde, R. L.; Sherry, B. D.; Kang, E. J.;Toste, F. D. *J. Am. Chem. Soc.* **2007**, *129*, 2452. (g). Chao, C.-M.; Beltrami, D.; Toullec, P. Y.; Michelet, V. *Chem. Commun.* **2009**, 6988. (h) Pradal, A.; Chao, C.-M.; Toullec, P. Y.; Michelet, V. *Beilstein J. Org. Chem* **2011**, *7*, 1021. (i). Tarselli, M.A.; Chianese, A.R.; Lee, S.J.; Gagne, M.R.; *Angew. Chem. Int. Ed.*, **2007**, *46*, 6670-6673

10.   Teller, H.; Corbet, M.; Mantilli, L.; Gopakumar, G.; Goddard, R.; Thiel, W.; Fürstner, A.; *J. Am. Chem. Soc.*, **2012** *134* (37), 15331-15342

11. For comprehensive review on TADDOL chemistry, see; Seebach, D.; Beck, A. K.; Heckel,A., *Angew. Chem., Int. Ed.,* **2001,** *40*, 92-138.

12. see reference 10

13. Gonzalez, A. Z.; Benitez, D.; Tkatchouk, E.; Goddard, W. A., III; Toste, F. D., *J. Am.Chem. Soc.,* **2011,** *133*, 5500-5507

14. Kleinbeck, F.; Toste, F. D., *J. Am. Chem. Soc.,* **2009,** *131*, 9178-9179.

15. Wang, Y-M.; Lackner, A.; Toste, F.D.; *Acc. Chem. Res.* **2014**, *47,* 889-901

16. Liu, C.; Widenhoefer, R. A., *Org. Lett.,* **2007,** *9*, 1935-1938

17. (a). Zhang, Z.; Liu, C.; Kinder, R. E.; Han, X.; Qian, H.; Widenhoefer, R. A., *J. Am. Chem. Soc.,* **2006,** *128*, 9066-9073. (b) Zhang, Z.; Bender, C. F.; Widenhoefer, R. A., *J. Am. Chem. Soc.,* **2007,** *129*, 14148-14149; (c) Zhang, Z.; Bender, C. F.; Widenhoefer, R. A., *Org. Lett.,* **2007,** *9*, 2887-2889.

18. (a) Hamilton, G. L.; Kang, E. J.; Mba, M.; Toste, F. D., *Science,* **2007,** *317*, 496-499; (b) Aponick, A.; Biannic, B., *Org. Lett.,* **2011,** *13*, 1330-1333. (c). Aikawa, K.; Kojima, M.; Mikami, K., *Adv. Synth. Catal.,* **2010,** *352*, 3131-3135

19. Sethofer, S. G.; Mayer, T.; Toste, F. D., *J. Am. Chem. Soc.,* **2010,** *132*, 8276-8277.

20. Nunez, E.J.; Echavarren, A.M. *Chem Rev*. **2008**, 108, 3326-3350. (b). Bartolome ́, C.; Ramiro, Z.; Pe ́rez-Gala ́n, P.; Bour, C.; Raducan, M.; Echavarren, A. M.; Espinet, P. *Inorg. Chem.* **2008**, 47, 11391−11397.

21. Watson, I. D. G.; Ritter, S.; Toste, F. D., *J. Am. Chem. Soc.,* **2009,** *131*, 2056-2057.

22. Wang, Y-M.; Lackner, A.; Toste, F.D.; *Acc. Chem. Res.* **2014**, *47,* 889-901

23. Chiarucci, M.; Bandini, M.; *Beilstein J. Org. Chem.*, **2013**, *9*, 2586-2614

24. Mukherjee, P.; Widenhoefer, R. A., *Angew. Chem., Int. Ed.,***2012,** *51*, 1405-1407.

25. Kanno, O., Kuriyama, W., Wang, Z. J. and Toste, F. D., *Angew. Chem. Int. Ed.*, 2011, *50*, 9919–9922.

26. Zhang, Z.; Lee, S. D.; Widenhoefer, R. A., *J. Am. Chem. Soc.,***2009,** *131*, 5372-5373.

27. Butler, K.L.; Tragni, M.; Widenhoefer, R.A., *Angew. Chem. Int. Ed.*, **2012**, *51*, 5175-5178

28. Johansson, M. J.; Gorin, D. J.; Staben, S. T.; Toste, F. D., *J. Am. Chem. Soc.,* **2005,** *127*, 18002-18003. (b) Teller, H.; Flugge, S.; Goddard, R.; Furstner, A., *Angew.Chem. Int. Ed.,***2010,** *49*, 1949- 1953.

29. Tschugajeff (Chugaev), L.; Skanawy-Grigorjewa, M. *J. Russ. Chem. Soc*. **1915**, 47, 776.

30. Moncada, A.; Khan, M.A.; Slaughter, L.M.; *Tett. Lett.* **2005**, *46*, 1399-1403, (b). Slaughter, L.M. *ACS Catal.* **2012**, *2,* 1802-1816

31. Kremzow, D., Seidel, G., Lehmann, C. W. and Fürstner, A. *Chem. Eur. J*., **2005**, *11*, 1833–1853.

32. Bartolome, C. ; Cuadrado, D.; Ramiro, Z.; Espinet, P.; *Inorg. Chem.*, **2010**, *49,* 9758-9764

33. Wang, Y.-M.; Kuzniewski, C. N.; Rauniyar, V.; Hoong, C.; Toste, F.D., *J. Am. Chem. Soc.,* **2011,** *133*, 12972-12975.

34. Handa, S.; Slaughter, L.M.; *Angew. Chem. Int. Ed.* **2012**, *51*, 2912-2915

35. Tarselli, M.A.; Chianese, A.R.; Lee, S.J.; Gagne, M.R.; *Angew. Chem. Int. Ed.*, **2007**, *46*, 6670-6673

CHAPTER IV

DEVELOPMENT AND CATALYTIC ACTIVITY OF CHIRAL MONODENTATE ACYCLIC

DIAMINOCARBENE GOLD COMPLEXES

4.1 Introduction

   Chiral monodentate ligands have recently emerged as a promising solution to solving some

of the challenges involved with achieving high asymmetric induction in enantioselective gold

catalysis.[1] The most successful monodentate ligand scaffold currently being used in gold

catalysis is the relatively weakly donating phosphoramidite ligand, typically containing either

BINOL **4-1** or TADDOL **4-2** backbones (**Figure 4.1**). These ligand have been successfully used

in numerous enantioselective gold catalyzed reactions.[2]

4-1   **4-2**
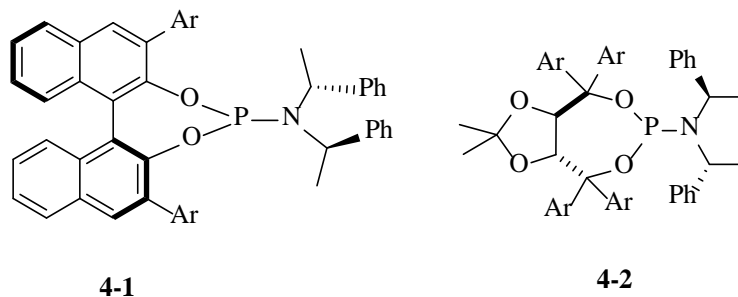
Figure 4.1 Phosphoramidites in Asymmetric Au[I] Catalysis

   However, strongly donating carbene ligands have recently started to emerge as another

potentially useful monodentate ligand type in gold catalysis (**Figure 4.2**).[3] Although they have

not achieved the generally high levels of selectivity seen with phosphoramidite ligands, there

have been some reported reactions where moderate to good selectivities were achieved (**Scheme

4.1**). Mascarenas and coworkers used a chiral NHC-Au(I) complex **4-3** to catalyze the [4+2]

cycloaddition reaction of allenamide (**1**) with dienes (**2**).[4a] The presence of two handles for steric

tuning on the N-substituent of the NHC as well as the 2'-substituent of the binaphthyl backbone allowed relatively high selectivities up to 91 %ee to be obtained.

4-3: R= *c*-hex

4-4

4-5: pyrrolidine
4-6: dimethyl

4-7
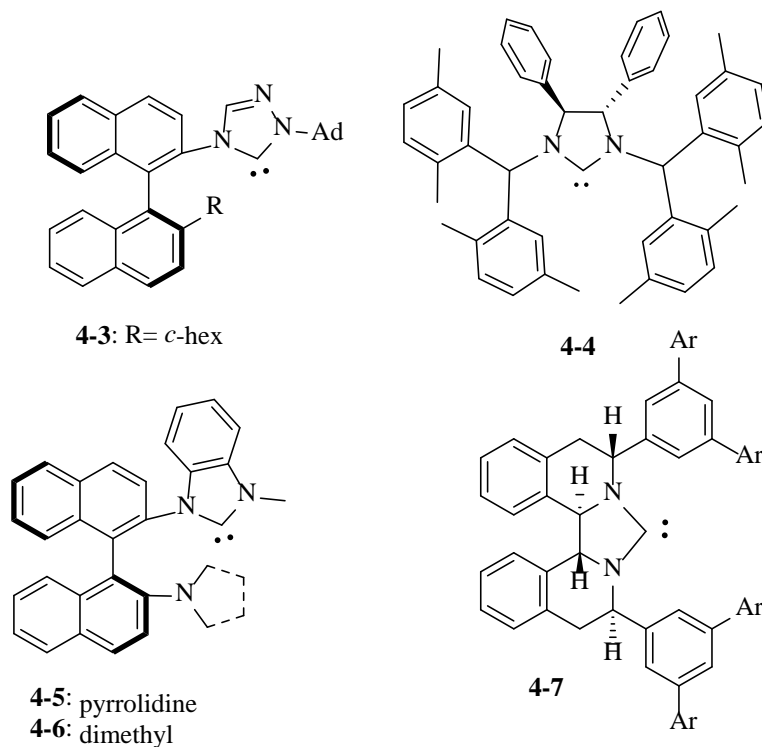
Figure 4.2 Chiral NHCs in Asymmetric Au^I Catalysis

1

2

(**4-3**)AuCl (5 mol%)
AgNTf$_2$ (5 mol%)
CH$_2$Cl$_2$, 10 ^{0}C, 3h

51% Yield, 91%ee

MeO$_2$C

MeO$_2$C

3

(**4-4**)AuCl (6 mol%)
AgSbF$_6$ (6 mol%)
MeOH rt 11h

MeO$_2$C

MeO$_2$C

MeO

91% Yield, 59%ee
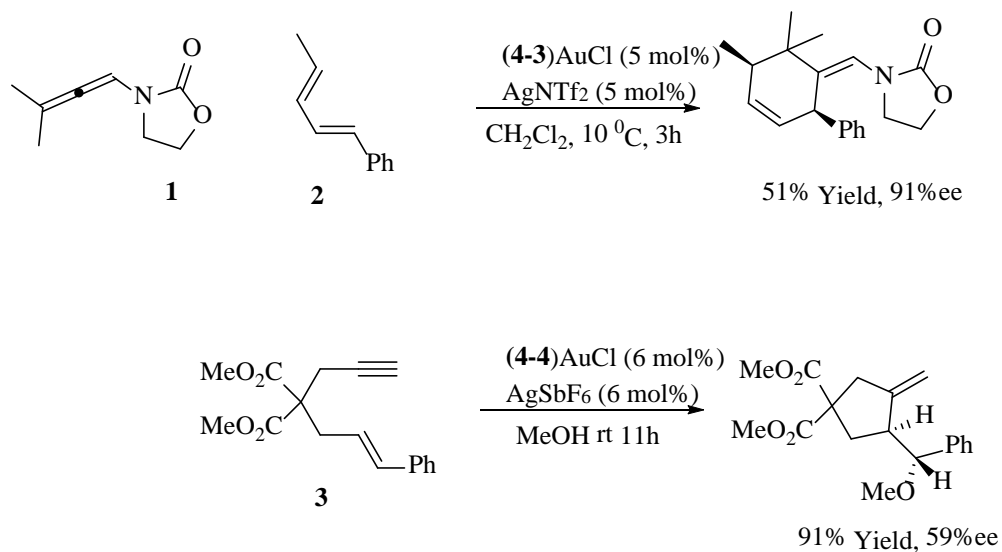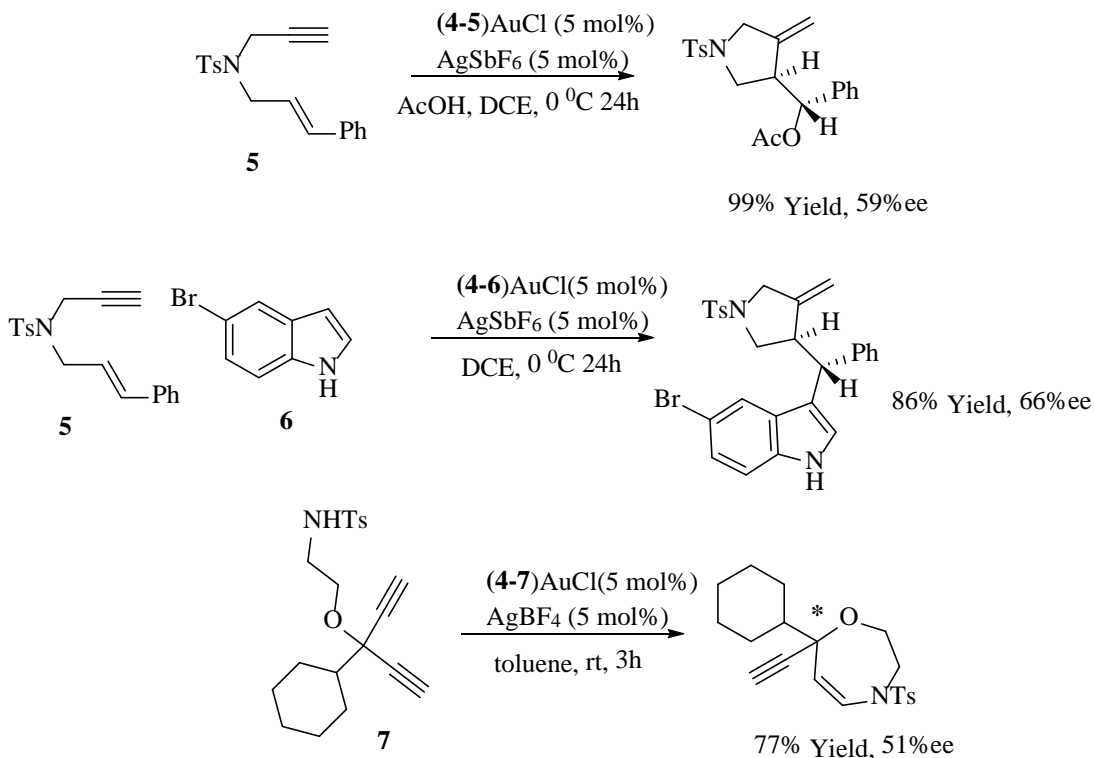
Scheme 4.1 Asymmetric NHC-Au^I Catalyzed Reactions

With the enyne cyclization being a ubiquitously studied reaction in gold catalysis,[5] it is not surprising that numerous groups have investigated asymmetric variants of this reaction.[6] Tomioka and coworkers used a new class of chiral NHC gold complexes **4-3** to catalyze the domino reaction of 1,6-enyne **3** in the presence of methanol to trap the carbenoid-type intermediate.[6c] Although good yields were achieved for the reaction, only modest selectivities up to 59 % ee were seen. Using the axially chiral binaphthyl backbone **4-5** and **4-6** with amino substituents at the 2'-position, Shi and coworkers were able to achieve similar selectivities around 60 % ee when performing the acetoxycyclization of 1,6 enyne **5** as well as the domino cycloisomerization/hydroarylation using an indole nucleophile **6**.[6d,6e] Using **4-7** the desymmetrization reaction of diyne **7** was studied by Czekelius and coworkers.[6f] In this reaction, only modest selectivities of 51 %ee were achieved.

Slaughter and coworker were the first to achieve high levels of asymmetric induction using a monodentate carbene ligand in gold catalysis (**Scheme 4.2**).[7] The use of acyclic diaminocarbene ligand **4-20a** in place of the more well-known NHCs allowed for significantly enhanced selectivities of up to 99 % ee to be obtained. Since one of the major issues is that the ligand is approximately 180° away from the active site in gold catalysis, ADCs offer some potential advantages over their NHC counterparts both electronically and conformationally.[8a]
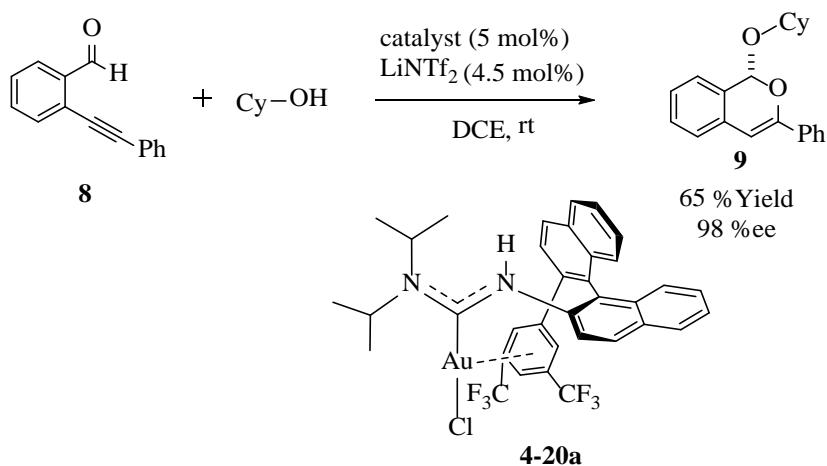
Scheme 4.2 First Highly Selective Au-catalyzed Reaction with Monodentate Carbene

ADCs have been suggested to be stronger σ-donors than NHCs based on a modified Tolman electronic parameter derived from Rh-CO stretching frequencies.[8b] However, one needs to be careful when correlating ligand properties measured on one metal with properties and reactivity at a different metal.[9] Since they lack cyclic backbones, ADCs have more conformational flexibility, which might allow them to have different types of interactions with the substrate. The wider N-C$_{carbene}$-N bond angles of 115-120°, compared with 104-107° for NHCs, might allow the chiral substituents to be closer to the catalytic active site, potentially resulting in higher asymmetric induction. In the work reported by Slaughter and coworkers, it was hypothesized that

an interaction between the aryl substituent at the binaphthyl 2'-position created a more rigid chiral pocket and caused the higher selectivities to be observed.

This chapter discusses the synthesis and catalytic application of an expanded series of chiral monodentate ADC gold complexes. The use of a gold-templated isocyanide route to synthesize a small library of ADC gold complexes has significant advantages over routes involving reaction of the free carbenes with the gold(I) precursor. Since free ADCs are very sensitive and prone to dimerization, the metal-templated isocyanide route allows for much easier synthesis of a large library of catalysts starting from commercially available chiral and achiral amines. The importance of the location of the substituent on the binaphthyl backbone was determined by comparing a series of 3-aryl substituted binaphthyl ADCs to a series of 2'-aryl substituted binaphthyl ADCs. This was followed up by determining what type of substituent was most effective at achieving high levels of asymmetric induction by expanding on the series of 2'-substituted binaphthyl ADCs to include alkyl, benzyl, and aryl substituents. The last influencing factor was determining what substituents from the amine used to synthesize the ADCs were most effective by screening a variety of commercially available amines. The goal of doing this was to allow for future rational ligand design by understanding some structure activity relationships.

4.2 Results and Discussion

Given previous successes in enantioselective catalysis with chiral ADC-gold complexes that bear aryl substituents at the 2'-position of the binaphthyl unit, it was decided to investigate how ADC ligands with substituents at the 3 position of the binaphthyl backbone would compare. There have been several protocols developed for attaching substituents at the 3 and 3' positions of BINOL (1,1′-Binaphthyl-2,2′-diol) and BINAM (1,1′-Binaphthyl-2,2′-diamine) derivatives.[10] A modification of a procedure reported by Chong and coworkers[10a] was used to attach a single

aryl group at the 3'-position of the binaphthyl backbone (**Scheme 4.3**). Commercially available

BINOL was converted into the MOM-protected alcohol **4-8** using the sequence listed below. **4-8**

was treated with n-Butyl lithium and the reaction was quenched with dibromotetrachloroethane

to brominate the 3-position resulting in **4-9**. This allowed for standard Suzuki coupling

procedures to be employed to attach various aryl substituents at the 3 position resulting in

products **4-10(a-c).** The yields for the Suzuki coupling are outlined in **Table 4.1**.
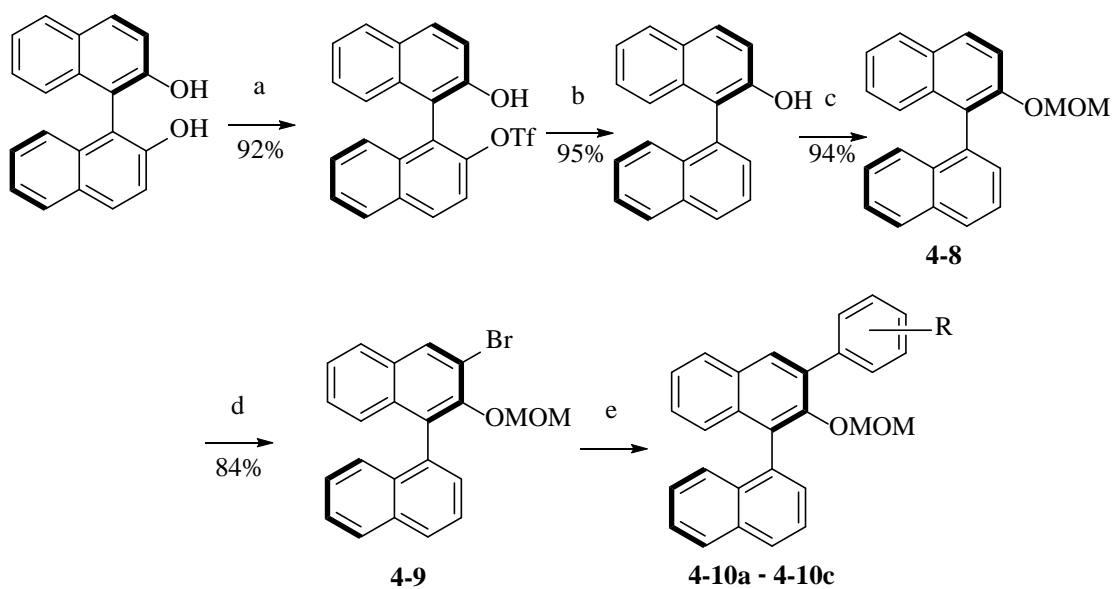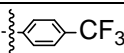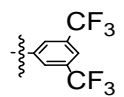
(a) Tf$_2$O, ^{i}Pr$_2$NEt, DCM; (b) H$_2$, Pd/C, EtOH; (c) NaH, MOMCl, THF (d) nBuLi, C$_2$Br$_2$Cl$_4$;

(e), ArB(OH)$_2$, Pd(Ph$_3$P)$_4$, Na$_2$CO$_3$ (2 *M*), DME

Scheme 4.3 Synthetic Outline for **4-10(a-c)**

Table 4.1: Suzuki Coupling Results

Entry	Label	Ar	% Yield
1	**4-10a**	$\{$⟨⟩-OMe	85

2	**4-10b**	⸝⟨⟩–CF₃	92
3	**4-10c**	⸝⟨⟩ with CF₃ / CF₃	84
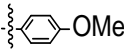
After removal of the alcohol protecting group, the remainder of the synthesis followed a procedure previously reported by the Slaughter group.[7] After converting the alcohol **4-11(a-c)** to the triflate **4-12(a-c)**, the resulting product underwent a Buchwald-Hartwig amination reaction with benzyl amine to give **4-13(a-c)** using conditions previously reported (**Scheme 4.4**).[7] Although the yields are only modest for the amination step, (**Table 4.2**) scaling up the reaction allowed for the synthesis of significant enough quantities to move forward with the syntheses.
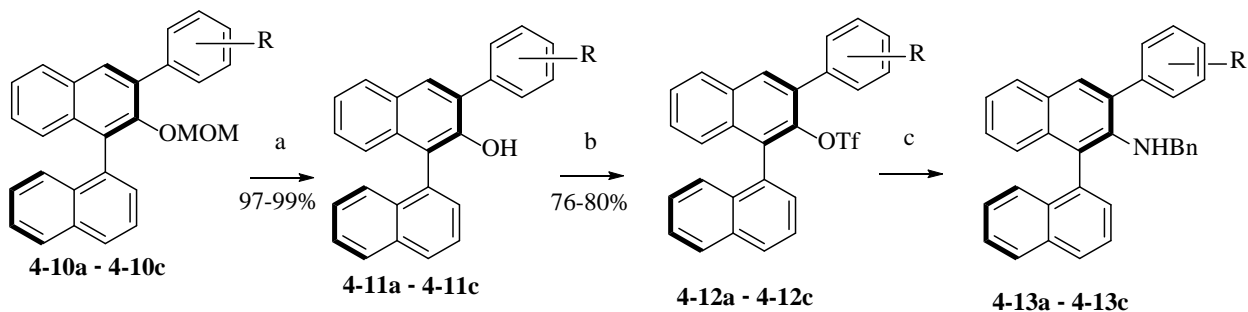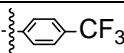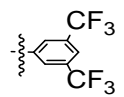
(a) Amberlyst-15, THF:MeOH (1:1); (b) Tf₂O, DIPEA, DCM; (c) Pd(OAc)₂, Xantphos, BnNH₂, Cs₂CO₃, Toluene

Scheme 4.4 Syntheses of 3-subsitituted Benzyl Amines **4-13(a-c)**

Table 4.2: Buchwald-Hartwig Amination Results

Entry	Label	Ar	% Yield
1	**4-13a**	⸝⟨⟩–OMe	56

2	**4-13b**	![CF3 aryl] -CF₃	49
3	**4-13c**	CF₃ / CF₃	51
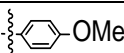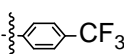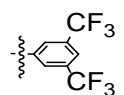
The straightforward synthesis of the isocyanide derivatives is outlined in **Scheme 4.5**. After removal of the benzyl group, the resulting primary amines **4-14(a-c)** were formylated using formic acid. The resulting formamides **4-15(a-c)** were then dehydrated using POCl₃, resulting in the desired isocyanides **4-16(a-c)**.
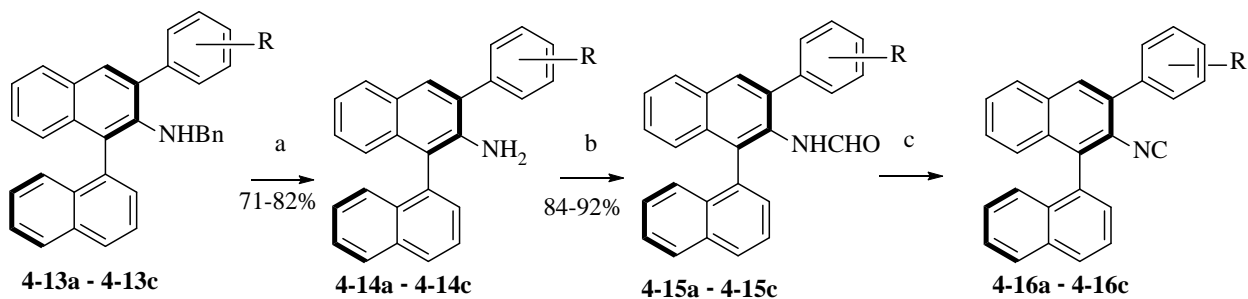
(a) H₂, Pd/C DCM:MeOH; (b) HCO₂H, benzene, Dean-Stark; (c) *i*Pr₂NH, POCl₃, DCM

Scheme 4.5 Synthetic Outline for Isocyanides **4-16(a-c)**

Table 4.3 Isocyanide Synthesis Results

Entry	Label	Ar	% Yield
1	**4-16a**	-OMe	95
2	**4-16b**	-CF₃	87
3	**4-16c**	CF₃ / CF₃	84

To complete the syntheses of the desired ADC gold complexes (**Scheme 4.6**) the isocyanides **4-16(a-c)** were allowed to react with (THT)AuCl. The resulting isocyanide gold complexes **4-17(a-c)** were purified by filtering through a plug of Celite and recrystallized from CH_2Cl_2:Hexanes. The high electrophilicity of gold allowed for the synthesis of ADC complexes **4-18(a-c)** via nucleophilic attack of amines on the gold-bound isocyanides **4-17(a-c)**. The ADC gold complexes were purified by filtering through a plug of Celite and recrystallizing from CH_2Cl_2:Hexanes to give analytically pure **4-18(a-c)**. Although a symmetrical amine was used in the synthesis of these complexes there still appears to be two conformational isomers in solution as can be seen in the NMR of **4-18c** shown in **Figure 4.3**.
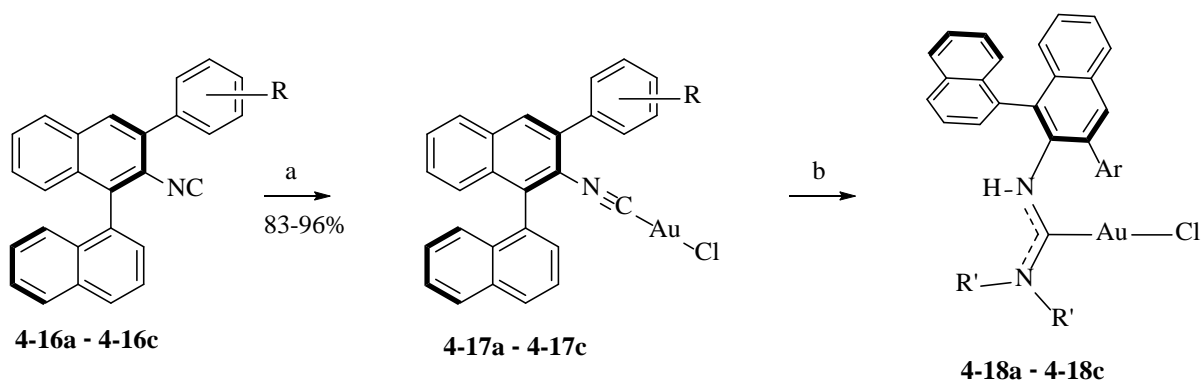
(a) (THT)AuCl, DCM; (b) R'$_2$NH, CHCl$_3$

Scheme 4.6 Syntheses of 3-Substitued Binaphthtyl Gold ADC Complexes.

Table 4.4 ADC Gold Complex Synthesis

Entry	Label	Ar	R'	% Yield
1	**4-18a**	$\{$◯-OMe	*i*Pr	78
2	**4-18b**	$\{$◯-CF$_3$	*i*Pr	72

3	**4-18c**		*i*Pr	71
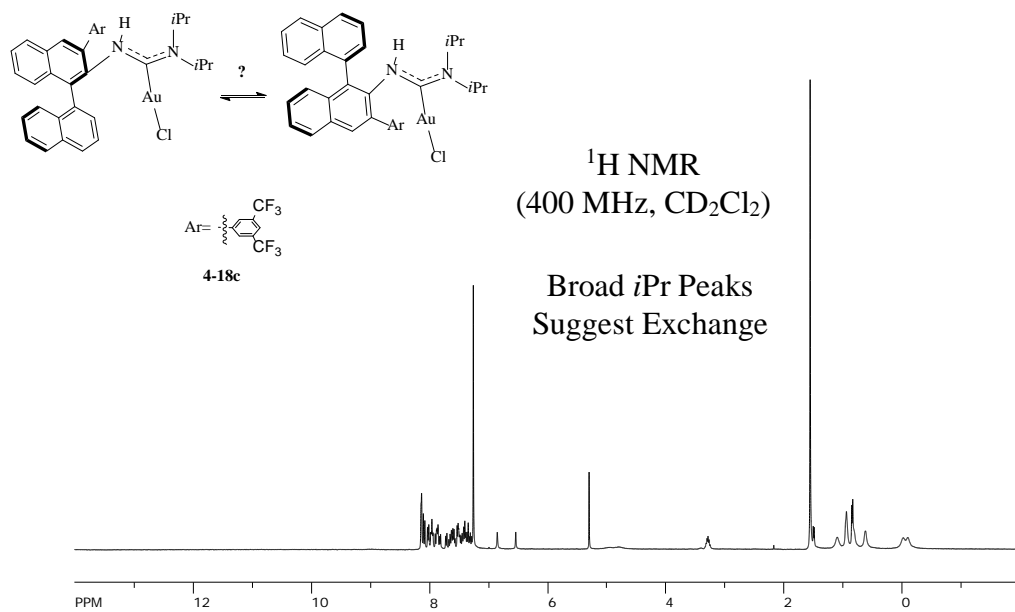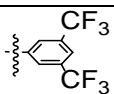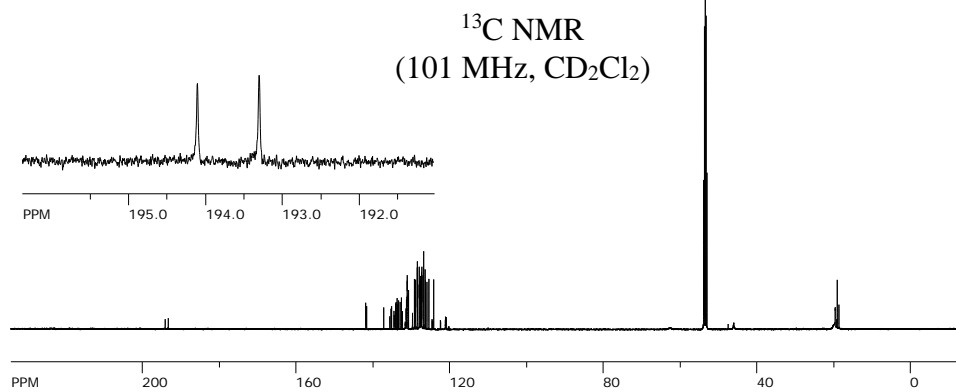
Figure 4.3 ^{1}H and ^{13}C NMR of **4-18c**

X-ray quality crystals were grown via slow diffusion of pentane into a saturated CH2Cl2 solution of **4-18a** and **4-18c** and are shown in **Figures 4.4** & **4.5**. Possible non-covalent secondary interactions can be seen for both structures. It was hypothesized that these types of interactions were responsible for achieving high levels of asymmetric induction in **Scheme 4.2**. These interactions can potentially create a more rigid chiral pocket as well as help stabilize catalytic intermediates allowing for higher turnover as well as better selectivity. Other structural features for the two structures are presented in **Table 4.7**.
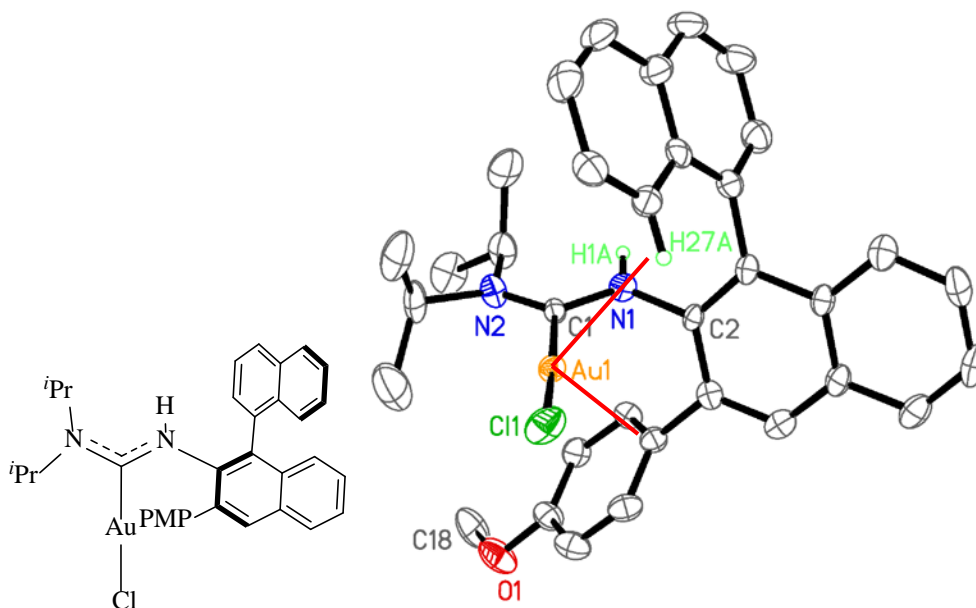
Potential Au-Secondary Interactions
Au-H$_{27A}$ 2.754 Å
Au-C 3.751 Å

Figure 4.4 X-ray Structure of **4-18a** With 50% Probability ellipsoids

Table 4.5 Structural Data for **4-18a**

Empirical formula	C34 H34 Au Cl N2 O
Formula weight	719.05

Temperature	100(2) K	
Wavelength	0.71073 Å	
Crystal system	Monoclinic	
Space group	P 21	
Unit cell dimensions	a = 12.8192(11) Å	$\alpha = 90°$.
	b = 15.3165(13) Å	$\beta = 95.629(2)°$.
	c = 15.3684(13) Å	$\gamma = 90°$.
Volume	3003.0(4) Å^3	
Z	4	
Density (calculated)	1.590 Mg/m^3	
Absorption coefficient	5.017 mm^{-1}	
F(000)	1424	
Crystal size	0.17 x 0.11 x 0.06 mm^3	
Theta range for data collection	1.60 to 27.12°.	
Index ranges	-16<=h<=16, -19<=k<=19, -19<=l<=19	
Reflections collected	40869	
Independent reflections	13231 [R(int) = 0.0326]	
Completeness to theta = 27.12°	99.9 %	
Absorption correction	Semi-empirical from equivalents	
Max. and min. transmission	0.7664 and 0.4862	
Refinement method	Full-matrix least-squares on F^2	
Data / restraints / parameters	13231 / 1 / 695	
Goodness-of-fit on F^2	1.029	

Final R indices [I>2sigma(I)]	R1 = 0.0264, wR2 = 0.0616
R indices (all data)	R1 = 0.0300, wR2 = 0.0629
Absolute structure parameter	0.003(4)
Largest diff. peak and hole	2.130 and -0.704 e.Å^{-3}
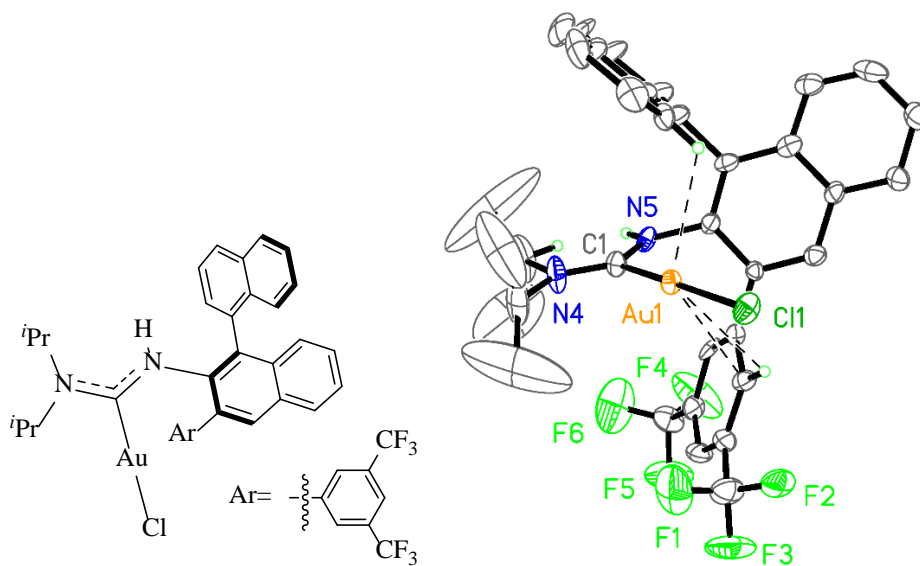
Potential Au-Secondary Interactions
Au-H 3.223 Å
Au-H 3.178 Å
Au-C 3.436 Å

Figure 4.5 X-ray Structure of **4-18c** 50% ellipsoids

Table 4.6 Structural Data for **4-18c**

Empirical formula	C34 H31 Au Cl F3 N2
Formula weight	757.02
Temperature	100(2) K
Wavelength	0.71073 Å
Crystal system	Monoclinic

Space group	P 21
Unit cell dimensions	a = 11.3330(5) Å α= 90°.
	b = 20.3948(8) Å β= 91.6450(10)°.
	c = 15.5881(6) Å γ = 90°.
Volume	3601.5(3) Å^3
Z	4
Density (calculated)	1.396 Mg/m^3
Absorption coefficient	4.196 mm^{-1}
F(000)	1488
Crystal size	0.38 x 0.19 x 0.05 mm^3
Theta range for data collection	1.31 to 28.28°.
Index ranges	-15<=h<=14, -27<=k<=27, -20<=l<=20
Reflections collected	39970
Independent reflections	17813 [R(int) = 0.0267]
Completeness to theta = 28.28°	99.9 %
Max. and min. transmission	0.8176 and 0.2985
Refinement method	Full-matrix least-squares on F^2
Data / restraints / parameters	17813 / 1 / 872
Goodness-of-fit on F^2	1.034
Final R indices [I>2sigma(I)]	R1 = 0.0422, wR2 = 0.1255
R indices (all data)	R1 = 0.0452, wR2 = 0.1280
Absolute structure parameter	0.027(6)
Largest diff. peak and hole	6.980 and -1.336 e.Å^{-3}

Table 4.7 ADC Gold Complex Structural Features From X-Ray Structure

Entry	Label	Au-Cl (Å)	Au-C$_{carbene}$ (Å)	C$_{carbene}$-N Avg (Å)	N-C-N (°)	Au-C-N$_{iPr}$ (°)	Au-C-N$_{Ar}$ (°)
1	**4-18a**	2.300	1.999	1.328	117.65	122.91	116.65
2	**4-18c**	2.284	2.022	1.326	119.35	123.83	116.80

These ADC gold complexes were tested as catalysts in an intramolecular hydroamination of an allene and compared with their 2'-substituted counterparts shown in **Figure 4.6** (**Scheme 4.7**). This study should help understand whether the interactions of the ring at the 3-position or the 2'-position of the binaphthyl are more important. As can be seen from the results in **Table 4.8** the 2'-substituted ADCs **entries 4-6** outperformed the 3-substituted ADCs **entries 1-3** in achieving higher selectivity.
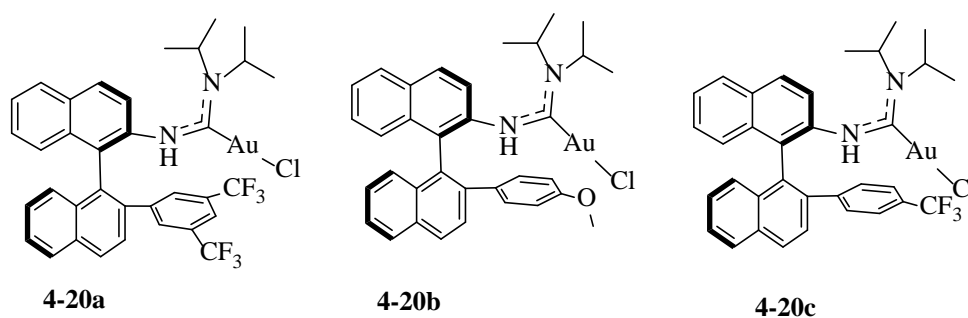
Figure 4.6 2'-Substituted ADC Gold Complexes

Reaction scheme: compound **10** (with NHMs and Ph, Ph substituents and allene) reacts under LAuCl (5 mol%), AgOTf (5 mol%), Toluene, -15°C, 24h to give compound **11**.

$$Ms= -\xi-\underset{\underset{O}{\|}}{\overset{\overset{O}{\|}}{S}}-CH_3$$
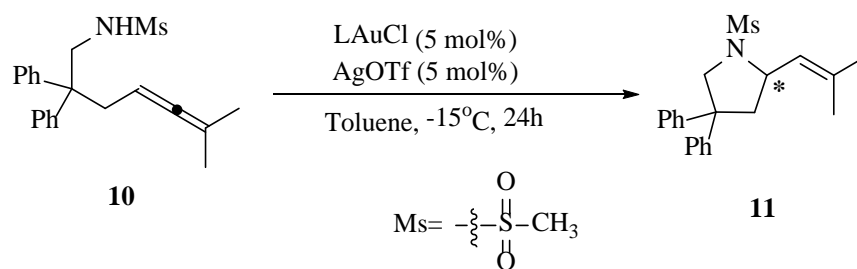
Table 4.8 Hydroamination Results

Entry	Catalyst	% Yield	% ee
1	**4-18a**	82	2
2	**4-18b**	79	20
3	**4-18c**	83	20
4	**4-20a**	74	66
5	**4-20b**	67	12
6	**4-20c**	36	74

Since the 2'-substituted ADC gold complexes appeared to outperform the 3-substituted binaphthyl ADC gold complexes, a small library of 2'-substituted ADC gold complexes (**Figure 4.7**) were synthesized according to procedures reported in a former student's dissertation.[11]
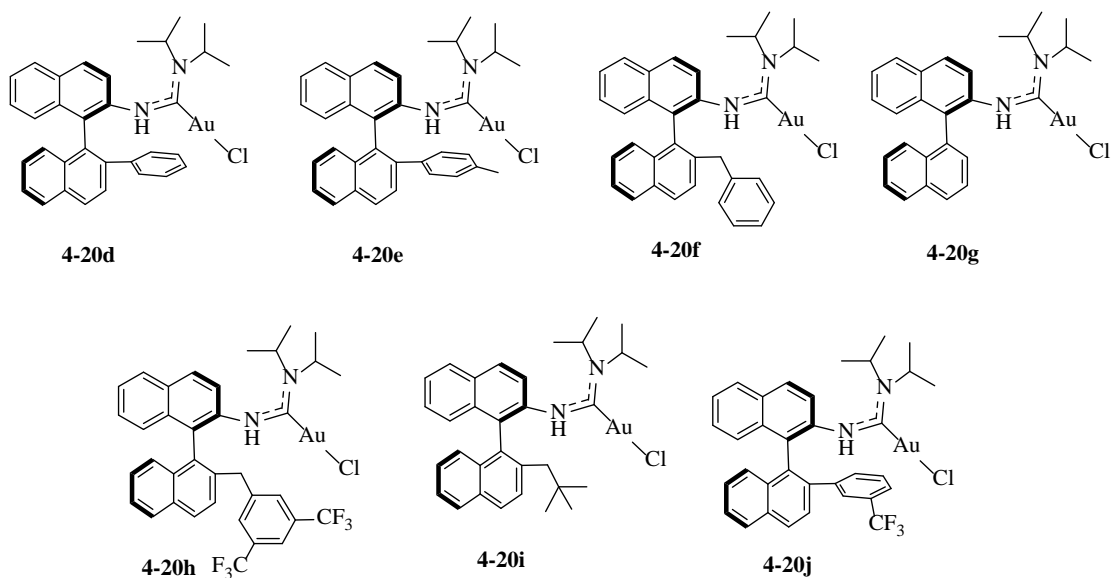
Figure 4.7 Additional 2'-Substituted ADC Gold Complexes

Out of the seven complexes in **Figure 4.7**, only **4-20h** and **4-20j** had not been previously synthesized. **4-20j** was synthesized to investigate whether the position of the trifluoromethyl group on the 2'- phenyl ring had any influence on catalytic activity or selectivity. **4-20h** was synthesized based on the hypothesis that the increased flexibility of the methylene linker in would facilitate the interaction between the aryl ring and gold. X-ray quality crystals were grown by slow diffusion of pentane into a saturated CH_2Cl_2 solution of **4-20h** and **4-20j** and **t**he structures of **4-20h** and **4-20j** were confirmed by X-ray crystallography shown in **Figure 4.8** & **Figure 4.9**. The anticipated Au-aryl interaction previously seen for **4-20a**, was not supported by the X-ray structure of **4-20h**. Instead, the aryl ring appears to π-stack with one naphthyl units of the binaphthyl backbone. Whereas **4-20j** adopts the "out"-conformation previously seen by **4-20d**.[7] If the hypothesis that these secondary interactions are necessary for achieving high levels of selectivity then these two compounds should perform worse than **4-20a**.
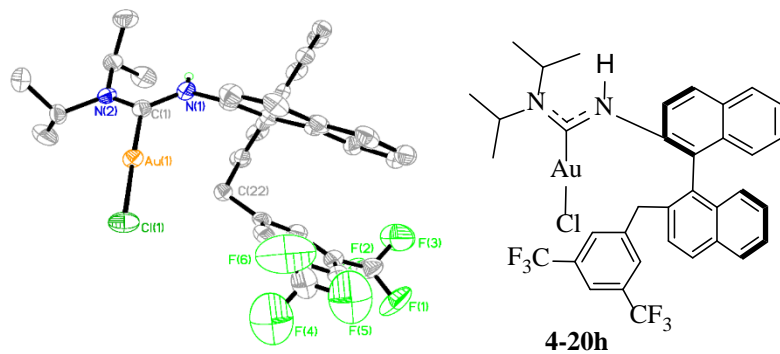
Figure 4.8 X-Ray Structure for **4-20h** with 50% ellipsoids

Table 4.9 Structural Data for **4-20h**

Empirical formula	C36 H32 Au Cl F6 N2
Formula weight	839.05
Temperature	200(2) K
Wavelength	0.71073 Å
Crystal system	Orthorhombic
Space group	P 21 21 21
Unit cell dimensions	a = 7.8291(3) Å $\quad$ α= 90°.
	b = 18.1999(7) Å $\quad$ β= 90°.
	c = 23.0975(9) Å $\quad$ γ = 90°.
Volume	3291.1(2) Å^3
Z	4
Density (calculated)	1.693 Mg/m^3
Absorption coefficient	4.614 mm^{-1}
F(000)	1648

Crystal size	0.27 x 0.07 x 0.04 mm^3
Theta range for data collection	1.76 to 27.13°.
Index ranges	-10<=h<=10, -23<=k<=23, -29<=l<=29
Reflections collected	44678
Independent reflections	7260 [R(int) = 0.0833]
Completeness to theta = 27.13°	99.9 %
Absorption correction	Semi-empirical from equivalents
Max. and min. transmission	0.8406 and 0.3656
Refinement method	Full-matrix least-squares on F^2
Data / restraints / parameters	7260 / 0 / 418
Goodness-of-fit on F^2	1.036
Final R indices [I>2sigma(I)]	R1 = 0.0301, wR2 = 0.0696
R indices (all data)	R1 = 0.0347, wR2 = 0.0718
Absolute structure parameter	0.004(6)
Extinction coefficient	0.00170(14)
Largest diff. peak and hole	0.890 and -0.705 e.Å^{-3}
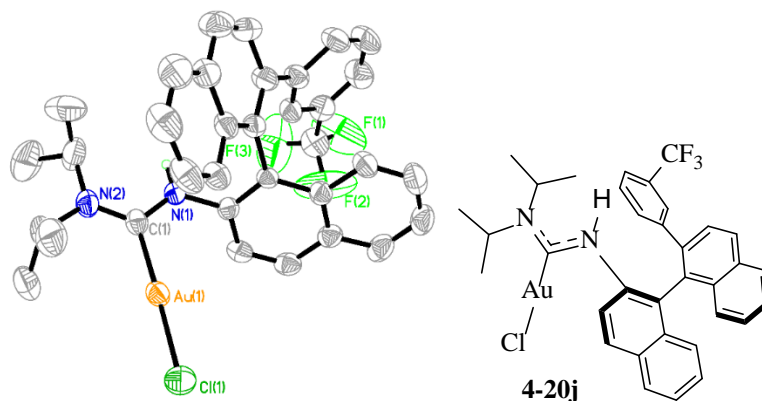
Figure 4.9 X-ray Structure of **4-20j** 50% ellipsoids

Table 4.10 Structure Data for **4-20j**

Empirical formula	C34 H31 Au Cl F3 N2
Formula weight	757.02
Temperature	296(2) K
Wavelength	0.71073 Å
Crystal system	Monoclinic
Space group	P 21
Unit cell dimensions	a = 8.1957(7) Å $\quad$ α= 90°.
	b = 11.4033(10) Å $\quad$ β= 99.4000(10)°.
	c = 16.4166(14) Å $\quad$ γ = 90°.
Volume	1513.7(2) Å^3
Z	2
Density (calculated)	1.661 Mg/m^3
Absorption coefficient	4.992 mm^{-1}
F(000)	744
Crystal size	0.20 x 0.14 x 0.12 mm^3
Theta range for data collection	2.18 to 30.85°.
Index ranges	-11<=h<=11, -16<=k<=16, -23<=l<=23
Reflections collected	26164
Independent reflections	9422 [R(int) = 0.0371]
Completeness to theta = 30.85°	99.5 %
Absorption correction	Semi-empirical from equivalents
Max. and min. transmission	0.5904 and 0.4427

Refinement method	Full-matrix least-squares on F^2
Data / restraints / parameters	9422 / 1 / 375
Goodness-of-fit on F^2	1.032
Final R indices [I>2sigma(I)]	R1 = 0.0378, wR2 = 0.0773
R indices (all data)	R1 = 0.0540, wR2 = 0.0827
Absolute structure parameter	0.013(7)
Largest diff. peak and hole	2.445 and -0.741 e.$Å^{-3}$.

These were then tested in the same allene hydroamination reaction to get an understanding of which substituents result in the best overall performance of the catalyst. Despite the wide variety of structural variants made, the original catalyst **4-20a** provided the best selectivities of 66 %ee. The lack of secondary interactions seen in the X-ray structures (**Fgiure 4.8 & 4.9**) between the aryl substituent in **4-20h** and **4-20j** and the poor selectivities observed in **Table 4.11** does support the hypothesis that somehow this interaction might play a crucial role in achieving the desired high levels of selectivity. To try and get an idea if this non-covalent secondary interaction is still occurring while in solution ^{19}F, ^{1}H-HOESY (Heteronuclear Overhauser Effect Spectroscopy) was done on **4-20a & 4-20j**. In the two spectra shown in **Figure 4.10** it is apparent there is an interaction between the CF$_3$ groups and the *i*Pr substituents of the ADCs for both **4-20a** & **4-20j**. Through space nuclear overhouser effects are typically limited to occur between atoms that are within 5Å other. This fits with **4-20a** with the CF$_3$ being only 2.49 Å away from the *i*Pr group. However, in the crystal structure in **4-20j** the CF$_3$ groups are locate 7.5 Å away from the *i*Pr groups. This result leads to the idea that the conformation adopted by the ADC is actually dynamic in nature. Either computational or low temperature NMR studies would be required to gain more insights into the

equilibrium between these two conformations to further understand the importance of these secondary interactions.
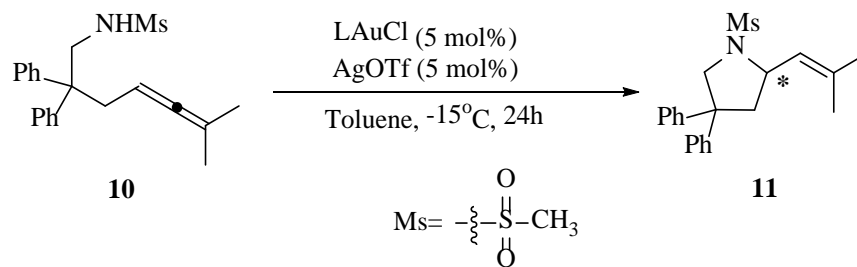
Table 4.11 2'-Substituted ADC Gold Complexes Hydroamination Results

Entry	Catalyst	% Yield	% ee
1	**4-20a**	74	66
2	**4-20b**	67	12
3	**4-20c**	36	74
4	**4-20d**	71	16
5	**4-20e**	63	16
6	**4-20f**	77	54
7	**4-20g**	68	6
8	**4-20h**	79	36
9	**4-20i**	74	38
10	**4-20j**	73	36
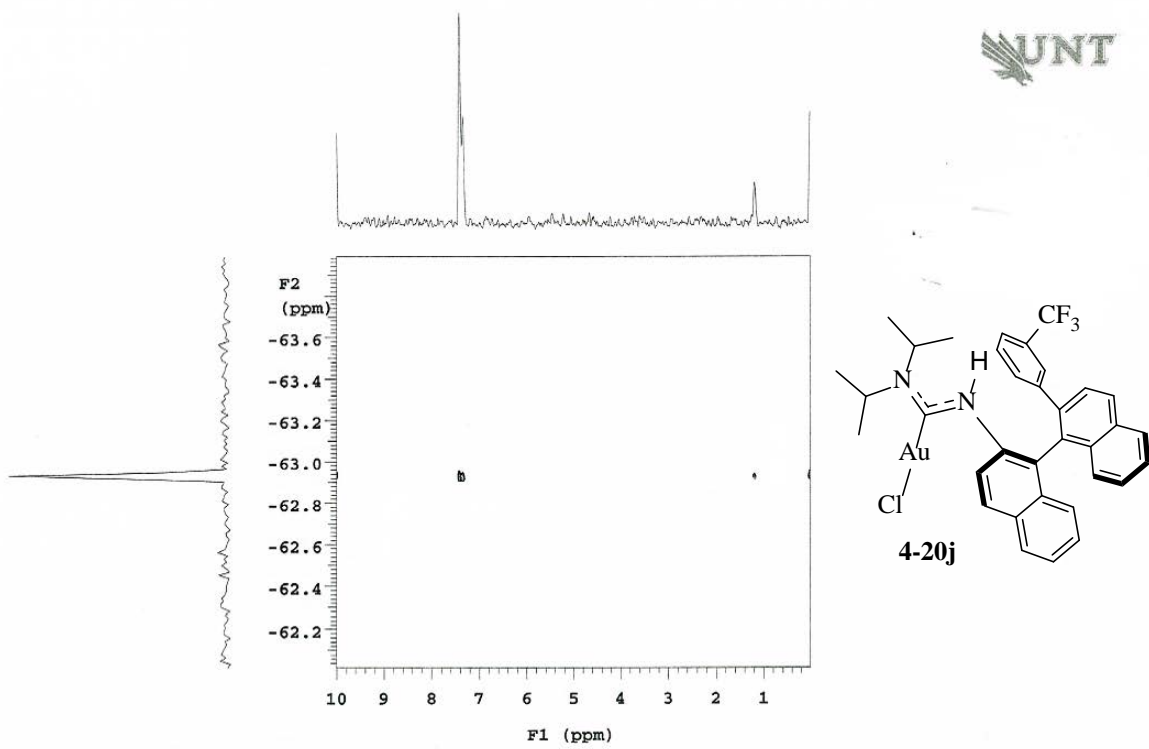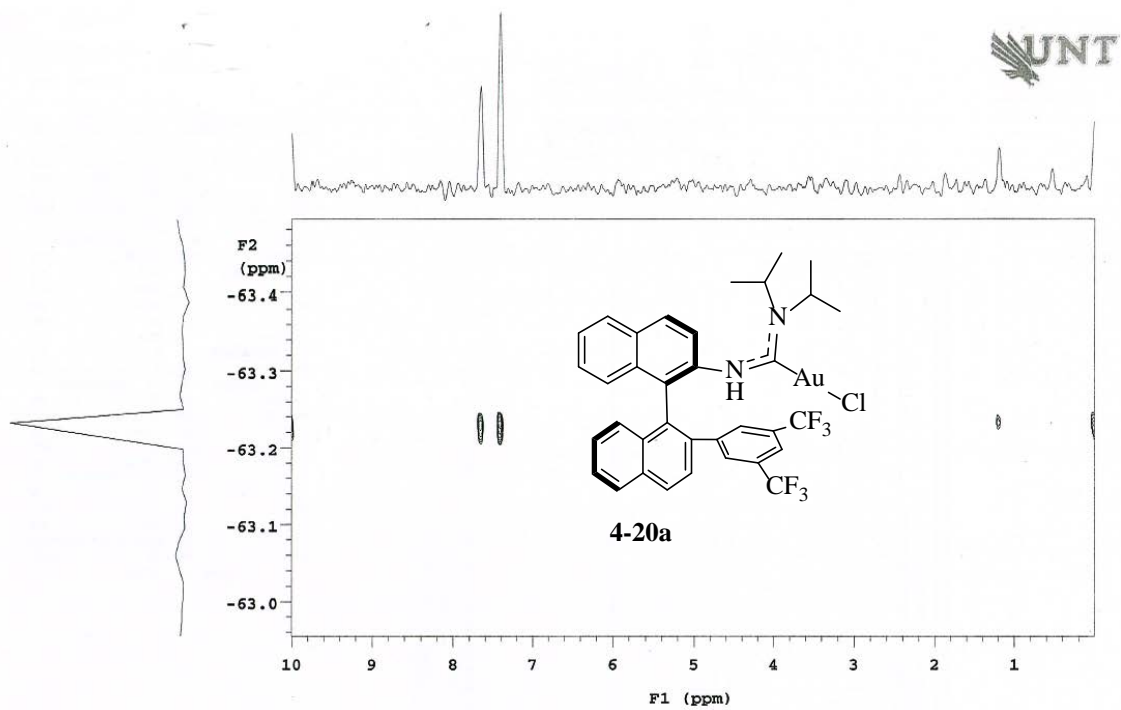
Figure 4.10 ^{19}F, [1]H-HOESY of **4-20a** & **4-20j**

The next variation made was to investigate the importance of the amine used to create the ADC. A small library of ADCs (**Figure 4.11**) containing the same bis(CF$_3$)phenyl 2'-substitutent as **4-20a** was synthesized by using various commercially available chiral and achiral amines. One of which **4-20m** has been previously reported.[7]

4-20k   **4-20l**

4-20m   **4-20n**
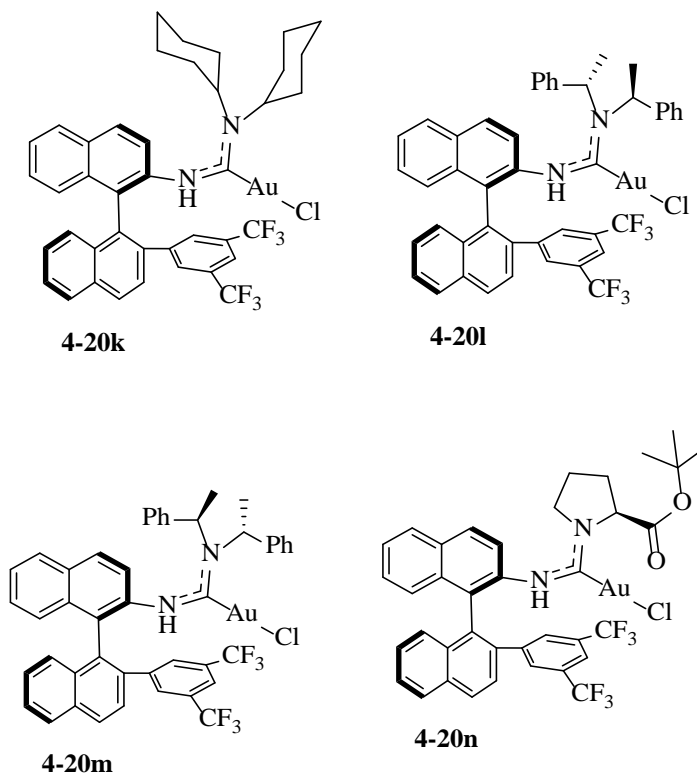
Figure 4.11 Various ADC Derivatives of **4-20a**
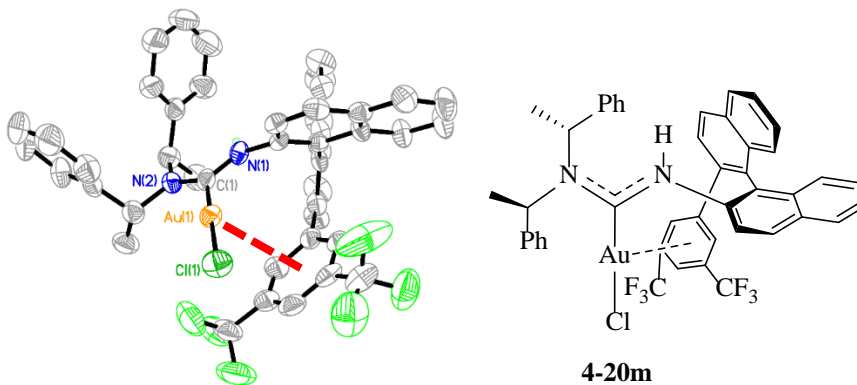
4-20m

Potential Au-Secondary Interactions
Au-centroid 3.540 Å

Figure 4.12 X-ray Structure of **4-20m** 50% ellipsoids

Table 4.12 Structure Data for **4-20m**

Empirical formula	C45 H34 Au Cl F6 N2
Formula weight	949.16
Temperature	220(2) K
Wavelength	0.71073 Å
Crystal system	Orthorhombic
Space group	P 21 21 21
Unit cell dimensions	a = 13.8723(11) Å $\quad$ $\alpha= 90°$.
	b = 16.2862(13) Å $\quad$ $\beta= 90°$.
	c = 17.5650(15) Å $\quad$ $\gamma = 90°$.
Volume	3968.4(6) Å^3
Z	4
Density (calculated)	1.589 Mg/m^3
Absorption coefficient	3.837 mm^{-1}
F(000)	1872
Crystal size	0.17 x 0.10 x 0.06 mm^3
Theta range for data collection	1.71 to 30.56°.
Index ranges	-19<=h<=19, -23<=k<=23, -24<=l<=25
Reflections collected	66730

Independent reflections	12126 [R(int) = 0.0904]
Completeness to theta = 30.56°	99.8 %
Absorption correction	Semi-empirical from equivalents
Max. and min. transmission	0.7969 and 0.5566
Refinement method	Full-matrix least-squares on F^2
Data / restraints / parameters	12126 / 0 / 498
Goodness-of-fit on F^2	1.012
Final R indices [I>2sigma(I)]	R1 = 0.0535, wR2 = 0.0668
R indices (all data)	R1 = 0.1035, wR2 = 0.0793
Absolute structure parameter	0.002(6)
Largest diff. peak and hole	1.072 and -0.521 e.Å^{-3}

These were then tested in the intramolecular hydroamination of **10** as shown in **Table 4.13**. Worth pointing out are the differences in selectivity between the two diastereomeric complexes **4-20l** and **4-20m**. The differences may be a result of a chiral match-mismatch scenario, in which the chirality of the amine is either reinforcing or interfering with the chirality of the binaphthyl backbone. There have been examples reported of chiral match and mismatch effects involving chiral ligands and chiral counterions in gold catalysis.[12a] The chiral match-mismatch scenario involving different parts of the ligand however are more rare.[12b] One example of such a case however is shown in **Scheme 4.9**. When the **L1** (R,S,S) diastereomer of the phosphoramidite is used moderate conversion (75%) and selectivity (66 %ee) are obtained whereas when another diastereomer **L2** (S,S,S) a higher conversion of 90% was achieved but significantly lower selectivity of only 4% was observed.

10 → **11**

LAuCl (5 mol%)
AgOTf (5 mol%)

Toluene, -15°C, 24h

$Ms= -\xi-\overset{O}{\underset{O}{\overset{\|}{\underset{\|}{S}}}}-CH_3$
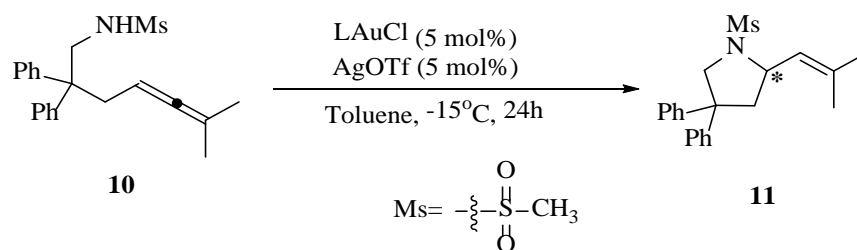
Table 4.13 Hydroamination Results

Entry	Catalyst	% Yield	% ee
1	**4-20a**	74	66
2	**4-20k**	63	59
3	**4-20l**	84	18
4	**4-20m**	71	90
5	**4-20n**	70	76

L (5 mol%)
(THT)AuCl (5 mol%)
AgOTf (5 mol%)

Toluene, -20°C, 20h

$Cbz= -\xi-\overset{O}{\overset{\|}{C}}-O-Ph$

10 → **11**

L1 75 %Conversion 66 %ee
L2 90 %Conversion 4 %ee

L1 (R,S,S)
L2 (S,S,S)
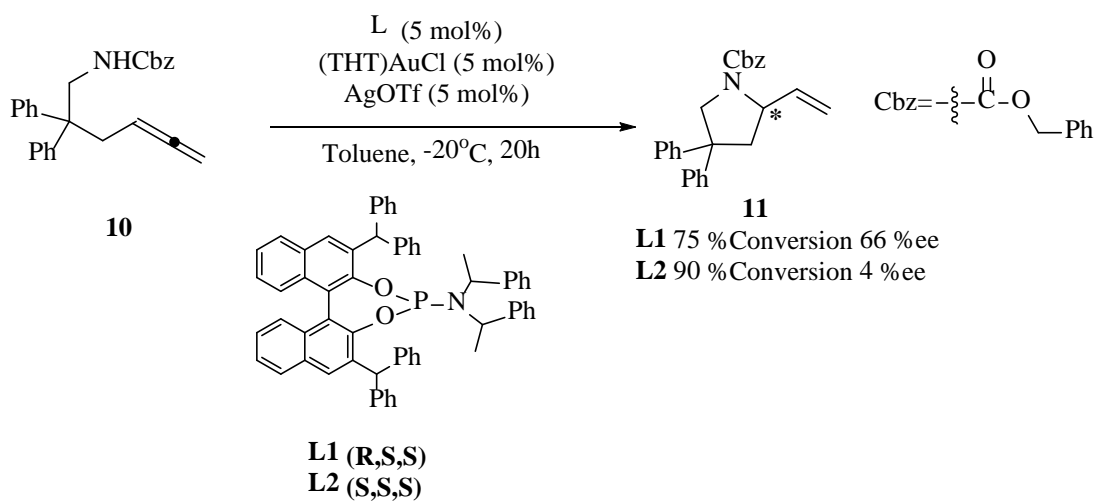
Scheme 4.9 Previous Ligand Based Chiral Match-Mismatch Scenario[12b]

137

With the best-performing catalyst in hand, **4-20l**, a substrate scope study will be undertaken (**Scheme 4.10**). Various protecting groups will be tested to see if there are any differences when switching from carbamates to sulfonamides. The terminal R-substituents of the allene will also be varied to see if there are any obvious effects on selectivity.
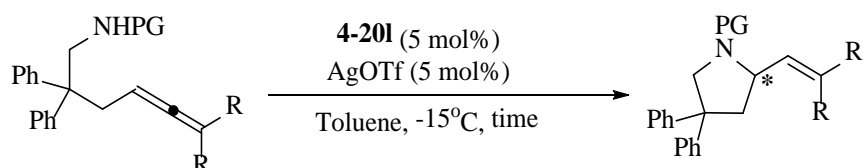
Scheme 4.10 Intramolecular Hydroamination Substrate Scope

In consideration of the rigorous amount of work needed to synthesize these binaphthyl-derived ADC ligands, another set of more readily prepared ADC gold complexes was targeted (**Scheme 4.11**) using the strategy that an achiral isocyanide gold complex could be converted into a chiral ADC simply by using a commercially available chiral amine as the nucleophile. This also potentially eliminates the problems seen with chiral match/mismatch effects between the chiral amine and binaphthyl scaffold.

4-21a: R= 3,5-bis CF3
4-21b: R= 4-CF3
4-21c: R= 4-OMe
4-21d: R= H

4-22a: R= 3,5-bis CF3
4-22b: R= 4-CF3
4-22c: R= 4-OMe
4-22d: R= H
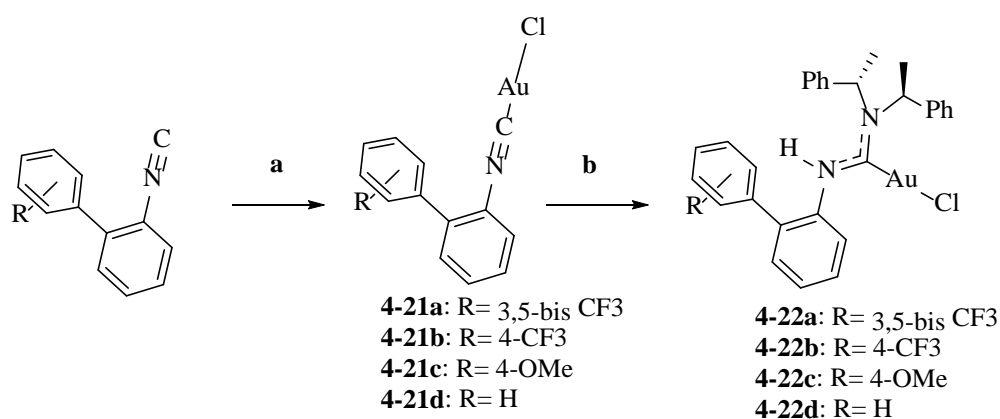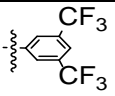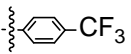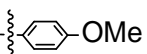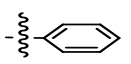
(a) (THT)AuCl, DCM; (b) (S,S)-bis[α-methylbenzylamine], CHCl₃

Scheme 4.11 Synthesis of Chiral ADC Gold Complexes from Achiral Gold Isocyanides

By using previously reported biphenyl isocyanides[13] and binding them to gold(I) as described above, a few new chiral ADC gold complexes **4-22(a-d)** could be synthesized by simply using a chiral amine (S,S)-bis[α-methylbenzylamine] or (R,R)-bis[α-methylbenzylamine].

Table 4.14 Chiral Biphenyl ADC Gold Complexes

Entry	Label	Ar	% Yield
1	**4-22a**	CF$_3$ / CF$_3$	62
2	**4-22b**	CF$_3$	57
3	**4-22c**	OMe	61
4	**4-22d**		71

X-ray quality crystals were grown by slow diffusion of pentane into a solution of the corresponding ADC Gold complex in CH$_2$Cl$_2$. The structures of these complexes were verified via X-ray crystallography shown in **Figures 4.13-4.15.** Unfortunately the desired gold aryl interactions were not observed in any of the following crystal structures. Structural details for the following crystal structures are tabulated in **Table 4.18**.
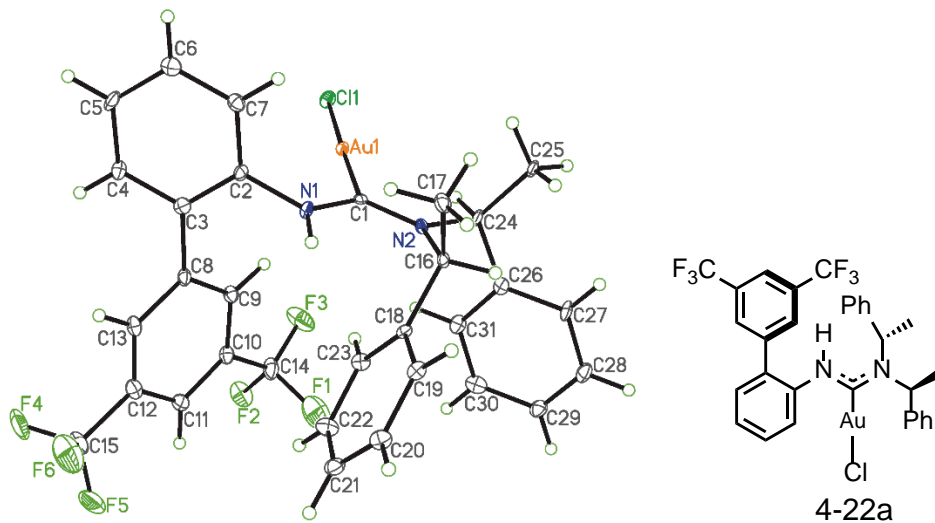
Potential Au-Secondary Interactions
Au-H$_{24A}$ 2.508 Å
Au-H$_{9A}$ 2.844 Å

Figure 4.13 X-ray Structure of **4-22a** With 50% Probability Ellipsoids Shown

Table 4.15 Structural Data for **4-22a**

Empirical formula	C31 H26 Au Cl F6 N2
Formula weight	772.95
Temperature	100(2) K
Wavelength	0.71073 Å
Crystal system	Orthorhombic
Space group	P 21 21 21
Unit cell dimensions	a = 8.6795(12) Å α= 90°.
	b = 9.3546(13) Å β= 90°.
	c = 35.324(5) Å γ = 90°.
Volume	2868.1(7) Å^3

Z	4
Density (calculated)	1.790 Mg/m^3
Absorption coefficient	5.286 mm^{-1}
F(000)	1504
Crystal size	0.29 x 0.09 x 0.04 mm^3
Theta range for data collection	2.25 to 27.12°.
Index ranges	-11<=h<=11, -11<=k<=11, -45<=l<=45
Reflections collected	29110
Independent reflections	6306 [R(int) = 0.0425]
Completeness to theta = 27.12°	99.8 %
Absorption correction	Semi-empirical from equivalents
Max. and min. transmission	0.8085 and 0.3103
Refinement method	Full-matrix least-squares on F^2
Data / restraints / parameters	6306 / 0 / 366
Goodness-of-fit on F^2	1.038
Final R indices [I>2sigma(I)]	R1 = 0.0261, wR2 = 0.0652
R indices (all data)	R1 = 0.0271, wR2 = 0.0655
Absolute structure parameter	0.032(6)
Largest diff. peak and hole	1.751 and -2.113 e.Å^{-3}
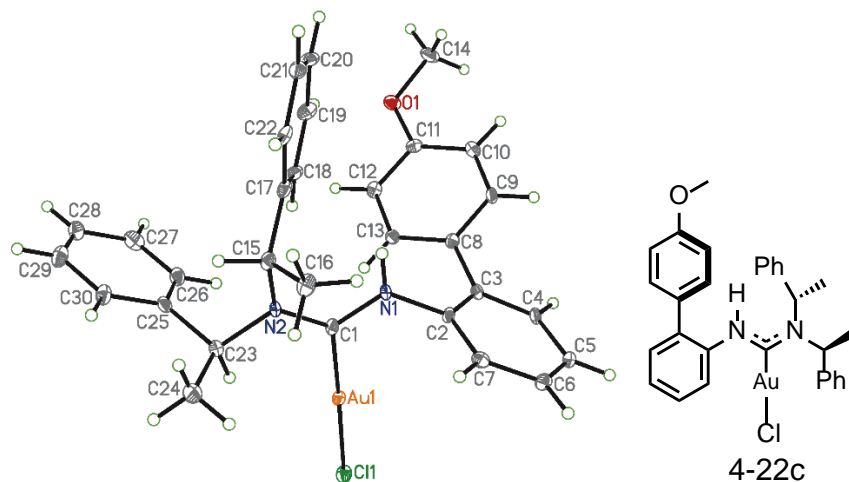
Potential Au-Secondary Interactions
Au-H$_{23A}$ 2.486 Å
Au-H$_{13A}$ 3.083 Å

Figure 4.14 X-ray Structure of **4-22c** With 50% ellipsoids Shown

Table 4.16 Structural Data for **4-22c**

Empirical formula	C30 H30 Au Cl N2 O
Formula weight	666.98
Temperature	100(2) K
Wavelength	0.71073 Å
Crystal system	Monoclinic
Space group	P 21
Unit cell dimensions	a = 9.5718(11) Å α= 90°.
	b = 8.8465(10) Å β= 99.789(2)°.
	c = 15.8700(18) Å γ = 90°.
Volume	1324.3(3) Å^3

|	
Z	2
Density (calculated)	1.673 Mg/m^3
Absorption coefficient	5.681 mm^{-1}
F(000)	656
Crystal size	$0.06 \times 0.05 \times 0.02$ mm^3
Theta range for data collection	2.16 to $27.60°$.
Index ranges	$-12<=h<=12, -11<=k<=11, -20<=l<=20$
Reflections collected	13809
Independent reflections	6040 [R(int) = 0.0395]
Completeness to theta = $27.60°$	99.2 %
Absorption correction	Semi-empirical from equivalents
Max. and min. transmission	0.8949 and 0.7268
Refinement method	Full-matrix least-squares on F^2
Data / restraints / parameters	6040 / 1 / 313
Goodness-of-fit on F^2	0.989
Final R indices [I>2sigma(I)]	R1 = 0.0303, wR2 = 0.0593
R indices (all data)	R1 = 0.0377, wR2 = 0.0613
Absolute structure parameter	0.001(7)
Extinction coefficient	0.0011(2)
Largest diff. peak and hole	1.753 and -1.168 e.Å^{-3}
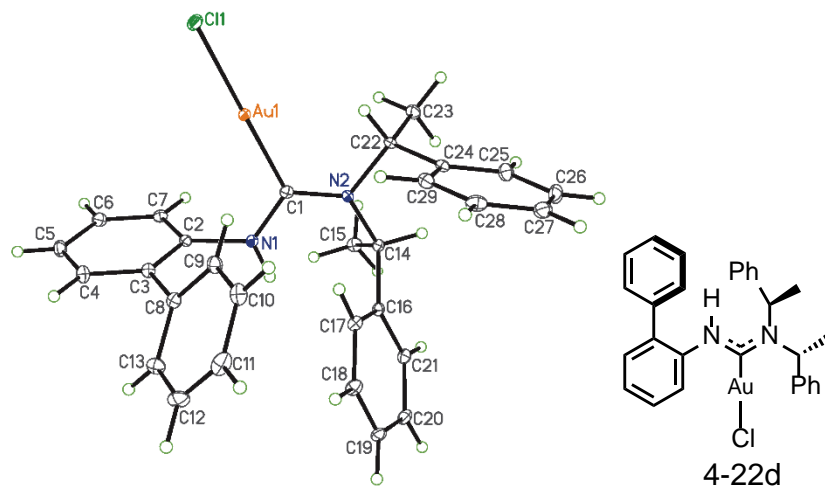
Potential Au-Secondary Interactions
Au-H$_{22A}$ 2.515 Å
Au-H$_{9A}$ 2.763 Å

Figure 4.15 X-ray Structure of **4-22d** With 50% Probability Ellipsoids Shown

Table 4.17 Structural Data for **4-22d**

Empirical formula	C29 H28 Au Cl N2
Formula weight	636.95
Temperature	100(2) K
Wavelength	0.71073 Å
Crystal system	Monoclinic
Space group	P 21
Unit cell dimensions	a = 9.4250(11) Å α= 90°.
	b = 8.5875(10) Å β= 104.782(2)°.
	c = 15.9237(18) Å γ = 90°.
Volume	1246.2(2) Å^3

Z	2
Density (calculated)	1.698 Mg/m^3
Absorption coefficient	6.029 mm^{-1}
F(000)	624
Crystal size	0.26 x 0.17 x 0.10 mm^3
Theta range for data collection	2.23 to 27.08°.
Index ranges	-12<=h<=12, -10<=k<=11, -20<=l<=20
Reflections collected	16473
Independent reflections	5398 [R(int) = 0.0214]
Completeness to theta = 27.08°	99.8 %
Absorption correction	Semi-empirical from equivalents
Max. and min. transmission	0.5728 and 0.3032
Refinement method	Full-matrix least-squares on F^2
Data / restraints / parameters	5398 / 1 / 304
Goodness-of-fit on F^2	0.815
Final R indices [I>2sigma(I)]	R1 = 0.0124, wR2 = 0.0306
R indices (all data)	R1 = 0.0127, wR2 = 0.0307
Absolute structure parameter	0.007(3)
Largest diff. peak and hole	1.404 and -0.726 e.Å^{-3}

Table 4.18 ADC Gold Complex Structural Features From X-Ray Structure

Entry	Label	Au-Cl (Å)	Au-C$_{carbene}$ (Å)	C$_{carbene}$-N Avg (Å)	N-C-N (°)	Au-C-N$_{C-H}$ (°)	Au-C-N$_{Ar}$ (°)
1	**4-22a**	2.286	2.015	1.336	118.73	123.04	118.19
2	**4-22c**	2.289	2.014	1.341	118.93	122.59	118.42
3	**4-22d**	2.287	2.005	1.334	118.01	123.00	118.89

To compare the ability of a chiral ADC without a binaphthyl scaffold to give chiral induction, these ligands were tested in the intramolecular hydroamination of **10**. The lower enantioselectivities observed with these catalysts shown in **Table 4.19** emphasizes the need for the binaphthyl backbone to achieve high levels of asymmetric induction. These result also emphasize the importance of the 3,5-bis trifluoromethylated aryl ring, which resulted in substantially better enantioselecivity of 57% (entry 1) than the other groups.
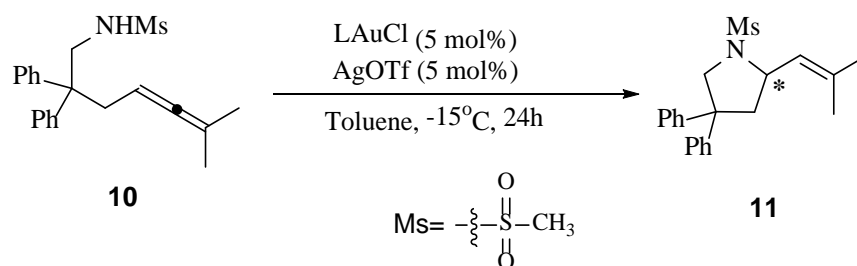
Table 4.19 Biphenyl ADC Hydroamination Results

Entry	Catalyst	% Yield	% ee
1	**4-22a**	71	57
2	**4-22b**	62	18

|			
3	**4-22c**	57	12
4	**4-22d**	61	15

4.3 Conclusion

A series of new modifications of chiral monodentate ADC gold complexes were synthesized and investigated as ligands for the asymmetric gold catalyzed intramolecular hydroamination of allenes. Through the screening of ligand substituents, some structure activity correlations were able to be determined, providing guidance for further rational ligand design. The inclusion of a 3,5-bis(trifluoromethyl)phenyl ring at the 2'-position of the binaphthyl scaffold proved to be essential in achieving high levels of asymmetric induction, whereas high enantioselectivities were not seen with the same ring present at the binaphthyl 3-position. This electron-deficient aryl substituent also proved to give better selectivities than alkyl, benzyl, phenyl, or electron-rich aryl substituents at the 2'-position. Effects of varying the amine used to create the ADC were also shown. When using chiral amines, it was shown that care must be taken when selecting the amine due to the possibility of chiral match/mismatch effects influencing enantioselectivities. A more detailed analysis of these effects should be the subject of future studies. The ability to create chiral ADC gold complexes from achiral gold-bound isocyanides by using commercially available chiral amines was shown. The lower selectivities observed in allene hydroaminations with these ADC ligands emphasizes the importance of the binaphthyl scaffold for achieving high levels of asymmetric induction. Given to the time, expense and number of steps required to synthesize these binaphthyl-containing ADC gold complexes, this study has provided valuable evidence for the importance of using a single binaphthyl scaffold with a 3,5-bis(trifluoromethyl)phenyl ring at the 2'-position and utilizing this as a starting point to build a catalyst library with the vast selection of commercially available amines as the only structural component that needs to be varied.

4.4 Experimental Section

General Information:

All air-sensitive synthesis steps were performed under an argon atmosphere using a vacuum line or under nitrogen atmosphere using a glovebox unless otherwise noted. All solvents for reactions were dried before use. Tetrahydrofuran, toluene, and 1, 4-dioxane were dried over and stored on sodium/benzophenone under vacuum. Dichloromethane was washed with concentrated sulfuric acid, deionized water, saturated sodium bicarbonate and deionized water, then pre-dried over anhydrous calcium chloride, followed by refluxing and distillation from phosphorus pentoxide under nitrogen and storage over phosphorus pentoxide under vacuum. The reported chemical shifts in NMR spectra were referenced to residual solvent peaks.[16] $CDCl_3$, ^1H NMR: 7.26 ppm, ^{13}C NMR: 77.16 ppm; DMSO-d_6, ^1H NMR: 2.50 ppm, ^{13}C NMR: 39.52 ppm; CD_2Cl_2, ^1H NMR: 5.32 ppm, ^{13}C NMR: 53.84 ppm ; Benzene-d_6, ^1H NMR: 7.16 ppm, ^{13}CNMR: 128.06 ppm. CD_2Cl_2 was dried over and stored on activated 4 Å molecular sieves under vacuum. Benzene- d_6 was dried over and stored on sodium/benzophenone. $Pd(OAc)_2$ (99.95+%-Pd) was purchased from Strem and purified according to Armarego and Chai.[17] $Pd(Ph_3P)_4$ (≥99.5%) was purchased from Chem-Impex and used as received. [4,5-bis(diphenylphosphino)-9,9-dimethylxanthene; 10 mol%] was purchased from strem and used as received. (THT)AuCl was synthesized using a Canadian Maple Leaf (99.99 %Au) following a publishd procedure.[18] Elemental analyses were performed by Midwest Microlab, Indianapolis, Indiana. Normal phase HPLC analysis of enantiomeric product mixtures was performed to determine %ee. Substrates were synthesized according to literature procedures.[19]

4-8
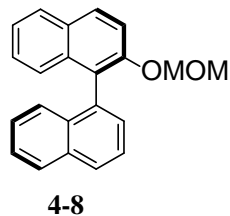
4-8 synthesized according to literature procedure and ^{1}H NMR matched , published data. [14]

Synthesis of 4-9:

A solution of **4-8** (2g) in diethyl ether (17mL/mmol) was treated with nBuLi (3.82ml, 2.5 *M* solution in hexanes, 1.5 equivalents) at room temperature, and the reaction mixture was stirred for 3 hours. THF (11mL/mmol) was distilled into the reaction mixture, and the mixture was stirred 1 hour. The mixture was cooled to 0 °C, and dibromotetrachloroethane (3.11g, 1.5 equivalents) was added all at once. The reaction mixture was stirred for 1 hour and then quenched with saturated ammonium chloride. The solvent was removed under reduced pressure, and the product was extracted into DCM. The organic layers were combined, washed with brine, and dried over sodium sulfate. **4-9** was purified by column chromatography over silica (1:10 EtOAc:Hexane) (84%).

4-9
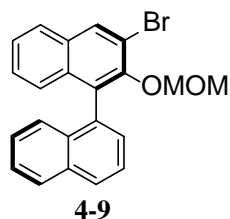
Yellow Oil, 2.1g (84 % Yield), R_f = 0.64 (CH$_2$Cl$_2$:hexane, 2:3) ^{1}H NMR (400 MHz, CDCl$_3$) δ = 8.29 (s, 1H), 8.01 (m, 2H), 7.84 (d, *J*= 8.0Hz, 1H), 7.66 (m, 1H), 7.55-7.23 (m, 7H), 4.78 (m, 2H), 2.67 (s, 3H) ppm. ^{13}C NMR (100.5 MHz, CDCl$_3$) δ= 149.2, 133.6, 133.6, 133.4, 133.0, 132.6, 131.7, 131.6, 129.2, 128.5, 128.2, 127.0, 126.7, 126.5, 126.5, 126.3, 126.1, 126.0, 125.4, 117.7, 99.2, 56.8 ppm. HRMS (ESI, [C$_{22}$H$_{17}$O$_2$Br + H]$^+$) Calcd: 392.0412, Found: m/z .

General Procedure for Suzuki Coupling

The resulting product **4-9** (1-3g, 1equiv.) was combined with 10 mol % of (Ph₃P)₄Pd in DME (7mL/mmol) at room temperature under argon. To the mixture was added the appropriate aryl boronic acid (1.75 equiv.) and 2 *M* sodium carbonate solution in water (2.6 equivalents). The mixture was refluxed at 90 °C for 48 hours. The mixture was filtered through Celite, and the solvent was removed under reduced pressure. The residue was dissolved in DCM and washed with saturated ammonium chloride, water, and brine, then dried over sodium sulfate, and concentrated to give the crude product. Compounds **4-10(a-c)** were purified by column chromatography over silica (1:9 Et₂O: Hexane)

4-10a Ar = -ξ⟨⟩-OMe
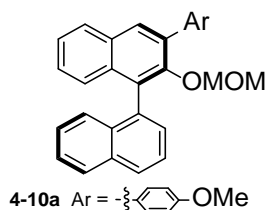
White Solid (mp = 118-120 °C), 908mg (85 % Yield), R_f = 0.59 (CH₂Cl₂:hexane, 2:3) ¹H NMR (400 MHz, CDCl₃) δ = 7.96-7.88 (m, 4H), 7.70-7.58 (m, 4H), 7.50-7.21 (m, 6H) 7.02 (m, 2H), 4.31 (m, 2H), 3.86 (s, 3H), 2.29 (s, 3H) ppm. ¹³C NMR (100.5 MHz, CDCl₃) δ= 159.2, 150.7, 135.2, 134.7, 133.7, 133.4, 133.3, 131.4, 131.1, 130.9, 130.3, 130.2, 129.2, 128.2, 128.0, 127.9, 126.7, 126.3, 126.2, 125.9, 125.5, 125.3, 113.9, 98.8, 56.3, 55.4 ppm. Anal Calcd for C₂₉H₂₄O₃: C, 82.83; H, 5.75%. Found: C, 82.82; H, 5.77%.


4-10b Ar = -ξ⟨⟩-CF₃
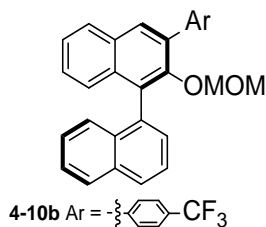
White Solid, (mp = 78-80 °C) 1493mg (92 % Yield), R_f = 0.61 (CH$_2$Cl$_2$:hexane, 2:3) ^{1}H NMR (500 MHz, CDCl$_3$) δ = 7.99-7.92 (m, 4H), 7.88 (d, J=7.5 Hz, 2H), 7.74 (d, J=8.5 Hz, 2H), 7.66-7.58 (m, 2H), 7.51-7.44 (m, 3H), 7.37-7.34 (m, 1H), 7.31-7.24 (m, 2H) 4.29 (m, 2H), 2.30 (s, 3H) ppm. ^{13}C NMR (125.6 MHz, CDCl$_3$) δ = 150.5, 142.9, 134.3, 134.3, 134.1, 133.8, 133.2, 130.9, 130.7, 130.6, 130.2, 129.9 (q, $^2J_{C\text{-}F}$= 32.4Hz), 129.3, 128.4, 128.3, 128.2, 127.7 (q, $^1J_{C\text{-}F}$= 272Hz) 126.9, 126.5, 126.4, 126.1, 125.7, 125.6, 125.4 (q, $^3J_{C\text{-}F}$ = 3.8Hz), 99.2, 56.4 ppm. ^{19}F NMR (376 MHz, CDCl$_3$) δ = -62.4 ppm. HRMS (ESI, [C$_{29}$H$_{21}$ F$_3$O$_2$ + Na]$^+$) Calcd: 481.1391, Found: 481.1403 m/z .

4-10c Ar =
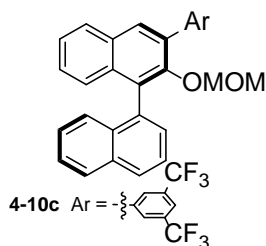
White Solid, (mp = 82-84 °C) 2440mg (84 % Yield), R_f = 0.62 (CH$_2$Cl$_2$:hexane, 2:3) ^{1}H NMR (400 MHz, CDCl$_3$) δ = 8.25 (m, 2H), 8.00 (m, 5H), 7.69-7.23 (m, 8H), 4.29 (m, 2H), 2.41 (m, 3H) ppm. ^{13}C NMR (100.5 MHz, CDCl$_3$) δ = 150.5, 141.4, 134.4, 133.9, 133.8, 133.1, 132.9, 132.2 (q, $^2J_{C\text{-}F}$ = 32.8Hz), 130.9, 130.8, 130.7, 130.2, 129.3, 128.5, 128.46, 128.3, 127.3, 126.6, 126.45, 126.4, 126.2, 126.0, 125.6, 127.7 (q, $^1J_{C\text{-}F}$ = 312Hz), 121.1, 99.5, 56.5 ppm. ^{19}F NMR (376 MHz, CDCl$_3$) δ = -62.6 ppm. HRMS (ESI, [C$_{30}$H$_{20}$ F$_6$O$_2$ + Na]$^+$) Calcd: 549.1265, Found: 549.1262 m/z

.

General Procedure for Removal of MOM protecting group

Under nitrogen, the resulting product **4-10(a-c)** (0.5-5g, 1equiv.) was dissolved in a 1:1 solution of THF:MeOH (16mL/mmol) and combined with Amberlyst-15 (0.25 g/mmol). The

resulting mixture was refluxed at 90 ^{0}C for 24 hours. The reaction was monitored by TLC. Upon completion, the mixture was filtered through a frit, and the solvent was removed under reduced pressure. The resulting products **4-11(a-c)** were purified by column chromatography over silica using CH$_2$Cl$_2$:hexane, 2:3

4-11a Ar = -§—⟨⟩—OMe
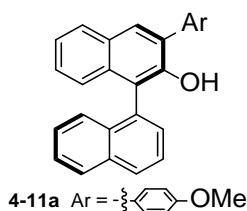
White Solid, (mp = 136-138 °C) 620mg 99 % Yield, R_f = 0.54 (CH$_2$Cl$_2$:hexane, 2:3) ^{1}H NMR (400 MHz, CDCl$_3$) δ = 8.05 (d, *J*= 8.4Hz, 1H), 8.00 (d, *J*= 8.4Hz, 1H), 7.92 (s, 1H), 7.89 (d, *J*= 8.0Hz, 1H), 7.70-7.22 (m, 9H), 7.11 (d, *J*= 8.4Hz, 1H), 7.04 (m, 2H), 5.15 (bs, 1H), 3.87 (s, 3H) ppm. ^{13}C NMR (100.5 MHz, CDCl$_3$) δ= 159.4, 148.8, 134.4, 133.5, 133.0, 132.3, 131.0, 130.3, 130.2, 129.8, 129.7, 129.3, 129.1, 128.6, 128.1, 126.9, 126.6, 126.5, 126.2, 126.1, 125.1, 123.8, 119.7, 114.1, 55.5 ppm. HRMS (ESI, [C$_{27}$H$_{20}$O$_2$ - H]$^-$) Calcd: 375.1385, Found: 375.1379 m/z .

4-11b Ar = -§—⟨⟩—CF$_3$
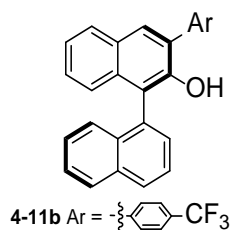
White Solid, (mp = 141-142 °C) 1320mg (97 % Yield), R_f = 0.57 (CH$_2$Cl$_2$:hexane, 2:3) ^{1}H NMR (500 MHz, CDCl$_3$) δ = 8.08 (d, *J*= 8.5Hz, 1H), 8.01 (d, *J*= 8.0Hz, 1H), 7.97 (s, 1H), 7.92 (d, *J*= 8.0Hz, 1H), 7.88 (d, *J*= 7.5Hz, 2H), 7.73-7.68 (m, 3H), 7.61 (d, *J*= 6.5Hz, 1H), 7.57 (m, 1H), 7.47 (d, *J*= 8.0Hz, 1H), 7.40 (m, 2H), 7.38 (m, 1H), 7.11 (d, *J*= 8.0Hz, 1H), 5.12 (s, 1H) ppm. ^{13}C NMR (125.6 MHz, CDCl$_3$) δ = 148.4, 141.9, 134.4, 133.9, 132.9, 131.4, 130.5, 130.2, 129.9, 129.7, 129.5 (q, $^2J_{C-F}$= 44.9Hz), 129.0, 128.8, 128.4, 127.2, 127.1, 126.8, 126.3, 125.8,

125.6 (q, $^1J_{C\text{-}F}$= 274Hz), 125.3 (q, $^3J_{C\text{-}F}$= 3.9Hz), 125.1, 124.2, 120.0 ppm. ^{19}F NMR (376 MHz, CDCl$_3$) δ = -62.4 ppm. HRMS (ESI, [C$_{27}$H$_{17}$F$_3$O - H]$^-$) Calcd: 413.1153, Found: 413.1125 m/z .


4-11c Ar =
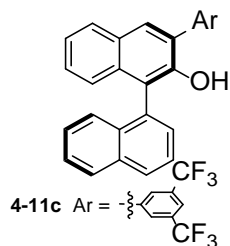
White Solid, (mp = 91-93 °C) 1843 99 % Yield, R_f = 0.58 (CH$_2$Cl$_2$:hexane, 2:3) ^{1}H NMR (400 MHz, CDCl$_3$) δ = 8.23 (s, 2H), 8.09 (d, J= 8.4 Hz, 1H), 8.02 (m, 2H), 7.95 (d, J= 8.4Hz, 1H), 7.89 (s, 1H), 7.73 (m, 1H), 7.62-7.54 (m, 2H), 7.45-7.28 (m, 4H), 7.12 (d, J= 8.4Hz, 1H), 5.19 (bs, 1H) ppm. ^{13}C NMR (100.5 MHz, CDCl$_3$) δ = 148.1, 140.4, 134.5, 134.1, 132.9, 132.1 (q, $^2J_{C\text{-}F}$= 32.9Hz), 130.9, 130.6, 130.1, 129.9, 129.0, 128.8, 127.7 (q, $^1J_{C\text{-}F}$= 273Hz), 128.5, 127.5, 127.4, 127.3, 126.9, 126.3, 125.7, 125.2, 125.0, 124.4, 121.2 (q, $^2J_{C\text{-}F}$= 3.8Hz), 120.3 ppm. ^{19}F NMR (376 MHz, CDCl$_3$) δ = -62.7 ppm. HRMS (ESI, [C$_{28}$H$_{16}$F$_6$O - H]$^-$) Calcd: 481.1027, Found: 481.1029 m/z .

General Procedure for Triflate Formation:

Under inert atmosphere, the 2-hydroxy-1,1'-binaphthyl derivative **4-11(a-c)** (0.5g-2.5g) was placed in an oven-dried two-neck flask containing dry CH$_2$Cl$_2$ (4 mL/mmol of **7**) at 0 °C. DIPEA (1.2 equiv) was added, followed by slow syringe addition of triflic anhydride (1.05 equiv). The reaction mixture was stirred at 0 °C. After complete consumption of starting material as monitored by TLC, the solution volume was doubled by addition of CH$_2$Cl$_2$. The mixture was washed with 1.0 *N* HCl, followed by water and saturated NaHCO$_3$ solution. The organic layer was separated and dried over anhydrous sodium sulfate. Solvent was evaporated to yield the solid triflate. The products **4i-12(a-c)** were purified by column chromatography over silica (1:10 EtOAc:Hexane)

4-12a Ar = -ξ-⟨⟩-OMe
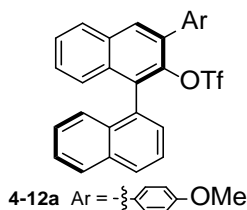
White Solid, (m.p. 97°C (decomp) 640mg (76 % Yield), R_f = 0.60 (CH₂Cl₂:hexane, 2:3) ^{1}H NMR (500 MHz, CDCl₃) δ = 8.05 (d, *J* = 8.0Hz, 1H), 8.01-7.95 (m, 3H), 7.68-7.33 (m, 10H), 7.05 (m, 2H), 3.88 (s, 3H) ppm. ^{13}C NMR (100.5 MHz, CDCl₃) δ = 160.0, 143.6, 134.1, 133.9, 133.0, 132.8, 132.2, 131.5, 131.2, 130.3, 129.6, 129.1, 128.5, 128.1, 127.5, 127.3, 127.2, 126.6, 126.2, 126.0, 125.4, 121.5 (q, $^1J_{C-F}$ = 320.4 Hz), 119.0, 116.4, 114.2, 55.5 ppm. ^{19}F NMR (377 MHz, CDCl₃) δ = -74.8 ppm. HRMS (ESI, [C₂₈H₁₉F₃SO₄ + Na]⁺) Calcd: 531.0854, Found: 531.0875 m/z

.

4-12b Ar = -ξ-⟨⟩-CF₃
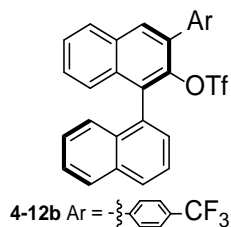
Unstable White Solid 1160mg (80 % Yield), R_f = 0.62 (CH₂Cl₂:hexane, 2:3) ^{1}H NMR (500 MHz, CDCl₃) δ = 8.05-7.95 (m, 3H), 7.76 (m, 4H), 7.66-7.49 (m, 4H), 7.39 (m, 4H), 7.25 (m, 1H) ppm. HRMS (ESI, [C₂₈H₁₇F₆SO₃ + Na]⁺) Calcd: 569.0622, Found: 569.3157 m/z.


4-12c Ar = -ξ-⟨⟩-CF₃ / CF₃
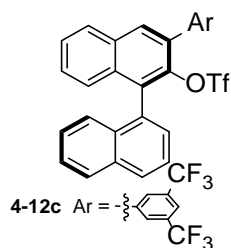
White Solid (m.p. 120°C (decomp) 2250mg (76 % Yield), R_f = 0.63 (CH₂Cl₂:hexane, 2:3) ^{1}H NMR (500 MHz, CDCl₃) δ = 8.08-7.99 (m, 7H), 7.69-7.62 (m, 3H), 7.55 (m, 1H), 7.46-7.35 (m, 4H) ppm. ^{13}C NMR (125.6 MHz, CDCl₃) δ = 142.2, 138.9, 133.9, 133.9, 133.4, 132.7 (q, $^2J_{C-F}$=

33.4Hz), 132.7, 132.5, 131.9, 131.2, 130.5, 130.3, 130.1, 129.9, 128.7, 128.4, 128.4, 128.2, 127.5, 126.9, 126.6 (q, $^1J_{C-F}$ = 273Hz), 126.4, 125.8, 125.4, 122.3 (q, $^3J_{C-F}$ = 3.9Hz), 121.5 (q, $^1J_{C-F}$ = 321Hz) ppm. ^{19}F NMR (376 MHz, CDCl$_3$) δ = -62.9 (6F), -74.9 (3F) ppm. HRMS (ESI, $[C_{29}H_{15}F_9SO_3 + Na]^+$) Calcd: 637.0496, Found: 637.1285 m/z .

General Procedure for Buchwald-Hartwig Amination:

Freshly recrystallized[17] Pd(OAc)$_2$ (10.0 mol%) and xantphos [4,5-bis(diphenylphosphino)-9,9-dimethylxanthene; 10 mol%] were added to freshly distilled dry toluene (3.0 mL/mmol of **4-12(a-c)**) in a sealable reaction vessel, and the reaction mixture was stirred at RT under argon. After 5 min, freshly prepared triflate **4-12(a-c)** (≤500mg, 1equiv), Cs$_2$CO$_3$ (1.2 equiv), and benzylamine (1.5 equiv) were added under argon counterflow, and the mixture was stirred for 3 d at 90 °C. The reaction mixture was then cooled to room temperature, diluted with CH$_2$Cl$_2$ and filtered through Celite. The solvent was evaporated to obtain crude product, which was purified by flash chromatography on silica gel using CH$_2$Cl$_2$:Hexane as the eluent, resulting in isolation of **4-13(a-c)**.

* Pd(OAc)$_2$ must be purchased from either Strem or Frontier Scientific and ideally freshly recrystallized.[17] Pd(OAc)$_2$ from other sources such as Chem-Impex resulted in irreproducible results.

4-13a Ar = -§⟨⟩-OMe
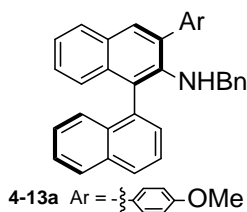
White Solid, (m.p. 87-89°C) 328mg (56 % Yield), R_f = 0.58 (CH$_2$Cl$_2$:hexane, 2:3) ^{1}H NMR (500 MHz, CDCl$_3$) δ = 7.95 (d, J= 8.5Hz, 2H), 7.83 (d, J= 8.5Hz, 1H), 7.81 (s, 1H), 7.71 (m, 2H),

7.56-7.49 (m, 2H), 7.45 (d, *J*= 8.5Hz, 1H), 7.33-7.27 (m, 3H), 7.17 (m, 1H), 7.05-6.97 (m, 6H), 6.56 (m, 2H), 3.88 (s, 3H), 3.54 (d, AB, *J*= 13Hz, 1H), 3.47 (d, AB, *J*= 13Hz, 1H) ppm. ^{13}C NMR (125.7 MHz, CDCl$_3$) δ= 159.1, 143.3, 139.6, 135.2, 134.1, 134.0, 133.6, 133.5, 133.3, 130.7, 130.4, 129.5, 129.2, 128.44, 128.4, 128.2, 128.0, 127.8, 127.0, 126.5, 126.3, 126.26, 126.2, 126.0, 125.5, 125.2, 123.7, 114.2, 55.5, 52.4 ppm. HRMS (ESI, [C$_{34}$H$_{27}$ON + H]$^+$) Calcd: 466.2171, Found: 466.2174 m/z .

4-13b Ar = -⸺⟨⟩-CF$_3$
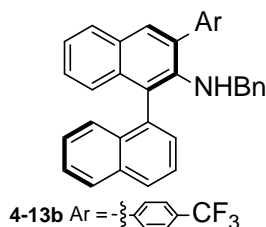
Yellow Oil, 226mg (49 % Yield), R_f = 0.60 (CH$_2$Cl$_2$:hexane, 2:3) ^{1}H NMR (500 MHz, CDCl$_3$) δ = 8.35 (s, 2H), 7.99 (m, 2H), 7.90 (m, 3H), 7.60-7.51 (m, 2H) 7.43-7.34 (m, 4H), 7.264 (m, 2H), 7.08-6.99 (m, 4H), 6.53 (m, 2H), 3.50 (d, AB, *J*= 13Hz, 1H), 3.46 (d, AB, *J*= 13Hz, 1H), 3.37 (bs, 1H) ppm. ^{13}C NMR (125.6 MHz, CDCl$_3$) δ = 143.4, 142.6, 138.6, 134.2, 134.2, 134.1, 133.2, 132.4 (q, $^2J_{C\text{-}F}$= 33.4Hz), 131.5, 131.4, 129.8, 129.4, 129.4, 129.0, 128.8, 128.6, 128.4, 128.2, 127.7, 127.4, 127.3, 127.3, 126.8, 126.5, 126.0, 125.9, 124.7 (q, $^1J_{C\text{-}F}$= 273Hz), 124.6, 121.1 (q, $^3J_{C\text{-}F}$= 3.9Hz), 53.5 ppm. ^{19}F NMR (376 MHz, CDCl$_3$) δ = -62.7 ppm. HRMS (ESI, [C$_{34}$H$_{24}$F$_3$N + H]$^+$) Calcd: 504.1939, Found: 504.1943 m/z .


4-13c Ar = -⸺⟨⟩⟨CF$_3$ / CF$_3$⟩
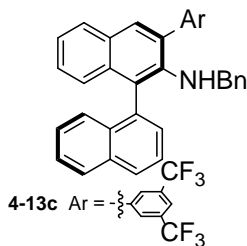
Yellow Oil, 291mg 51 % Yield, R_f = 0.61 (CH$_2$Cl$_2$:hexane, 2:3) ^{1}H NMR (500 MHz, CDCl$_3$) δ = 8.35 (s, 2H), 7.98 (m, 2H), 7.89-7.88 (m, 3H), 7.59-7.51 (m, 2H), 7.43-7.34 (m, 4H), 7.25 (m,

1H), 7.08-6.99 (m, 4H), 6.52 (m, 2H), 3.49 (d, AB J= 13Hz, 1H), 3.46 (d, AB J= 13Hz, 1H), 3.34 (bs, 1H) ppm. ^{13}C NMR (125.6 MHz, CDCl$_3$) δ = 143.4, 142.7, 138.7, 134.2, 134.2, 134.1, 133.2, 132.4 (q, $^2J_{C-F}$= 33.4Hz), 131.5, 131.4, 129.8, 129.4, 129.4, 129.0, 128.8, 128.6, 128.4, 128.2, 127.7, 127.4, 127.3, 127.3, 126.9 (q, $^1J_{C-F}$= 273Hz), 126.8, 126.5, 126.0, 125.9, 124.6, 121.1 (q, $^3J_{C-F}$= 3.8Hz), 53.4 ppm. ^{19}F NMR (376 MHz, CDCl$_3$) δ = -62.7 ppm. HRMS (ESI, [C$_{35}$H$_{23}$F$_6$N + H]$^+$) Calcd: 572.1813, Found: 572.1816 m/z .

General Procedure for Removal of Benzyl Protecting Group:

A solution of **4-13(a-c)** (1-2g, 1equiv) was dissolved in a mixture of dry MeOH (20 mL MeOH/g of amine) and dry CH$_2$Cl$_2$ (40 mL CH$_2$Cl$_2$/g of amine) in an oven-dried two-neck flask equipped with a nitrogen supply. Under nitrogen, 10% Pd/C (10 wt% total with respect to **4-13(a-c)**) was added. The nitrogen atmosphere was then removed under vacuum, and the apparatus was placed under 1 atm of H$_2$ (hydrogen balloon). The mixture was stirred for 1-2 hours at RT, until complete consumption of starting material was indicated by TLC. The hydrogen atmosphere was then removed under vacuum, and the reaction mixture was flushed generously with nitrogen. The suspended Pd/C was removed by filtration through Celite, and the solvent was evaporated to obtain the solid products **4-14(a-c)**. The product was purified by column chromatography over silica (1:10 Et$_2$O:Hexane)

4-14a Ar =-ξ⟨ ⟩-OMe
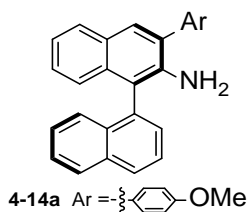
White Solid, (mp = 92-93°C) 1145mg (71 % Yield), R_f = 0.53 (CH$_2$Cl$_2$:hexane, 2:3) ^{1}H NMR (400 MHz, CDCl$_3$) δ = 7.99 (m, 2H), 7.79 (d, J= 8.0Hz, 1H), 7.73 (s, 1H), 7.68 (m, 1H), 7.56-7.49

(m, 5H), 7.36 (m, 1H), 7.24-7.15 (m, 2H), 7.04-6.97 (m, 3H), 3.89 (s, 3H), 3.63 (bs, 2H) ppm. ^{13}C NMR (100 MHz, CDCl$_3$) δ= 159.3, 140.3, 135.2, 134.4, 133.9, 132.6, 131.6, 130.7, 130.3, 129.4, 129.2, 128.5, 128.4, 127.9, 127.86, 126.6, 126.4, 126.35, 126.3, 126.0, 124.5, 122.5, 117.6, 114.4, 55.5 ppm. HRMS (ESI, [C$_{27}$H$_{21}$ON + H]$^+$) Calcd: 376.1701, Found: 376.1703 m/z .


4-14b Ar = -ξ⟨ ⟩-CF$_3$
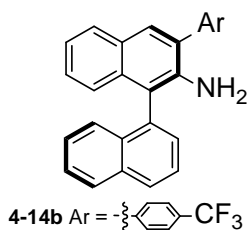
White Solid, (mp = 92-93°C) 583mg (71 % Yield), R_f = 0.56 (CH$_2$Cl$_2$:hexane, 2:3) ^{1}H NMR (500 MHz, CDCl$_3$) δ = 8.01 (m, 2H), 7.81-7.75 (m, 6H), 7.69 (m, 1H), 7.55- 7.47 (m, 3H), 7.37 (m, 1H), 7.27-7.18 (m, 2H), 7.01 (d, J= 8.5Hz, 1H), 3.56 (bs, 2H) ppm. ^{13}C NMR (125.6 MHz, CDCl$_3$) δ = 143.3, 139.5, 134.8, 134.4, 134.3, 132.6, 130.4 (q, $^2J_{C-F}$= 32.4Hz), 130.0, 129.7, 129.3, 129.2, 128.6, 128.59, 128.1, 127.8, 127.6 (q, $^1J_{C-F}$= 272Hz), 126.9, 126.7, 126.5, 126.4, 126.0 (q, $^3J_{C-F}$= 3.8Hz), 125.9, 124.7, 122.9, 118.3 ppm. ^{19}F NMR (376 MHz, CDCl$_3$) δ = -62.5 ppm. HRMS (ESI, [C$_{27}$H$_{18}$F$_3$N + H]$^+$) Calcd: 414.1470, Found: 414.1474 m/z .

4-14c Ar =-ξ⟨ ⟩-CF$_3$ / CF$_3$
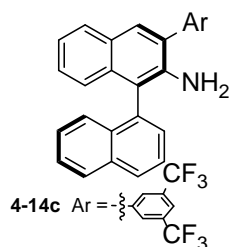
White Solid, (mp = 117-118°C) 691mg (82 % Yield), R_f = 0.57 (CH$_2$Cl$_2$:hexane, 2:3) ^{1}H NMR (500 MHz, CDCl$_3$) δ = 8.47 (s, 2H), 8.36-8.32 (m, 2H), 8.27 (s, 1H), 8.17 (m, 1H), 8.10 (s, 1H), 8.03 (m, 1H), 7.89-7.85 (m, 2H), 7.80 (d, J= 8.5Hz, 1H), 7.72 (m 1H), 7.63-7.55 (m, 2H), 7.36 (d, J= 8.0Hz, 1H), 3.88 (bs, 2H) ppm. ^{13}C NMR (125.6 MHz, CDCl$_3$) δ = 141.8, 139.2, 134.6, 134.5, 134.4, 132.8 (q, $^2J_{C-F}$= 33.3Hz), 132.5, 130.1, 129.9, 129.3, 128.7, 128.69, 128.2, 127.9, 127.5,

127.3, 126.8, 126.7 (q, $^1J_{C\text{-}F}$ = 273Hz), 126.5, 126.4, 125.8, 124.8, 123.2, 121.7 (q, $^3J_{C\text{-}F}$ = 3.8Hz), 119.0 ppm. ^{19}F NMR (376 MHz, CDCl$_3$) δ = -62.7 ppm. HRMS (ESI, [C$_{28}$H$_{17}$F$_6$N + H]$^+$) Calcd: 482.1343, Found: 482.1345 m/z .

General Procedure for Formamide Formation:

95% formic acid (10 equiv) was added to a solution of **4-14(a-c)** (1-2g, 1equiv.) in benzene. The solution was heated to 95 ^{0}C in a flask equipped with Dean-Stark apparatus to remove water, until the starting material had been consumed as judged by TLC. The reaction mixture was then cooled, diluted with EtOAc, and washed successively with water and saturated sodium carbonate solution. The organic layer was dried over anhydrous sodium sulfate and concentrated under vacuum to yield crude product, which was purified by flash column chromatography on silica (1:5 Et$_2$O:Hexane), resulting in the isolation of **4-15(a-c)**.

4-15a Ar = -ξ⟨ ⟩–OMe
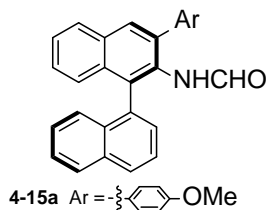
White Solid, (mp = 124-125°C) 1400mg (92 % Yield), R_f = 0.42 (CH$_2$Cl$_2$:hexane, 2:3) ^{1}H NMR (500 MHZ, CDCl$_3$): mixture of isomer δ= 8.00 (m, 4H), ppm. ^{13}C NMR (125.6MHZ, CDCl$_3$): δ= 164.1, 159.8, 159.4, 138.3, 135.0, 134.6, 134.1, 133.8, 133.0, 132.8, 132.5, 132.4, 132.0, 131.8, 131.0, 130.7, 130.5, 130.3, 130.0, 129.9, 129.2, 129.0, 128.7, 128.6, 128.5, 128.3, 128.1, 127.2, 127.0, 126.8, 126.6, 126.56, 126.5, 126.3, 125.9, 125.85, 125.6, 125.2, 114.7, 113.8, 55.5 ppm. IR (Neat) 3415, 1647 cm^{-1} HRMS (ESI, [C$_{28}$H$_{21}$O$_2$N + H]$^+$) Calcd: 404.1651, Found: 404.1654 m/z .

4-15b Ar = -§-⟨benzene⟩-CF$_3$
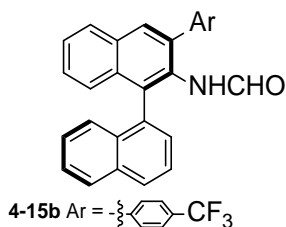
White Solid, (mp = 111-112°C) 1879mg (88 % Yield), R_f = 0.53 (CH$_2$Cl$_2$:hexane, 2:3) ^{1}H NMR (500 MHz, CDCl$_3$) mixture of isomers: δ = 8.03-7.95 (m, 7H), 7.76-7.22 (m, 27H), 6.66 (bd, J = 11.5Hz, 1H), 6.56 (bs, 1H) ppm. ^{13}C NMR (125.6 MHz, CDCl$_3$) δ = 163.9, 159.7, 143.9, 142.7, 137.3, 135.7, 134.2, 134.1, 134.0, 133.9, 133.5, 133.3, 133.2, 132.9, 132.8, 132.4, 132.3, 132.0, 131.1, 130.3, 130.2, 130.1, 129.8, 129.7, 129.5, 129.4, 129.3, 129.1, 128.8, 128.7, 128.67, 128.3, 127.7, 127.3, 127.1, 127.03, 127.0, 126.9, 126.8, 126.77, 126.7, 126.5, 126.2, 126.19, 125.93, 125.9, 125.5, 125.3, 125.27, 125.0, 123.3, 123.1 ppm. ^{19}F NMR (376 MHz, CDCl$_3$) δ = -62.4, -62.6 ppm. IR (Neat) 3411, 1660 cm^{-1} HRMS (ESI, [C$_{28}$H$_{18}$F$_3$NO + H]$^+$) Calcd: 442.1419, Found: 442.1414 m/z .

4-15c Ar = -§-⟨benzene⟩ with CF$_3$, CF$_3$
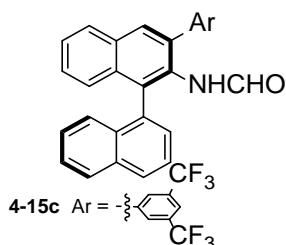
White Solid, (mp = 121-122°C) 889mg (84 % Yield), R_f = 0.57 (CH$_2$Cl$_2$:hexane, 2:3) ^{1}H NMR (500 MHz, CDCl$_3$) mixture of isomers δ = 8.05-7.88 (m, 14H), 7.74-7.22 (m, 18H), 6.69 (m 2H) ppm. ^{13}C NMR (125.6 MHz, CDCl$_3$) δ = 163.6, 159.4, 142.4, 141.3, 135.4, 135.3, 134.2, 134.0, 133.9, 133.7, 133.4, 133.0, 132.8, 132.6, 132.5, 132.3, 132.0, 131.7, 131.5, 131.3, 131.2, 130.4, 130.0, 129.5, 129.4, 129.3, 129.1, 129.07, 128.7, 128.6, 128.3, 128.1, 127.5, 127.4, 127.3, 127.22, 127.2, 126.9, 126.8 (q, $^1J_{C-F}$ = 273Hz), 126.7, 126.6, 126.5 (q, J_{C-F} = 273Hz), 125.9, 125.4, 125.0, 121.9, 121.2 (q, $^3J_{C-F}$ = 3.8Hz), ppm. ^{19}F NMR (376 MHz, CDCl$_3$) (70:30 ratio) δ = -62.7, -62.8

ppm. IR (Neat) 3385, 1667 cm^{-1} HRMS (ESI, $[C_{29}H_{17}F_6NO + H]^+$) Calcd: 510.1293, Found: 510.1302 m/z .

General Procedure for Isocyanide Synthesis:

To a solution of **4-15(a-c)** (0.5-1.5g, 1equiv.) in dry CH_2Cl_2 (3mL/mmol) was added $^iPr_2NH$ (5.0 equiv), and the reaction mixture was stirred for 5 min under nitrogen at 0 °C. POCl$_3$ (1.2 equiv.) was then added dropwise, and the reaction mixture was stirred under nitrogen at RT. After consumption of starting material as monitored by TLC, the solution was diluted with CH_2Cl_2 (~30mL) and washed sequentially with 0.5 N Na$_2$CO$_3$ and water. The organic layer was dried over anhydrous sodium sulfate and concentrated under reduced pressure. The crude product was purified by flash chromatography on silica (1:6 EtOAc:Hexane), resulting in the isolation of **4-16(a-c).**

4-16a Ar = -§⟨◯⟩-OMe
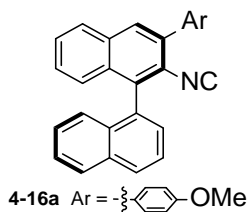
White Solid, (m.p. 79°C (decomp)) 1083mg (81 % Yield), R_f = 0.60 (CH$_2$Cl$_2$:hexane, 2:3) ^{1}H NMR (400 MHZ, CDCl$_3$): δ= 8.05 (d, J=8.4 Hz. 1H), 8.00-7.94 (m, 3H), 7.69-7.49 (m, 6H), 7.37-7.28 (m, 4H), 7.07 (m, 2H), 3.88 (s, 3H) ppm. ^{13}C NMR (100.5 MHZ, CDCl$_3$): δ= 168.9, 159.8, 137.5, 135.6, 133.9, 133.7, 133.0, 132.1, 132.0, 130.8, 130.0, 129.5, 129.2, 128.7, 128.2, 128.0, 127.4, 127.3, 126.7, 126.3, 125.7, 125.5, 123.2, 114.1, 55.5 ppm. IR (Nujol) 2112 cm^{-1} HRMS (ESI, $[C_{28}H_{19}ON + H]^+$) Calcd: 386.1545, Found: 386.1546 m/z .

4-16b Ar = ξ—⟨benzene⟩—CF_3
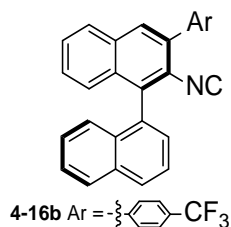
White Solid (m.p. 70°C (decomp)) 590mg (82 % Yield), R_f = 0.67 (CH$_2$Cl$_2$:hexane, 2:3) ^{1}H NMR (500 MHz, CDCl$_3$) δ = 8.13 (s, 2H), 8.07 (d, J= 8.0Hz, 1H), 8.03-7.99 (m, 4H), 7.70-7.62 (m, 2H), 7.55 (m, 2H), 7.44-7.33 (m, 3H), 7.26 (m, 2H) ppm. ^{13}C NMR (125.6 MHz, CDCl$_3$) δ = 170.4, 139.6, 138.3, 133.8, 132.8, 132.7, 132.6, 132.6, 132.4 (q, $^2J_{C-F}$= 33.3Hz), 131.8, 129.9, 129.7, 129.7, 129.5, 128.7, 128.5, 128.3, 128.3, 128.0, 127.4, 126.8, 126.5 (q, $^1J_{C-F}$= 273Hz), 126.3, 125.6, 125.1, 122.2 (q, $^3J_{C-F}$= 3.8Hz), ppm. ^{19}F NMR (376 MHz, CDCl$_3$) δ = -62.8 ppm. IR (Neat) 2113 cm^{-1} HRMS (ESI, [C$_{28}$H$_{16}$F$_3$N + H]$^+$) Calcd: 424.1313, Found: 424.1318 m/z .

4-16c Ar = -ξ—⟨benzene⟩ with CF_3, CF_3
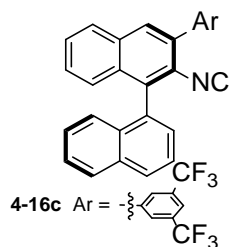
White Solid, (m.p. 70°C (decomp)) 405mg (84 % Yield), R_f = 0.67 (CH$_2$Cl$_2$:hexane, 2:3) ^{1}H NMR (500 MHz, CDCl$_3$) δ = 8.15 (s, 2H), 8.08 (d, J= 8.5Hz, 1H), 8.04-8.00 (m, 4H), 7.71-7.24 (m, 8H) ppm. ^{13}C NMR (125.6 MHz, CDCl$_3$) δ = 170.6, 139.8, 138.4, 134.0, 132.9, 132.9, 132.9, 132.8, 132.7, 132.6 (q, $^2J_{C-F}$= 33.4Hz), 132.0, 130.1, 129.9, 129.9, 129.6, 128.8, 128.7, 128.5, 128.5, 128.2, 127.0, 126.6 (q, $^1J_{C-F}$= 273Hz), 126.5, 125.8, 125.3, 122.4 (q, $^3J_{C-F}$= 3.9Hz) ppm. ^{19}F NMR (376 MHz, CDCl$_3$) δ = -62.7 ppm. IR (Neat) 2116 cm^{-1} HRMS (ESI, [C$_{29}$H$_{15}$F$_6$N + H]$^+$) Calcd: 492.1187, Found: 492.1187 m/z .

General Procedure for Isocyanide Gold Complex Synthesis:

To a solution of binaphthyl isocyanide **4-16(a-c)** (0.1-05.g) in dry CH_2Cl_2 (0.2 M) was added Au(THT)Cl (0.95 equiv), and the reaction mixture was stirred overnight at RT under nitrogen. The solvent was evaporated under reduced pressure, and the crude products **4-17(a-c)** were washed with pentane to obtain a white solid, which was recrystallized from CH_2Cl_2/pentane.

4-17a Ar = -§-⟨◯⟩-OMe
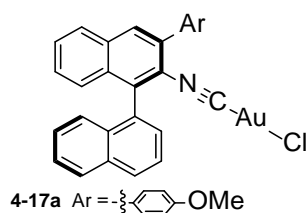
White solid, 399mg (83 % Yield). ^{1}H NMR (400 MHZ, CDCl$_3$): δ= 8.10 (d, J=8.4 Hz. 1H), 8.04-7.94 (m, 3H), 7.71-7.36 (m, 9H), 7.21 (d, J=8.4 Hz, 1H), 7.08 (d, J=8.4 Hz, 2H), 3.90 (s, 3H) ppm. ^{13}C NMR (100.5 MHZ, CD$_2$Cl$_2$): δ= 160.6, 145.8, 140.1, 135.6, 134.2, 132.5, 132.0, 132.0, 130.8, 130.3, 130.2, 129.5, 129.2, 129.0, 128.7, 128.4, 128.2, 127.6, 127.4, 126.9, 126.0, 125.2, 121.5, 114.7, 55.8 ppm. IR (Nujol) 2213 cm^{-1} Anal calcd For $C_{28}H_{19}AuClNO$: C, 54.43; H, 3.10; N, 2.27 % Found C, 54.27; H, 3.09; N, 2.21 %

4-17b Ar = -§-⟨◯⟩-CF$_3$
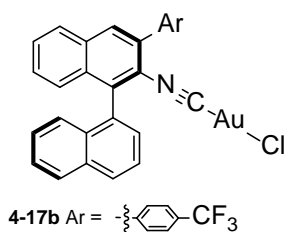
White Solid, 595mg (96 % Yield), ^{1}H NMR (500 MHz, CD$_2$Cl$_2$) δ = 8.15-8.06 (m, 4H), 7.86-7.70 (m, 6H), 7.60-7.39 (m,5H), 7.25 (d, J= 8.4Hz, 1H) ppm. ^{13}C NMR (125.7 MHz, CD$_2$Cl$_2$) δ = 145.7, 140.8, 140.6, 134.3, 134.2, 134.1, 132.6, 132.1, 131.9, 131.5 (q, [2]J_{C-F}= 32.4Hz), 130.9, 130.4, 130.1, 129.9, 129.3, 129.0, 129.0, 128.5, 127.7 (q, [1]J_{C-F}= 273Hz), 127.7, 127.6, 127.0, 126.4 (q, [3]J_{C-F}= 3.8Hz), 126.1, 125.1, 120.8 ppm. ^{19}F NMR (376 MHz, CD$_2$Cl$_2$) δ = -62.9 ppm. IR (nujol)

2213 cm^{-1} Anal. calcd For $C_{28}H_{16}F_3AuClN$: C, 51.28; H, 2.46; N, 2.14 % Found C, 51.82 ; H, 2.59 ; N, 2.06 %

4-17c Ar =
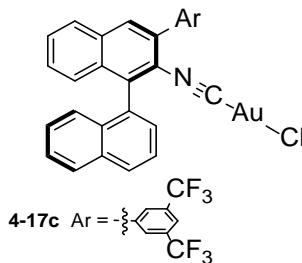
White Solid, 707mg (96 % Yield), ^{1}H NMR (500 MHz, CD$_2$Cl$_2$) δ = 8.15-8.07 (m, 7H), 7.77-7.73 (m, 2H), 7.61-7.51 (m, 3H), 7.43 (m, 2H), 7.23 (d, *J*= 8.5Hz, 1H) ppm. ^{13}C NMR (125.7 MHz, CD$_2$Cl$_2$) δ = 145.9, 141.2, 139.0, 134.3, 134.0, 133.1 (q, $^2J_{C-F}$= 33.4Hz), 132.9, 132.5, 131.1, 130.6, 130.3, 130.1, 130.0, 129.4, 129.3, 129.1, 128.5, 127.9, 127.7, 127.1, 126.8 (q, $^1J_{C-F}$= 273Hz), 126.1, 125.0, 123.2 (q, $^3J_{C-F}$= 3.8Hz), 120.6 ppm. ^{19}F NMR (376 MHz, CD$_2$Cl$_2$) δ = -63.1 ppm. IR (nujol) 2214 cm^{-1} Anal. calcd For $C_{29}H_{15}F_6AuClN$: C, 48.12; H, 2.09; N, 1.94 % Found C, 48.23 ; H, 2.15 ; N, 1.97 %

General Procedure for ADC-Au Complex Formation

To a solution of **4-17(a-c)** (0.1-0.3g, 1equiv) in CHCl$_3$ (2mL) under nitrogen was added the desired amine (2 equiv) all at once, and the mixture was heated to 60 $^{°}$C. The reaction was monitored by IR by disappearance of the CN stretching frequency. The solvent was removed under reduced pressure, and the products **4-18(a-c)** were filtered through Celite and were recrystallized from CH$_2$Cl$_2$/pentane.

4-18a
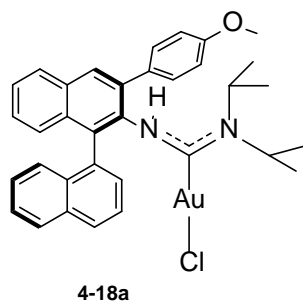
White solid, 97mg (83 % Yield). ^{1}H NMR (400 MHZ, CD$_2$Cl$_2$): mixture of isomer δ= 8.07-7.30 (m, 14H), 7.28 (m, 2H), 6.83 (s, 1H), 6.56 (s, 1H), 4.91 (bm, 1H), 3.33 (m, 1H), 1.12-0.64 (m, 10H), 0.11- -0.07 (bm, 4H) ppm. ^{13}C NMR (100.5 MHZ, CD$_2$Cl$_2$): δ= 194.0, 193.2, 159.4, 159.3, 139.0, 138.7, 137.0, 135.8, 135.6, 135.5, 134.9, 134.5, 134.3, 134.27, 133.546, 133.53, 133.2, 133.0, 132.9, 1132.8, 132.78, 132.6, 132.4, 132.2 132.0, 131.9, 130.6, 130.4, 130.3, 129.9, 129.2, 128.8, 128.5, 128.4, 128.2, 128.1, 127.9, 127.6, 127.55, 127.3, 127.2, 127.0, 126.9, 126.8, 126.4, 126.38, 126.3, 126.2, 126.0, 125.9, 125.5, 125.0, 124.5, 114.6, 114.0, 133.7, 113.1, 55.8, 55.6, 46.1, 20.4, 19.6, 19.0 ppm Anal. calcd For C$_{34}$H$_{34}$AuClN$_2$O: C, 56.79; H, 4.77; N, 3.90 % Found C, 57.69 ; H, 4.69; N, 3.78 %

4-18b
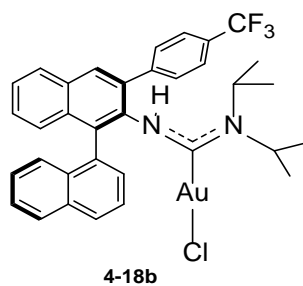
White Solid, 111mg (96 % Yield), ^{1}H NMR (500 MHz, CD$_2$Cl$_2$) mixture of isomers 1:1 δ = 9.28 (bs, 1H), 8.12-7.91 (m, 8H), 7.79-7.32 (m, 21H), 6.86 (bs, 1H), 6.57 (bs, 1H), 4.88 (bm, 2H), 3.39 (m, 4H), 1.09-0.636 (m, 18H), 0.10 (bs, 3H), -0.07 (bs, 3H) ppm. ^{13}C NMR (125.7 MHz, CD$_2$Cl$_2$) δ = 194.2, 193.4, 143.8, 143.7, 138.0, 137.5, 137.2, 135.7, 135.3, 135.2, 134.5, 134.4,

134.4, 134.2, 133.5, 133.5, 133.4, 133.0, 132.8, 131.8, 131.76, 131.7, 130.9, 130.5, 130.1, 129.4, 129.3, 128.8, 128.7, 128.7, 128.24, 128.2, 128.0, 127.7, 127.7, 127.7, 127.6, 127.6, 127.5, 127.4, 127.1, 126.8, 126.6, 126.3, 125.9, 125.8, 125.7, 125.3 (q, $^3J_{C-F}$= 3.8Hz),, 124.6, 63.0, 47.8, 46.2, 20.5, 19.64, 19.6, 19.0 ppm. ^{19}F NMR (376 MHz, CD$_2$Cl$_2$) δ = -62.7, -62.8 ppm. Anal. calcd For C$_{34}$H$_{31}$F$_3$AuClN$_2$: C, 53.94; H, 4.13; N, 3.70 % Found C, 53.71 ; H, 4.57 ; N, 4.20 %

4-18c
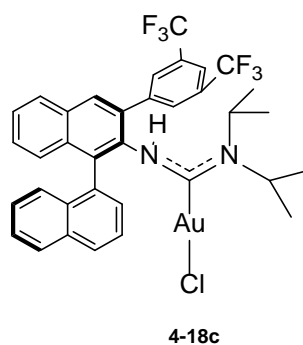
White Solid, 109mg (96 % Yield), ^{1}H NMR (500 MHz, CD$_2$Cl$_2$) mixture of isomers δ = 8.18-8.14 (m, 6H), 8.08-8.06 (m, 2H), 8.02-7.90 (m, 6H), 7.81 (m, 1H), 7.70-7.50 (m 9H), 7.45-7.30 (m, 7H), 6.91 (bs, 1H), 6.59 (bs, 1H), 4.91 (bm, 2H), 3.34 (m, 3H), 1.45 (d, J= 6.5 Hz, 3H), 1.07-0.64 (m, 20H), 0.02 (bs, 3H), -0.068 (bs, 3H) ppm. ^{13}C NMR (125.7 MHz, CDCl$_3$) δ = 194.5, 193.7, 142.3, 142.1, 137.6, 136.0, 135.7, 135.6, 134.9, 134.9, 134.5, 134.4, 134.1, 134.0, 133.8, 133.7, 132.0 (q, $^2J_{C-F}$= 33.4Hz), 132.0 (q, $^2J_{C-F}$= 33.4Hz), 131.7, 131.5, 131.5, 131.5, 131.4, 131.4, 131.1, 130.1, 129.6, 129.3, 128.9, 128.8, 128.8, 128.4, 128.4, 128.1, 128.1, 128.0, 127.8, 127.7, 127.7, 127.7, 127.2 (q, $^1J_{C-F}$= 273Hz), 127.1 (q, $^1J_{C-F}$= 273Hz), 126.8, 126.7, 126.3, 125.8, 124.6, 121.6 (q, $^3J_{C-F}$= 3.9Hz), 121.3 (q, $^3J_{C-F}$= 3.8Hz), 62.7, 47.9, 46.4, 20.0, 20.0, 19.6, 19.5, 19.0 ppm. ^{19}F NMR (376 MHz, CDCl$_3$) δ = -62.80, -62.73 ppm. Anal. calcd C$_{35}$H$_{30}$F$_6$AuClN$_2$: C, 50.95; H, 3.67; N, 3.40 % Found C, 50.83 ; H, 3.59 ; N, 3.41 %

4-20h
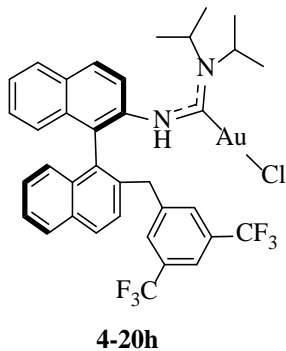
White Solid, 48mg (84 % Yield), ^{1}H NMR (400 MHz, CD$_2$Cl$_2$) δ = 8.31 (d, *J*= 8.8Hz, 1H), 8.12 (d, *J*= 8.8Hz, 1H), 8.05 (d, *J*= 8.4Hz, 1H), 7.97 (t, *J*= 8.8Hz, 1H), 7.65 (d, *J*= 8.8Hz, 1H), 7.53-7.34 (m, 4H), 7.24-7.12 (m, 4H), 6.90 (d, *J*= 8.4Hz, 1H), 6.79 (bs, 1H), 5.26 (bs, 1H), 4.06 (d, *J$_{AB}$*= 14.8Hz, 1H), 3.94 (d, *J$_{AB}$*= 14.8Hz, 1H), 3.44 (sept, *J*= 7.2Hz, 1H), 1.17 (d, *J*= 6.8Hz, 3H), 1.10 (d, *J*= 6.4Hz, 3H), 0.46 (d, *J*= 7.2Hz, 3H), 0.29 (d, *J*= 7.2Hz, 3H), ppm. ^{13}C NMR (100.5 MHz, CD$_2$Cl$_2$) δ = 190.6, 142.8, 137.3, 133.6, 132.7, 132.5, 131.9 (q, $^2J_{C-F}$= 32.9Hz), 130.1, 129.6, 129.4, 128.9, 128.7, 128.3, 128.1, 127.5, 126.9, 126.4, 127.6 (q, $^1J_{C-F}$= 272Hz), 127.5, 126.9, 126.4, 125.7, 125.6, 124.8, 120.5 (q, $^3J_{C-F}$= 4.4Hz), 63.5, 43.4, 40.6, 20.6, 19.8, 19.4 ppm. ^{19}F NMR (376 MHz, CD$_2$Cl$_2$) δ = -63.15 ppm. Anal. calcd For C$_{36}$H$_{32}$F$_6$AuClN$_2$: C, 51.53; H, 3.84; N, 3.34 % Found C, 51.46; H, 3.62 ; N, 3.32 %

4-20j
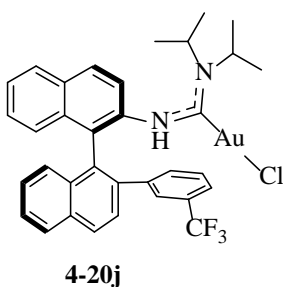
White Solid, 37mg (64 % Yield), ^{1}H NMR (500 MHz, CDCl$_3$) δ = 8.21(d, *J*= 9.0Hz, 1H), 8.10 (d, *J*= 8.5Hz, 1H), 8.01 (d, *J*= 8.0Hz, 1H), 7.96 (d, *J*= 8.5Hz, 1H), 7.85 (d, *J*= 8.0Hz, 1H), 7.73 (d, *J*= 8.5Hz, 2H), 7.58 (m, 1H). 7.45-7.15 (m, 10H), 5.32 (bs, 1H), 3.54 (sept, *J*= 7.0Hz, 1H),

1.17 (d, *J*= 6.5Hz, 3H), 1.11 (d, *J*= 6.0Hz, 3H), 0.70 (d, *J*= 7.0Hz, 3H), 0.47 (d, *J*= 7.5Hz, 3H)

ppm. ^{13}C NMR (125.7 MHz, CDCl$_3$) δ = 190.4, 140.8, 138.9, 137.0, 133.5, 133.1, 132.3, 132.0,

131.3, 130.8 (q, $^2J_{\text{C-F}}$= 32.1Hz), 129.7, 129.5, 128.8, 128.7, 128.6, 127.7, 127.3, 127.3 (q, $^1J_{\text{C-F}}$=

272Hz), 127.1, 126.0, 125.9, 125.8, 125.5 (q, $^3J_{\text{C-F}}$= 3.77Hz), 124.6 (q, $^3J_{\text{C-F}}$= 3.77Hz), 123.6,

63.3, 45.9, 20.5, 19.9, 19.4 ppm. ^{19}F NMR (470 MHz, CD$_2$Cl$_2$) δ = -62.91 ppm. Anal. calcd For

C$_{34}$H$_{31}$F$_3$AuClN$_2$: C, 53.94; H, 4.13; N, 3.70 % Found C, 53.97 ; H, 4.68 ; N, 4.30 %

4-20k
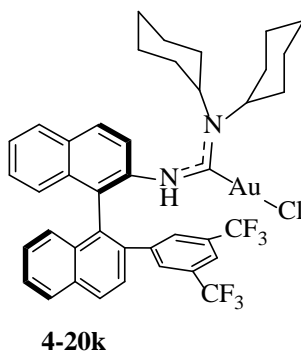
White Solid, 47mg (75 %Yield), ^{1}H NMR (500 MHz, CD$_2$Cl$_2$) δ = 8.20 (d, *J*= 8.5Hz, 1H),

8.12 (d, *J*= 8.5Hz, 1H), 8.08 (d, *J*= 8.0Hz, 1H), 8.01 (d, *J*= 9.0Hz, 2H), 7.77 (d, *J*= 8.5Hz, 1H),

7.66 (s, 1H), 7.63 (m, 1H), 7.57 (m, 1H), 7.46 (m, 2H), 7.36-7.33 (m, 4H), 7.05 (bs, 1H), 4.81 (m,

1H), 3.04 (m, 2H), 2.13 (m, 1H), 1.81-0.86 (m, 16H), -0.18 (m, 1H), -0.55 (m, 1H)   ppm. ^{13}C

NMR (125.7 MHz, CD$_2$Cl$_2$) δ = 190.4, 142.0, 138.0, 137.2, 134.6, 134.1, 132.9. 132.2. 132.2.

131.7 (q, $^2J_{\text{C-F}}$= 33.4Hz), 130.2, 129.5, 129.4, 129.2, 128.9, 128.6, 128.2 127.9, 127.4, 126.8, (q,

$^1J_{\text{C-F}}$= 273Hz), 126.4, 126.2, 125.9, 124.2, 122.6, 72.4, 57.2, 30.9, 30.1, 26.3, 26.2, 15.8, 25.6,

25.4, 25.3, 24.8 ppm. ^{19}F NMR (376 MHz, CD$_2$Cl$_2$) δ = -63.18 ppm. Anal. calcd For

C$_{41}$H$_{38}$F$_6$AuClN$_2$: C, 54.40; H, 4.23; N, 3.09 % Found C, 54.42; H, 4.11 ; N, 3.58 %
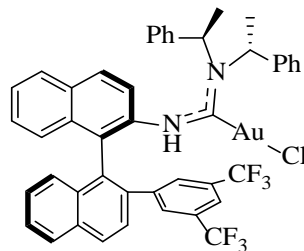
4-20l

White Solid, 75 mg (71% Yield), ^{1}H NMR (500 MHz, CDCl$_3$) δ = 8.19 (d, *J*= 8.5Hz, 1H), 8.13 (d, *J*= 8.5Hz, 1H), 7.71 (m, 2h), 7.82 (d, *J*= 9.0Hz, 1H), 7.56-7.26 (m, 11H), 7.20 (d, *J*= 8.5Hz, 1H), 7.08 (d, *J*= 8.5Hz, 1H), 6.88 (m, 1H), 6.76 (s, 1H), 6.74 (sept, *J*=7Hz, 1H), 6.62 (m, 2H), 5.69 (d, *J*= 8.0Hz, 1H), 4.59 (sept, *J*= 6.5Hz, 1H), 1.75 (d, *J*= 7.0Hz, 3H), 0.99 (d, *J*= 7.0Hz, 3H) ppm. ^{13}C NMR (101 MHz, CDCl$_3$) δ = 190.6, 141.7, 138.0, 137.3, 136.5, 136.2, 134.0, 133.5, 132.5, 132.1, 132.0, 131.7 (q, $^2J_{C\text{-}F}$= 33.3Hz), 130.0, 129.6, 129.2, 129.1, 129.0, 128.9, 128.5, 128.2, 128.1, 128.1, 128.0, 127.9, 127.7, 127.3, 126.8, 126.4, 126.2 (q, $^1J_{C\text{-}F}$= 273Hz), 125.7, 124.9, 124.7, 122.4 (q, $^3J_{C\text{-}F}$= 3.77Hz), 69.3, 52.4, 16.9, 16.3 ppm. ^{19}F NMR (376 MHz, CDCl$_3$) δ = -62.7 ppm. Anal. calcd For C$_{45}$H$_{34}$F$_6$AuClN$_2$: C, 56.94; H, 3.61; N, 2.95 % Found C, 56.86 ; H, 3.55 ; N, 3.03 %
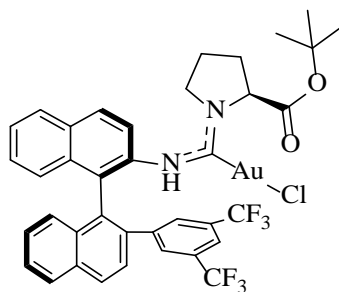
4-20n

White Solid, 42 mg (67% Yield), Mixture of isomers (2:1) ^{1}H NMR (500 MHz, CDCl$_3$) δ = 8.32 (d, *J*= 9.0Hz, 1H, major), 8.24 (d, *J*= 8.0Hz, 1H, minor), 8.18 (d, *J*= 8.0Hz, 1H, major) 8.16 (d, *J*= 9.0Hz, 1H, minor) 8.14-7.13 (m, 13H, majpr and minor), 6.77 (bs, 1H, major), 4.82 (m,

169

1H), 4.14 (m, 1H), 3.86 (m, 1H0, 3.53 (m, 1H), 2.76 (m, 1H), 2.31 (m,1H), 1.99 (m, 2H), 1.47 (s, 9H, major), 1.06 (s, 9H, minor) ppm. ^{13}C NMR (101 MHz, CD$_2$Cl$_2$) δ = 191.7, 190.0, 170.5, 168.5, 142.5, 142.3, 136.9, 136.9, 136.3, 135.3, 134.0, 133.7, 133.5, 133.3, 132.6, 132.2, 132.0, 131.9, 131.7, 131.6, 131.5, 131.4, 131.3, 131.1, 131.1, 130.8, 130.4, 130.2, 130.1, 129.8, 129.1, 129.0, 128.9, 128.9, 128.8, 128.5, 128.4, 128.3, 128.2, 127.9, 127.9, 127.8, 127.4, 127.2, 127.1, 127.0, 126.9, 126.8, 126.4 (q, $^1J_{C\text{-}F}$= 273Hz), 126.3, 126.2, 126.2, (q, $^1J_{C\text{-}F}$= 273Hz) 125.8, 125.6, 123.4, 122.7, 121.4 (q, $^3J_{C\text{-}F}$= 3.77Hz), 84.2, 83.3, 68.5, 61.8, 571, 45.1, 31.8, 28.7, 28.1, 27.5, 23.3, 22.9 ppm. ^{19}F NMR (376 MHz, CDCl$_3$) δ = -63.33 (minor) -63.35 (major) ppm. Anal. calcd For C$_{38}$H$_{32}$F$_6$AuClN$_2$O$_2$: C, 50.99; H, 3.60; N, 3.13 % Found C, 50.88 ; H, 3.22 ; N, 2.91 %
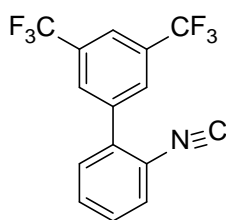
2-isocyano-3',5'-bis(trifluoromethyl)-1,1'-biphenyl

Light blue solid (m.p. 95°C) 2.3g (84 % Yield), R$_f$ 0.50 (1:5 acetone/hexanes); ^{1}H NMR (400 MHz, CDCl$_3$): δ = 7.98 (d, J = 5.2 Hz, 3 H), 7.58-7.46 (m, 4 H). ^{13}C NMR (101 MHz, CDCl$_3$): δ = 168.5, 139.1, 139.1, 135.9, 135.8, 132.7 (q, $^2J_{C,F}$ = 33.1 Hz), 131.5, 131.2, 131.0, 130.8, 130.7, 130.5, 130.5, 130.3, 130.2, 130.2, 129.9, 129.6, 129.4, 129.4, 128.9, 128.8, 128.8, 128.6, 128.4, 128.2, 127.9, 127.7, 127.3, 126.6, 124.8, 124.6, 123.4, 122.5 (sept, $^3J_{C,F}$ = 3.6 Hz), 121.9, 121.3, 120.3, 119.2. ^{19}F NMR (377 MHz, CDCl$_3$): δ = -63.85. IR (neat): ν = 2122 cm^{-1} (CN). Anal Calcd for C$_{15}$H$_7$F$_6$N: C, 57.16; H, 2.24; N, 4.44 %. Found: C, 57.19; H, 2.30; N, 4.49 %.
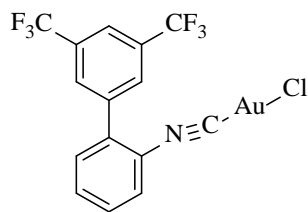
4-21a

Chloro(2-isocyano-3',5'-bis(trifluoromethyl)-1,1'-biphenyl)gold(I)

White solid, yield 1040 mg (76%). ^{1}H NMR (400 MHz, CDCl$_3$): δ = 8.03 (s, 1 H), 7.92 (d, J = 0.4 Hz, 2 H), 7.76-7.72 (m, 2 H), 7.65 (dt, J = 7.2, 1.2 Hz, 1 H), 7.58 (dd, J = 7.2, 0.8 Hz, 1 H). ^{13}C NMR (101 MHz, CDCl$_3$): δ = 144.8, 138.1, 137.4, 133.7 (q, $^2J_{C,F}$ = 34.6 Hz), 132.8, 131.5, 130.8, 129.5, 129.1, 127.4 (q, $^1J_{C,F}$ = 273.2 Hz), 123.7 (septet, $^3J_{C,F}$ = 3.7 Hz), 123.2. ^{19}F NMR (377 MHz, CDCl$_3$): δ = -63.75. IR (neat): ν = 2227 cm^{-1} (CN). Anal Calcd for C$_{15}$H$_7$AuClF$_6$N: C, 32.90; H, 1.29; N, 2.56 %. Found: C, 32.96; H, 1.24; N, 2.49 %.
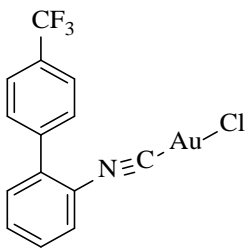
4-21b

Chloro(2-isocyano-4'-(trifluoromethyl)-1,1'-biphenyl)gold(I)

White solid, yield 1.0g (83%). ^{1}H NMR (400 MHz, CDCl$_3$): δ = 7.82 (d, J = 8.0 Hz, 2 H), 7.70 (dt, J = 7.2, 1.6 Hz, 2 H), 7.59-7.56 (m, 3 H), 7.54-7.51 (m, 1 H). ^{13}C NMR (101 MHz, CDCl$_3$): δ = 143.5, 139.4, 138.7, 132.1, 131.9 (q, $^2J_{C,F}$ = 33.2 Hz), 131.1, 129.7, 129.3, 128.7, 128.0 (q, $^1J_{C,F}$ = 272.4 Hz), 126.3 (q, $^3J_{C,F}$ = 3.6 Hz), 122.6. ^{19}F NMR (377 MHz, CDCl$_3$): δ = -

63.71. IR (neat): $\nu = 2216$ cm^{-1} (NC). Anal Calcd for $C_{14}H_8AuClF_3N$: C, 35.06; H, 1.68; N, 2.92 %. Found: C, 35.10; H, 1.49; N, 2.93 %.

4-21c
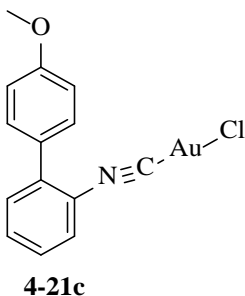
Chloro(2-isocyano-4'-(methoxy)-1,1'-biphenyl)gold(I)

White solid, yield 1950 mg (88%). ^{1}H NMR (400 MHz, CDCl$_3$): δ = 7.63-7.59 (m, 2 H), 7.50-7.42 (m, 2 H), 7.37 (dd, J = 6.8, 2.4 Hz, 2 H), 7.05 (dd, J = 4.8, 2.4 Hz, 2 H), 3.89 (s, 3 H). ^{13}C NMR (101 MHz, CDCl$_3$): δ = 160.4, 142.6, 140.2, 131.9, 131.1, 130.0, 128.3, 128.2, 127.9, 122.3, 114.7, 55.6. IR (neat): ν = 2218 cm^{-1} (NC). Anal Calcd for $C_{14}H_{11}AuClNO$: C, 38.07; H, 2.51; N, 3.17 %. Found: C, 38.00; H, 2.55; N, 3.13 %.

4-21d
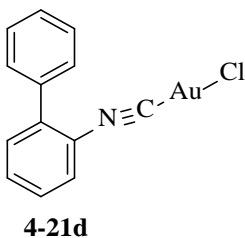
^{1}H NMR matched literature data.[15]

General Procedure for Biaryl ADC-Au Complex Formation

To a solution of **4-21(a-9)** (0.1-0.3g, 1equiv) in CHCl$_3$ (2mL) under nitrogen was added the desired amine (2 equiv) all at once, and the mixture was heated to 60 $^\circ$C. The reaction was monitored by IR by disappearance of the CN stretching frequency. The solvent was removed under

reduced pressure, and the products **4-22(a-9)** were filtered through Celite and were recrystallized from CH_2Cl_2/pentane.

4-22a
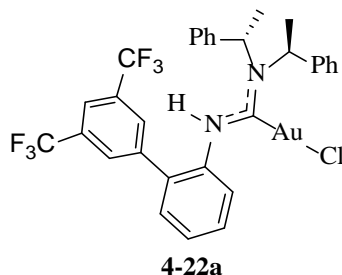
White solid, 95mg (67 % Yield) ^{1}H NMR (500 MHz, CD_2Cl_2): δ = 7.84 (s, 1H), 7.70 (m, 4H), 7.50-7.41 (m, 6H), 7.25 (m, 1H), 7.12 (bs, 1H), 6.94-6.86 (m, 3H), 6.84 (q, J = 7.5 Hz, 1H), 6.48 (d, J = 8.5 Hz, 2H), 4.89 (q, J = 7.5 Hz, 1H), 1.86 (d, J = 7.0 Hz, 3H), 1.68 (d, J = 7.0 Hz, 3H) ppm ^{13}C NMR (126 MHz, CD_2Cl_2): δ = 193.6, 140.9, 138.3, 138.1, 137.2, 135.4, 132.3 (q, $^2J_{C-F}$= 33.4Hz) 131.. 130.2. 130.2. 130.1. 129.5. 129.5. 129.5. 129.4. 128.8. 128.6. 126.9 (q, $^1J_{C-F}$= 273Hz), 126.0, 122.0 (q, $^3J_{C-F}$= 3.77Hz), 69.7, 17.4, 17.1 ppm. ^{19}F NMR (377 MHz, CD_2Cl_2): δ = -62.96 ppm. Anal. calcd $C_{31}H_{26}F_6AuClN_2$: C, 48.14; H, 3.39; N, 3.62 % Found C, 48.19 ; H, 3.16 ; N, 3.60 %

4-22b
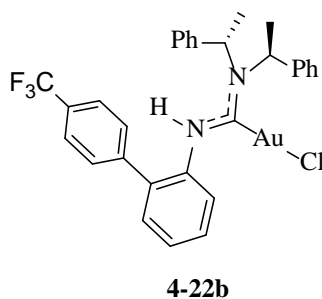
White solid, 191mg (65 % Yield) ^{1}H NMR (500 MHz, CD_2Cl_2): δ = 7.63 (m, 2H), 7.58 (m, 2H), 7.49 (m, 5H), 7.26 (m, 2H), 7.17 (bs, 1H), 7.04 (m, 1H), 6.98 (m, 2H), 6.80 (q, J= 7.0Hz, 1H), 6.48 (d, J= 8.0Hz, 2H), 4.86 (q, J= 7.0Hz, 1H), 1.83 (d, J= 7.0Hz, 3H), 1.65 (d, J= 7.5Hz,

3H) ppm ^{13}C NMR (126 MHz, CD$_2$Cl$_2$): δ = 193.4, 142.5, 138.5, 138.1, 137.3, 137.2, 132.4, 130.4, 129.5, 129.5, 129.3, 129.3, 128.8, 128.6, 128.0 (q, $^1J_{C-F}$= 272Hz), 126.1, 125.8 (q, $^3J_{C-F}$= 3..90Hz), 69.5, 53.5, 17.3, 17.1 ppm. ^{19}F NMR (377 MHz, CD$_2$Cl$_2$): δ = -62.80 ppm. Anal. calcd C$_{30}$H$_{27}$F$_3$AuClN$_2$: C, 51.11; H, 3.86; N, 3.97 % Found C, 48.04 ; H, 3.07 ; N, 3.70 %
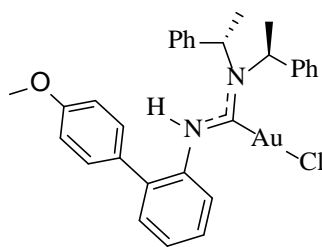
4-22c

White solid, 306mg (81 %Yield) ^{1}H NMR (500 MHz, CD$_2$Cl$_2$): δ = 7.66 (m, 2H), 7.53 (m, 1H), 7.46-7.31 (m, 5H), 7.22 (m, 1H), 7.16 (bs, 1H), 7.07-6.98 (m 5H), 6.89 (m, 2H), 6.83 (q, J= 7.0Hz, 1H), 6.52 (m, 2H), 4.84 (q, J= 7.5Hz, 1H), 1.84 (d, J= 7.5Hz, 3H), 1.58 (d, J= 7.0Hz, 3H) ppm ^{13}C NMR (126 MHz, CD$_2$Cl$_2$): δ = 192.5, 159.6, 138.7, 138.3, 138.0, 137.3, 131.1, 131.1, 130.7, 129.4, 129.3, 129.2, 128.6, 128.6, 128.1, 128.0, 127.7, 126.2, 114.4, 69.4, 55.7, 17.4 ppm. Anal. calcd C$_{30}$H$_{30}$OAuClN$_2$: C, 54.02; H, 4.53; N, 4.20 % Found C, 54.39 ; H, 4.44 ; N, 4.22 %
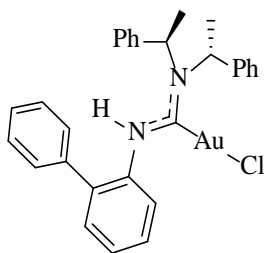
4-22d

White solid, 404mg (87 %Yield) ^{1}H NMR (500 MHz, CD$_2$Cl$_2$): δ = 7.66 (m, 2H), 7.56 (m,1H), 7.46 (m, 2H), 7.40 (m, 6H), 7.25 (m, 2H), 7.17 (m, 2H), 7.11 (bs, 1H), 7.08-7.00 (m,

3H), 6.83 (q, $J= 7.0$Hz, 1H), 6.53 (m, 2H), 4.83 (q, $J= 7.0$Hz, 1H), 1.82 (d, $J= 6.5$Hz, 3H), 1.50

(d, $J= 7.0$Hz, 3H) ppm ^{13}C NMR (126 MHz, CD$_2$Cl$_2$): δ = 192.4, 138.6, 138.4, 138.1, 137.1,

130.9, 130.0, 129.4, 129.3, 129.2, 129.0, 128.6, 129.6, 128.5, 128.1, 128.0, 127.6, 126.1, 69.4,

53.3, 17.5, 17.4 ppm. Anal. calcd C$_{29}$H$_{28}$AuClN$_2$: C, 54.68; H, 4.43; N, 4.40 % Found C, 54.59;

H, 4.30 ; N, 4.36 %

General Procedure for ADC Au^{I} Catalyzed Intramolecular Hydroamination:

In a nitrogen filled glovebox, **LAuCl** (5 mol%) was dissolved in dry toluene (0.5 mL) and

AgOTf (5 mol%) was added. These were allowed to stir for ~10 minutes to allow for activation of

the gold complex. These were filtered into a separate vial through Celite to remove AgCl. In a

separate 4-dram vial, **10** (50mg) was dissolved in dry toluene (0.5 mL), and both vials were closed

and wrapped with paraflm. The two vials were brought out of the glovebox and partially

submerged in an ethylene glycol/dry ice bath (-15 ºC). The vials were allowed to reach temperature

by waiting ~10 min before transferring the solution of **10** to the vial containing the activated

catalyst via syringe. The reaction was kept at -15 ºC for 24 hours, after which the reaction mixture

was directly added to a silica column and purified using EtOAc:Hexane (1:8) as the eluent. The

enantiomeric ratio was determined via chiral HPLC using conditions shown below.
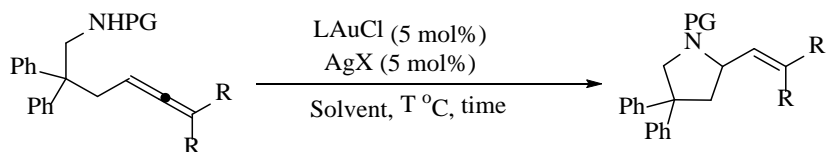
Entry	Catalyst	AgX	PG	R	solvent	Temp ºC	Time (h)	% Yield	% ee
1	**4-20a**	OTf	Boc	H	Toluene	rt	24	80	40
2	**4-20a**	BF$_4$	Boc	H	Toluene	rt	24	95	30

3	**4-20a**	NTf$_2$	Boc	H	Toluene	rt	24	95	30
4	**4-20a**	SbF$_6$	Boc	H	Toluene	rt	24	95	30
5	**4-20a**	PF$_6$	Boc	H	Toluene	rt	24	95	30
6	**4-20a**	OBz	Boc	H	Toluene	rt	24	N.R.	-
8	**4-20a**	OTf	Boc	H	Benzene	rt	24	80	32
9	**4-20a**	OTf	Boc	H	DCE	rt	24	10	5
10	**4-20a**	OTf	Boc	H	CH$_2$Cl$_2$	rt	24	50	11
11	**4-20a**	OTf	Boc	H	Dioxane	rt	24	15	22
12	**4-20a**	OTf	Boc	H	THF	rt	24	75	7

Scheme 4.12 Intramolecular Hydroamination Optimization Table
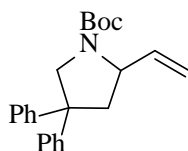
^{1}H NMR matched literature data.[19]

Method: CHIRALPAK $^®$ IB column, mobile phase: hexanes/ i-PrOH= 92.5/7.5, flow rate:

1.0mL/min $t_R(1) = 4.69$ min. $t_R(2) = 5.10$ min.
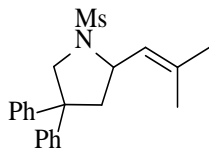
^{1}H NMR matched literature data.[19]

Method: CHIRALPAK ® IB column, mobile phase: hexanes/ *i*-PrOH= 70/30, flow rate:

1.2mL/min $t_R(1)$ = 7.29 min. $t_R(2)$ = 9.71 min.

4.5 References

1.   Cera, G.; Bandini, M.; *Isr. J. Chem.* **2013**, *53*, 848-855

2.   (a) H. Teller, S. Flugge, R. Goddard, A Furstner, *Angew. Chem.* **2010**, *122*, 1993– 1997; *Angew. Chem., Int. Ed.* **2010**, *49*, 1949 –1953; (b) H. Teller, A. Furstner, *Chem. Eur. J.* **2011**, *17*, 7764–7767; (c) H. Teller, M. Corbet, L. Mantilli, G. Gopakumar, R. Goddard, W. Thiel, A. Furstner, *J. Am. Chem. Soc*. **2012**, *134*, 15331–15342. (d) S. Suarez-Pantiga, C. Hernandez-Diaz, E. Rubio, J. M. Gonzalez, *Angew. Chem*. **2012**, *124*, 11720 –11723; *Angew. Chem., Int. Ed*. **2012**, *51*, 11552–11555. (e) J. Francos, F. Grande-Carmona, H. Faustino, J. Iglesias-Siguenza, E. D_ez, I. Alonso, R. Fernandez, J. M. Lassaletta,F. L_pez, J. L. MascareÇas, *J. Am. Chem. Soc*. **2012**, *134*,14322 – 14325; from the same group see also: (f) I. Alonso,B. Trillo, F. Lopez, S. Montserrat, G. Ujaque, L. Castedo, A.Lledos, J. L. MascareÇas, *J. Am. Chem. Soc*. **2009**, *131*,13020 – 13030.

3.   F. Wanga, L.-J. Liua, W. Wanga, S. Li, M. Shi, *Coord. Chem. Rev*. **2012**, *256*, 804–853, and references therein.

4.   S. P. Nolan, *Acc. Chem. Res*. **2011**, *44*, 91–100.

5.   Nunez, E.J.; Echavarren, A.M. *Chem Rev*. **2008**, 108, 3326-3350. (b). Bartolome, C.; Ramiro, Z.; Perez-Galan, P.; Bour, C.; Raducan, M.; Echavarren, A. M.; Espinet, P. *Inorg. Chem*. **2008**, 47, 11391−11397. (c). Leseurre, L.; Toullec, P.Y.; Genet, J-P.; Michelet, V.; *Org. Lett.*, **2007**¸*9*, 4049-4052. (d). Reeds. J.P.; Whitwodd, A.C.; Healy,

M.P.; Fairlamb, I.J.S.; *Organometallics,* **2013**, 3108-3120. (e). Rao, W.; Koh, MJ.; Chan, P.W.H. *J. Org. Chem.* **2013**, *78*, 3183-3195 (f). Zhang, L.; Sun, J.; Kozmin, S.A.; *Adv. Synth. Catal.* **2006**¸ *348*, 2271-2296.

6.   (a). A. Furstner, L. Morency, *Angew. Chem.* **2008**, *120*, 5108 –5111; *Angew. Chem., Int. Ed*. **2008**, *47*, 5030 –5033 (b). M. P. MuCoz, J. Adrio, J. C. Carretero, A. M. Echavarren, *Organometallics* **2005**, *24*, 1293 –1300. (c). Y. Matsumoto, K. B. Selim, H. Nakanishi, K. Yamada, Y. Yamamoto, K. Tomioka, *Tetrahedron Lett*. **2010**, *51*, 404 –

406. (d). Wang, W.; Yang, J.; Wang, F.; Shi, M. *Organometallics*, **2011**, *30*, 3859-3869. (e). Yang, J.; Zhang, R.; Wang, W.; Zhang, Z.; Shi, M.; *Tetrahedron: Asymmetry*, **2011**, *22,* 2029-2038 (f). K. Wilckens, D. Lentz, C. Czekelius, *Organometallics*, **2011**, *30*, 1287–1290.

7.   Handa, S.; Slaughter, L.M.; *Angew. Chem. Int. Ed.* **2012**, *51*, 2912-2915

8   (a) Slaughter, L.M., *ACS Catalysis*, **2012**, 2, 1802-1816. (b) Denk, K.; Sirsch, P.; Herrmann, W. A. *J. Organomet. Chem.* **2002**, *649*, 219−224.

9.   Cianacaleoni, G.; Scafuri, N.; Belpassi, L.; et al. *Inorg. Chem.*, **2014**, 53, 9907-9916

10.   (a) Wu, R.T.; Shen, L.; Chong, M.J.; *Org. Lett*, **2004**, *6*, 2701-2704 (b) Wang, Y.-M.; Kuzniewski, C. N.; Rauniyar, V.; Hoong, C.; Toste, F.D., *J. Am. Chem. Soc.,* **2011,** *133*, 12972-12975. (c). Chen, Y.; Yekta, S.; Yudin, A. K. *Chem. Rev*. **2003**, *103*, 3155−3211. (d). Brunel, J.M. *Chem. Rev.* **2005**, *105,* 857-897. (e). Pu, L. *Chem. Rev.* **1998**, *98,* 2405-2494.

11.   S. Handa, Ph-D. thesis, Oklahoma State University (USA), **2013**.

12. Hamilton, G. L.; Kang, E. J.; Mba, M.; Toste, F. D., *Science,***2007,** *317*, 496-499 (b). Michon, C.; Medina, F.; Abadie, M-A.; Niedercorn, F.A., *Organometallics*, **2013**, *32*, 5589-5660

13. Yamaguchi, *J. Antibiot.*, 2006, 59(11), 729-734. Wang, Q.; Dong, X.; Xiao, T.; Zhou, L.; *Org. Lett.,* **2013**, 15, 4846-4849.

14. Rhode, V.H.G.; Muller, M.F.; Oestreich, M. *Organometallics*, **2015**, *34*, 3358-3373

15. Riedel, D.; Wurm, T.; Graf, K.; Rudolph. M.; Rominger, F.; Hashmi, S.K.; *Adv. Synth Catal.* **2015**, *357*, 1515-1523

16. Fulmer, G.R.; Miller, A.J.M.; Stoltz, B.M.; Bercaw, J.E.; Goldberg, K.I.; *Organometallics*, **2010**, *29*, 2176-2179

17. *Purification of Laboratory Chemicals*, 5th Ed. Elsevier, **2003**.

18. Inorg. Synth., Volume 26, Pg 86

19. K Aikawa, M. Kojima, K. Mikami, *Adv. Synth. Cat.* **2010**, *352*, 3131-3135; correction: Aikawa, M. Kojima, K. Mikami, *Adv. Synth. Cat.* **2011**, *353*, 2875-2883. (b). LaLonde, R. L.; Sherry, B. D.; Kang, E. J.; Toste, F. D. *J. Am. Chem. Soc.* **2007**, *129*, 2452-2453. (c). Zhang, Z.; Bender, C. F.; Widenhoefer, R. A. *Org. Lett.* **2007**, *9*, 2887-2889. (d). Teller, H.; Mantilli, L.; Gopakumar, G.; Goddard, R.; Thiel, W.; Furstner, A.; *J. Am. Chem. Soc.* **2012**, *134*, 15331-15342

CHAPTER V

SYNTHESIS AND CATALYTIC APPLICATION OF C_3-SYMMETRIC CHIRAL

MONODENTATE PHOSPHITE LIGANDS AND THEIR Au[I] COMPLEXES

5.1 Introduction

The need for enantiopure compounds in the pharmaceutical and agrochemical industries has

resulted in numerous methods for their synthesis. One approach is the use of enantioselective

transition metal catalysis. The importance of this field is emphasized by the 2001 Nobel Prize

awarded to Knowels, Noyori, and Sharpless for the development of asymmetric catalysis.[1] One of

the most crucial parameters for achieving high levels of enantioselectivity is the choice of chiral

ligand. Probably the most prevalent ligand type in asymmetric catalysis are chiral phosphine

ligands.[2] Phosphites emerged in the early 1990s as a new chiral ligand type in the Rh-catalyzed

asymmetric hydroformylation **(Scheme 5.1)**[3] and have since been used in numerous other types of

transition metal catalyzed reactions.[4] Probably the most attractive feature of phosphite type ligands

is that they are easily synthesized from readily available chiral alcohols.
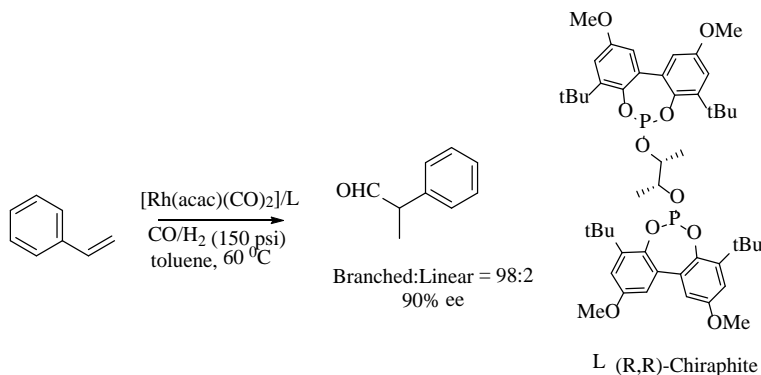
Scheme 5.1 Asymmetric Hydroformylation Using Rh-Phosphite Complex[3]

Another major advantage of phosphite based ligands is that they are less prone to oxidation

and thus less sensitive to air than phosphines, although they do undergo other decomposition

180

pathways such as hydrolysis, alcoholysis, and the Arbuzov reaction **(Scheme 5.2)**. Through rational ligand design, making a more sterically hindered phosphite typically can hinder these decomposition processes.
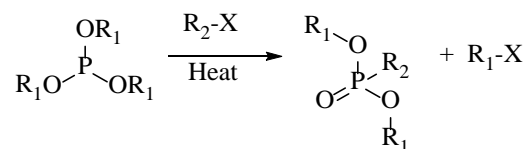
Scheme 5.2 Decomposition of Phosphites Via Arbuzov Reaction

Some notable chiral phosphite ligands are shown in **Figure 5.1**.[2,4,5] Phosphites based on the atropisomeric 1,1′-binaphthyl backbone have probably been the most widely developed.
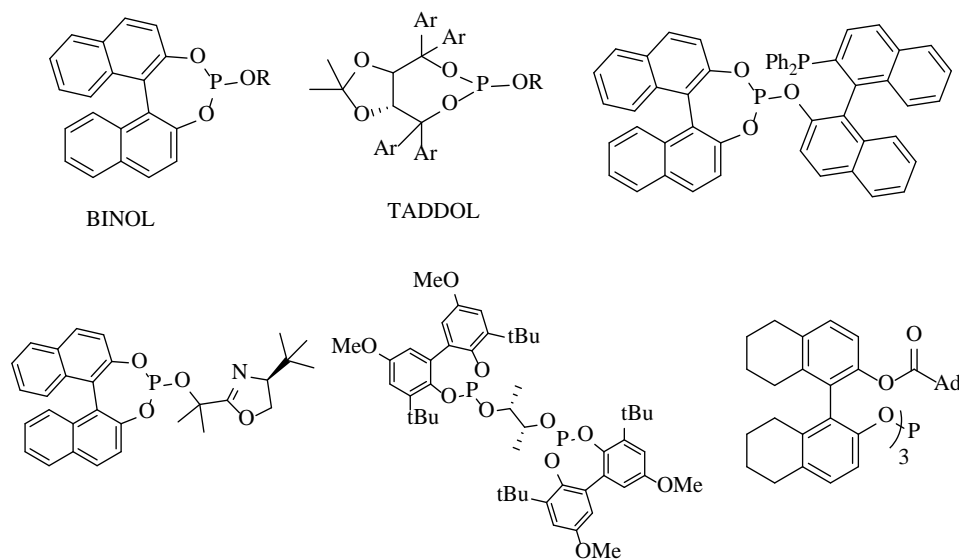
Figure 5.1 Notable Chiral Phosphites Used in Asymmetric Catalysis[2,4,5]

In 2000, Reetz and coworkers reported the use of BINOL-based monodenatte phosphite ligands as excellent chiral auxiliaries for Rh-catalyzed olefin hydrogenation **(Scheme 5.3)**.[5] These C_2-symmetric ligands[5] allowed for very high levels of asymmetric induction. Shortly after this work Reetz developed helical or screwlike C_3-symmetric phosphite ligands which were used for

asymettric Rh-catalyzed hydrogenation reactions **(Scheme 5.4)**.[6] Using the optimized conditions

98% ee was achieved in the Rh-catalyzed hydrogenation reaction.Helical or screwlike ligands are

sometimes viewed as a special chirality class.[7]
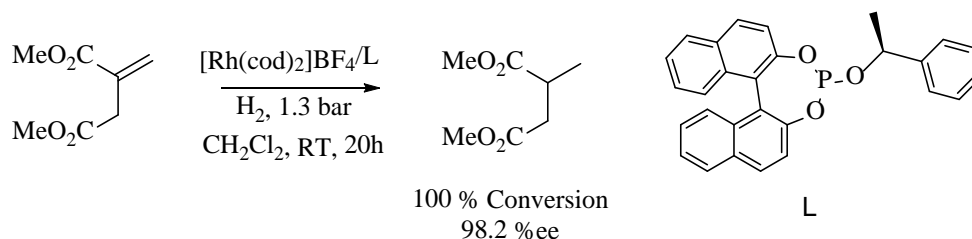
Scheme 5.3 Asymmetric Rh-catalyzed hydrogenation of itaconic acid dimethyl ester[6a]
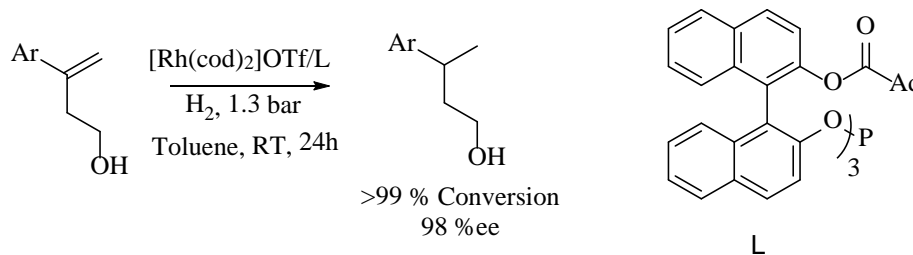
Scheme 5.4 Helical C_3-symmetric phosphite ligands for Rh-catalyzed hydrogenation[6d]

Although the first asymmetric reaction catalyzed by gold was published in 1986,

enantioselective gold catalysis has only recently become a major area of research.[8] With Au[I]

preferring a two-coordinate geometry and most mechanisms involving an anti-attack of a

nucleophile on a gold-activated π-bond, achieving high levels of asymmetric induction has been

considered a major challenge. The most common ligands used in enantioselective gold catalysis

are sterically hindered, chiral, bidentate phosphine ligands. The need to drastically augment the

steric environment by creating walls to enclose the gold center and allowing the chiral ligand exert

a close influence on the catalytic active site has resulted in some novel ligand designs. Although

bidentate ligands are have been the focus of most studies, a few notable monodentate ligands have

been able to achieve high levels of selectivity in various reactions **(Scheme 5.5)**.[9] There are only a

few reports of phosphite gold complexes achieving high levels of asymmetric induction **(Scheme**

5.6).[13]

(a).

79-88% Yield
79-96.5% ee

L=

(b). + R²-OH

65-68% Yield
84-98% ee

catalyst=
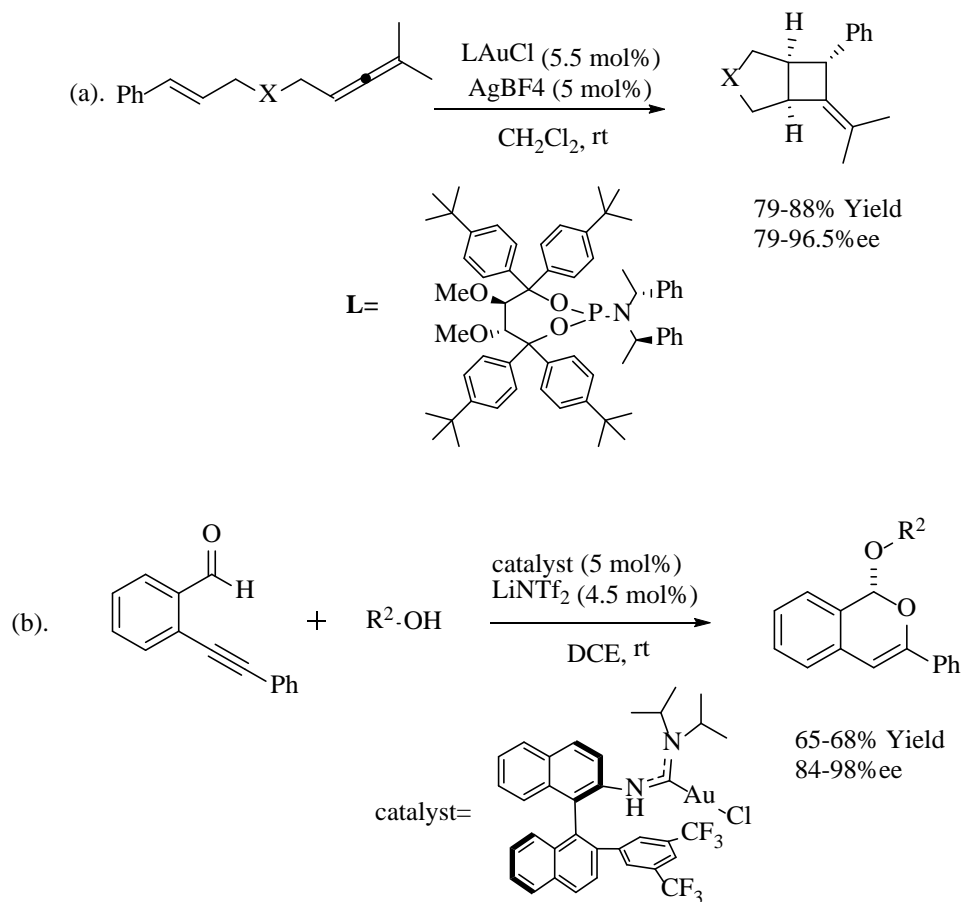
Scheme 5.5 Notable monodentate ligands that achieved high levels of asymmetric induction[10,12]

84-90 % Yield
34-92% ee
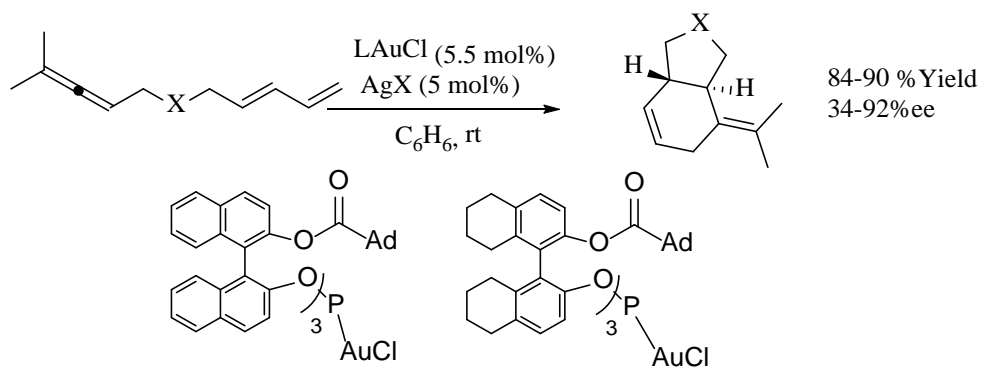
The ability to synthesize various 2`-substituted binaphthyl alcohols makes these compounds ideal for synthesizing new chiral phosphites and studying structure activity relationships in various phosphite-gold catalyzed reactions. With the ligand synthesis only being three steps and the resulting products being less sensitive than typical phosphines makes them very attractive to a wide variety of chemist and not just specialist in the field. The remainder of this chapter will discuss the synthesis novel C_3-symmetric phosphites and their gold complexes. These were then tested in an intramolecular hydroamination reaction of allenes. Various parameters of the ligands such as cone angle and hydrodynamic radius were determined and used to explain observed selectivities.

5.2 Results and Discussion

Our group has previously described the synthesis of novel 2`-aryl substituted binaphthol derivatives **(Scheme 5.7)**.[11] These were originally converted to chiral acyclic diaminocarbenes ligands which provided high levels of asymmetric induction in a gold-catalyzed alkynyl benzaldehyde cyclization shown in **Scheme 5.5(b)**.[12]
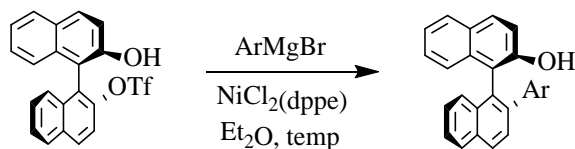
Scheme 5.7 Ni-Catalyzed Kumada Coupling Previously Reported by the Slaughter Group[11]

Given ease of converting alcohols into phosphites, these new chiral binaphthyl alcohol derivatives were viewed as convenient precursors for the synthesis of a small library of new C_3-symmetric phosphite ligands. **(Scheme 5.8)**. The phosphites were readily synthesized by treating

the 2,2' binaphthol derivatives with sodium hydride followed by quenching with phosphorus trichloride. The resulting phosphites were easily purified via flash column chromatography. X-ray quality crystals were obtained via slow diffusion of pentane into dichloromethane solutions of the phosphites (**Figure 5.2**).
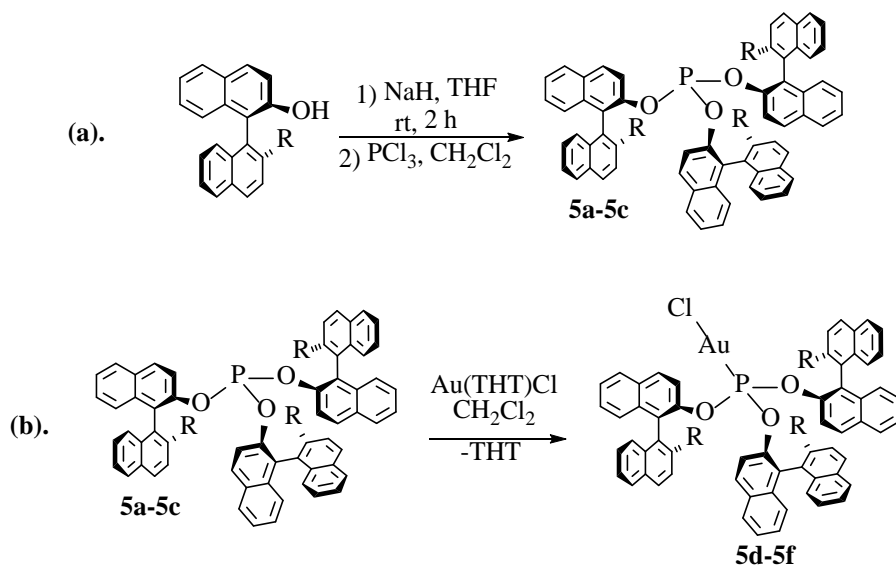
Scheme 5.8 Phosphite Synthesis

Table 5.1 Phosphite Synthetic Results

Entry	R	% Yield
5a	H	81
5b	PMP	52
5c	(4-CF$_3$)Ph	66
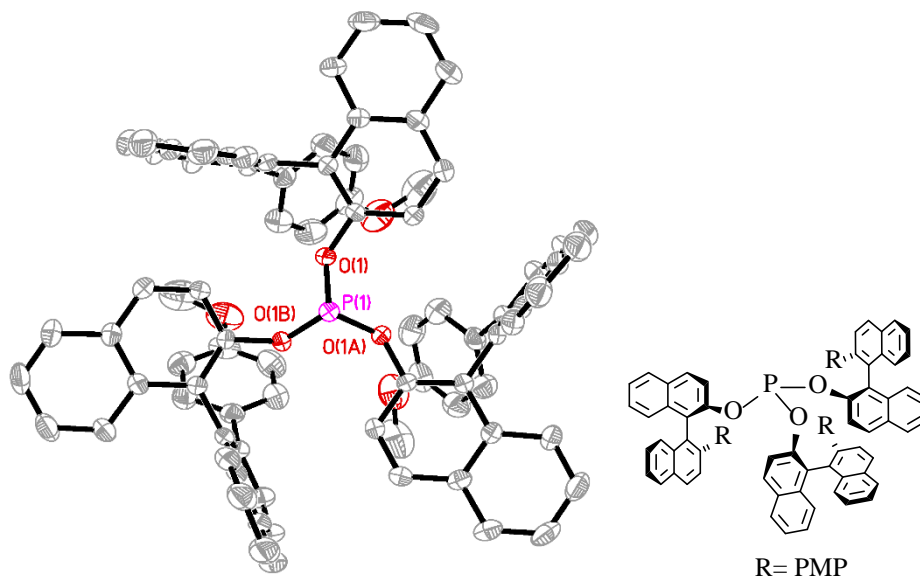
Figure 5.2 X-ray Crystal Structure of **5b** with 50% ellipsoids

Table 5.2 Structural Data for **5b**

Empirical formula	C81 H57 O6 P
Formula weight	1157.24
Temperature	200(2) K
Wavelength	0.71073 Å
Crystal system	Trigonal
Space group	R 3
Unit cell dimensions	a = 22.9494(7) Å $\quad$ α= 90°.
	b = 22.9494(7) Å $\quad$ β= 90°.
	c = 10.0633(4) Å $\quad$ γ = 120°.
Volume	4590.0(3) Å^3
Z	3
Density (calculated)	1.256 Mg/m^3

Absorption coefficient	0.103 mm^{-1}
F(000)	1818
Crystal size	0.29 x 0.25 x 0.23 mm^3
Theta range for data collection	1.77 to 27.11°.
Index ranges	-29<=h<=29, -29<=k<=29, -12<=l<=12
Reflections collected	15395
Independent reflections	4494 [R(int) = 0.0758]
Completeness to theta = 27.11°	100.0 %
Absorption correction	Semi-empirical from equivalents
Max. and min. transmission	0.9763 and 0.9706
Refinement method	Full-matrix least-squares on F^2
Data / restraints / parameters	4494 / 1 / 266
Goodness-of-fit on F^2	1.013
Final R indices [I>2sigma(I)]	R1 = 0.0439, wR2 = 0.1114
R indices (all data)	R1 = 0.0459, wR2 = 0.1138
Absolute structure parameter	-0.02(10)
Largest diff. peak and hole	0.763 and -0.205 e.Å^{-3}
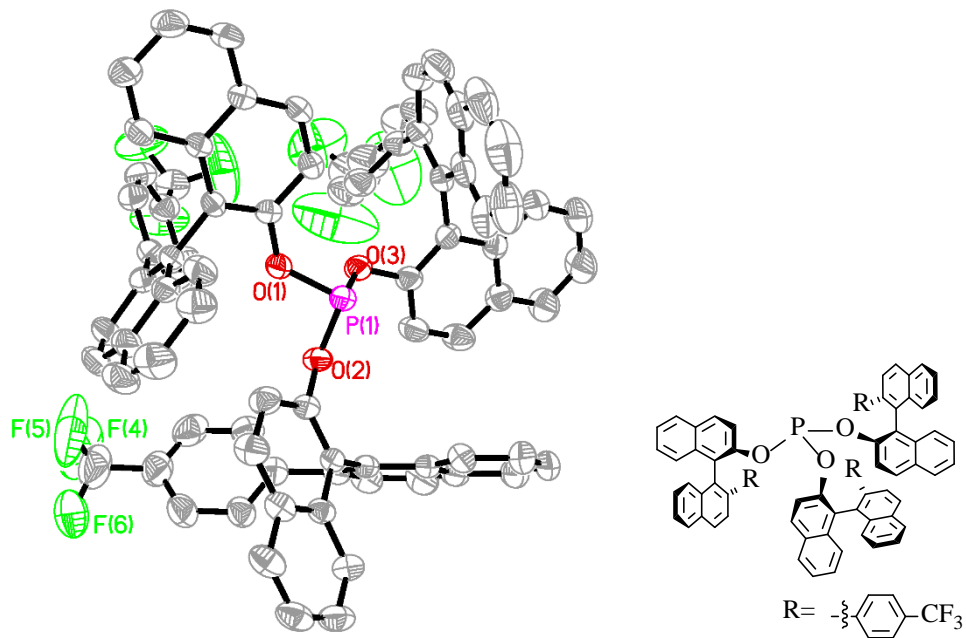
Figure 5.3 X-ray Crystal Structure of **5c** with 50% ellipsoids

Table 5.3 Structural Data for **5c**

Empirical formula	C81 H48 F9 O3 P
Formula weight	1271.16
Temperature	200(2) K
Wavelength	0.71073 Å
Crystal system	Monoclinic
Space group	P 21
Unit cell dimensions	a = 12.8298(10) Å α= 90°.
	b = 19.5303(15) Å β= 95.924(2)°.
	c = 12.8951(10) Å γ = 90°.
Volume	3213.9(4) Å^3
Z	2

Density (calculated)	1.314 Mg/m^3
Absorption coefficient	0.120 mm^{-1}
F(000)	1308
Crystal size	0.26 x 0.18 x 0.18 mm^3
Theta range for data collection	1.59 to 27.23°.
Index ranges	-16<=h<=16, -25<=k<=24, -16<=l<=16
Reflections collected	43812
Independent reflections	14293 [R(int) = 0.0543]
Completeness to theta = 27.23°	99.7 %
Absorption correction	Semi-empirical from equivalents
Max. and min. transmission	0.9787 and 0.9699
Refinement method	Full-matrix least-squares on F^2
Data / restraints / parameters	14293 / 1 / 847
Goodness-of-fit on F^2	1.043
Final R indices [I>2sigma(I)]	R1 = 0.0547, wR2 = 0.1369
R indices (all data)	R1 = 0.0717, wR2 = 0.1482
Absolute structure parameter	-0.07(10)
Largest diff. peak and hole	0.507 and -0.317 e.Å^{-3}

The gold complexes were readily synthesized by treating the phosphites with tetrahydrothiophene gold chloride as shown in **Scheme 5.8(b)** and followed by recrystallization to yield pure material **(Table 5.4).** X-ray quality crystals were grown in a similar manner as the free phosphites **(Figure 5.4)**.

Table 5.4 Synthetic Results for Phosphite Gold Complexes

Entry	R	% Yield
5d	H	83
5e	PMP	81
5f	(4-CF$_3$)Ph	82
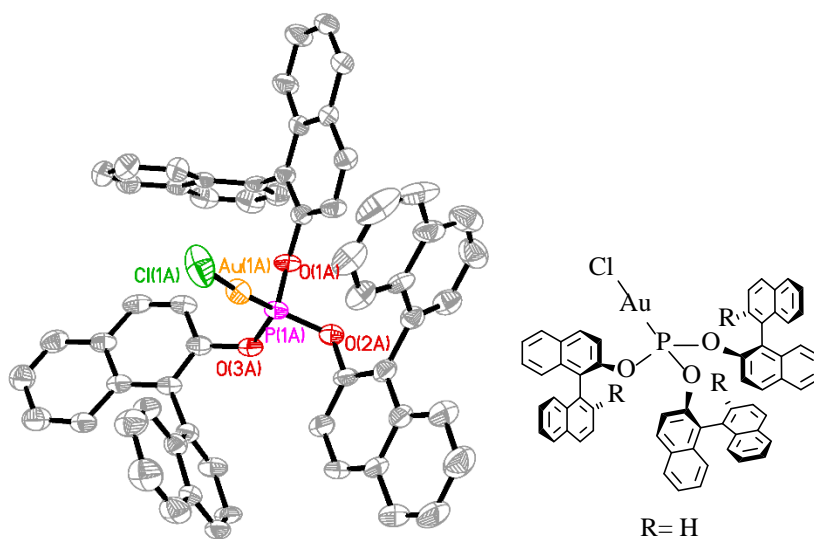
Figure 5.4 X-ray Crystal Structure of **5d** with 50% ellipsoids

Table 5.5 Structural Data for **5d**

Empirical formula	C62.50 H47 Au Cl O4 P
Formula weight	1125.39
Temperature	200(2) K
Wavelength	0.71073 Å
Crystal system	Monoclinic
Space group	C 2

Unit cell dimensions	a = 27.2866(10) Å	α= 90°.
	b = 15.1737(5) Å	β= 91.2950(10)°.
	c = 24.1283(9) Å	γ = 90°.

Volume	9987.5(6) $Å^3$
Z	8
Density (calculated)	1.497 Mg/m^3
Absorption coefficient	3.081 mm^{-1}
F(000)	4520
Crystal size	0.29 x 0.15 x 0.08 mm^3
Theta range for data collection	1.49 to 27.14°.
Index ranges	-34<=h<=34, -19<=k<=19, -30<=l<=30
Reflections collected	51139
Independent reflections	21844 [R(int) = 0.0340]
Completeness to theta = 27.14°	99.7 %
Absorption correction	Semi-empirical from equivalents
Max. and min. transmission	0.7906 and 0.4686
Refinement method	Full-matrix least-squares on F^2
Data / restraints / parameters	21844 / 1 / 1177
Goodness-of-fit on F^2	1.029
Final R indices [I>2sigma(I)]	R1 = 0.0332, wR2 = 0.0822
R indices (all data)	R1 = 0.0382, wR2 = 0.0843
Absolute structure parameter	0.018(4)
Largest diff. peak and hole	1.169 and -0.703 e.$Å^{-3}$
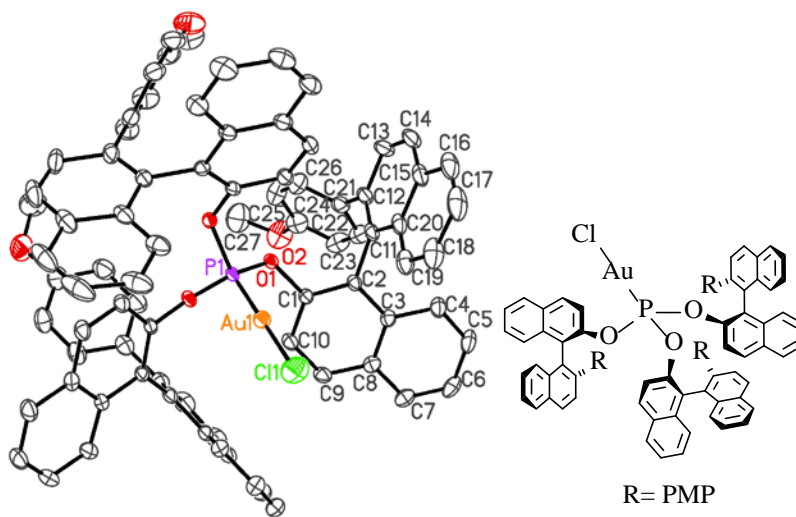
Figure 5.5 X-ray Crystal Structure of **5e** with 50% ellipsoids

Table 5.6 Structural Data **5e**

Empirical formula	C81 H57 Au Cl O6 P
Formula weight	1389.65
Temperature	200(2) K
Wavelength	0.71073 Å
Crystal system	Trigonal
Space group	R 3
Unit cell dimensions	a = 22.7722(10) Å α= 90°.
	b = 22.7722(10) Å β= 90°.
	c = 11.0243(6) Å γ = 120°.
Volume	4951.0(4) Å^3
Z	3

Density (calculated)	1.398 Mg/m^3
Absorption coefficient	2.348 mm^{-1}
F(000)	2106
Crystal size	0.20 x 0.16 x 0.11 mm^3
Theta range for data collection	1.79 to 27.07°.
Index ranges	-29<=h<=29, -29<=k<=29, -14<=l<=14
Reflections collected	18055
Independent reflections	4557 [R(int) = 0.0627]
Completeness to theta = 27.07°	96.2 %
Absorption correction	Semi-empirical from equivalents
Max. and min. transmission	0.7872 and 0.6497
Refinement method	Full-matrix least-squares on F^2
Data / restraints / parameters	4557 / 1 / 272
Goodness-of-fit on F^2	0.791
Final R indices [I>2sigma(I)]	R1 = 0.0258, wR2 = 0.0563
R indices (all data)	R1 = 0.0260, wR2 = 0.0564
Absolute structure parameter	0.012(5)
Largest diff. peak and hole	0.289 and -0.409 e.Å^{-3}

These phosphite gold complexes were then tested in an asymmetric gold catalyzed intramolecular allene hydroamination reaction. This is one of the benchmark reactions used to test new chiral gold catalyst, as it has been studied by several groups before.[14] The initial screening of silver salts revealed that triflate was the superior counterion as can be seen by comparing entries **1-5** of **Table 5.7** below. Running the reaction in toluene led to the highest levels of asymmetric

induction which can be seen by comparing entry **1** to entries **6-10**. In general less polar solvents appeared to be better with benzene being the next best choice. Coordinating solvents such as acetonitrile completely inhibited the reaction. The reaction appeared to be sensitive to substrate structure as well. When comparing entry **12** to entry **17** the addition of two methyl groups on the allene resulted in lower yields and selectivity. It is also worth pointing out that in general carbamate protected substrates out performed sulfonamide protected substrates (entry **12** vs. entry **19**) and that increasing the sterics of the protecting group had little effect (entry **12** vs. entry **16**).
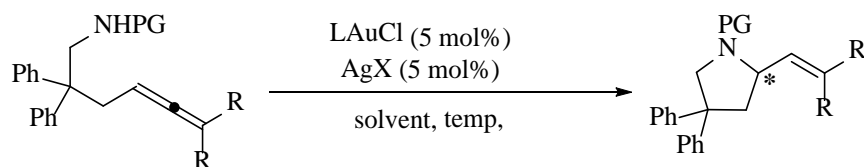
Table 5.7 Phosphite Hydroamination Results

Entry	Catalyst	AgX	Solvent	Temp (^{0}C)	Protecting Group (PG)	R	% Yield	% ee
1	**5f**	OTf	Toluene	-40	Cbz	H	72	46
2	**5f**	SbF$_6$	Toluene	-40	Cbz	H	68	25
3	**5f**	NTf$_2$	Toluene	-40	Cbz	H	71	43
4	**5f**	BF$_4$	Toluene	-40	Cbz	H	13	53
5	**5f**	ClO$_4$	Toluene	-40	Cbz	H	11	42
6	**5f**	OTf	Benzene	rt	Cbz	H	60	42
7	**5f**	OTf	THF	rt	Cbz	H	N.R.	-
8	**5f**	OTf	MTBE	rt	Cbz	H	N.R.	-
9	**5f**	OTf	CH$_2$Cl$_2$	rt	Cbz	H	56	24
10	**5f**	OTf	CH$_3$CN	rt	Cbz	H	N.R	-

11	**5f**	OTf	Toluene	rt	Cbz	H	78	40
12	**5f**	OTf	Toluene	-15	Cbz	H	84.	48
13	**5f**	BF$_4$	Toluene	-15	Cbz	H	N.R.	-
14	**5d**	OTf	Toluene	-15	Cbz	H	62	5
15	**5e**	OTf	Toluene	-15	Cbz	H	71	11
16	**5f**	OTf	Toluene	-15	Cbz	Me	42	20
17	**5f**	OTf	Toluene	-15	Mes	H	81	42

The three different phosphites were tested under optimized conditions (entries **14-16**), and **5f** was found to be superior. To aid in understanding why **5f** gave higher levels of selectivity, ligand steric parameters were calculated. Buried volumes were calculated for each ligand by putting in X-ray coordinates into the online SambVca program. These were correlated to the Tolman cone angle parameter using Nolan's published method **(Table 5.8)**.[14]

Table 5.8 Phosphite Buried Volume and Estimated Tolman Cone Angles

Entry	R	%V$_{bur}$	θ	$\theta_{corrected}$
5d	H	47.5	219°	194°
5e	PMP	39.8	189°	164°
5f	(4-CF$_3$)Ph	52.2	238°	213°

The corrected value is reported due to the fact the one phosphite in Nolans paper didn't fit and was located below the trend line. Therefore, to make the cone angle more accurate the calculated values were decreased by twenty-five degrees. The increased cone angle of **5f** allows for the chiral

ligand to be closer to the substrate binding site, thereby resulting in higher levels of asymmetric induction compared with **5d** or **5e**. However, it is possible that the increased cone angle may have deleterious effects once the steric bulk of the substrate is increased, as can be seen in **Table 5.7** entry **16.** The increased steric bulk of the ligand might interfere with the binding of a more sterically encumbered substrate and cause a decrease in reactivity as well as selectivity.

5.3 Conclusions

A set of three new C_3-symmetric phosphite gold complexes were synthesized and tested in an intramolecular hydroamination reaction of allenes. The observed reactivities and selectivities were dependent on several factors, including counterion, choice of solvent, nitrogen protecting group, substrate steric hindrance, and choice of ligand. Carbamates appear to be the optimal protecting group when compared to sulfonamides in terms of achieving moderate enantioselectivies. Although increasing the steric hindrance of the protecting group seemed to have little effect on the observed selectivity, increasing the number of substituents on the allene seemed to have a deleterious effect on both the yield and observed selectivity. This can potentially be understood as a result of the phosphite ligand having such large cone angles that activation of the allene might be inhibited by an increase in steric hindrance on the allene. Although only modest enantioselectivities were observed, the fact that these phosphites can be synthesized in only three steps and readily tuned by simple modification of the binaphthyl 2'-substituents makes them promising candidates for determining structure-selectivityrelationships in asymmetric gold catalysis and in other metal-catalyzed enantioselective reactions in which phosphites have been previously shown to be successful.

5.4 Experimental Section

General Information:

All air-sensitive synthesis steps were performed under an argon atmosphere using a vacuum line or under nitrogen atmosphere using a glovebox unless otherwise noted. All solvents for reactions were dried before use. Tetrahydrofuran, toluene, and 1, 4-dioxane were dried over and stored on sodium/benzophenone under vacuum. Dichloromethane was washed with concentrated sulfuric acid, deionized water, saturated sodium bicarbonate and deionized water, then pre-dried over anhydrous calcium chloride, followed by refluxing and distillation from phosphorus pentoxide under nitrogen and storage over phosphorus pentoxide under vacuum. The reported chemical shifts in NMR spectra were referenced to residual solvent peaks:[16] $CDCl_3$, ^{1}H NMR: 7.26 ppm, ^{13}C NMR: 77.16 ppm; DMSO-d_6, ^{1}H NMR: 2.50 ppm, ^{13}C NMR: 39.52 ppm; CD_2Cl_2, ^{1}H NMR: 5.32 ppm, ^{13}C NMR: 53.84 ppm ; Benzene-d_6, ^{1}H NMR: 7.16 ppm, ^{13}CNMR: 128.06 ppm. CD_2Cl_2 was dried over and stored on activated 4 Å molecular sieves under vacuum. Benzene-d_6 was dried over and stored on sodium/benzophenone. Elemental analyses were performed by Midwest Microlab, Indianapolis, Indiana. Normal phase HPLC analysis of enantiomeric product mixtures was performed to determine %ee. Various protected allenamines were synthesized according to literature procedures.[14] THT(AuCl) was synthesized from published procedure starting with Canadian Maple Leaf Gold Coin (99.99 %Au).[17]

General Procedure for Phosphite 5a-5c Synthesis:

The binaphthyl alcohol (3.1 equiv) was treated with NaH (3.15 equiv, 60 wt% in mineral oil) in THF (0.1 M) at 0 °C for 2 hours. PCl$_3$ (1 equiv) was added to the reaction at 0 °C, and the reaction was allowed to slowly warm to room temperature and was stirred overnight. The resulting mixture was filtered through Celite to remove NaCl and then concentrated. The resulting product was

purified using column chromatography followed by recrystallization using CH$_2$Cl$_2$:Hexane.

5a
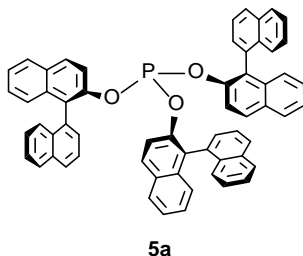
White solid, (mp = 166-168°C), 419mg (81 % Yield). R$_f$ = 0.61 (CH$_2$Cl$_2$:Hexane, 2:1), ^{1}H NMR (400 MHz, C$_6$D$_6$): δ= 7.65 (m, 6H), 7.55 (m, 3H), 7.22-7.12 (m, 21H), 6.95-6.87 (m, 6H), 6.57 (d, J= 8.8Hz, 3H) ppm. ^{13}C NMR (101 MHz, CD$_2$Cl$_2$): δ= 146.8, 134.3, 134.1, 133.8, 133.1, 130.8, 129.4, 129.2, 128.6, 128.4, 128.2, 127.1 (d, $^3J_{p\text{-}c}$= 2.9Hz), 126.6, 126.4, 126.3, 126.2, 125.6, 125.1, 120.9, 120.8, ^{31}P NMR (162MHz, C$_6$D$_6$): δ= 132.0 Anal. Calcd. for C$_{60}$H$_{39}$O$_3$P: C, 85.90; H, 4.69 %. Found: C, 86.10; H, 4.77 %.

5b R = -⌇〈 〉—OMe
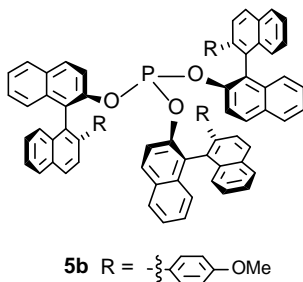
White solid, (dec 265°C), 266mg (52 % Yield). R$_f$ = 0.56 (CH$_2$Cl$_2$:Hexane, 2:1), ^{1}H NMR (400 MHz, C$_6$D$_6$): δ= 7.87 (d, J=8.8Hz, 3H), 7.75 (d, J=7.6 Hz, 3H), 7.67 (d, J=8.8Hz, 3H), 7.57 (d, J=8 Hz, 3H), 7.25 (d, J=8.4Hz, 3H), 7.17-6.83 (m, 24H), 6.43 (d, J=9.2 Hz, 3H), 6.34 (m, 6H), 3.08 (s, 9H) ppm. ^{13}C NMR (125 MHz, CD$_2$Cl$_2$): δ= 158.6, 147.7, 147.6, 140.4, 134.4, 134.1, 133.5, 133.2, 131.1, 130.3, 130.26, 129.4, 129.2, 128.9, 128.4, 128.2, 127.0, 126.5, 126.1, 125.9, 125.7(d, $^3J_{p\text{-}c}$= 3.8Hz), 124.8, 119.8, 119.7, 113.2, 55.2 ppm. ^{31}P NMR (162 MHz, C$_6$D$_6$): δ= 131.8 Anal. Calcd. for C$_{81}$H$_{57}$O$_6$P: C, 84.06; H, 4.96 %. Found: C, 84.07; H, 4.95 %.

5c R = —CF$_3$
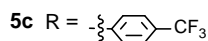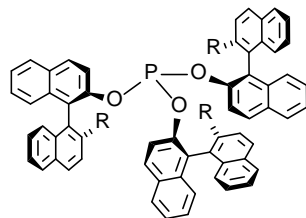
White solid (dec 210°C), 337mg (66 % Yield). R$_f$ = 0.59 (CH$_2$Cl$_2$:Hexane, 2:1), ^{1}H NMR (400 MHz, C$_6$D$_6$): δ= 7.77 (d, J=8.8Hz, 3H), 7.71 (d, J=8.0 Hz, 3H), 7.56 (d, J=8.0Hz, 3H), 7.42 (d, J=8.0Hz, 3H), 7.19-6.74 (m, 33H), 6.27 (d, J=9.2 Hz, 3H) ppm. ^{13}C NMR (125MHz, CD$_2$Cl$_2$): δ= 147.33, 147.3, 145.8, 139.4, 134.2, 133.6, 133.3, 131.4, 130.3, 129.8, 129.5, 129.1, 128.9 (q, $^2J_{C-F}$= 32 Hz), 128.5, 128.4, 128.4, 127.9 (q, $^1J_{C-F}$ = 272Hz), 127.1, 127.0, 126.9, 126.6, 125.9, 125.0, 124.8 (d, $^3J_{p-c}$= 3.8Hz), 124.5 (q, $^3J_{C-F}$ = 3.9 Hz) ppm. ^{31}P NMR (162MHZ, C$_6$D$_6$): δ= 130.1 ^{19}F NMR (376 MHz, C$_6$D$_6$): δ= -62.1 ppm. Anal. Calcd. for C$_{81}$H$_{48}$O$_3$F$_9$P: C, 76.53; H, 3.81 %. Found: C, 76.50.10; H, 3.87 %.

General Procedure for Phosphite Gold Complex 5d-5f

Phosphites **5a-5c** (1 equiv.) where mixed with (THT)AuCl (0.95 equiv.) in dry CH$_2$Cl$_2$ under nitrogen and allowed to stir overnight. The reaction mixture was filtered through a plug of Celite and recrystallized using CH$_2$Cl$_2$:Hexane. The resulting crystal were collected via vacuum filtration and dried under reduced pressure to give the desired product.
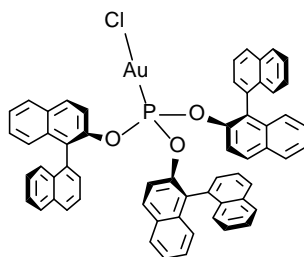
5d

White solid, 106mg (83 % yield). ^{1}H NMR (400 MHZ, CD$_2$Cl$_2$): δ= 7.98 (d, J= 8.4Hz, 3H), 7.86-7.81 (m, 6H), 7.57-7.53 (m, 3H), 7.50-7.45 (m, 9H), 7.33-7.24 (m, 6H), 7.14 (d, J= 8.8Hz, 3H), 7.09 (m, 6H), 5.96 (d, J= 8.8Hz, 3H) ppm. ^{13}C NMR (101MHZ, CD$_2$Cl$_2$): δ= 144.5 (d, $^3J_{p-c}$= 4.6Hz), 134.2, 132.9, 132.4, 131.7, 130.1, 129.9, 129.0, 128.9, 128.4, 128.1 (d, $^2J_{p-c}$= 6.9Hz), 127.2, 127.0, 126.6, 126.5, 126.2, 126.16, 126.1, 119.6, 119.55 ppm. ^{31}P NMR (162 MHz, CD$_2$Cl$_2$): δ= 109.8 ppm. Anal. Calcd. for C$_{60}$H$_{39}$O$_3$PAuCl: C, 67.27; H, 3.67%. Found: C, 66.99 ; H, 3.63 %.
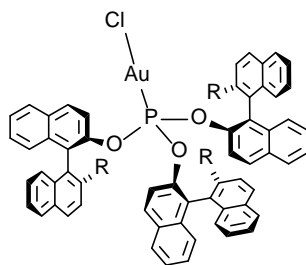
5e R = $-\xi$⟨◯⟩—OMe

White solid, 97mg (81 % Yield). ^{1}H NMR (400 MHZ, CD$_2$Cl$_2$): δ= 8.13 (d, J= 8.4 Hz, 3H), 8.03 (d, J= 8.4 Hz, 3H), 7.74 (d, J= 7.6 Hz, 3H), 7.64 (d, J= 8.4 Hz, 3H), 7.53 (t, J= 7.6 Hz, 3H), 7.41 (t, J= 8.0 Hz, 3H), 7.24 (t, J= 7.6 Hz, 6H), 7.04 (d, J= 8.8 Hz, 3H), 6.95 (m, 6H), 6.73 (d, J= 8.4 Hz, 6H), 6.44 (d, J= 8.8 Hz, 6H), 5.86 (d, J= 8.8 Hz, 3H), 3.64 (s, 9H) ppm. ^{13}C NMR (101MHZ, CD$_2$Cl$_2$): δ=158.8, 145.4, 140.8, 134.5, 134.1, 133.4, 133.2, 131.0, 130.15, 130.1, 129.7, 129.4, 129.1, 128.54, 128.52, 128.1, 127.5, 127.1, 126.6, 126.5, 126.4 (d, $^3J_{p-c}$= 7.6Hz), 125.9, 117.9, 117.8, 113.4, 55.4 ppm. ^{31}P NMR (162 MHZ, CD$_2$Cl$_2$): δ= 106.9 ppm. Anal. Calcd. for C$_{81}$H$_{57}$O$_6$PAuCl: C, 70.01; H, 4.13%. Found: C, 69.91 ; H, 4.19 %.

5f R = -§⟨benzene⟩-CF$_3$
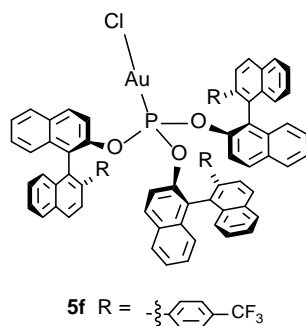
White solid, 97mg (82 % Yield). ^{1}H NMR (400 MHz, CD$_2$Cl$_2$): δ= 8.14 (d, J= 8.8 Hz, 3H), 8.03 (d, J= 8.4 Hz, 3H), 7.75 (d, J= 8.4 Hz, 3H), 7.60 (m, 6H), 7.43 (m, 3H), 7.27-7.18 (m, 12H), 7.03 (d, J= 8.8 Hz, 3H), 6.98 (d, J= 8.4 Hz, 3H), 6.90 (d, J= 8.8 Hz, 9H), 5.82 (d, J= 9.2 Hz, 3H) ppm. ^{13}C NMR (101MHZ, CD$_2$Cl$_2$): δ= 145.6, 145.33, 145.3, 139.6, 134.4, 133.5, 133.1, 131.1, 130.6, 130.1, 129.8, 129.4, 129.1 (q, $^2J_{C\text{-}F}$= 32 Hz), 128.7, 128.6, 128.4 (q, $^1J_{C\text{-}F}$= 272 Hz), 128.5, 127.9, 127.2, 126.4, 126.2, 125.8, 124.8 (q, $^3J_{C\text{-}F}$= 3.8 Hz), 117.5, 117.47 ppm. ^{31}P NMR (162 MHz, CD$_2$Cl$_2$): δ= 108.1 ^{19}F NMR (376 MHz, CD$_2$Cl$_2$): δ= -62.7 ppm. Anal. Calcd. for C$_{81}$H$_{48}$O$_3$F$_9$PAuCl: C, 64.70; H, 3.22%. Found: C, 64.45; H, 2.93 %.
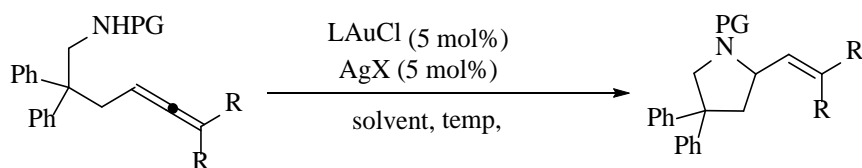
General Procedure for Gold Catalyzed Hydroamination Study

In a nitrogen filled glovebox phosphite gold complexes **5d-5f** (5 mol%) where mixed with AgOTf (5 mol%) and dry toluene (0.5mL) in a 4 dram vial equipped with a stir bar and stirred at room temperature for 10 minutes. The reaction mixture was filtered through a plug of Celite and microfiber filter to remove AgCl into a new 4 dram vial equipped with a stir bar and septum. The substrate (1 equiv) was placed in a separate 4 dram vial equipped with a septum and dissolved in

toluene (0.5mL). Both vials were sealed and brought out of the glove box and placed in an ethylene glycol-dry ice bath (-15 °C) and allowed to cool down for 10 minutes before the substrate solution was transferred via syringe to the solution containing the active catalyst. The resulting mixture was stirred at -15 °C 24 hours until complete consumption of the starting material was observed via TLC. Upon completion the resulting products were purified via silica column chromatography using literature procedures and analyzed via Chiral HPLC. All racemates were synthesized using IPrAuCl and AgOTf in toluene at room temperature.

5.5 References

1. (a). The Nobel Prize in Chemistry 2001". *Nobelprize.org*. Nobel Media AB 2014. Web. 13 Jan 2016. http://www.nobelprize.org/nobel_prizes/chemistry/laureates/2001/

2. (a). Tang, W.; Zhang, X. *Chem Rev.* **2003**, *103*, 3029-3070. (b). Whitesell, J.K. *Chem. Rev.* **1989**, *89*, 1581-1590. (c). Trost, B.M., Vranken, D.L.V.; *Chem. Rev.* **1996**, *96*, 395-422. (d). Leeuwen, P.; Kamer, P.C.; Claver, C.; Dieguez, M.; Pamies, O.; *Chem. Rev.* **2011**, *111*, 2077-2118. (e). Zhang, X. *Tetrahedron: Asymmetry*, **2004**, *15*, 2009-2100. (f). Jerphagon, T.; Renaud, J-L; Bruneau, C.; *Tetrahedron: Asymmetry*, **2004**, *15*, 2101-2111. (g). Wu, S.; He, M.; Zhang, X. *Tetrahedron: Asymmetry*, **2004**, *15*, 2177-2180. (h). *Catalytic Asymmetric Synthesis*, 3rd Ed. Wiley, **2010.** (i). Zhang, w.; Chi, Y.; Zhang, X. *Acc. Chem. Res. 2007, 40*, 1278-1290.

3. Babin, J.E.; Whiteker, G.T. (**1992**) (Union Carbide Chem. Plastics. Tech. Co.) U.S. Patent 5,360,938.

4. (a). Klosin, J.; Landis, C.R. *Acc. Chem. Res.* **2007**, *40*, 1251-1259. (b). Dieguez, M.; Pamies, O.; *Acc. Chem. Res.* **2010**, *43*, 312-322. (c). Leeuwen, P.; Kamer, P.C.; Claver,

C.; Dieguez, M.; Pamies, O.; *Chem. Rev.* **2011**, *111*, 2077-2118. (d). Dieguez, M.; Pamies, O.; Claver, C. *Tetrahedron: Asymmetry*, **2004**, *15*, 2113-2122.

5.   Whitesell, J.K. *Chem. Rev.* **1989**, *89*, 1581-1590.

6.   (a) Reetz, M.T.; Mehler, G. *Angew. Chem., Int. Ed.*, **2000**, *39*, 3889-3890. (b). Reetz, M.T.; Meiswinkel, A.; Mehler, G.; Angermund, K.; Graf, M.; Thiel, W.; Mynott, R.; Blackmond, D.G, *J. Am. Chem. Soc.*, **2005**, *127*, 10305-10313. (c). Reetz, M. T.; Mehler, G.; Meiswinkel, A. Patent WO 01/94278 A1, **2001**. (d). Reetz, M.T.; Guo, H.; Ma, J-A.; Goddard, R.; Mynott, R.J.; *J. Am. Chem. Soc.* **2009**, *34*, 1642-1643

7.   a) Prelog V.; Helmchen, G. *Angew. Chem.***1982**, *94*, 614-631; Prelog, V.; Helmchen, G. *Angew. Chem., Int. Ed. Engl*. **1982**, *21*, 567-583.(b) Helmchen, G. InHouben-Weyl *Methods in Organic Chemistry:Stereoselective Synthesis*, 4th ed.; Helmchen, G., Hoffmann, R. W.,Mulzer, J., Schaumann, E., Eds.; *Thieme Verlag: Stuttgart*, Germany, **1995**; Vol. E21a, pp 1-74.(3) (a) Reetz, M. T.; Beuttenmuller, E. W.; Goddard, R. *Tetrahedron Lett*. **1997**, *38*, 3211–3214. (b) Reetz, M. T.; Sostmann, S. *J. Organomet.Chem*. **2000**, *603*, 105–109.(4) (a) Gilbertson, S. R.; Wang, X. *Tetrahedron* **1999**, *55*, 11609–11618.(b) Gilbertson, S. R.; Chen, G.; McLoughlin, M. *J. Am. Chem. Soc*. **1994**, *116*, 4481–4482.

8.   For pertinent reviews on asymmetric gold catalysis, see: (a) Pradal, A.; Toullec, P. Y.; Michelet, V. *Synthesis* **2011**, 1501. (b) Shapiro, N. D.; Toste, F. D. *Synlett* **2010**, 675. (c) Bongers, N.;Krause, N. *Angew. Chem., Int. Ed*. **2008**, *47*, 2178. (d) Widenhoefer, R.A. *Chem. Eur. J.* **2008**, *14*, 5382.

9.   Cera, G.; Bandini, M.; *Isr. J. Chem.* **2013**, *53*, 848-855

10.   Wang, Y-M.; Lackner, A.; Toste, F.D.; *Acc. Chem. Res.* **2014**, *47,* 889-901

11.   Handa, S.; Arachchige, Y.L.N.M.; Slaughter, L.M.; *J. Org. Chem.* **2013**, *78*, 5694-5699

12.   Handa, S.; Slaughter, L.M.; *Angew. Chem. Int. Ed.* **2012**, *51*, 2912-2915

13.   Gonzalez, A.Z.; Toste, D.F. *Org. Lett.* **2010**, *12*, 200-203.

14.   (a). Zhang, Z.; Liu, C.; Kinder, R. E.; Han, X.; Qian, H.; Widenhoefer, R. A., *J. Am. Chem. Soc.,***2006,** *128*, 9066-9073. (b) Zhang, Z.; Bender, C. F.; Widenhoefer, R. A., *J. Am. Chem. Soc.,***2007,** *129*, 14148-14149; (c) Zhang, Z.; Bender, C. F.; Widenhoefer, R. A., *Org. Lett.,***2007,** *9*, 2887-2889. (d). Wang, Y-M.; Lackner, A.; Toste, F.D.; *Acc. Chem. Res.* **2014**, *47,* 889-901 (e). Michon, C.; Medina, F.; Abadie, M-A.; Nidercorn, F.A. *Organometallics,* **2013**, *32*, 5589-5600. (f). Teller, H.; Mantilli, L.; Gopakumar, G.; Goddard, R.; Thiel, W.; Furstner, A.; *J. Am. Chem. Soc.* **2012**, *134*, 15331-15342

15.   (a). Clavier, H.; Nolan, S.P.; *Chem. Comm.* **2010**, 46, 841 (b). http://www.molnac.unisa.it/OMtools/sambvca.php.

16.   Fulmer, G.R.; Miller, A.J.M.; Stoltz, B.M.; Bercaw, J.E.; Goldberg, K.I.; *Organometallics*, **2010**, *29*, 2176-2179

17.   Inorg. Synth., Volume 26, Pg 86

GOLD-CATALYZED DOMINO ALKYNYL BENZALDEHYDE CYCLIZATION/DIELS-

ALDER SEQUENCE FOR THE SYNTHESIS OF AMINO SUBSTITUTED TETRACYCLIC

COMPOUNDS

6.1 Introduction

The ability of gold to activate π-bonds toward nucleophilic attack and access complex

mechanistic pathways has opened the doors to accessing complex molecules in few synthetic

steps.[1] One of the more popular areas of research that has emerged over recent years are domino

processes.[2] A domino reaction is defined as "a reaction in which two or more bonds are formed

under the same reaction conditions, and in which subsequent reactions result as a consequence of

the functionality formed in the previous step."[3] Gold is very well known to promote such

reactions.[4] A select few of the reactions are outlined in **Scheme 6.1**. All of these reactions begin

with gold activating a π-bond toward nucleophilic attack, upon which the intermediate can then

undergo protodeauration or continue to react in various labyrinths of mechanisms.

E= CO$_2$Me
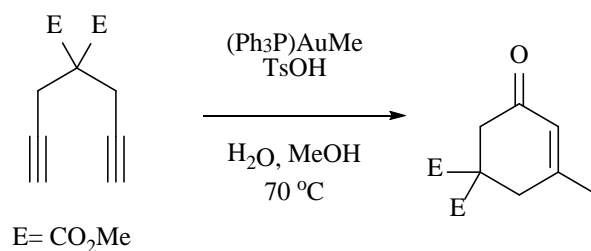
(a). Gold catalyzed hydration/*6-endo-dig* cyclization sequence[5]
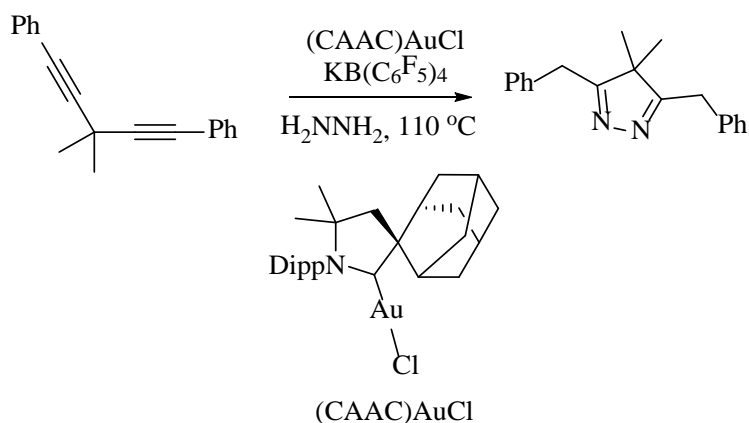
(b). Gold Catalyzed hydroamination cyclization sequence[6]

R= SO$_2$Ph

R= SO$_2$Ph
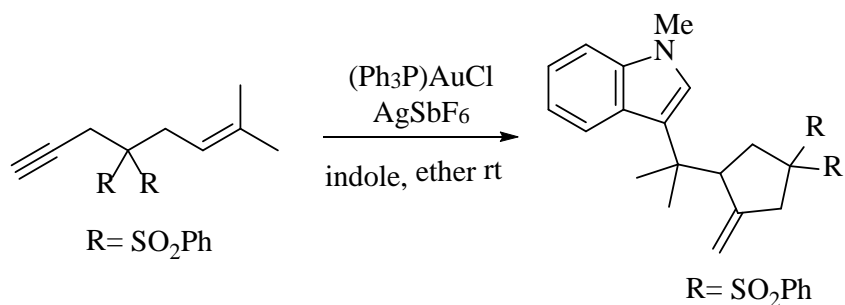
(c). Gold Catalyzed 1,6-enyne cyclization/hydroarylation reaction[7]

Scheme 6.1: Gold Catalyzed Domino Processes

With one of the original reactions catalyzed by gold being hydration of alkynes, it is fitting to start with a domino process involving that step. In **Scheme 6.1(a)** the diyne first undergoes hydration of one the alkynes, resulting in an enol which then undergoes a 6-endo-dig cyclization to the remaining alkyne. This is followed by protodeauration and isomerization of the double bond, resulting in the cylcohexenone derivative. The related gold-catalyzed hydroamination cyclization sequence was used in the synthesis of various nitrogen containing heterocycles as shown in **Scheme 6.1(b).** Krause's group conducted a study in which a 1,6-enyne cyclization reaction was followed by hydroarylation of the gold carbenoid intermediate **Scheme 6.1 (c).** This is but a brief introduction to the numerous types of domino reactions that gold can catalyze. For a more thorough introduction, numerous reviews have been written.[2] One particular domino reaction that is relevant

to this chapter **(Scheme 6.2)** has been studied by our group before as well as by many other groups.[8] This reaction involves intramolecular cyclization of the alkynylbenzaldehyde substrate resulting in an isochromenylium intermediate which can be trapped by various nucleophiles as shown below.
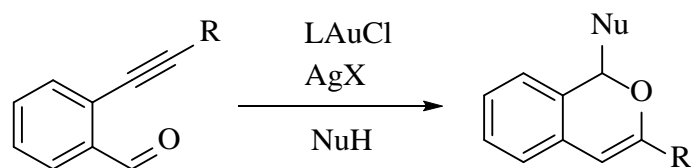
Table 6.1 Au Catalyzed Alkynyl Benzaldehyde Cyclization

L	NuH	Ref
	ROH	9
None[a]	ArH	10
Me₃P		11

(a). Only AgOTf used as catalyst; no gold was required.

Out of all the possible nucleophiles one could potentially try with this reaction, amine based nucleophiles apparently have not been thoroughly studied. Reported gold-catalyzed intermolecular reactions involving amines are actually fairly limited, including only hydroamination of alkynes using aniline derivatives and a few other examples.[12] This can be understood as due to the fact that amines have a stronger binding affinity toward gold compared with alkynes whereas alcohols

being less basic than amines are less problematic.[13] The higher binding affinity results in the amine binding to the cationic gold center, and because Au^I is only two-coordinate, deactivation of the catalyst may occur.

Another reaction pathway available in alkynylbenzaldehyde cyclizations involves the isochromenylium ion intermediates undergoing [4+2] Diels-Alder cycloaddition reactions (**Scheme 6.3),** which can result in the synthesis of some very elaborate structures.[14-17]
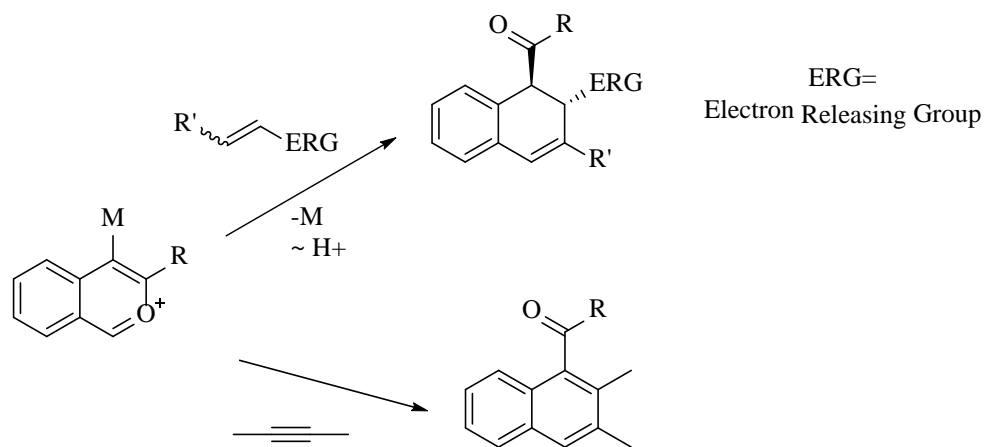
Scheme 6.3 [4+2] Cycloaddition Reactions of Isochromenylium Intermediate

The reaction of isochromenylium ions with alkynes results in the formation of substituted naphthalene derivatives.[15] Replacement of the alkyne with an olefin that has an electron releasing substituent results in a reverse electron demand Diels-Alder reaction.[16,17] This reaction results in the formation of biologically relevant tetrahydronaphthalene derivatives. One example is podophyllotoxin (**Figure 6.1)** Outlined in red is the tetrahydronaphthalene framework. This particular structure is a well-known anticancer natural drug candidate.[18] This is just one of many examples illustrating the ability of gold to dramatically shorten the number of reaction steps in the synthesis of biologically relevant compounds.[19]
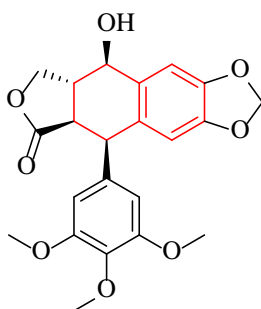
Figure 6.1: Podophyllotoxin

This chapter describes the discovery of a new gold-catalyzed domino reaction that utilizes both an alkynylbenzaldehyde cyclization/hydroamination sequence and a Diels-Alder reaction between the resulting isochromene derivative and a second isochromenylium intermediate. This reaction highlights gold's ability to access very complex structures in a minimal number of steps. The resulting tetracyclic products have various structural features some of which are similar to Podophylotoxin that potentially allow for biological activity and have been sent for screening.

6.2 Results and discussion

While screening conditions for the gold-catalyzed synthesis of new amine-substituted isochromene derivatives **(Scheme 6.4),** an unusual reactivity pattern was observed. Upon testing various amine nucleophiles and gold precatalysts with alkynylbenzaldehyde **1a**, most of the tested conditions resulted either in recovery of the substrate or in complex reaction mixtures with no identifiable products. However, when diisopropyl amine was used as the nucleophile in combination with the Buchwald-type ligand cyclohexyl Johnphos[27], a recoverable product **6a** was obtained.
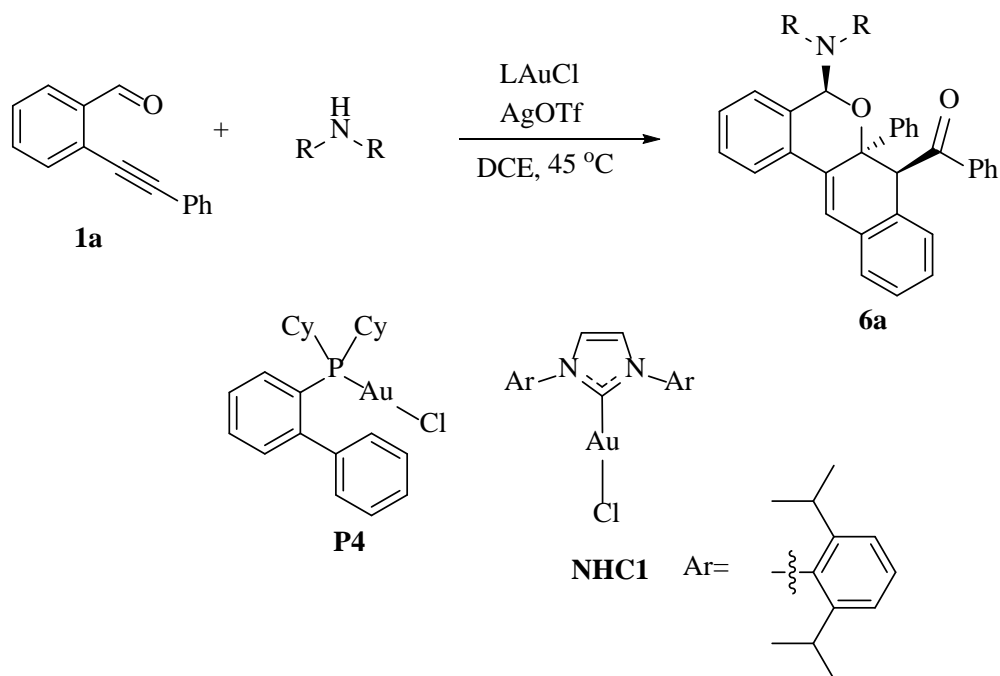
Table 6.2 Screening Amines

Entry	L	Amine	Result
1	**NHC1**	iPr2NH	N.R.
2	**NHC1**	Aniline	N.R.
3	**P4**	iPr2NH	26 % Yield
4	**P4**	Aniline	unidentifiable mixture

(a). reaction conditions: 1 equiv alkynylbenzaldehyde, 1equiv. amine, 5mol% **P4** 5mol% AgOTf,

DCE 45°C, 3 days.

However, the obtained product turned out not to be the expected isochromene derivative. X-ray crystallography revealed the product to be an unexpected tetracyclic compound shown in **Figure 6.2**. 1H-isochromene frameworks are found in numerous pharmaceuticals, bioactive molecules, and natural products.[19] They have been investigated for having antitumor properties.[20]
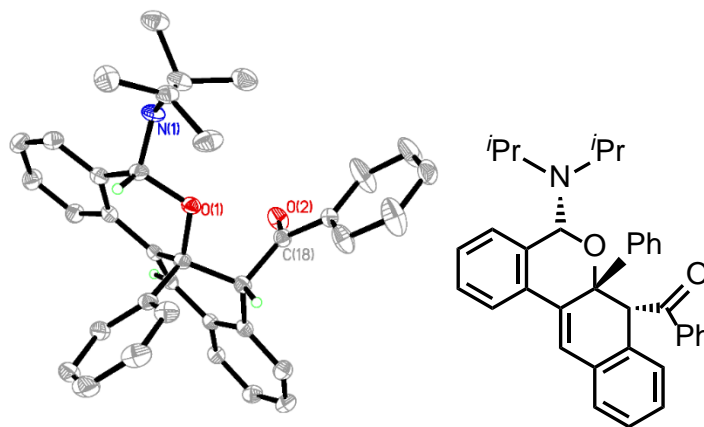
Figure 6.2: X-ray Crystal Structure of **6a** with 50% ellipsoids

Table 6.3 X-ray Structural Data for **6a**

Empirical formula	C36 H35 N O2
Formula weight	513.65
Temperature	100(2) K
Wavelength	0.71073 Å
Crystal system	Monoclinic
Space group	P 21/n
Unit cell dimensions	a = 10.8442(8) Å a= 90°.
	b = 13.8546(11) Å b= 92.1160(10)°.
	c = 18.5750(14) Å g = 90°.
Volume	2788.8(4) Å^3
Z	4
Density (calculated)	1.223 Mg/m^3
Absorption coefficient	0.075 mm^{-1}
F(000)	1096
Crystal size	0.23 x 0.17 x 0.14 mm^3

Theta range for data collection	1.83 to 27.14°.
Index ranges	-13<=h<=13, -17<=k<=17, -23<=l<=23
Reflections collected	37386
Independent reflections	6167 [R(int) = 0.0444]
Completeness to theta = 27.14°	99.8 %
Absorption correction	Semi-empirical from equivalents
Max. and min. transmission	0.9899 and 0.9827
Refinement method	Full-matrix least-squares on F^2
Data / restraints / parameters	6167 / 0 / 357
Goodness-of-fit on F^2	1.027
Final R indices [I>2sigma(I)]	R1 = 0.0403, wR2 = 0.0971
R indices (all data)	R1 = 0.0497, wR2 = 0.1039
Extinction coefficient	0.0018(4)
Largest diff. peak and hole	0.338 and -0.352 e.Å^{-3}

To gain insights into the mechanism, a stoichiometric reaction was carried out between the alkynylbenzaldehyde **1a** and **P4** that was activated in situ by stirring with $AgSbF_6$. Instead of isolating the desired isochromenyilum intermediate, a chloro-bridged gold dimer **5a** was formed **(Figure 6.3).** These bridging compounds are known to form upon attempted activation of gold catalysts by reaction with silver salts in non-coordinating solvents.[21] Echavarren's group recently showed these complexes to be poor catalysts in various gold catalyzed organic transformations.[21]
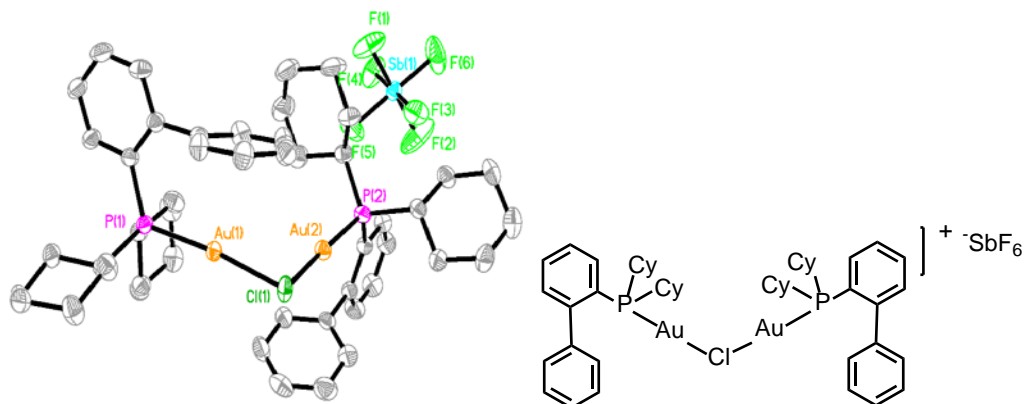
Figure 6.3: X-ray Crystal Structure of **5a** with 50% ellipsoids

Table 6.4 X-Ray Structural Data for **5a**

Empirical formula	C50 H66 Au2 Cl3 F6 P2 Sb
Formula weight	1465.00
Temperature	200(2) K
Wavelength	0.71073 Å
Crystal system	Triclinic
Space group	P -1
Unit cell dimensions	a = 13.2790(6) Å $\quad$ α= 100.2770(10)°.
	b = 14.4620(7) Å $\quad$ β= 96.4260(10)°.
	c = 15.6401(12) Å $\quad$ γ = 115.8120(10)°.
Volume	2598.8(3) Å^3
Z	2
Density (calculated)	1.872 Mg/m^3
Absorption coefficient	6.418 mm^{-1}
F(000)	1420
Crystal size	0.26 x 0.21 x 0.20 mm^3

Theta range for data collection	1.62 to 27.08°.
Index ranges	-16<=h<=17, -18<=k<=18, -20<=l<=20
Reflections collected	34962
Independent reflections	11422 [R(int) = 0.0524]
Completeness to theta = 27.08°	99.9 %
Absorption correction	Semi-empirical from equivalents
Max. and min. transmission	0.3572 and 0.2862
Refinement method	Full-matrix least-squares on F^2
Data / restraints / parameters	11422 / 1 / 578
Goodness-of-fit on F^2	1.034
Final R indices [I>2sigma(I)]	R1 = 0.0291, wR2 = 0.0798
R indices (all data)	R1 = 0.0327, wR2 = 0.0829
Extinction coefficient	0.00068(10)
Largest diff. peak and hole	1.410 and -1.228 e.Å^{-3}

To circumvent formation of the bridged chloro-complex, the acetonitrile-ligated cationic gold complex of **P4** was synthesized [22] and used for the remainder of the reactions. In an attempt to increase the yield and shorten the reaction time, the temperature was increased to 75 °C. During optimization, it was observed that the desired reactivity was very limited in scope with respect to the amine. This is not surprising given the difficulties associated with amines as nucleophiles in gold catalysis (vide supra).[13] The only two amines that underwent the desired reaction were two sterically bulky secondary amines, diisopropylamine and dicyclohexylamine. Fortunately, the reaction was less sensitive with respect to the alkynylbenzaldehyde substrate, (**Scheme 6.5.)** although there were some limitations. When electron-withdrawing substituents were present, the

yield did drop. This might be due to the fact that amines have higher binding affinities for gold compared with alkynes, and electron-withdrawing groups on the alkynes increase this effect, resulting in no activation of the alkyne towards cyclization. X-ray quality crystals were obtainable for compounds **6e, 6g,** and **6l**, and are shown in **Figures 6.4-6.6**
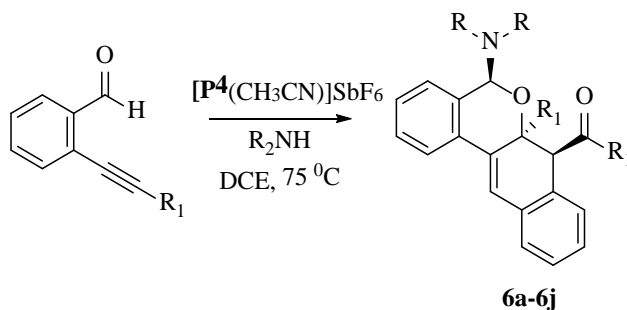
Scheme 6.5 Substrate Scope of Reaction

(i). reaction conditions: 1 equiv alkynylbenzaldehyde, 1.5equiv. amine, 10mol%

[P4(CH$_3$CN)]SbF$_6$ DCE 75ºC, 2 days.

Table 6.5 Substrate Scope

Entry	R	Product Assignment	Amine	Yield
1	Ph	**6a**	^{i}Pr$_2$NH	70
2	Ph	**6b**	Cy$_2$NH	67
3		**6c**	^{i}Pr$_2$NH	52
4		**6d**	Cy$_2$NH	57
5	PMP	**6e**	^{i}Pr$_2$NH	62
6	PMP	**6f**	Cy$_2$NH	68
7		**6g**	^{i}Pr$_2$NH	76
8		**6h**	Cy$_2$NH	73
9		**6i**	^{i}Pr$_2$NH	32
10		**6j**	Cy$_2$NH	37
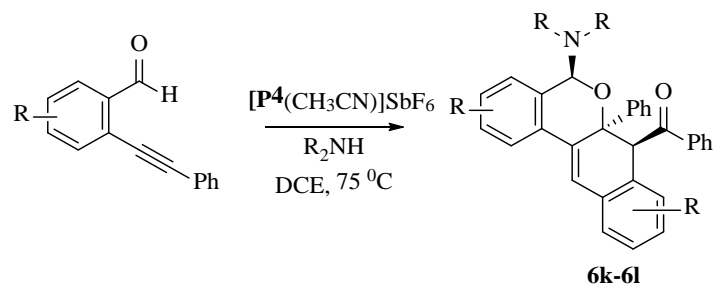
(i). reaction conditions: 1 equiv alkynylbenzaldehyde, 1.5equiv. amine, 10mol%

[**P4**(CH₃CN)]SbF₆, DCE, 75°C, 2 days.

Table 6.5b Substrate Scope

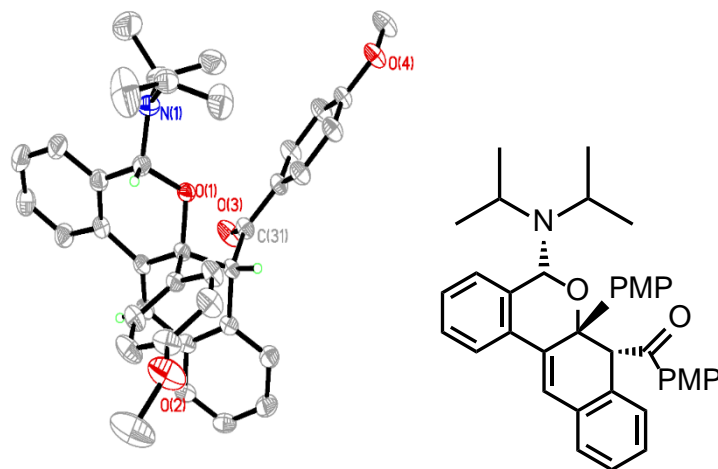| Entry	R	Product Assignment	Amine	Yield
1	4-F	6k	^{i}Pr₂NH	61
2	4-F	6l	Cy₂NH	63

Figure 6.4: X-ray Crystal Structure of **6e** with 50% ellipsoids

Table 6.6 X-ray Structural Data for **6e**

Empirical formula	C38 H39 N O4

Formula weight	573.70	
Temperature	200(2) K	
Wavelength	0.71073 Å	
Crystal system	Monoclinic	
Space group	P 21/n	
Unit cell dimensions	a = 12.6921(10) Å	$\alpha = 90°$.
	b = 17.3656(14) Å	$\beta = 99.9860(10)°$.
	c = 14.0302(12) Å	$\gamma = 90°$.
Volume	3045.5(4) $Å^3$	
Z	4	
Density (calculated)	1.251 Mg/m^3	
Absorption coefficient	0.080 mm^{-1}	
F(000)	1224	
Crystal size	0.35 x 0.34 x 0.12 mm^3	
Theta range for data collection	1.88 to 27.09°.	
Index ranges	-16<=h<=16, -22<=k<=22, -17<=l<=17	
Reflections collected	40435	
Independent reflections	6715 [R(int) = 0.0779]	
Completeness to theta = 27.09°	99.9 %	
Absorption correction	Semi-empirical from equivalents	
Max. and min. transmission	0.9903 and 0.9724	
Refinement method	Full-matrix least-squares on F^2	
Data / restraints / parameters	6715 / 6 / 407	

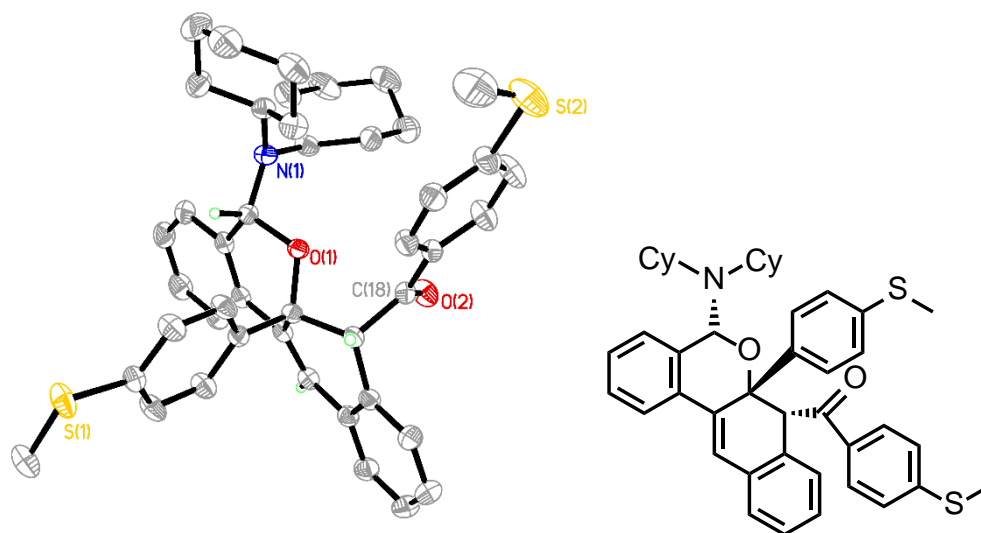| Goodness-of-fit on F^2	1.050
Final R indices [I>2sigma(I)]	R1 = 0.0490, wR2 = 0.1215
R indices (all data)	R1 = 0.0614, wR2 = 0.1326
Extinction coefficient	0.0110(10)
Largest diff. peak and hole	0.390 and -0.354 e.Å^{-3}

Figure 6.5: X-ray Crystal Structure of **6g** with 50% ellipsoids

Table 6.7 X-ray Structural Data for **6g**

Empirical formula	C47 H54 N O2 S2	
Formula weight	729.03	
Temperature	200(2) K	
Wavelength	0.71073 Å	
Crystal system	Monoclinic	
Space group	P 21/n	
Unit cell dimensions	a = 16.9652(11) Å	$\alpha = 90°$.
	b = 13.3015(8) Å	$\beta = 108.1600(10)°$.

218

|	
	$c = 18.3142(11)$ Å $\qquad \gamma = 90°.$
Volume	$3927.0(4)$ Å^3
Z	4
Density (calculated)	1.233 Mg/m^3
Absorption coefficient	0.175 mm^{-1}
F(000)	1564
Crystal size	$0.30 \times 0.26 \times 0.11$ mm^3
Theta range for data collection	1.43 to $27.08°.$
Index ranges	$-21 <= h <= 21, -17 <= k <= 17, -23 <= l <= 23$
Reflections collected	52005
Independent reflections	8655 [R(int) = 0.0633]
Completeness to theta = 27.08°	100.0 %
Absorption correction	Semi-empirical from equivalents
Max. and min. transmission	0.9813 and 0.9491
Refinement method	Full-matrix least-squares on F^2
Data / restraints / parameters	8655 / 2 / 484
Goodness-of-fit on F^2	1.004
Final R indices [I>2sigma(I)]	R1 = 0.0440, wR2 = 0.1155
R indices (all data)	R1 = 0.0528, wR2 = 0.1246
Largest diff. peak and hole	0.475 and -0.473 e.Å^{-3}
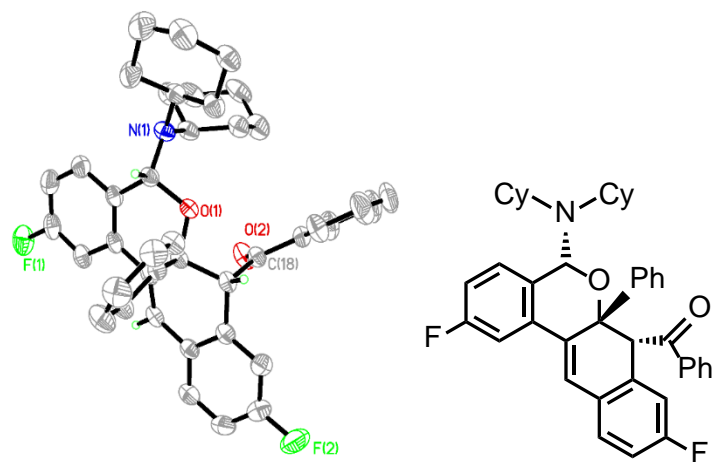
Figure 6.6: X-ray Crystal Structure of **6l** with 50% ellipsoids

Table 6.8 X-ray Structural Data for **6l**

|	
Empirical formula	C42.50 H42 Cl F2 N O2
Formula weight	672.22
Temperature	200(2) K
Wavelength	0.71073 Å
Crystal system	Triclinic
Space group	P -1
Unit cell dimensions	a = 11.0496(7) Å $\quad$ α= 64.7740(10)°.
	b = 12.2287(8) Å $\quad$ β= 82.4240(10)°.
	c = 14.2619(10) Å $\quad$ γ = 88.2690(10)°.
Volume	1727.4(2) Å^3
Z	2
Density (calculated)	1.292 Mg/m^3
Absorption coefficient	0.160 mm^{-1}

F(000)	710
Crystal size	0.17 x 0.16 x 0.12 mm^3
Theta range for data collection	1.59 to 27.16°.
Index ranges	-14<=h<=14, -15<=k<=15, -18<=l<=18
Reflections collected	23652
Independent reflections	7670 [R(int) = 0.0307]
Completeness to theta = 27.16°	99.9 %
Absorption correction	Semi-empirical from equivalents
Max. and min. transmission	0.9806 and 0.9736
Refinement method	Full-matrix least-squares on F^2
Data / restraints / parameters	7670 / 1 / 437
Goodness-of-fit on F^2	1.040
Final R indices [I>2sigma(I)]	R1 = 0.0723, wR2 = 0.1933
R indices (all data)	R1 = 0.0926, wR2 = 0.2113
Largest diff. peak and hole	1.754 and -1.153 e.Å^{-3}

Heterocyclic alkynyl benzaldehydes such as 2-(phenylethynyl)-3-formylpyridine shown below also didn't undergo the desired reaction. Electron rich substrates also did not react very cleanly, resulting in a complex reaction mixture from which a clean isolated product could be found.

No Reaction   No Identifiable Products
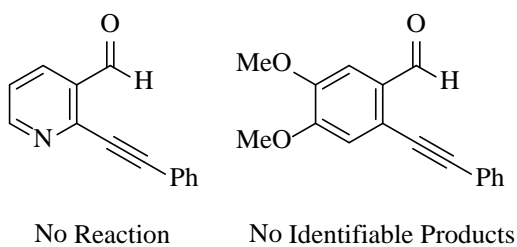
A reasonable mechanism for the formation of this product is outlined in **Scheme 6.7**. The

reaction is initiated by activation of the alkyne by gold, resulting in a 6-endo-dig cyclization upon attack of the aldehyde. The resulting isochromenylium ion then undergoes nucleophilic attack by the amine, followed by protodeauration, resulting in the initially desired isochromene derivative. As shown in **Scheme 6.3,** this isochromene derivative has an olefin with an adjacent electron-releasing group. This allows for an inverse electron-demand Diels-Alder reaction to occur between the initially desired product and another isochromenylium ion intermediate. After elimination followed by protodeauration, the desired product is formed. The excess amine is likely required to facilitate the elimination reaction.
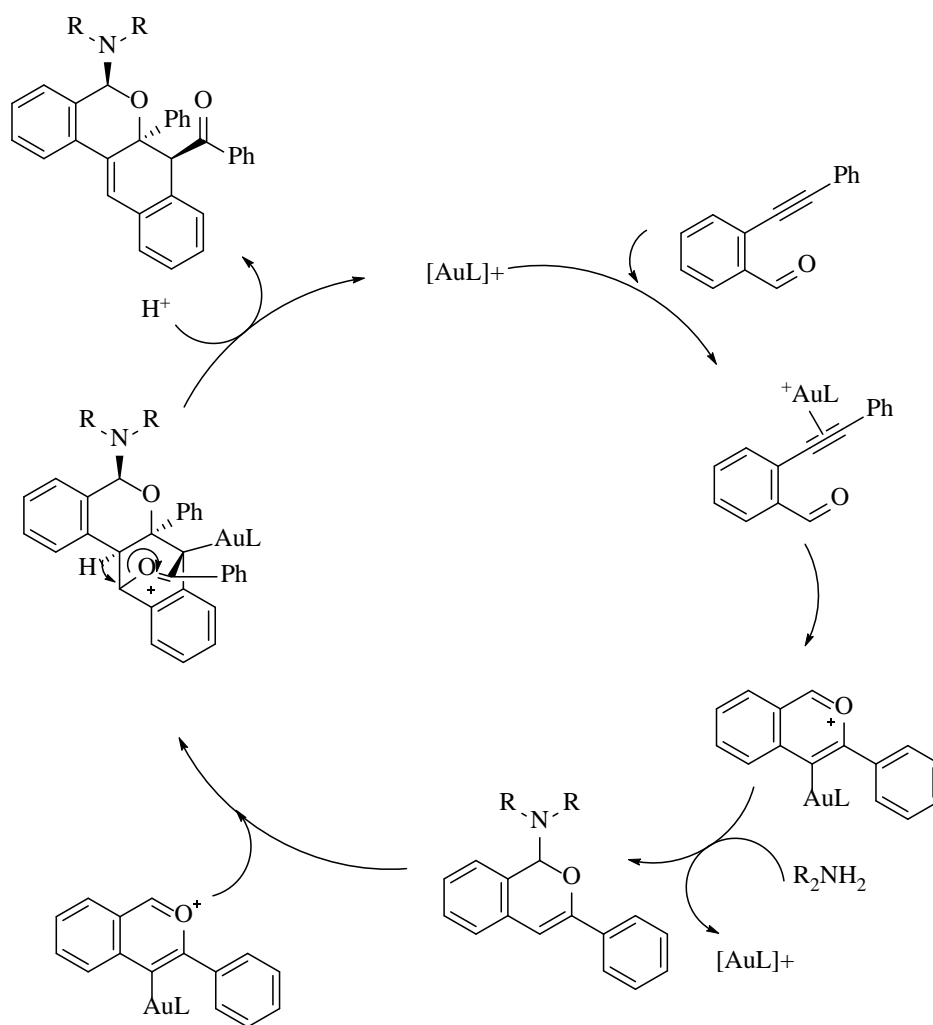
**Scheme 6.7** Mechanistic Proposal for Formation of Tetracyclic Products.

During the process of determining the substrate scope, other reaction pathways leading to other products were discovered **(Scheme 6.8)**. The first pathway resulted in the originally desired isochromene derivative upon simple change of the solvent from DCE to THF and lowering of the reaction temperature to 60 °C. The product proved to be unstable to chromatography on silica and had to be isolated via a basic alumina chromatography column or recrystallization. Although the reaction does work for various secondary amines by inspection of the crude NMR only two products have been isolated **7a** and **7b**. The second alternative pathway was discovered when morpholine was used as the nucleophile. The result was formation of phenylcinnamalone derivatives,[23] albeit in yields below twenty percent. The product was identified by x-ray crystallography **(Figure 6.4)**.

7a R= *i*Pr 42 % Yield
7b R=Bn 56 % Yield
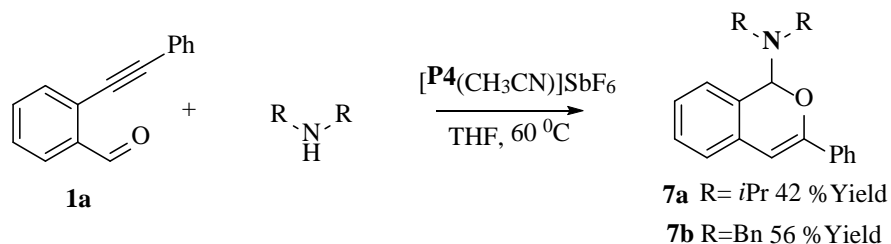
(i). reaction conditions: 1 equiv alkynylbenzaldehyde, 1.5 equiv. amine, 10mol%

[**P4**(CH₃CN)]SbF₆ THF 60°C, 24hr.

(a). Synthesis and isolation of desired isochromene derivative

8b 20 % Yield
8d 14 % Yield
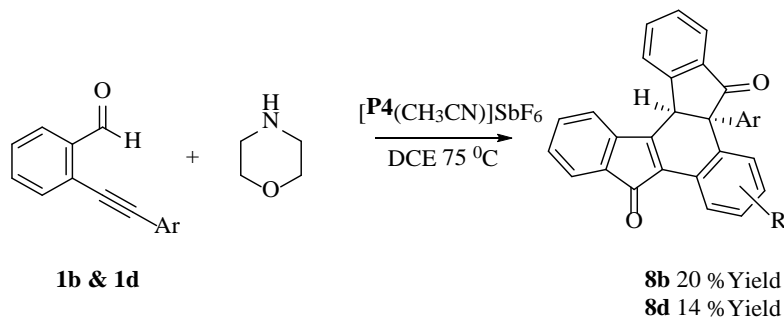
(ii). reaction conditions: 1 equiv alkynylbenzaldehyde, 1.5equiv. amine, 10mol%

[**P4**(CH₃CN)]SbF₆ DCE 75°C, 2 days.

(b). Synthesis and isolation of phenylcinnamalone derivatives

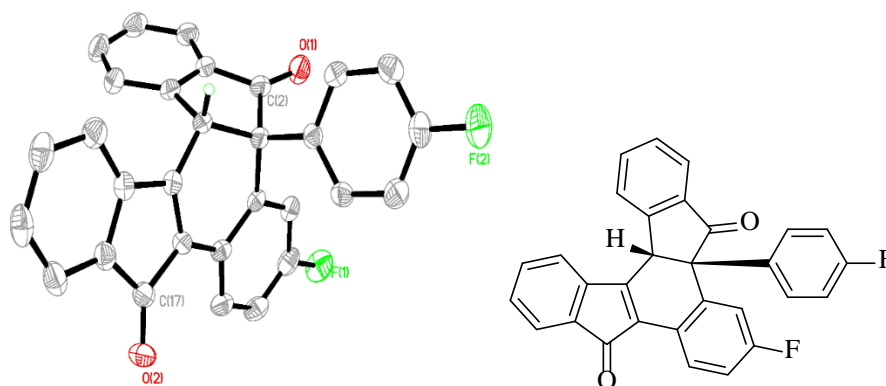**Scheme 6.8**: Alternative Reaction Pathways Discovered.

**Figure 6.7** X-ray Crystal Structure of **8b** with 50% ellipsoids

Table 6.9: X-ray Structural Data for **8b**

Empirical formula	C30 H16 F2 O2	
Formula weight	446.43	
Temperature	200(2) K	
Wavelength	0.71073 Å	
Crystal system	Monoclinic	
Space group	P 21/c	
Unit cell dimensions	a = 10.8296(9) Å	$\alpha= 90°$.
	b = 15.2564(13) Å	$\beta= 112.090(2)°$.
	c = 13.7596(12) Å	$\gamma = 90°$.
Volume	2106.5(3) Å^3	
Z	4	
Density (calculated)	1.408 Mg/m^3	
Absorption coefficient	0.099 mm^{-1}	

F(000)	920
Crystal size	0.34 x 0.11 x 0.05 mm^3
Theta range for data collection	2.03 to 27.11°.
Index ranges	-13<=h<=13, -19<=k<=19, -17<=l<=17
Reflections collected	20991
Independent reflections	4645 [R(int) = 0.0747]
Completeness to theta = 27.11°	99.9 %
Absorption correction	Semi-empirical from equivalents
Max. and min. transmission	0.9952 and 0.9674
Refinement method	Full-matrix least-squares on F^2
Data / restraints / parameters	4645 / 0 / 308
Goodness-of-fit on F^2	1.006
Final R indices [I>2sigma(I)]	R1 = 0.0472, wR2 = 0.1041
R indices (all data)	R1 = 0.0745, wR2 = 0.1188
Extinction coefficient	0.0097(12)
Largest diff. peak and hole	0.300 and -0.202 e.Å^{-3}

Similarly, only two phenylcinnamolone derivatives from the side reaction shown in **Scheme 6.8 (b)** have been isolated, with Ar= 4-thiomethylphenyl **(8d)** (14% yield) and Ar=4-fluorophenyl **(8b)** (20% yield). Given the low yields, no attempt was made to isolate this side product for the whole series of alkynylbenzaldehyde derivatives. A proposed mechanism for the formation of the phenylcinnamalone derivatives is outlined in **Scheme 6.9**. The [4+2] cycloaddition between two 2-phenylindenone, resulting in the formation of the parent phenylcinnamalone derivative, was reported by Wawzonek an coworkers in 1969.[23b] Considering the reaction can be achieved at 75

^0C the [4+2] cycloaddition might be gold catalyzed. The rearrangement of the cyclic oxonium intermediate is based on a proposed mechanism for indenyl ether synthesis shown in **Scheme 6.10**.[24a] The mechanism could be similar to one proposed in a recent publication shown in **Scheme 6.11**.[24b] This mechanism does explain the need for the use morpholine however the catalyst used in the cited reference was a Au^{III} catalyst and the amine source was ammonia which could react substantially different than current conditions.
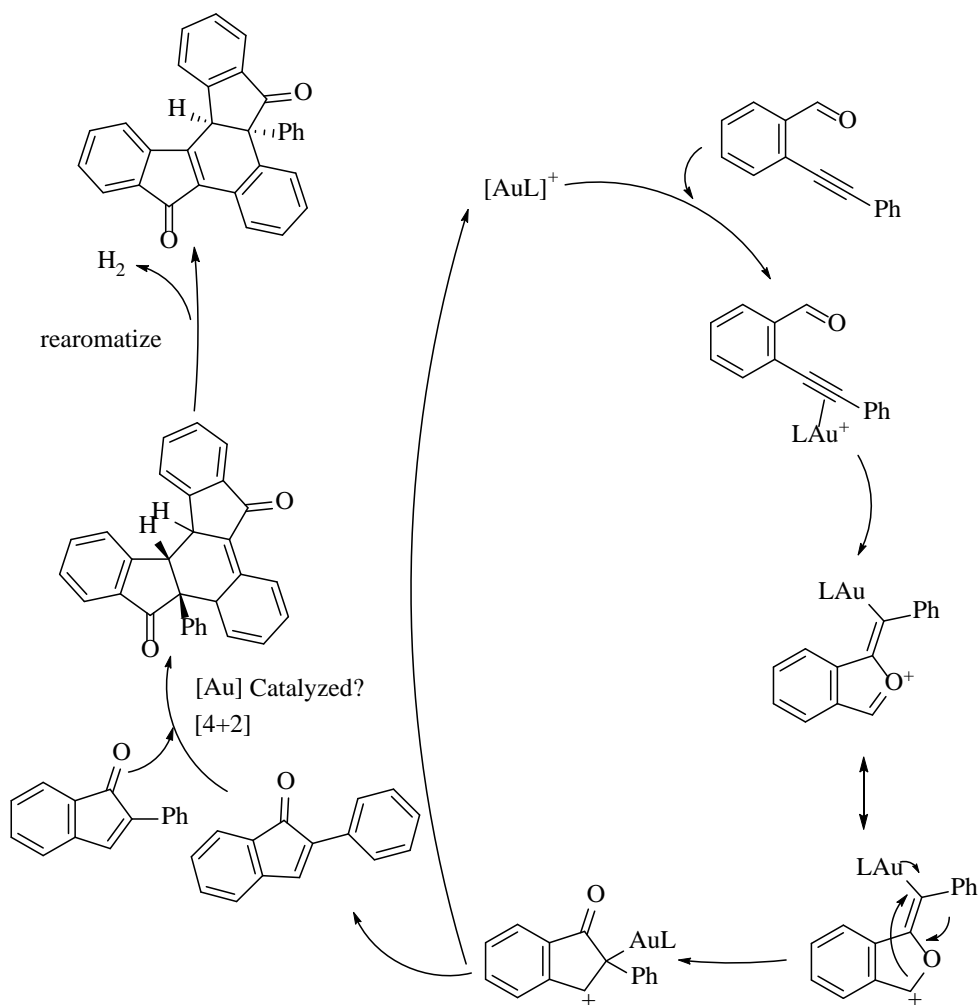

Scheme 6.9 Proposed Mechanism for Phenylcinnamalone Derivatives.

The role of the amine in the above reaction mechanism is unclear. It might be involved in sequestering the excess hydrogens. Given that there was no observation of hydrogen gas evolution

during the reaction, the amines might just be involved in the rearomatization of the product. The other possibility which is shown in **Scheme 6.11** is the amine is involved in the synthesis of the indenone which then undergoes the Diels-Alder reaction.
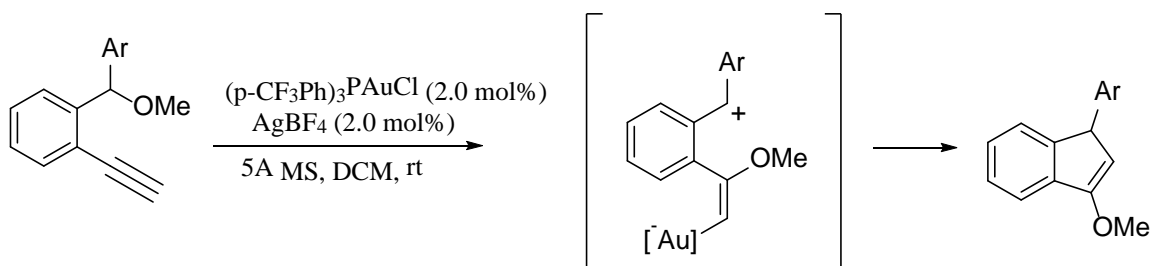
Scheme 6.10 Gold Catalyzed Indenyl Ether Synthesis[24a]
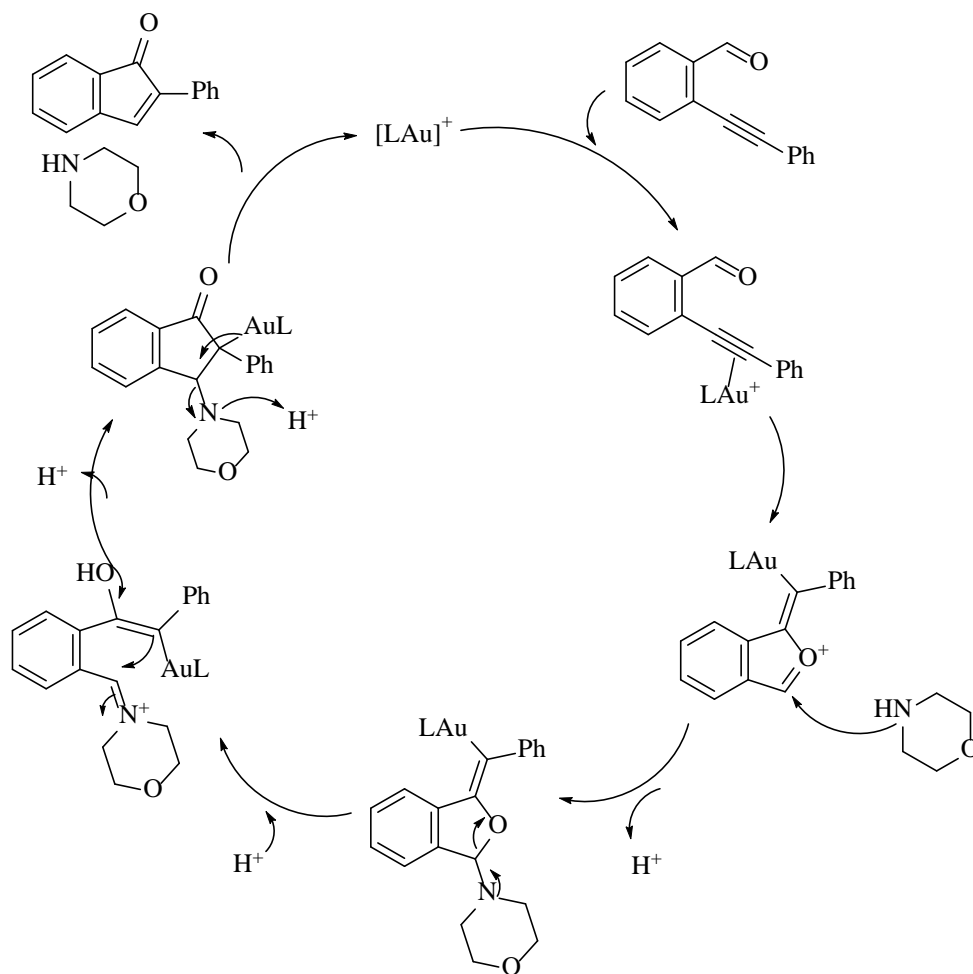
Scheme 6.11 Proposed Mechanism for Gold Catalyzed Indenone Synthesis[24b]

6.3 Conclusion

The gold catalyzed tandem alkynyl benzaldehyde cyclization in the presence of sterically bulky secondary amines resulted in the formation of three new product classes depending on the conditions used. With amine nucleophiles, the scope of the reaction was fairly limited but still allowed the formation of novel 6a,7-dihydro-5-amino-dibenzo[c,g]chromene derivatives. These compounds have been sent to Eli Lilly for biological activity screening. During optimization processes and substrate scope studies, the originally desired isochromene derivative could be synthesized in two cases, while in other cases novel phenylcinnamalone derivatives were isolated. In only one other case has there been a nitrogen-based nucleophile used in a domino alkynylbenzaldehyde cyclization.[14c] This study highlights the ability of gold to access a variety of complex mechanistic pathways even under similar reaction conditions. It also highlights the ability of gold to access elaborate structures that would normally be very complicated if not impossible to synthesize by other routes from accessible starting materials. More mechanistic studies may be required to fully understand the mechanisms behind the various pathways. This understanding could allow for the identification of better catalysts, which then might allow for the substrate scope to be expanded and yields to be improved.

6.4 Experimental Section

General Information:

All air-sensitive synthesis steps were performed under Argon atmosphere using vacuum line or under Nitrogen atmosphere using glovebox unless otherwise noted. All solvent for reactions were dried before use. (Tetrahydrofuran, toluene and 1, 4-Dioxane were dried over and stored on sodium with benzophenone under vacuum. Dichloromethane were washed with concentrated sulfuric acid, deionized water, saturated Sodium bicarbonate and deionized water, then pre-dried

over anhydrous calcium chloride, followed by refluxed and distilled from phosphorus pentoxide under nitrogen, stored over phosphorus pentoxide under vacuum.). All other reagents were used directly from the vendors. The reported chemical shifts in NMR spectra were referenced to residual solvent peaks.[25] (CDCl$_3$, ^{1}HNMR: 7.26 ppm, ^{13}CNMR: 77.18 ppm; CD$_2$Cl$_2$, ^{1}HNMR: 5.32 ppm, ^{13}CNMR: 53.84 ppm) CD$_2$Cl$_2$ was dried over and stored on activated 4 Å molecular sieves under vacuum. (THT)AuCl[26], **P4**[27], and substrates **1a-1g**[28] were synthesized according to literature procedures. IR spectra were performed by dissolving compound in DCM then placing drop on salt plate and allowing DCM to evaporate leaving behind thin film of compound which was ran on a FT-IR spectrometer. ^{1}H and ^{13}C NMR were taken on Varian Unity INOVA (400 and 500 MHz) spectrometers. Elemental analyses were performed by Midwest Microlab, Indiana. HRMS was performed at University of Kansas.

General Procedure for Synthesis of 6a-6l and 8b,d

In a nitrogen filled glovebox a 4-dram reaction vial equipped with a stir bar was charged with corresponding alkynyl benzaldehyde derivative (1 equiv.) and [**P4**(CH$_3$CN)]SbF$_6$ (10 mol%) in 2mL of dry DCE. The vial was closed and removed from the box and the corresponding amine was injected through a septum and the reaction was heated at 75 ^{0}C for 48 hours and monitored by TLC until complete consumption of starting material was observed. Upon completion the reaction was purified via silica column using pure DCM as eluent. Any remaining impurities were removed via recrystallization from DCM and hexane.

6a
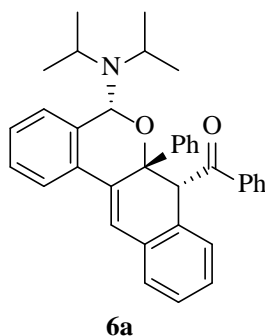
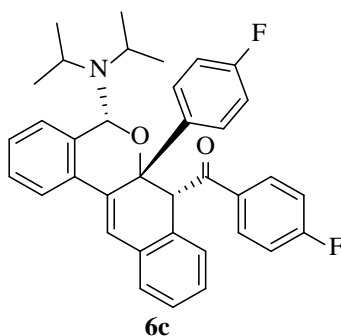## 5-(diisopropylamino)-6a-phenyl-6a,7-dihydro-5H-dibenzo[c,g]chromen-7-yl)(phenyl)methanone 6a

White solid (mp = 267-269°C), 87mg (70% Yield) R_f = 0.37 (CH$_2$Cl$_2$:Hexane, 2:3), ^{1}H NMR (400 MHz, CDCl$_3$) δ = 8.22 (d, J= 7.2Hz, 2H), 8.0 (d, J= 7.22 Hz, 1H), 7.63-7.48 (m, 6H), 7.33-7.11 (m, 8H), 6.92 (t, J=7.6 Hz, 1H), 6.72 (d, J=7.2Hz, 1H), 5.32 (s, 1H), 5.20 (s, 1H), 3.13 (septet, J= 6.4Hz, 1H), 2.76 (septet, J=6.4Hz, 1H), 1.18 (d, J=6.8Hz, 3H), 0.99 (d, J=7.2 Hz, 3H), 0.71 (d, J= 6.8Hz, 3H), 0.38 (d, J= 6.8Hz, 3H). ^{13}C NMR (101MHz, CDCl$_3$) δ = 196.6, 141.1, 138.6, 137.6, 135.1, 132.9, 132.8, 130.7, 129.6, 128.7, 128.5, 128.2, 128.0, 127.6, 127.6, 127.4, 127.4, 127.3, 127.2, 123.1, 121.4, 83.0, 82.3, 58.6, 47.1, 43.5, 24.9, 23.9, 22.3, 21.5. IR (Neat) 1686 (s), 1595 (w), 1488 (w), 1447 (m) cm^{-1} Anal Calcd for C$_{36}$H$_{35}$NO$_2$: C, 84.18; H, 6.87; N, 2.73%. Found: C, 83.97; H, 6.97; N, 2.71%.

6b
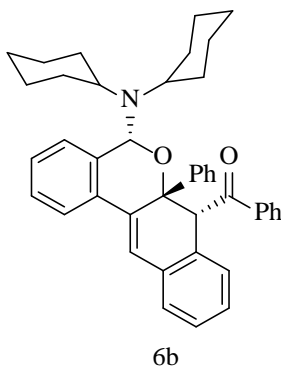
5-(dicyclohexylamino)-6a-phenyl-6a,7-dihydro-5H-dibenzo[c,g]chromen-7-yl)(phenyl)methanone 6b

White solid (mp = 242-244°C), 96mg (67% Yield) R_f = 0.39 (CH$_2$Cl$_2$:Hexane, 2:3), ^{1}H NMR

(400 MHz, CDCl$_3$) δ = 8.22 (d, J=7.6 Hz, 2H), 7.99 (d, J= 7.6Hz, 1H), 7.64-7.48 (m, 6H), 7.33-7.08 (m, 9H), 6.91 (t, J=7.6Hz, 1H), 6.72 (d, J= 7.2Hz, 1H), 5.31 (s, 1H), 5.15 (s, 1H), 2.57 (m, 1H), 2.23 (m, 1H), 1.844-0.59 (m, 20H) ppm. ^{13}C NMR (100.5MHz, CDCl$_3$) δ = 196.4, 141.2, 138.5, 137.8, 135.2, 132.9, 132.9, 132.7, 130.7, 129.6, 128.6, 128.4, 128.2, 128.15, 128.0, 127.6, 127.6, 127.5, 127.4, 127.3, 127.2, 123.1, 121.3, 83.6, 82.2, 58.1, 55.9, 53.7, 35.9, 35.4, 32.8, 27.1, 27.0, 26.4, 26.3, 26.27, 26.0 ppm. IR (Neat) 1680 (s), 1595 (w), 1491 (m), 1447 (m) cm^{-1} Anal Calcd for C$_{42}$H$_{43}$NO$_2$: C, 84.95; H, 7.30; N, 2.36%. Found: C, 84.67; H, 7.52; N, 2.43%.

6c

5-(diisopropylamino)-6a-(4-fluorophenyl)-6a,7-dihydro-5H-dibenzo[c,g]chromen-7-yl)(4-fluorophenyl)methanone 6c

White solid (mp = 271-273°C), 64mg (52% Yield) R$_f$ = 0.40 (CH$_2$Cl$_2$:Hexane, 2:3), ^{1}H NMR (500 MHz, CDCl$_3$) δ = 8.21 (m, 2H), 7.98 (m,1H), 7.58 (m, 2H), 7.51 (s, 1H), 7.33-7.13 (m, 7H), 6.97-6.92 (m, 3H), 6.73 (d, J= 7.5Hz, 1H), 5.19 (s, 1H), 5.18 (s, 1H), 3.15 (septet, J= 6.5Hz, 1H), 2.74 (septet, J= 6.5Hz, 1H), 1.16 (d, J= 7.0Hz, 3H), 1.01 (d, J= 6.5Hz, 3H), 0.72 (d, J= 7.0Hz, 3H), 0.39 (d, J= 7.0Hz, 3H), ppm. ^{13}C NMR (100.5MHz, CDCl$_3$) δ = 194.9, 167.2 (d, $^1J_{C-F}$= 254Hz), 163.7 (d, $^1J_{C-F}$= 247Hz), 137.4, 136.7, 136.7, 135.0, 135.0, 132.5, 132.4, 132.1, 132.0, 130.4, 129.2, 129.1, 128.4, 128.1, 127.7, 127.7, 127.6, 127.5, 127.4, 123.1, 121.4, 115.8, 115.7, 115.5, 115.5, 83.0, 81.8, 58.7, 47.1, 43.5, 24.9, 24.0, 22.2, 21.5 ppm. ^{19}F NMR (376MHz, CDCl$_3$)

δ = -106.0 (m, 1F), -114.5 (m, 1F) ppm. IR (Neat) 1687 (s), 1595 (s), 1501 (s) cm^{-1} Anal Calcd for

C$_{36}$H$_{33}$NO$_2$F$_2$: C, 78.67; H, 6.05; N, 2.55%. Found: C, 78.68; H, 6.13; N, 2.63%.
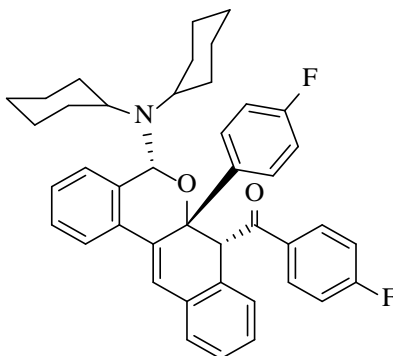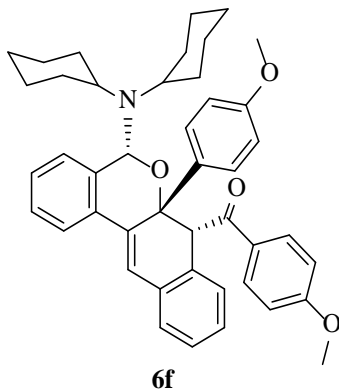

6d

5-(dicyclohexylamino)-6a-(4-fluorophenyl)-6a,7-dihydro-5H-dibenzo[c,g]chromen-7-yl)(4-fluorophenyl)methanone 6d

White solid (mp = 287-289°C), 80mg (57% Yield) R$_f$ = 0.41 (CH$_2$Cl$_2$:Hexane, 2:3), ^{1}H NMR

(400 MHz, CD$_2$Cl$_2$) δ = 8.23 (m, 2H), 8.01 (d, *J*=8Hz, 1H), 7.62 (m, 2H), 7.52 (s, 1H), 7.36-7.14

(m, 7H), 7.01-6.94 (m, 3H), 6.76 (d, *J*=7.6Hz, 1H), 5.22 (s, 1H), 5.12 (s, 1H), 2.62 (m, 1H), 2.15

(m, 1H), 1.86-1.60 (m, 5H), 1.46-0.69 (m, 17H) ppm. ^{13}C NMR (126MHz, CD$_2$Cl$_2$) δ = 194.8,

167.2 (d, ^{1}*J$_{C-F}$*= 254Hz), 163.8 (d, ^{1}*J$_{C-F}$*= 247Hz), 137.9, 137.03, 137.0, 135.4, 135.2, 135.1, 132.8,

132.5, 132.4, 132.3, 130.6, 129.6, 129.6, 128.6, 128.0, 127.9, 127.9, 127.7, 127.6, 123.1, 121.5,

115.8, 115.7, 115.6, 115.6, 83.9, 82.0, 58.4, 56.3, 36.1, 35.8, 32.9, 32.8, 27.1, 27.1, 26.6, 26.4,

26.1 ppm. ^{19}F NMR (376MHz, CD$_2$Cl$_2$) δ = -106.0 (m, 1F), -114.5 (m, 1F) ppm. IR (Neat) 1685

(s), 1595 (s), 1498 (s) cm^{-1} HRMS (ESI, [C$_{42}$H$_{41}$O$_2$F$_2$N + H]$^+$) Calcd: 630.3184, Found: 630.3195

m/z

6e
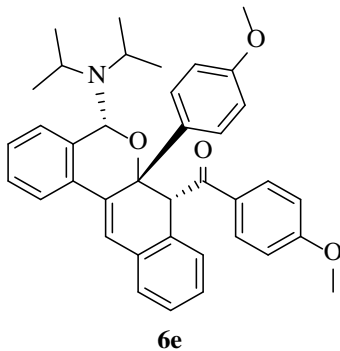
5-(diisopropylamino)-6a-(4-methoxyphenyl)-6a,7-dihydro-5H-dibenzo[c,g]chromen-7-yl)(4-methoxyphenyl)methanone 6e

White solid (mp = 224-227°C), 75mg (62% Yield) R_f = 0.31 (CH$_2$Cl$_2$:Hexane, 2:3), ^{1}H NMR (400 MHz, CDCl$_3$) δ = 8.19 (d, J=8.8Hz, 2H), 7.99 (d, J=8.0Hz, 1H), 7.53 (d, J=8.8Hz, 2H), 7.50 (s, 1H), 7.31-7.10 (m, 5H), 7.0 (m, 2H), 6.92 (m, 1H), 6.80 (d, J=8.8Hz, 2H), 6.74 (d, J=7.2Hz, 1H), 5.29 (s, 1H), 5.17 (s, 1H), 3.89 (s, 3H), 3.72 (s, 3H), 3.14 (septet, J=6.8Hz, 1H), 2.76 (septet, J=6.8Hz, 1H), 1.17 (d, J=6.8Hz, 2H), 1.00 (d, J=6.8Hz, 2H), 0.72 (d, J=6.8Hz, 2H), 0.41 (d, J=6.8Hz, 2H), ppm. ^{13}C NMR (100.5MHz, CDCl$_3$) δ = 195.2, 163.5, 159.2, 127.7, 135.2, 133.2, 133.1, 132.9, 131.9, 131.8, 130.9, 128.7, 128.1, 128.0, 127.5, 127.4, 127.2, 127.17, 123.0, 121.1, 114.0, 113.7, 82.7, 81.8, 58.4, 55.6, 55.3, 47.1, 43.5, 25.0, 24.0, 22.3, 21.5 ppm. IR (Neat) 1679 (s), 1595 (s), 1508 (m), 1164 (s) cm^{-1} HRMS (ESI, [C$_{38}$H$_{39}$O$_4$N + H]$^+$) Calcd: 574.2957, Found: 574.2972 m/z .

6f

233

5-(dicyclohexylamino)-6a-(4-methoxyphenyl)-6a,7-dihydro-5H-dibenzo[c,g]chromen-7-yl)(4-methoxyphenyl)methanone 6f

White solid (mp = 259-260°C), 94mg (68% Yield) R_f = 0.33 (CH$_2$Cl$_2$:Hexane, 2:3), ^{1}H NMR (400 MHz, CDCl$_3$) δ = 8.18 (m, 2H), 7.97 (d, *J*=7.6Hz, 1H), 7.52 (d, *J*=8.4Hz, 2H), 7.49 (s, 1H), 7.30-7.07 (m, 5H), 6.98 (m ,2H), 6.91 (t, *J*=7.6Hz, 1H), 6.78 (d, *J*=7.2Hz, 2H), 6.73 (d, *J*=7.6Hz, 1H), 5.22 (s, 1H), 5.11 (s, 1H), 3.89 (s, 3H), 3.71 (s, 3H), 2.57 (m,1H), 2.23 (m,1H), 1.84-0.62 (2, 20H) ppm.^{13}C NMR (100.5MHz, CDCl$_3$) δ = 195.0, 163.5, 159.2, 137.9, 135.2, 133.2, 133.2, 132.7, 131.8, 131.7, 130.9, 128.7, 128.1, 128.0, 127.6, 127.5, 127.3, 127.2, 127.1, 123.0, 121.0, 113.9, 113.5, 83.4, 81.7, 58.2, 55.9, 55.6, 55.3, 53.7, 35.9, 35.4, 32.8, 32.77, 27.1, 27.0, 26.4, 26.3. 26.3, 26.1 ppm. IR (Neat) 1676 (s), 1597 (s), 1507 (m), 1165 (s) cm^{-1} Anal Calcd for C$_{44}$H$_{47}$NO$_4$: C, 80.82; H, 7.25; N, 2.14%. Found: C, 80.60; H, 7.31; N, 2.22%.

6g
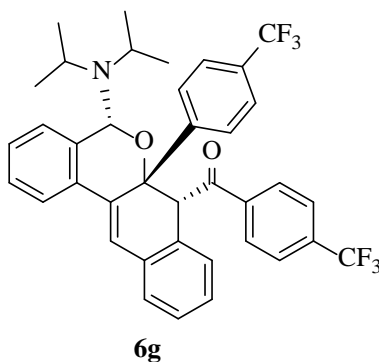
5-(diisopropylamino)-6a-(4-(trifluoromethyl)phenyl)-6a,7-dihydro-5H-dibenzo[c,g]chromen-7-yl)(4-(trifluoromethyl)phenyl)methanone 6g

White solid (mp = 258-259°C), 38mg (32% Yield) R_f = 0.44 (CH$_2$Cl$_2$:Hexane, 2:3), ^{1}H NMR (500 MHz, CDCl$_3$) δ = 8.27 (d, *J*=8Hz, 2H), 8.00 (d, *J*=8Hz, 1H), 7.79 (d, *J*=8Hz, 2H), 7.74 (d, *J*=8Hz, 2H), 7.56 (s, 1H), 7.54 (m, 2H), 7.37 (d, *J*=7.5Hz, 1H), 7.31-7.16 (m, 4H), 6.96 (t, *J*=7.5Hz, 1H), 6.71 (d, *J*=7Hz, 1H), 5.25 (s, 1H), 5.19 (s, 1H), 3.18 (septet, *J*=7Hz, 1H), 2.76 (septet, *J*=6.5Hz, 1H), 1.18 (d, *J*=7Hz, 3H), 1.03 (d, *J*=6.5Hz, 1H), 0.73 (d, *J*=6.5Hz, 1H), 0.40 (d, *J*=6.5Hz, 1H) ppm.^{13}C NMR (125MHz, CDCl$_3$) δ = 195.5, 145.0, 141.1, 137.0, 134.7 ($^2J_{CF,}$

$J= 33.1$ Hz), 132.1, 131.5, 130.7 ($^2J_{CF}$, $J= 32.7$ Hz), 130.0, 129.7, 128.7, 128.2, 128.0, 127.9, 127.7, 127.66, 127.6, 127.4 ($^1J_{CF}$, $J= 272.1$ Hz), 127.1 ($^1J_{CF}$, $J= 272.6$ Hz), 126.0 ($^3J_{CF}$, $J= 3.3$ Hz), 125.7 ($^3J_{CF}$, $J= 3.8$ Hz), 123.2, 121.7, 83.4, 82.0, 59.0, 47.1, 43.5, 24.9, 24.1, 22.1, 21.6 ppm. ^{19}F NMR (376MHz, CDCl$_3$) δ = -62.6, -63.0 ppm. IR (Neat) 1695 (s), 1616 (s), 1494 (m) cm^{-1} HRMS (ESI, [C$_{38}$H$_{33}$O$_2$F$_6$N + H]$^+$) Calcd: 650.2494, Found: 650.2510 m/z .

6h
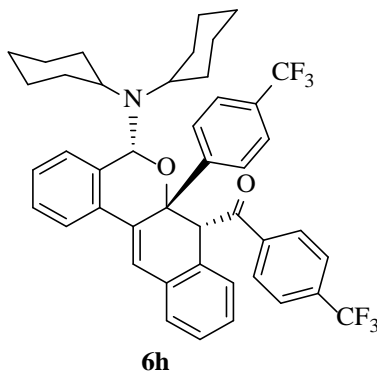
5-(dicyclohexylamino)-6a-(4-(trifluoromethyl)phenyl)-6a,7-dihydro-5H-dibenzo[c,g]chromen-7-yl)(4-(trifluoromethyl)phenyl)methanone 6h

White solid (mp = 263-264ºC), 49mg (37% Yield) R$_f$ = 0.45 (CH$_2$Cl$_2$:Hexane, 2:3), ^{1}H NMR (500 MHz, CDCl$_3$) δ = 8.27 (d, J=8Hz, 2H), 7.98 (d, J=8Hz, 1H), 7.78 (d, J=8Hz, 2H), 7.73 (d, J=8Hz, 2H), 7.55 (s, 1H), 7.54 (m, 2H), 7.36 (d, J=7.5Hz, 1H), 7.29-7.20 (m, 4H), 7.16 (t, J=7.0Hz, 1H) 6.96 (t, J=7.5Hz, 1H), 6.70 (d, J=7Hz, 1H), 5.19 (s, 1H), 5.17 (s, 1H), 2.60 (m, 1H), 2.22 (m, 1H), 1.84-0.69 (m, 20H) ppm. ^{13}C NMR (125MHz, CDCl$_3$) δ = 195.2, 145.1, 140.9, 137.2, 134.7, 134.7 ($^2J_{CF}$, $J= 30.3$ Hz), 131.9, 131.5, 130.7 ($^2J_{CF}$, $J= 32.6$ Hz), 130.1, 129.7, 128.7, 128.2, 127.9, 127.9, 127.8, 127.7, 127.7, 127.5, 127.4 ($^1J_{CF}$, $J= 272.1$ Hz), 127.1 ($^1J_{CF}$, $J= 272.6$ Hz), 125.9 ($^3J_{CF}$, $J= 3.8$ Hz), 125.6 ($^3J_{CF}$, $J= 3.6$ Hz), 123.2, 121.6, 84.0, 81.9, 58.7, 55.9, 53.6, 35.9, 35.7, 32.9, 26.9, 26.8, 26.3, 26.2, 25.8 ppm. ^{19}F NMR (376MHz, CDCl$_3$) δ = -62.6, -63.0 ppm. IR (Neat) 1692 (s), 1618 (m), 1494 (m) cm^{-1} HRMS (ESI, [C$_{44}$H$_{41}$O$_2$F$_6$N + H]$^+$) Calcd: 730.3120,
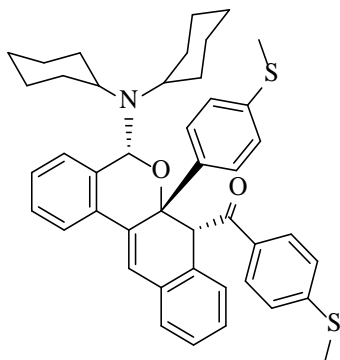
Found: 730.3127 m/z .
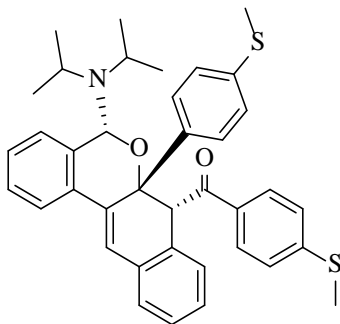
6i

5-(diisopropylamino)-6a-(4-(methylthio)phenyl)-6a,7-dihydro-5H-dibenzo[c,g]chromen-7-yl)(4-(methylthio)phenyl)methanone 6i

White solid (mp = 206-208 °C), 91mg (76% Yield) R_f = 0.36 (CH$_2$Cl$_2$:Hexane, 2:3), ^{1}H NMR (500 MHz, CDCl$_3$) δ = 8.10 (m, 2H), 7.98 (d, *J*=8Hz, 1H), 7.52 (d, *J*=7.5Hz, 2H), 7.50 (s, 1H), 7.32-7.12 (m ,9H), 6.92 (m, 1H), 6.72 (d, *J*=7Hz, 1H), 5.21 (s, 1H), 5.19 (s, 1H), 3.142 (septet, *J*=7.0Hz, 1H), 2.75 (d, *J*=6.5Hz, 1H), 2.55 (s, 3H), 2.40 (s, 3H), 1.17 (d, *J*=6.5Hz, 3H), 1.01 (d, *J*=6.5Hz, 3H), 0.72 (d, *J*=6.5Hz, 3H), 0.42 (d, *J*=6.5Hz, 3H) ppm.^{13}C NMR (100.5MHz, CDCl$_3$) δ = 195.6, 145.5, 138.1, 137.8, 137.5, 135.0, 134.9, 130.5, 129.9, 128.2, 128.1, 127.9, 127.6, 127.54, 127.5, 127.3, 127.25, 126.4, 125.0, 123.1, 121.3, 82.9, 81.8, 58.4, 47.1, 43.5, 25.0, 24.0, 22.3, 21.5, 15.5, 15.0 ppm. IR (Neat) 1678 (s), 1586 (m), 1494 (s) cm^{-1} Anal Calcd for C$_{38}$H$_{39}$NO$_2$S$_2$: C, 75.33; H, 6.49; N, 2.31%. Found: C, 75.40; H, 6.53; N, 2.29%.

6j

5-(dicyclohexylamino)-6a-(4-(methylthio)phenyl)-6a,7-dihydro-5H-dibenzo[c,g]chromen-7-yl)(4-(methylthio)phenyl)methanone 6j
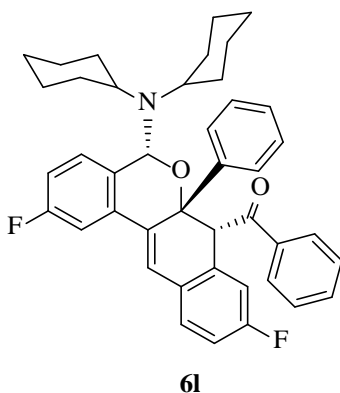
White solid (color change 195°C), 99mg (73% Yield) R_f = 0.36 (CH$_2$Cl$_2$:Hexane, 2:3), ^{1}H NMR (500 MHz, CDCl$_3$) δ = 8.11 (m, 2H), 7.97 (d, *J*=8Hz, 1H), 7.52 (d, *J*=7.5Hz, 2H), 7.51 (s, 1H), 7.32-7.09 (m ,9H), 6.92 (m, 1H), 6.72 (d, *J*=7Hz, 1H), 5.17 (s, 1H), 5.16 (s, 1H), 2.59 (m, 1H), 2.56 (s, 3H), 2.40 (s, 3H), 2.23 (m,1H), 1.84-0.68 (m, 20H) ppm.^{13}C NMR (100.5MHz, CDCl$_3$) δ = 195.3, 145.5, 138.0, 137.9, 137.6, 135.0, 134.8, 132.7, 132.4, 130.6, 129.9, 128.2, 127.9, 127.6, 127.57, 127.4, 127.3, 127.2, 126.3, 124.9, 123.0, 121.2, 83.5, 81.8, 58.2, 55.9, 53.6, 35.9, 35.5, 32.8, 32.7, 27.0, 26.9, 26.3, 26.25, 26.0, 15.5, 15.0 ppm. IR (Neat) 1669 (s), 1585 (m), 1486 (m) cm^{-1} Anal Calcd for C$_{44}$H$_{47}$NO$_2$S$_2$: C, 77.04; H, 6.91; N, 2.04%. Found: C, 77.31; H, 7.34; N, 1.86%.

6k
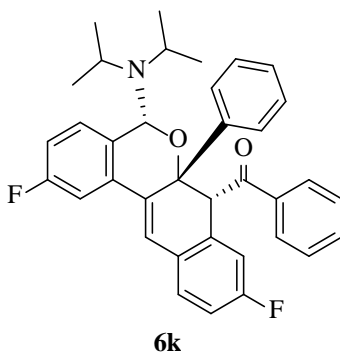
5-(diisopropylamino)-2,9-difluoro-6a-phenyl-6a,7-dihydro-5H-dibenzo[c,g]chromen-7-yl)(phenyl)methanone 6k

White solid (mp = 272-274°C), 75mg (61% Yield) R_f= 0.39 (CH$_2$Cl$_2$:Hexane, 2:3), ^{1}H NMR (500 MHz, CDCl$_3$) δ = 8.19 (m, 2H), 7.62 (m, 4H), 7.53 (m, 2H), 7.42 (s, 1H), 7.32-7.15 (m, 5H), 6.88 (m, 2H), 6.47 (m, 1H), 5.29 (s, 1H), 5.14 (s, 1H), 3.12 (septet, *J*= 6Hz, 1H), 2.72 (septet, *J*= 6.5Hz, 1H), 1.15 (d, *J*= 6.5Hz, 3H), 0.96 (d, *J*= 7Hz, 3H), 0.70(d, *J*= 6.5Hz, 3H), 0.35 (d, *J*= 6.5Hz, 3H) ppm.^{13}C NMR (125MHz, CDCl$_3$) δ = 195.9, 163.6 (d, $^1J_{C-F}$= 254Hz), 163.1 (d, $^1J_{C-F}$= 248Hz), 140.5, 138.2, 135.1, 135.0, 134.7, 134.6, 133.3, 133.29, 133.25, 131.0, 130.98, 129.8, 129.7, 129.6,

129.2, 129.1, 128.9, 128.6, 128.3, 127.3, 121.5, 115.8, 115.6, 115.0, 114.8, 109.0, 108.8, 82.8, 82.0, 58.4, 46.9, 43.5, 24.9, 23.8, 22.3, 21.4 ppm. ^{19}F NMR (376MHz, CDCl$_3$) δ = -113.4, -115.7 ppm. IR (Neat) 1684 (s), 1582 (m), 1500 (m) cm^{-1} HRMS (ESI, [C$_{36}$H$_{33}$O$_2$F$_2$N + H]$^+$) Calcd: 550.2558, Found: 550.2572 m/z .


6l

5-(dicyclohexylamino)-2,9-difluoro-6a-phenyl-6a,7-dihydro-5H-dibenzo[c,g]chromen-7-yl)(phenyl)methanone 6l

White solid (color change 205°C), 88mg (63% Yield) R$_f$ = 0.40 (CH$_2$Cl$_2$:Hexane, 2:3), ^{1}H NMR (500 MHz, CDCl$_3$) δ = 8.20 (m, 2H), 7.62 (m, 4H), 7.53 (m, 2H), 7.43 (s, 1H), 7.32-7.20 (m, 5H), 6.88 (m, 2H), 6.47 (m, 1H), 5.28 (s, 1H), 5.09 (s, 1H), 2.55 (m, 1H), 2.19 (m, 1H), 1.84-0.61 (m, 20H) ppm.^{13}C NMR (125MHz, CDCl$_3$) δ = 195.6, 163.5 (d, $^1J_{C-F}$= 254Hz), 163.1 (d, $^1J_{C-F}$= 248Hz), 140.5, 138.1, 135.1, 135.05, 134.5, 134.5, 133.5, 133.45, 133.3, 131.03, 131.0, 129.9, 129.8, 129.6, 129.3, 129.2, 129.1, 128.8, 128.5, 128.3, 127.3, 121.4, 115.8, 115.6, 115.0, 114.9, 114.8, 114.7, 108.9, 108.7, 83.5, 82.0, 58.2, 55.8, 53.6, 35.8, 35.3, 32.8, 32.7, 27.0, 26.9, 26.4, 26.3, 26.2, 25.9 ppm. ^{19}F NMR (376MHz, CDCl$_3$) δ = -113.5, -115.8 ppm. IR (Neat) 1682 (s), 1581 (m), 1499 (m) cm^{-1} HRMS (ESI, [C$_{42}$H$_{41}$O$_2$F$_2$N + H]$^+$) Calcd: 630.3184, Found: 630.3196 m/z .

**General Procedure for Synthesis of 7a & 7b**

In a nitrogen filled glovebox a 4-dram reaction vial equipped with a stir bar was charged with

corresponding alkynyl benzaldehyde derivative (1 equiv.) and [**P4**(CH$_3$CN)]SbF$_6$ (10 mol%) in 2mL of dry THF. The vial was closed and removed from the box and the corresponding amine was injected through a septum and the reaction was heated at 60 ^{0}C and monitored by TLC until complete consumption of starting material was observed. Upon completion products were purified via recrystalization

7a
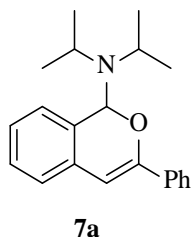
N,N-diisopropyl-3-phenyl-1H-isochromen-1-amine 7a

Off-White solid (mp = 84-87°C), % Yield ^{1}H NMR (500 MHz, CDCl$_3$) δ = 7.82 (m, 2H), 7.43 (m, 2H), 7.37 (m, 1H), 7.28 (m, 2H), 7.22 (m, 1H), 7.12 (d, J= 7.5Hz, 1H), 6.45 (s, 1H), 6.36 (s, 1H), 3.47 (sept, J=7.0Hz, 2H), 1.31 (bs, 6H), 1.15 (bs, 1H) ppm. ^{13}C NMR (125MHz, CDCl$_3$) δ = 153.4, 135.6, 134.1, 130.1, 128.5, 128.4, 128.0, 126.2, 125.7, 125.0, 123.8, 98.0, 89.5, 45.5, 23.7 ppm. HRMS (ESI, [C$_{21}$H$_{25}$ON + H]$^+$) Calcd: 308.2014, Found: 308.2016 m/z .

7b
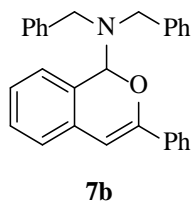
N,N-dibenzyl-3-phenyl-1H-isochromen-1-amine 7b

Off-White solid (mp= 96-98°C), 110mg (56% Yield) ^{1}H NMR (500 MHz, CDCl$_3$) δ = 7.89 (m, 2H), 7.52 (m, 2H), 7.46-7.24 (m, 14H), 7.12 (m, 1H), 6.36 (s, 1H), 6.20 (s, 1H), 4.08 (d, J_{AB}= 14.0 Hz, 2H), 3.92 (d, J_{AB}= 14.0 Hz, 2H) ppm. ^{13}C NMR (125MHz, CDCl$_3$) δ = 152.5,

139.4, 135.1, 133.0, 129.0, 128.8, 128.6, 128.6, 128.5, 128.4. 127.2, 126.6, 126.0, 125.1, 124.0, 98.7, 88.9, 52.4 ppm. HRMS (ESI, $[C_{29}H_{25}ON + H]^+$) Calcd: 404.2014 , Found: 404.2002 m/z .
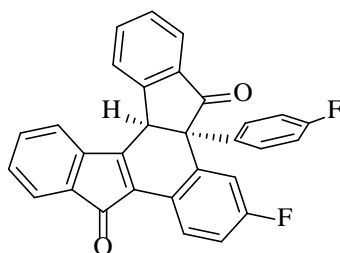
8b

7-fluoro-5a-(4-fluorophenyl)-5a,14c-dihydrobenzo[a]indeno[2,1-c]fluorene-5,10-dione 8b

Red solid (mp = 261-263 °C), 20mg (20% Yield) ^{1}H NMR (400 MHz, CDCl$_3$) δ = 8.43 (m, 1H), 7.93 (d, *J* = 7.6Hz, 1H), 7.66 (m, 1H), 7.55-7.26 (m, 7H), 7.06 (m, 1H), 6.98 (m, 4H), 4.59 (s, 1H) ppm. ^{13}C NMR (101MHz, CDCl$_3$) δ = 204.3, 195.1, 164.1, 163.2, 161.6, 160.8, 152.5, 152.5, 150.2, 143.7, 139.4, 139.3, 136.5, 135.8, 135.1, 135.1, 134.2, 132.3, 130.0, 129.9, 129.8, 129.3, 127.0, 126.9, 126.7, 125.2, 124.6, 123.4, 120.2, 117.0, 116.8, 116.0, 115.9, 115.8, 115.7, 62.4, 48.9 ppm. ^{19}F NMR (376 MHz, CDCl$_3$) δ = −109.3, −114.7 ppm. IR (Neat) cm^{-1} HRMS (ESI, $[C_{30}H_{16}O_2F_2 + H]^+$) Calcd: 447.1197 , Found: 447.1125 m/z .
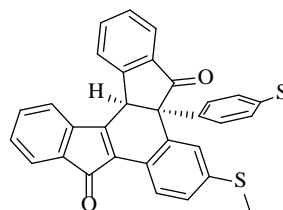

8d

7-(methylthio)-5a-(4-(methylthio)phenyl)-5a,14c-dihydrobenzo[a]indeno[2,1-c]fluorene-5,10-dione 8d

Red solid (mp = 272-273 °C), 14mg (14% Yield) ^{1}H NMR (400 MHz, CDCl$_3$) δ = 8.32 (d, *J* =

8.4Hz, 1H), 7.91 (d, J= 7.6Hz, 1H), 7.63-7.12 (m, 12H), 6.88 (m, 2H), 4.58 (s, 1H), 2.45 (s, 3H), 2.42 (s, 3H) ppm. ^{13}C NMR (101MHz, CDCl$_3$) δ = 204.5, 195.1, 152.0, 150.2, 143.8, 140.5, 140.1, 137.6, 136.0, 135.8, 133.9, 132.6, 132.2, 129.5, 128.9, 128.5, 127.1, 126.8, 126.5, 125.6, 125.1, 124.9, 124.8, 123.0, 120.0, 62.6, 49.0, 31.6, 22.6 ppm. IR (Neat) 1711 (s) cm^{-1} Anal. Calcd: C, 76.47; H, 4.41 % Found: C, 76.19; H, 4.02 %

5a
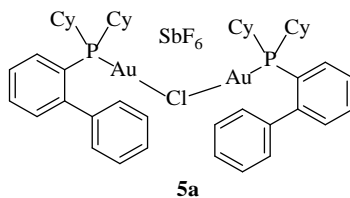
White solid 103mg (88 % Yield) ^{1}H NMR (500 MHz, CD$_2$Cl$_2$) δ = 7.65–7.52 (m, 8H), 7.44 (m, 4H), 7.36 (m, 2H), 7.19 (m, 4H), 2.25 (m, 4H), 1.98 (m, 4H), 1.83-1.65 (m, 18H), 1.38-1.10 (m, 18H) ppm. ^{13}C NMR (125MHz, CD$_2$Cl$_2$) δ = 149.2, 149.1, 142.3, 142.2, 133.1, 133.0, 133.0, 131.9, 131.8, 129.9, 129.2, 128.8, 128.6, 128.6, 123.5, 123.0, 37.0, 36.7, 31.6, 31.6, 29.9, 26.8, 26.7, 26.7, 26.6, 26.0, 26.0 ppm. ^{31}P NMR 202MHz, CD$_2$Cl$_2$) δ = 39.7 ppm. Anal Calcd for C$_{48}$H$_{62}$Au$_2$ClSbP$_2$F$_6$: C, 42.20; H, 4.57 %. Found: C, 41.50; H, 4.39 %.

6.5 References

1.   (a). Hashmi, S.K.; Toste, D. <u>Modern Gold Catalyzed Synthesis</u>, Wiley-VCH, Weinheim **2012** (b). Toste, D.; Michelet, V. <u>Gold Catalysis: an homogeneous approach</u> Imperial College Press, London. **2014** (c). Slaughter, L.M. *Topics in Current Chemistry 357* <u>Homogeneous Gold Catalysis</u> Springer **2015** (d). Forin, D. J.; Toste, F. D.; *Chem. Rev.* **2008**, *108*, 3351-3378.

2.   Tietze, L.F., *Chem. Rev.,* **1996**, *96*, 115-136.

3.   Fogg, D.E.; dos Santos, E.N. *Coord. Chem Rev.* **2004**, *248*, 2365-2379

4.   Poli, G.; Giambastiani, G.; Heumann, A.; *Tetrahedron*, **2000**, *56*, 5959-5989

5.   (a). Teles, J. H.; Brode, S.; Chabanas, M. *Angew. Chem.* **1998**, *110*, 1475; *Angew. Chem., Int. Ed.* **1998**, *37*, 1415-1418. (b). Zhang, C.; Cui, D.M.; Yao, L.M.; Wang, B.S.; Hu, Y.Z.; Hayashi, T. *J. Org. Chem*, **2008**, 73, 7811-7813.

6.   Orbradors, C.; Echavarren, A.M.; *Acc. Chem. Res.* **2014**, 47, 902-912.

7.   Bongers, N.; Krause, N.; *Angew. Chem. Int. Ed.* **2008**, *47*, 2178-2181.

8.   (a). Nucleophiles, Ar: (a) Ouyang, B.; Yuan, J.; Yang, Q.; Ding, Q.; Peng, Y.; Wu, J. *Heterocycles* **2010**, *82*, 1239-1249. (b) Tang, R.-Y.; Li, J.-H. *Chem. Eur. J.* **2010**, *16*, 4733-4738. (c) Mariaule, G.; Newsome, G.; Toullec, P. Y.; Belmont, P.; Michelet, V. *Org. Lett*. **2014**, *16*, 4570-4573. Terminal alkynes: (d) Yao, X.; Li, C.-J. *Org. Lett*. **2006**, *8*, 1953-1955. Phosphites: (e) Yu, X.; Ding, Q.; Wang, W.; Wu, J. *Tetrahedron Lett*. **2008**, *49*, 4390-4393. Nitrogen: (f) Dyker, G.; Hildebrandt, D.; Liu, J.; Merz, K. *Angew. Chem., Int. Ed*. **2003**, *42*, 4399-4402. Activated-methylenes: (g) Beeler, A. B.; Su, S.; Singleton, C. A.; Porco, J. A., Jr. *J. Am. Chem. Soc*. **2007**, *129*, 1413-1419. (h) Leng, B.; Chichetti, S.; Su, S.; Beeler,   A. B.; Porco, J. A., Jr. *Beilstein J. Org. Chem*. **2012**, *8*, 1338-1343.

9.   Handa, S.; Slaughter, L.M.; *Angew. Chem. Int. Ed.* **2012**, 51, 2912-2915.

10.   Gaëlle Mariaule, Gregory Newsome, Patrick Y. Toullec, Philippe Belmont, and Véronique Michelet *Org. Lett.* **2014,** *16*, 4570-4573

11.   Xiaoquan Yao, Chao-Jun Li *Org. Lett.* **2006** *8*, 1953-1955

12.   Xiaoming Zeng, Guido D. Frey, Rei Kinjo, Bruno Donnadieu, and Guy Bertrand

J. Am. Chem. Soc. **2009** *131*, 8690-8696

13.   Zhdanko, A., Ströbele, M. and Maier, M. E., *Chem. Eur. J.* **2012**, *18*, 14732-14744

14.   (a) Selvi, T.; Srinivasan, K. *Org. Biomol. Chem.* **2013**, *11*, 2162-2167 (b) N. Asao, T. Kasahara and Y. Yamamoto, *Angew. Chem., Int. Ed.*, **2003**, 42, 3504-3506. (c) G. Dyker, D. Hildebrandt, J. Liu and K. Merz, *Angew. Chem., Int. Ed.*, **2003**, 42, 4399-4402, (d) Z.-L. Hu, W.-J. Qian, S. Wang, S.-z. Wang and Z.-J. Yao, *Org. Lett.*, **2009**, 11, 4676-4679 (e) Z.-L. Hu, W.-J. Qian, S. Wang, S.-z. Wang and Z.-J. Yao, *J. Org. Chem.*, **2009**, 74, 8787-8793. (f). Jagdale, A.R.; Park, J.H.; Youn, S.W.; *J. Org. Chem.* **2011**, *76*, 7204-7215. (g) Asao, N.; Chan, C. S.; Takahashi, K.; Yamamoto, Y. *Tetrahedron* **2005**, *61*, 11322-11326. (h) Asao, N.; Nogami, T.; Takahashi, K.; Yamamoto,Y. *J. Am. Chem. Soc.* **2002**, *124*, 764-765. (i) Patil, N. T.; Yamamoto, Y. *J. Org. Chem.* **2004**, *69*, 5139-5142. (j) Mondal, S.; Nogami, T.;   Asao, N.;Yamamoto, Y. *J. Org. Chem.* **2003**, *68*, 9496-9498. (k) Wei, L.-L.; Wei, L.-M.; Pan, W.-B.; Wu, M.-J. *Synlett* **2004**, 1497-1502. (l) Gulias, M.; Rodriguez,J. R.; Castedo, L.; Mascareñas, J. L. *Org. Lett.* **2003**, *5*, 1975-1977. (m) Bhunia,S.; Wang, K.-C.; Liu, R.-S. *Angew. Chem., Int. Ed.* **2008**, *47*, 5063-5066. (n) Jha, R. R.; Aggarwal, T.; Verma, A. K. *Tetrahedron Lett.* **2014**, *55*, 2603-2608.

15.   N. Asao, K. Takahashi, S. Lee, T. Kasahara, Y. Yamamoto, *J. Am. Chem. Soc.* **2002**, 124, 12650 – 12651. (b). Asao, N.; Nogami, T.; Takahashi, K.; Yamamoto, Y. *J. Am.Chem. Soc.* **2002**, 124, 764−765.

16.   Zhang, M.; Ruan, W.; Zhang, H-J; Li, W.; Wen, T-B.; *J. Org. Chem.* ASAP. DOI: 10.1021/acs.joc.5b02340

17. (a). Katz, T.J.; Woodward, R.B.; *Tetrahedron*, **1959**, 5, 70-89. (b). Woodward, R.B.; Hoffman, R.; *Acc. Chem. Res.* **1968**, 1, 17-22. (c). Carey, F.A.; Sundberg, R.J.; Advanced Organic Chemistry, Part B. 5th edition, Springer, **2007**, p 475.

18. (a) Ward, R.-S. *Nat. Prod. Rep*. **1999**, 16, 75– 96. (b) Wu, Y.; Zhao, J.; Chen, J.; Pan, C.; Li, L.; Zhang, H. *Org. Lett.* **2009**, 11, 597– 600. (c) Stadler, D.; Bach, T. *Angew. Chem., Int. Ed*. **2008**, 47, 7557– 7559 (d) Reynolds, A.-J.; Scott, A.-J.; Turner, C.-I.; Sherburn, M.-S. *J. Am. Chem. Soc.* **2003**, 125, 12108– 12109 (e) Bush, E.-J.; Jones, D. W. *J. Chem. Soc., Perkin Trans.* 1 **1996**, 151– 155 (f) Hadimani, S.-B.; Tanpure, R.-P.; Bhat, S.-V. *Tetrahedron Lett.* **1996**, 37, 4791– 4794 (g) Speybroeck, R.-V.; Guo, H.; Eycken, J.-V.; Vandewalle, M. *Tetrahedron* **1991**, 47, 4675– 4682 (h) Andrews, R.-C.; Teague, S.-T.; Meyers, A.-I. *J. Am. Chem. Soc.* **1988**, 110, 7854– 7858.

19. (a). Panda, B.; Sarkar, T.K.; *J. Org. Chem.* **2013** *78* (6), 2413-2421 (b). Liu, Y.; Xu, W.; Wang, X.; *Org. Lett.*, **2010**, 12 (7), pp 1448–1451 (c) Shi, H.; Fang, L.; Tan, C.; Shi, L.; Zhang, W.; Li, C-C.; Luo, T.; Yang, Z.; *J. Amer. Chem. Soc.* **2011** *133* (38), 14944-14947.

20. (a) Wang, W.; Li, T.; Milburn, R.; Yates, J.; Hinnant, E.; Luzzio, M. J.; Noble, S. A.; Attardo, G. *Bioorg. Med. Chem. Lett*. **1998**, *8*, 1579-1584. (b) Shishido, Y.; Wakabayashi, H.; Koike, H.; Ueno, N.; Nukui, S.; Yamagishi, T.; Murata, Y.; Naganeo, F.; Mizutani, M.; Shimada, K.; Fujiwara, Y.; Sakakibara, A.; Suga, O.; Kusano, R.; Ueda, S.; Kanai, Y.; Tsuchiya, M.; Satake, M. *Bioorg. Med. Chem*. **2008**, *16*, 7193-7205. (c) Liu, M.; Xiao, H.-T.; He, H.-P.; Hao, X.-Y. *Chem. Nat. Compd*. **2008**, *44*, 588-590.

21.   (a). Homs, A.; Escofet, I.; Echavarren, A.M.; *Org. Lett.* **2013**, 15, 5782-5785. (b) Y. Zhu, C. S. Day, L. Zhang, K. J. Hauser and A. C. Jones, *Chem. Eur. J.*, **2013**, 19, 12264-12271.

22.   Nieto-Oberhuber, C.; López, S.; Muñoz, M. P.; Cárdenas, D. J.; Buñuel, E.; Nevado, C.; Echavarren, A. M. *Angew. Chem. Int. Ed.* **2005**, *44*, 6146–6148.

23.   (a) Bednowitz, A.L.; Hamilton, W.C.; Brown, r.; Donaruma, L.G.; Southwick, P.L.; Kropf, R.; Stanfield, R.A. *J. Amer. Chem. Soc.* **1968** *90* (2), 291-296 (b). Wawzonek, S.; Hansen, G.R.; Zigman, A.R., *J. Chem. Soc. D.* **1969**, 6a-6a

24.   (a). Dubé, P.; Toste, F. D. *J. Am. Chem. Soc.* **2006**, *128*, 12062-12063. (b). Domaradzki, M.E.; Long, Y.; She, Z.; Liu, X.; Zhang, G.; Chen, Y.; *J. Org. Chem.*, **2015**¸ *80*, 11360-11368.

25   Fulmer, G.R.; Miller, A.J.M.; Stoltz, B.M.; Bercaw, J.E.; Goldberg, K.I.; *Organometallics*, **2010**, *29*, 2176-2179

26.   Inorg. Synth., Volume 26, Pg 86

27.   (a) Nieto-Oberhuber, C.; Lopez, S.; Echavarren, A. M. *J. Am. Chem. Soc*. **2005**, *127*, 6178. (b) Al-SaAdy, A. K.; McAuliffe, C. A.; Parish, R. V.; Sandbank, J. A. *Inorg. Synth*. **1985**, *23*, 191.

28.   Rustagi, V.; Tiwari, R.; Verma, A.K.; *Eur. J. Org. Chem.* **2012**, 4590-4602

CHAPTER VII

CONCLUSIONS

The research projects presented herein are interconnected under the common theme of wanting to design and synthesize new monodentate ligands and explore their catalytic activity in homogeneous transition metal catalysis. The study of acyclic diaminocarbenes (ADCs) was the major focus of the research with phosphites being the second class of ligands studied. With a larger N-C$_{carbene}$-N bond angle and more conformational flexibility the ADC-Au^I catalyst proved to be efficient catalyst in the asymmetric intramolecular hydroamination of sulfonamide protected allenamines as long as the 2'-position of the binaphthyl was equipped with a 3,5-bis(trifluoromethyl)phenyl derivative. When using a chiral amine to synthesize the ADC-Au^I complex it was shown care must be taken to avoid any chiral-mismatch situations. Derivatives with other substituents at the 2'-position or 3-position of the binaphthyl proved to be less effective. Chiral ADC-Au^I complexes lacking the binaphthyl backbone also proved to be less efficient. The phosphite-Au^I catalyst proved be somewhat complementary to the ADC-Au^I in that they worked better for the intramolecular hydroamination of carbamate protected allenamines.

Both classes of ligands could be synthesize from similar starting chiral binaphthyl alcohols, that were accessible via a Kumada coupling procedure developed by the Slaughter group. The alcohols could be converted to the desired isocyanides after using a Buchwald-Hartwig amination procedure also developed by the Slaughter group.

A series of sterically hindered achiral ADCs were also synthesized and studied in a domino enyne-cyclization/hydroarylation reaction as well as a Nazarov cyclization. Structure-activity and structure-selectivity correlations were made to determine what factors influence the regioselectivity in aforementioned reactions. Due to the increased steric bulk this series of ADC-

Au^I complexes have distorted dihedral angles which potentially might make them more π-accepting in nature. This would explain the selectivity seen for the domino enyne-cyclization/hydroarylation reaction. The regioselectivity of the Nazarov cyclization correlated well with the calculated steric parameters %V$_{bur}$ and solid angle. A proposed mechanism is given to explain how sterics might influence the termination step of the Nazarov cyclization.

In conclusion, a series of tunable chiral and achiral monodentate ligands for Au^I were synthesized and their catalytic activity were tested in various gold-catalyzed organic transformations. Structure-activity and structure-selectivity correlations were made that will potentially allow for more rational ligand design to be performed in the future. Future expansion on the library of 2'-substituted ADC-Au^I complexes should focus on having 3,5-bis(trifluoromethyl)phenyl substituent and using the countless number of chiral and achiral amines that are commercially available. Although only moderate selectivities were achieved in Au^I catalysis, the ease of synthesis of the phosphite ligands makes them great candidates for the use in other transition metal symmetric catalysis. These new catalyst can potentially provide the means to overcome the fundamental problems associated with achieving high levels of enantioselectivty in gold catalysis and can be potentially used with other transition metals.